

Comparative physiology and the predictability of evolution in extreme environments

by

Nick Barts

B.S., University of Illinois, 2015

AN ABSTRACT OF A DISSERTATION

submitted in partial fulfillment of the requirements for the degree

DOCTOR OF PHILOSOPHY

Division of Biology
College of Arts and Sciences

KANSAS STATE UNIVERSITY
Manhattan, Kansas

2020

Abstract

The physiological mechanisms underlying adaptation, and how physiological differences observed in natural populations relate to underlying genetic variation, remain largely unknown for many natural systems. My dissertation seeks to close these gaps in knowledge by addressing three major questions: 1) How does variation across levels of biological organization integrate to explain divergence in organismal phenotypes? 2) Are patterns of physiological adaptation predictable across populations experiencing similar sources of selection? 3) What are the evolutionary origins of physiological traits facilitating adaptation to novel environmental conditions? Organisms inhabiting extreme environments are ideal systems to investigate questions about the mechanisms underlying adaptation and the predictability of evolution at molecular scales. These habitats are characterized by harsh physiochemical stressors that often target specific biochemical and physiological pathways, allowing for hypothesis-driven tests of the effects of the stressor on organismal function and trait evolution. Additionally, powerful comparisons can be made between closely related lineages inhabiting extreme and ancestral habitats, which allows for investigations into the predictability of evolution in response to similar sources of selection. In my research, I leveraged a unique study system of fishes that have independently colonized extreme aquatic habitats rich in hydrogen sulfide (H₂S), a naturally occurring toxin that is known to interfere with oxygen transport and mitochondrial function address four objectives: 1) I determined the predictability and repeatability of molecular evolution and changes in gene expression of oxygen transport genes in ten lineages of sulfide-tolerant fishes, 2) I assessed the convergence in biochemical, physiological, and organismal function in pathways exhibiting evidence of molecular evolution and gene expression variation, 3) I measured the functional consequences of genetic variation on the metabolic function of

enzymes, mitochondria, and whole organisms to identify the predictability of metabolic evolution across levels of organization and between sulfide-tolerant and -intolerant lineages of fish, and 4) I identified potential adaptive plasticity in gene expression in ancestral freshwater species that may represent pre-adaptations for the colonization of H₂S-rich springs. Through the integration of genomic, biochemical, and organismal data, I found that (1) oxygen transport genes are predictable targets of natural selection in sulfide spring fishes, but the modifications in gene expression and sequence variation were not repeatable across groups, (2) both H₂S detoxification and oxidative phosphorylation are predictable targets of natural selection in H₂S-rich environments, and modification of these integral pathways results in functional differences at the biochemical, physiological, and organismal levels, (3) the degree to which metabolic physiology varies between sulfide-tolerant and -intolerant fish differs depending on the level of organization observed, suggesting that researchers must be cautious when making inferences about function solely from genetic data, and (4) genes exhibiting adaptive plasticity in H₂S detoxification, metabolic pathways, and oxygen sensing may have been pre-adaptations that facilitated colonization of sulfide-rich springs. The research detailed in this dissertation has important implications for how scientists perceive the predictability of both evolution and phenotype, highlighting the role environmental and physiological constraints play in our ability to predict the outcomes of natural variation across habitats and within organisms.

Comparative physiology and the predictability of evolution in extreme environments

by

Nick Barts

B.S., University of Illinois, 2015

A DISSERTATION

submitted in partial fulfillment of the requirements for the degree

DOCTOR OF PHILOSOPHY

Division of Biology
College of Arts and Sciences

KANSAS STATE UNIVERSITY
Manhattan, Kansas

2020

Approved by:

Major Professor
Michael Tobler

Copyright

© Nicholas Barts 2020.

Abstract

The physiological mechanisms underlying adaptation, and how physiological differences observed in natural populations relate to underlying genetic variation, remain largely unknown for many natural systems. My dissertation seeks to close these gaps in knowledge by addressing three major questions: 1) How does variation across levels of biological organization integrate to explain divergence in organismal phenotypes? 2) Are patterns of physiological adaptation predictable across populations experiencing similar sources of selection? 3) What are the evolutionary origins of physiological traits facilitating adaptation to novel environmental conditions? Organisms inhabiting extreme environments are ideal systems to investigate questions about the mechanisms underlying adaptation and the predictability of evolution at molecular scales. These habitats are characterized by harsh physiochemical stressors that often target specific biochemical and physiological pathways, allowing for hypothesis-driven tests of the effects of the stressor on organismal function and trait evolution. Additionally, powerful comparisons can be made between closely related lineages inhabiting extreme and ancestral habitats, which allows for investigations into the predictability of evolution in response to similar sources of selection. In my research, I leveraged a unique study system of fishes that have independently colonized extreme aquatic habitats rich in hydrogen sulfide (H₂S), a naturally occurring toxin that is known to interfere with oxygen transport and mitochondrial function address four objectives: 1) I determined the predictability and repeatability of molecular evolution and changes in gene expression of oxygen transport genes in ten lineages of sulfide-tolerant fishes, 2) I assessed the convergence in biochemical, physiological, and organismal function in pathways exhibiting evidence of molecular evolution and gene expression variation, 3) I measured the functional consequences of genetic variation on the metabolic function of

enzymes, mitochondria, and whole organisms to identify the predictability of metabolic evolution across levels of organization and between sulfide-tolerant and -intolerant lineages of fish, and 4) I identified potential adaptive plasticity in gene expression in ancestral freshwater species that may represent pre-adaptations for the colonization of H₂S-rich springs. Through the integration of genomic, biochemical, and organismal data, I found that (1) oxygen transport genes are predictable targets of natural selection in sulfide spring fishes, but the modifications in gene expression and sequence variation were not repeatable across groups, (2) both H₂S detoxification and oxidative phosphorylation are predictable targets of natural selection in H₂S-rich environments, and modification of these integral pathways results in functional differences at the biochemical, physiological, and organismal levels, (3) the degree to which metabolic physiology varies between sulfide-tolerant and -intolerant fish differs depending on the level of organization observed, suggesting that researchers must be cautious when making inferences about function solely from genetic data, and (4) genes exhibiting adaptive plasticity in H₂S detoxification, metabolic pathways, and oxygen sensing may have been pre-adaptations that facilitated colonization of sulfide-rich springs. The research detailed in this dissertation has important implications for how scientists perceive the predictability of both evolution and phenotype, highlighting the role environmental and physiological constraints play in our ability to predict the outcomes of natural variation across habitats and within organisms.

Table of Contents

List of Figures	xi
List of Tables	xv
Acknowledgements	xvii
Dedication	xx
Preface	xxi
Chapter 1 - Molecular evolution and expression of oxygen transport genes in livebearing fishes (Poeciliidae) from hydrogen sulfide rich springs	1
Abstract	1
Introduction	2
Materials and methods	6
Sample collection	6
RNA extraction, cDNA library preparation, and sequencing	7
Identifying focal and background genes	8
Variant detection and consensus sequence generation	9
Phylogenetic analysis	10
Evolution of gene expression	11
Quantifying positive selection	12
Results	13
Focal oxygen transport genes	13
Expression variation	13
Evidence for positive selection	14
Discussion	15
Shared and unique patterns of expression and evolution of oxygen transport genes	16
Open questions	19
Conclusions	21
Figures	23
Tables	29
Chapter 2 - Convergent evolution of conserved mitochondrial pathways underlies repeated adaptation to extreme environments	35
Abstract	35
Introduction	36
Results and Discussion	39
Sulfide spring <i>P. mexicana</i> exhibit a resistant toxicity target	39
Sulfide spring <i>P. mexicana</i> can regulate mitochondrial H ₂ S through increased detoxification	39
Sulfide spring <i>P. mexicana</i> can maintain mitochondrial function in presence of H ₂ S	40
Convergence among <i>P. mexicana</i> populations is shaped by selection on de novo mutations and standing genetic variation	42
Convergent modifications of toxicity targets and detoxification pathways are evident at macroevolutionary scales	43
Conclusions	44
Methods	46
Background and hypotheses	46

Enzyme activity assays	50
Cytochrome c oxidase (COX) activity	51
Sulfide:quinone oxireductase (SQR) activity	53
In vivo measurement of endogenous H ₂ S with MitoA	54
Mitochondrial Function.....	57
Comparative genomics and local ancestry analysis	61
Comparative Transcriptomics	63
Figures	70
Chapter 3 - Molecular consequences of metabolic function: Does genetic variation predict physiological differences?	76
Abstract	76
Introduction.....	77
Methods	82
Study sites and fish care.....	82
Measuring activity of OxPhos and detoxification enzymes.....	82
Isolation of mitochondria.....	83
Measurement of enzyme activity	84
Mitochondrial respiration.....	85
Isolation of mitochondria.....	85
Mitochondrial coupling assay.....	86
Whole organism performance.....	86
Measuring aerobic scope.....	87
Measurement of critical oxygen tension	88
Statistical analyses	89
Results.....	90
OxPhos and SQR enzyme activity	90
Mitochondrial respiration.....	91
Whole organism metabolism	92
Discussion.....	92
Variation in OxPhos and detoxification enzyme activity across populations and H ₂ S exposure	93
Mitochondrial and organismal respiration	96
Maintenance of aerobic respiration under environmental stress.....	97
Conclusions.....	99
Figures	100
Tables.....	105
Chapter 4 - The role of plasticity in facilitating the colonization of extreme environments	113
Abstract.....	113
Introduction.....	114
Methods	120
Study sites and fish collection.....	120
H ₂ S exposure.....	120
RNA isolation and cDNA library preparation	121
Transcriptome assembly and gene annotation	121
Quantifying expression of orthogroups.....	122
Results and discussion	124

Species-specific responses to H ₂ S exposure	124
Adaptive plasticity as evidence for pre-adaptation to H ₂ S-rich environments	125
Maladaptive plasticity and post-colonization evolution	129
Future considerations	130
Conclusions.....	131
Figures	133
Tables.....	137
Chapter 5 - Synthesis	142
The predictability of biological processes	142
The role of environment in predicting evolutionary outcomes.....	143
Predicting the consequences of phenotypic variation	145
Convergent and nonconvergent patterns of evolution	147
Appendix A - Molecular evolution and expression of oxygen transport genes in livebearing fishes (Poeciliidae) from hydrogen sulfide rich springs	149
Appendix A Figures.....	149
Appendix A Tables	150
Appendix B - Convergent evolution of conserved mitochondrial pathways underlies repeated adaptation to extreme environments	156
Appendix B Figures	156
Appendix B Tables	165
Appendix C - The role of plasticity in facilitating colonization of extreme environments	174
Appendix C Tables	174
References.....	175

List of Figures

- Figure 1-1: Phylogenetic relationships and collection localities of focal lineages of poeciliid fishes that have colonized H₂S-rich environments, along with relevant reference lineages from non-sulfidic habitats. A. Phylogeny of lineages included in analyses of expression variation and evolution of oxygen transport genes. Lineages from H₂S-rich environments (S) are underlined, lineages from non-sulfidic lineages are designated as NS. Asterisks indicate bootstrap support $\geq 99\%$. B. Location of collection sites in the US, Mexico, and the Dominican Republic. C. Detailed view of collection localities in Southern Mexico, which harbors the highest diversity of sulfide spring fishes. Roads (black lines) and major towns (shaded areas) are included for orientation. Note that yellow symbols correspond to sulfidic sites, blue symbols to non-sulfidic sites. Numbers correspond to lineages as listed in Table 1..... 23
- Figure 1-2: Overall expression levels of focal genes across all lineages investigated. Overall expression levels (\log_{10} -transformed) of focal genes (one myoglobin gene and eleven hemoglobin genes) across all lineages investigated. Boxes cover the first through third quartile of the data; vertical black lines indicate the median. Open diamonds indicate the mean for each group, and closed dots indicate outliers. 24
- Figure 1-3: Results of EVE analyses testing for gene expression differences between sulfidic and non-sulfidic lineages overall, as well as in specific lineages that have colonized sulfidic environments. Depicted are empirical LRT_{θ} distributions for each comparison, including LRT_{θ} values for background genes (gray) and oxygen-transport genes (red). The vertical red line represents the top 5% cut-off value; i.e., genes with LRT_{θ} values above this line are considered having significant evidence for an expression shift in the focal lineage. 25
- Figure 1-4: Lineage-specific expression variation for oxygen-transport genes with significant evidence for expression shifts associated with the colonization of H₂S-rich environments as established by EVE. Non-sulfidic lineages are in blue, sulfidic lineages in yellow, and lineages with significant expression shifts are highlighted with asterisks (also see Table 2). Boxes cover the first through third quartile of the \log_{10} -transformed expression levels of each lineage; vertical black lines indicate the median. Open diamonds indicate the mean for each group, and closed dots indicate outliers. The phylogenetic trees depict the evolutionary relationships across lineages; numbers correspond to lineage IDs in Table 1..... 26
- Figure 1-5: Amino acid sequence alignment of HEMOAA, which had significant evidence for selection on specific codons based on a branch-site test in codeml (see Table 4). Highlighted in red are amino acid positions that exhibited evidence for positive selection based on a Bayes Empirical Bayes (BEB) analysis (position 73, probability of 0.996; position 143, probability of 0.989). Amino acid substitutions in sulfidic lineages are highlighted in bold; substitutions with significant functional effects based on Provean analyses are underlined. 27
- Figure 1-6: Amino acid sequence alignment of HEMOBAL, which had significant evidence for selection on one codon based on a branch-site test in codeml (see Table 4). Highlighted in red is the amino acid position that exhibited evidence for positive selection based on a Bayes Empirical Bayes (BEB) analysis (position 26, probability of 0.954). Amino acid substitutions in sulfidic lineages are highlighted in bold; substitutions with significant functional effects based on Provean analyses are underlined. 28
- Figure 2-1: A. Physiological pathways associated with H₂S toxicity and detoxification are located in the inner mitochondrial membrane. H₂S inhibits OxPhos (orange enzymes) by

binding to COX (Complex IV). H₂S can be detoxified through the nuclear-encoded SQR (green enzyme) and additional enzymes (indicated by asterisks). **B.** Relative activity of COX upon H₂S exposure, which was primarily explained by an interaction between habitat type of origin and ambient H₂S concentration (Tables S2-S3). **C.** Activity of SQR as a function of H₂S concentration, which was explained by an interaction between habitat type of origin and H₂S concentration (Tables S4-S5). **D.** Relative change in mitochondrial H₂S concentrations in the liver of live fish exposed to different levels of environmental H₂S. Variation in mitochondrial H₂S levels were explained by habitat type of origin and exogenous H₂S concentration (Tables S6-S7). **E.** Relative spare respiratory capacity of isolated liver mitochondria at different levels of H₂S. The interaction between habitat type of origin and drainage of origin best explained variation in spare respiratory capacity (Tables S11-S12). For all graphs, yellow colors denote *P. mexicana* from H₂S-rich habitats, blue from nonsulfidic habitats. Symbols stand for populations from different river drainages (■: Tac; ▲: Puy; ●: Pich; see Figure S1). 70

Figure 2-2: **A.** Phylogeny of different population in the *P. mexicana* species complex (with *P. reticulata* as an outgroup) based on genome-wide SNPs. Colors indicate sulfidic (yellow) and nonsulfidic (blue) lineages. **B.** Local ancestry patterns around genes encoding two enzymes involved in H₂S detoxification, *SQR* and *ETHE1*. Gray bars represent the local ancestry pattern (cactus) associated with each region. Unrooted trees represent local ancestry relationships, with sulfidic lineages colored in yellow and nonsulfidic lineages in blue. Cacti 10 and 19 show clear clustering by ecotype. In cacti 1, 5, and 12, four of five sulfidic individuals cluster together. 72

Figure 2-3: **A.** Multidimensional scaling (MDS) plot of overall gene expression patterns across 20 lineages of poeciliid fishes. Black lines represent phylogenetic relationships among lineages; color represents habitat type of origin (yellow: sulfidic; blue: nonsulfidic). **B.** Expression variation of 186 genes with evidence for convergent expression shifts (*z*-transformed FPKM). Colors represent expression levels as indicated by the scale. The neighbor-joining tree on the left organizes species based on expression similarity. The cladogram on the right shows the phylogenetic relationship among lineages. Pictures on the side are examples of sulfide spring fishes (from top to bottom): *X. hellerii*, *P. bimaculatus*, *G. holbrooki*, *G. sexradiata*, *G. eurystoma*, *P. latipinna*, *P. sulphuraria* (Pich), *P. mexicana* (Tac), *P. mexicana* (Puy), and *L. sulphurophila*. **C.** MDS plot of the expression of 186 genes with evidence for convergent expression shifts. **D.** Boxplot with mean expression levels of different components of the SQR pathway across lineages from sulfidic (yellow) and nonsulfidic (blue) habitats. 73

Figure 2-4: Amino acid differences in *COX1* and *COX3* between lineages from sulfidic (yellow) and nonsulfidic (blue) habitats. Derived amino acids are shown in red. Bold letters indicate codons with convergent amino acid substitutions in different clades (separated by black horizontal lines) of sulfide spring fishes. 75

Figure 3-1: Relative enzyme activity of OxPhos enzymes from sulfide-tolerant (yellow) and intolerant (blue) populations of *Poecilia mexicana* from two independent lineages (▲: Tac; ●: Puy). **A.** Relative activity of Complex I along a gradient of H₂S exposure was best explained by the interaction between habitat of origin, drainage of origin, and H₂S concentration (Table 3-2). **B.** The relative enzyme activity of Complex II was primarily explained by the three-way interaction between habitat of origin, drainage of origin, and ambient H₂S concentration (Table 3-2). **C.** Complex III activity was best explained by the

two-way interaction between drainage of origin and H₂S (Table 3-2). D: The relative activity of. Complex IV (COX) was primarily explained by both H₂S and an additive effect of H₂S and drainage of origin (Table 3-2). 100

Figure 3-2: SQR enzyme activity in sulfide-tolerant (yellow) and intolerant (blue) populations of *P. mexicana* from two independent drainages(▲: Tac; ●: Puy). SQR activity was best explained by ambient H₂S and an additive effect of habitat of origin and H₂S concentration (Table 3-2)..... 101

Figure 3-3: Measures of mitochondrial (A-C) and organismal (D-F) respiration collected from sulfide-tolerant (yellow) and intolerant (blue) populations of *P. mexicana* in the absence of H₂S. A. Variation in the basal respiration of mitochondria was best explained by an interaction between habitat of origin and drainage of origin (Table 3-3). B. Measures of maximal mitochondrial respiration indicated variation was best explained by a two-way interaction between habitat of origin and drainage of origin (Table 3-3). C. Spare respiratory capacity, which is the difference between maximal and basal respiration rates, exhibited similar patterns of variation explained by the interaction between habitat and drainage of origin (Table 3-3). D. No variation was observed in standard metabolic rate (Table 3-4). E. Maximum metabolic rate did not exhibit any variation across habitats or drainages and was best explained by the null model (Table 3-4). F. Absolute aerobic scope, which is the difference between standard and maximum metabolic rates, was best explained by the null model (Table 3-4)..... 102

Figure 3-4: Critical oxygen tension (P_{crit}) of sulfide-tolerant (yellow) and intolerant (blue) populations of *P. mexicana*. Habitat of origin primarily explained the variation observed in P_{crit} (Table 3-4)..... 104

Figure 4-1: Conceptual framework detailing the three potential categories of gene expression responses to H₂S exposure in ancestral populations of fish compared to locally adapted populations of sulfide-tolerant *Poecilia mexicana* (optimal expression levels). A. In this scenario, optimal gene expression does not differ between ancestral and derived populations. Upon exposure to H₂S, these genes may exhibit no plasticity and remain equal in expression, or they may exhibit maladaptive plasticity in freshwater populations due to the presence of expression variation that is lacking in locally adapted populations. B. This scenario considers that there are expression differences between ancestral and derived populations. Under these conditions, we can identify evidence of adaptive plasticity if exposure to H₂S results in similar expression profiles between freshwater ancestors and locally adapted sulfide-tolerant populations. Alternatively, we can identify a lack of plasticity, in which gene expression does not change upon exposure to H₂S, or maladaptive plasticity, in which plasticity drives expression variation in the opposite direction predicted by patterns observed in adapted populations. C. A visualization of our predicted results, in which species with a derived sulfidic ecotype will exhibit evidence for adaptive plasticity (green arrows), while species that did not successfully colonize sulfide springs will exhibit for a lack of plasticity or maladaptive plasticity (red lines)..... 133

Figure 4-2: MDS plot visualizing the change of gene expression in each species upon exposure to H₂S. The center point represents expression under control conditions, and each outward point represents the lineage-specific expression profile upon exposure. Unsuccessful species are represented by blue lines and successful species are represented by orange lines. 135

Figure 4-3: Relative gene expression patterns within the three potential categories of plasticity. Blue boxes indicate unsuccessful colonizing species and yellow boxes indicate successful

colonizing species. There was no statistically significant difference across measures of
plasticity..... 136

List of Tables

Table 1-1: List of lineages from sulfidic and non-sulfidic habitats included in this study. The table provides descriptions of the collection localities, information about the presence or absence of H ₂ S, latitude and longitude, as well as the number of individuals (<i>N</i>) collected from each site.	29
Table 1-2: List of focal oxygen transport genes investigated in this study, including eleven hemoglobin genes and one myoglobin gene. The table includes the gene ID from the <i>X. maculatus</i> reference genome annotation file (XM ID), the accession ID, percent sequence similarity, and <i>E</i> -value from the top BLAST hit in Swiss-Prot. The table also contains the results of branch tests that evaluated shifts in gene expression associated with the colonization of H ₂ S-rich habitats as implemented in EVE. We list the likelihood ratio test statistic (LRT _θ) for all sulfidic lineages combined (overall) as well as for each sulfidic lineage individually. Genes with evidence for divergence in expression are highlighted in bold.	31
Table 1-3: Results of branch tests evaluating differences in non-synonymous to synonymous amino acid substitution rates (ω) between non-sulfidic and sulfidic lineages. Branch test models ($\omega_{NS} \neq \omega_S$) were evaluated against a null model ($\omega_{NS} = \omega_S$) using a likelihood ratio test, and we present the log-likelihoods ($\ln L$) for each model, the test statistic ($2\Delta \ln L$), and the corresponding <i>P</i> -value. In addition, we provide ω of the null model or separate estimates of ω for non-sulfidic and sulfidic lineages, depending on which model was supported. Genes with evidence for $\omega_{NS} \neq \omega_S$ are highlighted in bold.	33
Table 1-4: Results of branch-site tests evaluating positive selection on specific codon between sulfidic and non-sulfidic lineages. Branch-site models were evaluated against a null model using a likelihood ratio test, and we present the log-likelihoods ($\ln L$) for each model, the test statistic ($2\Delta \ln L$), and the corresponding <i>P</i> -value. Genes with evidence for significant branch-site models are highlighted in bold.	34
Table 3-1: Predictions for the plasticity of OxPhos enzyme activity in the presence of H ₂ S and the evolution of enzyme activity in sulfide-tolerant lineages of <i>Poecilia mexicana</i> based on biochemical studies of OxPhos function and previously collected data from wild-caught individuals.	105
Table 3-2: Results of mixed-effect linear models analyzing absolute variation of OxPhos enzyme activity under control conditions and relative activity under H ₂ S exposure. Models are ordered based on dAICc values. Models in bold exhibit a dAICc < 2.	108
Table 3-3: Results of mixed-effect linear models analyzing variation in basal respiration, maximal respiration, and spare respiratory capacity of mitochondria. Models are ordered based on dAICc values. Models in bold exhibit a dAICc < 2.	111
Table 3-4: Results of mixed-effect linear models analyzing variation in the standard metabolic rate, maximum metabolic rate, absolute aerobic scope, and critical oxygen tension of whole fish. Models are ordered based on dAICc values. Models in bold exhibit a dAICc < 2.	112
Table 4-1: List containing the species name, family, colonizing success, and sample size for each treatment used for comparative transcriptomics analyses.	137
Table 4-2: Descriptive sequencing and mapping statistics for each species and treatment. All numbers represent means (\pm standard deviation).	138

Table 4-3: Comparisons between control and H₂S exposed individuals within species were used to identify lineage-specific and universal trends of orthogroup expression plasticity induced by H₂S toxicity. Additionally, comparisons between the expression profiles of exposed individuals and wild-caught sulfidic *Poecilia mexicana* were used to identify patterns of plasticity. For each species, we provide the number of up and downregulated orthogroups and the number of orthogroups exhibiting adaptive, maladaptive, or a lack of plasticity. Underlined values indicate the number of shared orthogroups within the group comparisons. 139

Table 4-4: List of universally upregulated genes in successful and unsuccessful ancestors. Included are the orthogroup ID, the accession number associated with the top BLAST hit, the gene name, the protein name, and the E-value..... 140

Acknowledgements

Land Acknowledgement

Kansas State University is founded on the ancestral lands of the Kaw People, and Kansas is currently home to four tribal nations: the Iowa, Kickapoo, Prairie Band Pottawatamie, and Sac and Fox. These nations and others were displaced by white settlers and colonizers who forcibly took their lands, and the work we conduct at Kansas State would not be possible without the sacrifice these individuals were forced to make. Therefore, Kansas State University and the work conducted at this institution are rooted in white colonialism, and I acknowledge that the research conducted in this dissertation took place on stolen land. We must all actively consider our role in perpetuating this colonial history and work to dismantle the system that white colonizers have built to establish a truly diverse and equitable future.

Personal Acknowledgements

I would like to first thank my advisor Michi Tobler for both supporting my wildest ideas and keeping me grounded throughout the pursuit of my doctoral degree. Michi provided advice and guidance in all aspects of my research, teaching, and life over the last five years, and I will always be incredibly thankful for his patience. Additionally, Michi recognized my passion for teaching and science communication, and he found and created opportunities for me to explore both of these avenues throughout my graduate career, which was an incredible experience and something I will always value in him as a mentor. I appreciate the friendship we have developed, and I look forward to our future collaborations and discussions regarding research and education.

I thank all of my committee members: Ted Morgan, Alice Boyle, and Kevin Brix. I appreciate their feedback and guidance that helped in my development as a scientist. In addition

to my committee, I also received extensive training and guidance from Joanna Kelley, and I appreciate her advice and guidance during my bioinformatics training over the last few years.

If you are familiar with my experience at KSU, you know that teaching and learning has been at the forefront of my professional development. I had the pleasure of teaching both organismic biology and ichthyology, and I want to thank all of my amazing students from over the years. Additionally, I would like to thank the members of the Division of Biology who I was lucky enough to teach with: Chu, Sam, CC, Caitlin, Bryan, and Emily. I am lucky to have been able to teach both amazing students and work with great people.

I owe thanks to the many members of the Tobler Lab that I have been lucky enough to have worked with over the last few years: Henry Camarillo, John Coffin, Zach Culumber, Bryan Frenette, Ryan Greenway, Garrett Hopper, Rachel McNemee, Nichole Nieves, Courtney Passow, and Libby Wilson. An eclectic bunch, these individuals provided much needed friendship, guidance, and support. I'd like to especially thank Nichole for helping me develop my own philosophies as a mentor and for being an incredibly amazing and resilient undergraduate researcher, Courtney for welcoming me to Kansas State and continuing to be a great friend, and Libby Wilson for quickly becoming one of the best friends I have ever known. I also had the privilege of meeting some amazing people at KSU who did not belong to the lab: Joel, Elsie, Sam, CC, Bliss, and Dustin. These humans were always there if I needed support, someone to listen to me rant about my issues with the American education system, or a friend to grab a beer. I wish them all the best of luck!

Without the unconditional support of my mother and sister, there is little doubt that completing my graduate career would have been as possible. I appreciate their understanding of my inability to travel home as frequently as I had previously, and I am thankful that they have

always been a phone call away when I needed to talk. My sister passed away two weeks after I completed my comprehensive exams, but I will never forget how important she was to my pursuit in science and a graduate degree in general. I am also thankful for my niece and nephews Joanna, Edward, and Hudson. They are bright lights and constant reminders of how important family can be.

I cannot dole out appreciation without mentioning my partner over the last five years, Clayton Kistner. We arrived in Manhattan at the same time, and I am very grateful to have met you that first semester. Graduate school is not easy, and Clayton was always there to remind me that my imposter syndrome did not deserve to get the best of me, that I am responsible for my own accomplishments, and that it is okay to take breaks now and then. Thank you so much for all that you've done and all that you continue to do.

This research would not have been possible without the support of Centro de Investigación e Innovación para la Enseñanza y Aprendizaje (CIIEA), the communities of Teapa and Tapijulapa, Villa Luz Nature Park, local landowners, and Dr. Lenin Arias-Rodriguez. These groups and individuals provided access to research spaces and study locations, and I am thankful to have been able to work with them while conducting my research.

Lastly, I would like to acknowledge the societies and agencies that funded my research; the National Science Foundation, the Army Research Office, the Society for Integrative and Comparative Biologists, the American Genetics Association, the Department of Education, the Kansas State University Graduate Student Council, the Kansas State University College of Arts and Sciences, and the Division of Biology at Kansas State University.

Dedication

I would like to dedicate this work to Janice Barts (my mother), Kayla Goscinski (my sister), and my niece and nephews. My sister encouraged me to pursue a PhD and supported me throughout the process, and although she passed away before I completed my dissertation, I know that she would be ecstatic to see me complete my graduate career.

Preface

Identifying whether and under what circumstances evolution is predictable remains a major goal of evolutionary biology (1-5). Convergent evolution is often cited as an example of the predictability of evolution, as there is evidence for convergence of organismal phenotypes across broad phylogenetic and environmental scales (6-9). Investigating the scenarios in which similar phenotypes evolve by similar mechanisms may shed light into the role of constraint in adaptation and facilitate the predictability of evolutionary change (2). Much of this research has emphasized the convergence of morphology in response to similar selective regimes, but little is known about the convergence of genetic, biochemical, and physiological mechanisms of adaptation in natural populations (2, 5, 8, 9). In particular, identifying the predictability of evolution in respect to physiological traits presents a challenge, as these complex phenotypes are the result of many interacting genetic and biochemical pathways that may evolve in many different ways (2). Therefore, in order to elucidate the predictability of physiological trait evolution, it is necessary to 1) identify the mechanisms linking genotype to phenotype to assess the consequences of molecular variation on physiological function and 2) conduct comparative analyses to identify if organisms inhabiting similar selection regimes overcome environmental stress using similar or unique mechanisms.

Extreme environments provide ideal systems to explore the physiological mechanisms of adaptation and the predictability of evolution (10, 11). These habitats are characterized by the harsh physiochemical stressors that are lethal to most organisms. The selection regimes within extreme environments are clearly defined, allowing for hypotheses-driven tests assessing the effects of selection on traits across biological levels of organization (12, 13). Another advantage of studying extreme environments is the ability to identify adjacent benign habitats in which

ancestral, non-extremophile lineages live (12). These benign and extreme habitat pairs often occur in a replicated fashion, which facilitates comparative analyses among independent evolutionary lineages and facilitates analyses of convergent evolution (12).

Freshwater springs rich in hydrogen sulfide (H₂S) are among the most extreme aquatic habitats (14). H₂S is a naturally occurring toxin that imposes biochemical constraints on organismal energetics, making it lethal to many metazoans at even micromolar concentrations (13-15). The primary toxicity target of H₂S is cytochrome c oxidase (COX; complex IV of the mitochondrial respiratory chain), in which the molecule reversibly binds to COX and disrupts mitochondrial respiratory function (16). Additionally, H₂S is known to bind to respiratory proteins, such as hemoglobin and myoglobin, which disrupts the ability of these proteins to transport oxygen to tissues necessary for carrying out aerobic respiration and sulfide detoxification (17). Not only does H₂S disrupt physiological function of oxygen-dependent pathways, but it also competitively consumes oxygen in the environment via oxidation reactions and results in environmental hypoxia (14, 18). Therefore, to survive in H₂S-rich environments, organisms must be able to increase the ability to acquire oxygen from their environment, effectively regulate internal H₂S concentrations by increasing detoxification efficiency, mitigate the toxicity of H₂S by preventing the inhibition of mitochondrial respiration and oxygen transport, and/or behaviorally avoid high concentrations of H₂S (14, 15). Previous investigations into the mechanisms of adaptation to chronic H₂S exposure reveal an important role of detoxification; however, these studies rely on comparisons of distantly related organisms (e.g., lugworms vs. rats) (19-21). Given the suite of alternative mechanisms potentially facilitating adaptation to H₂S-rich habitats, it is necessary to make comparisons in closely related organisms inhabiting sulfidic and non-sulfidic environments (22).

Livebearing fishes within the family Poeciliidae provide an ideal study system to explore the mechanisms of adaptation and the predictability of evolution in response to inhabiting H₂S-rich environments. Within this family of fishes, ten lineages—including species from multiple genera—have independently colonized shallow sulfidic springs across Latin America and the Caribbean (23, 24). Much research investigating adaptation to these extreme environments has focused on the *Poecilia mexicana* species complex from Southern Mexico. *Poecilia mexicana* has independently colonized H₂S-rich environments on three occasions, and sulfidic and non-sulfidic populations are known to differ in a number of traits that are largely convergent across sulfidic populations (25, 26). Morphological (25, 27, 28) and behavioral (29) evolution is well-documented across habitats, and recent work is beginning to highlight the genetic and physiological mechanisms underlying adaptation to these environments (22, 24, 30-34). The results of these studies highlight differences that exist at the genetic and organismal levels, but the functional mechanisms linking the variation observed at these two biological scales remains unknown.

My dissertation seeks to provide novel insights into the physiological mechanisms underlying adaptation to extreme environments and the predictability of evolution of physiological traits. Using a comparative approach, I leveraged the existence of sulfide-tolerant and intolerant species to focus on four objectives.

Chapter 1: It is hypothesized that the predictability of molecular evolution increases when organisms inhabit an environment that constrains the number of solutions to the same evolutionary problem (1). H₂S toxicity dramatically influences the functionality of a number of physiological pathways, including oxygen transport (13, 15). H₂S reversibly binds the porphyrin ring of both hemoglobin and myoglobin, resulting in the formation of sulfhemoglobin and

sulfmyoglobin (17). These proteins suffer reduced oxygen-binding affinity and may result in their overall inability to function in oxygen transport (35). I tested if the constraints imposed by H₂S on oxygen transport function results in predictable shifts in gene expression and molecular evolution in ten independent lineages of sulfide-tolerant poeciliids using a phylogenetic comparative approach (24).

Chapter 2: Investigations into the mechanisms underlying adaptation to H₂S-rich environments have identified a number of genetic differences that exist between sulfide-tolerant and intolerant species (13); however, little is known about the functional consequences of that genetic variation. As part of a large collaborative effort, we were able to identify macroevolutionary patterns in the H₂S detoxification and oxidative phosphorylation pathways across sulfidic lineages of poeciliids (36). I assessed the functional consequences of this genetic variation by measuring variation in enzyme activity as a function of H₂S concentration and the ability to regulate internal H₂S concentrations in three sulfidic and non-sulfidic population pairs of *P. mexicana* (36).

Chapter 3: A major goal of comparative physiology is to identify the mechanisms that link genotypic variation to differences in organismal phenotypes (37, 38). Frequently, studies invoke that patterns of genetic variation have predictable consequences on function at higher levels of biological organization; however, tests investigating these assumptions have identified this is often not the case (38, 39). Genetic variation has been identified in a number of genes associated with aerobic metabolism and H₂S detoxification in sulfidic populations of *P. mexicana* (22, 36). I assessed oxidative phosphorylation and detoxification enzyme activity, mitochondrial respiration, and organismal respiration to test if genetic variation within these pathways has

resulted in identifiable differences in metabolic function between habitats and lineages of *P. mexicana*.

Chapter 4: A primary goal of evolutionary biology is to identify the origin of adaptive traits, which remains a challenging task due to the inability to turn back time and measure phenotypes at evolutionarily important events (40, 41). Therefore, it is often necessary to identify systems in which relatively recent divergence has occurred in organisms inhabiting native and non-native environments, as this allows scientists to assess variation that exists between the same or closely related species exposed to native and novel selection regimes (42-45). Invasion and evolutionary biologists have identified two primary mechanisms facilitating the successful colonization of novel environments: 1) post-colonization adaptation or 2) pre-adaptation (46). Post-colonization mechanisms mediating adaptation to H₂S-rich springs are well known, and some are described in Chapters 1-3. However, little is known about whether pre-adaptations may have facilitated success in these extreme environments initially. Using a comparative transcriptomics approach, I measured gene expression responses to H₂S exposure in nine species of fish from three families who differed in their success of colonizing H₂S-rich habitats. I then compared gene expression identified in our study to previous data that identified gene expression differences in locally adapted populations of sulfide-tolerant fish to test if gene expression plasticity may serve as a pre-adaptation to surviving in sulfidic habitats.

Synthesis and future research

Defining the circumstances in which evolution is predictable remains a critical goal of evolutionary biology (1), and despite advances in determining what drives predictable evolution at the organismal level, little is known about what processes influence the predictability at lower

biological levels of organization (1, 2, 5). In chapters 1 and 2, I found evidence that convergent molecular evolution and shifts in gene expression occurred in physiological pathways predicted to be targeted by selection in H₂S-rich environments (24, 36). H₂S readily binds to both oxygen transport proteins (17, 35) and cytochrome c oxidase (COX) (16), rendering them non-functional, and enzymatic reactions driven via the sulfide:quinone oxidoreductase (SQR) pathway are the primary mechanisms for sulfide detoxification in most organisms (19, 21). I found that hemoglobin and myoglobin genes were predictable targets of selection and exhibit evolutionary shifts in gene expression across sulfide-tolerant poeciliids; however, the patterns of evolved differences were not consistent across groups (24). This mirrors patterns observed in the molecular evolution of COX, in which identified amino acid substitutions largely differed across lineages (36). Although modification of toxicity targets differs across lineages, phylogenetic shifts in gene expression of detoxification enzymes suggest that all sulfide-tolerant poeciliids rely on this mechanism to tolerate chronic H₂S exposure in the wild (36). Overall, my research found that molecular aspects of evolution becomes increasingly predictable when environments limit the evolutionary solutions available to overcome sources of selection.

Classical studies of adaptation assumed that evidence of genetic variation within candidate pathways likely impacts function at higher levels of biological organization. This issue has further been exacerbated by the advent of next-generation sequencing technology, which creates a cheap way to assess gene expression variation and is often used to infer physiological function. However, this same technology has allowed scientists to identify that genetic variation, both at the molecular and gene expression levels, does not necessarily confer consequences on function (38, 39). In Chapters 2 and 3, I sought out to identify if the genetic variation that exists within the oxidative phosphorylation and sulfide detoxification pathways had consequences on

physiological function at higher levels of biological organization. In wild-caught populations of *Poecila mexicana*, I identified that genetic variation resulted in observable functional differences across biological scales, such that sulfide-tolerant fish exhibited differences in physiological function at the enzymatic and cellular scales (36). Despite the evidence for selection acting on oxidative phosphorylation and detoxification pathways, I found that the metrics of metabolic physiology measured in Chapter 3 did not exhibit obvious functional consequences due to these changes as were observed in Chapter 2.

We found that as levels of biological scale increased, it became more difficult to identify variation in metabolism. Overall, these results indicate that the consequences of genetic variation may be predictable when it occurs in predictable targets of selection; however, the ability to predict the consequences of variation becomes increasingly difficult at higher levels of organization, likely due to the complexity of interactions that occur at larger biological scales.

In the pursuit of identifying the mechanisms that underly adaptation, much research has focused primarily on how organisms respond upon exposure to novel sources of selection. Because of this, little is known about the mechanisms that initially facilitate colonization of novel environments (46). Invasion biologists have identified that pre-adaptations often play a role in the ability of a species to become invasive within non-native ranges, and I hypothesized that pre-adaptations in candidate physiological pathways may allow some species to persist under extreme environmental conditions. In Chapter 4, I compared gene expression between sulfide-tolerant *P. mexicana* and the ancestral populations of successfully colonizing species, and I identified several genes associated with H₂S detoxification, metabolism, and ion transport that may have initially been necessary to colonize H₂S-rich habitats. The results of this study

highlight the importance of assessing pre- and post-colonization mechanisms facilitating colonization of extreme environments.

Overall, my research has implications for understanding the predictability of evolution and the mechanisms underlying adaptation to extreme environments. I identified that evolution may indeed be predictable when organisms inhabit environments imposing large constraints on physiological or biochemical function. Many studies examining the mechanisms of adaptation focus on a single biological scale; however, my research sought to bridge the gap that exists between genotypes and phenotypes of organisms. In the presence of environmental constraints, genetic variation seems to allow for increased predictability of physiological function, as was the case considering modification of toxicity targets and detoxification mechanisms. The consequences of variation become increasingly difficult to identify at higher levels of biological organization, however, and this is likely due to complex interactions between other biochemical and physiological pathways. My research, as that of many others interested in adaptation, focused largely on post-colonization adaptations, but I was also able to identify that pre-adaptations may similarly play important roles in facilitating persistence in novel habitats. Pre-adaptations may be necessary to initially invade new environments, and this has important implications for considering the mechanisms facilitating species distributions and predicting what traits may be subject to selection upon exposure to new selection regimes. Future studies should address the role pre-adaptations play in facilitating colonization and adaptation to other environments and at larger evolutionary scales.

Chapter 1 - Molecular evolution and expression of oxygen transport genes in livebearing fishes (Poeciliidae) from hydrogen sulfide rich springs

Nick Barts, Ryan Greenway, Courtney N. Passow, Lenin Arias-Rodriguez, Joanna L. Kelley, and Michael Tobler

Abstract

Hydrogen sulfide (H₂S) is a natural toxicant in some aquatic environments that has diverse molecular targets. It binds to oxygen transport proteins, rendering them non-functional by reducing oxygen-binding affinity. Hence, organisms permanently inhabiting H₂S-rich environments are predicted to exhibit adaptive modifications to compensate for the reduced capacity to transport oxygen. We investigated 10 lineages of fish of the family Poeciliidae that have colonized freshwater springs rich in H₂S—along with related lineages from non-sulfidic environments—to test hypotheses about the expression and evolution of oxygen transport genes in a phylogenetic context. We predicted shifts in the expression of and signatures of positive selection on oxygen transport genes upon colonization of H₂S-rich habitats. Our analyses indicated significant shifts in gene expression for multiple hemoglobin genes in lineages that have colonized H₂S-rich environments, and three hemoglobin genes exhibited relaxed selection in sulfidic compared to non-sulfidic lineages. However, neither changes in gene expression nor signatures of selection were consistent among all lineages in H₂S-rich environments. Oxygen transport genes may consequently be predictable targets of selection during adaptation to sulfidic

environments, but changes in gene expression and molecular evolution of oxygen transport genes in H₂S-rich environments are not necessarily repeatable across replicated lineages.

*Published as: Barts, N., et al. (2018). "Molecular evolution and expression of oxygen transport genes in livebearing fishes (Poeciliidae) from hydrogen sulfide rich springs." *Genome* **61**(4): 273-286.

Introduction

Whether and under what circumstances evolution is repeatable and predictable remains a core question in biology. Phenotypic convergence is frequently invoked as evidence for the repeatability and predictability of evolution (6, 47, 48). Indeed, phenotypic convergence has been documented across broad phylogenetic scales and in response to a wide variety of sources of selection (7, 9, 49, 50). Nonetheless, convergent evolution is not ubiquitous, and disparate lineages can respond to shared evolutionary problems with unique adaptive solutions (51-53). Historical, ecological, genetic, and functional factors can all contribute to the degree of shared (convergent) versus unique (non-convergent) evolutionary changes that are observed when independent lineages are exposed to the same sources of selection (52, 54, 55). But even when phenotypic convergence is common, convergent functional outcomes frequently arise from non-convergent modifications at lower hierarchical levels of biological organization (1, 4), which suggests that multiple molecular changes can result in equivalent function and fitness (56). This begets questions about the circumstances under which we can actually anticipate convergent changes at a molecular level (5). Evolutionary repeatability and predictability at a molecular level may be particularly high if constraints limit the number of solutions that maximize fitness under given environmental conditions. Such constraints may be evident when populations are exposed to sources of selection with clear-cut biochemical targets and physiological

consequences (57). Indeed, some of the best examples of repeated modifications of the same molecular pathways—and even genes—come from systems that are exposed to physiochemical stressors. For example, killifish have repeatedly evolved loss of function mutations in aryl hydrocarbon receptor signaling pathway to cope with anthropogenic pollution in the form of aromatic hydrocarbons (58), exposure to secondary plant metabolites lead to the repeated modification of sodium–potassium pumps in insects (59), snakes have repeatedly evolved tetrodotoxin-resistant sodium channels to cope with prey toxicity (60), and poison frogs have repeatedly modified sodium channels to tolerate their own toxins (61). Consequently, natural systems in which selection is mediated by biochemically and physiologically explicit stressors provide excellent models to test for evolutionary repeatability and predictability at a molecular level.

Hydrogen sulfide (H₂S) is a naturally occurring toxicant with well-documented biochemical and physiological effects (62, 63). The primary toxic effect of H₂S is the cessation of aerobic respiration. H₂S readily and reversibly binds to the heme group of cytochrome *c* oxidase (COX, complex IV of the mitochondrial respiratory chain), inhibiting aerobic ATP production (16, 64). Hence, exposure to H₂S is lethal in micromolar concentrations for most metazoans (65, 66). Nonetheless, animals can enzymatically oxidize and detoxify H₂S at low concentrations through the highly conserved sulfide:quinone oxidoreductase (SQR) pathway (20). Organisms living in naturally H₂S-rich environments—such as deep sea hydrothermal vents, cold seeps, anoxic sediments, and freshwater sulfide springs—are consequently expected to either exhibit modifications of direct toxicity targets or enzymes associated with detoxification (14). Indeed, H₂S-resistant COX (67, 68) and modification of enzymes associated with the SQR pathway (22, 69-72) have been documented in various taxa.

Besides COX and detoxification enzymes, H₂S has a variety of other putative molecular targets (65, 73). In particular, H₂S can bind to heme proteins involved in oxygen transport, including myoglobin and hemoglobin (74). H₂S effectively reduces the porphyrin ring within the globin structure, forming sulfmyoglobin and sulfhemoglobin (75). Sulfmyoglobin and sulfhemoglobin are characterized by drastically reduced oxygen binding affinity, rendering them almost non-functional for oxygen transport (76, 77). Consequently, theory predicts that myoglobin and hemoglobin proteins are likely targets of adaptation to chronic H₂S exposure. Several marine invertebrates that inhabit H₂S-rich environments (e.g., the bivalve *Lucina pectinata* and the giant tubeworm *Riftia pachytila*) have evolved specialized heme proteins that function in H₂S binding and are critical for supplying symbiotic sulfur-oxidizing microbes with resources (78-80). In addition, a polychaete worm (*Methanoaricia dendrobranchiata*) that inhabits environments with low oxygen and high H₂S concentrations along hydrocarbon seeps exhibits hemoglobin with exceptionally high oxygen binding affinity and a pronounced Bohr effect (81). However, it largely remains untested whether hemoglobin and myoglobin are repeatable and predictable targets of selection across a diversity of lineages that have colonized H₂S-rich environments.

We investigated multiple lineages of fish of the family Poeciliidae that have independently colonized freshwater springs rich in H₂S in parts of North and Latin America, as well as the Caribbean (23). These sulfide springs exhibit continuously high concentrations of H₂S and low concentrations of oxygen (27). Fish populations in sulfide springs are locally adapted and characterized by divergence in complex phenotypic traits from ancestral populations in non-sulfidic environments (13, 82). Trait evolution in independent sulfide spring lineages is governed by patterns of convergence in molecular (22, 72), physiological (32, 68), morphological (83, 84),

and life history traits (85, 86). Furthermore, sulfide spring populations are often reproductively isolated from adjacent, non-sulfidic populations, even when physical barriers that prevent fish movement are absent (87, 88).

Here, we collected samples of sulfide spring poeciliids from a broad geographic and phylogenetic range (Fig. 1) to test whether evolution in H₂S-rich environments has led to the repeatable and predictable modification of oxygen transport genes. We sought to address two broad questions: (i) Is there evidence for potential shifts in the expression of myoglobin and hemoglobin genes associated with the colonization of H₂S-rich habitats? Both the presence of H₂S and the rampant hypoxia in sulfide springs could cause differential transcription of oxygen transport genes either plastically or through evolved changes in gene regulation. If H₂S reduces the functionality of hemoglobin and myoglobin in oxygen transport and storage (76, 77), organisms in sulfidic habitats may compensate through up-regulation of associated genes. Similarly, up-regulation of hemoglobins and myoglobin could also be related to an increased capacity for H₂S sequestration and oxidation that might mitigate toxic effects (89). Finally, variation in ambient oxygen concentrations have been documented to induce complex transcriptional changes in oxygen transport genes (90), and hypoxia can be associated with increased gene expression of hemoglobins and myoglobin (91-94). (ii) Is there evidence for positive selection on oxygen transport genes, and are there specific codons that have been the target of selection across different lineages of sulfide spring fishes? Selection on oxygen transport genes is expected to shape the proteins' oxygen binding affinity in a way that simultaneously optimizes oxygen uptake from the environment and its delivery to mitochondria in tissues where oxygen is consumed by aerobic metabolism. Selection may also act to shape the proteins' propensity to interact with allosteric effectors—like H₂S—that affect their function (95-

97). Theoretical considerations suggest that adaptive modifications of oxygen transport proteins should be restricted to specific amino acids that are involved in heme binding, inter-subunit contacts, or interaction with allosteric effectors, which collectively shape oxygen-binding affinity (56, 98). Hence, if there is positive selection on oxygen transport genes in H₂S-rich environments, we predict convergent modifications of specific codons in replicated lineages inhabiting sulfide spring environments. We addressed these questions by analyzing the expression levels and molecular evolution of hemoglobin and myoglobin genes in an explicit phylogenetic context, including 10 lineages from sulfide springs and 10 reference lineages from non-sulfidic habitats.

Materials and methods

Sample collection

To analyze variation in oxygen transport gene expression and evolution, we collected specimens from multiple lineages of poeciliid fishes that have independently colonized H₂S-rich springs in the United States, Mexico, and the island of Hispaniola, as well as from geographically and phylogenetically proximate lineages in non-sulfidic habitats (Fig. 1) (23). This approach led to sets of closely related lineages found in sulfidic and non-sulfidic habitats, including populations of *Poecilia latipinna* and *Gambusia holbrooki* in Florida; populations of the *Poecilia mexicana* species complex (including *Poecilia mexicana*, *Poecilia sulphuraria*, and *Poecilia limantouri*) (99), the *Gambusia sexradiata* species complex (including *G. sexradiata* and *Gambusia eurystoma*) (100), *Pseudoxiphophorus bimaculatus*, and *Xiphophorus hellerii* in Mexico; as well as populations of the *Limia perugiae* species complex (*L. perugiae* and *Limia sulphurophila*) (101) in the Dominican Republic (see Table 1 for localities

and habitat associations of specific lineages). Note that data for some lineages of the *P. mexicana* species complex were reanalyzed from a previous study (GenBank BioProject accession number: PRJNA290391) (22). In addition, we used published genomic data from *Xiphophorus maculatus* (for mapping of RNA-seq reads; GenBank accession number: AGAJ000000000.1) (102) and *Fundulus heteroclitus* (as an outgroup in phylogenetic analyses; GenBank accession number: JXMV000000000.1) (103).

All fish were caught using a seine (2 m × 5 m; 3 mm mesh size). Immediately upon capture, adult females ($N = 5\text{--}6$ per site; Table 1) were euthanized, and the gills were extracted from both sides of the body using sterilized scissors and forceps. Tissues were then preserved in RNAlater (Ambion Inc.) for subsequent analysis in the laboratory. We focused on gill tissues, because they are in direct contact with the toxic environment (14), mediate a variety of physiological processes involved in the maintenance of homeostasis (104, 105), and exhibit strong transcriptional responses upon exposure to H₂S (106, 107). Procedures for these experiments were approved by the Institutional Animal Care and Use Committee at Kansas State University (Protocol #3418).

RNA extraction, cDNA library preparation, and sequencing

The general protocols for RNA extraction, library preparation, and sequencing of all new samples closely followed procedures previously employed for *Poecilia* (22, 106). In brief, 10–30 mg of gill tissues from each individual were sealed in a Covaris TT1 TissueTube (Covaris, Inc., Woburn, Mass., USA), frozen in liquid nitrogen, and pulverized. Total RNA was extracted from pulverized tissue using the NucleoSpin RNA kit (Machery-Nagel, Düren, Germany) following the manufacturer's protocol. mRNA isolation and cDNA library preparation were conducted

using the NEBNext Poly(A) mRNA Magnetic Isolation Module (New England Biolabs, Inc., Ipswich, Mass., USA) and NEBNext Ultra Directional RNA Library Prep Kit for Illumina (New England Biolabs, Inc., Ipswich, Mass., USA) following the manufacturers' protocol with minor modifications. All cDNA libraries were individually barcoded (so that reads could be linked back to a specific individual), quantified using Qubit and an Agilent 2100 Bioanalyzer High Sensitivity DNA chip, and pooled in sets of 11–12 samples based on nanomolar concentrations. Samples were split into pools such that samples from different species and habitat types were sequenced together. Libraries were sequenced on an Illumina HiSeq. 2500 with paired-end 101 base pair (bp) reads at the Washington State University Spokane Genomics Core. Because of low coverage, some samples were re-sequenced, and reads from separate runs were combined for each sample for data analysis. There was no evidence for significant lane effects. After sequencing, all raw RNA-seq reads were sorted by barcode and trimmed twice (quality 0 to remove adapters and then quality 24) using the program Trim Galore! (v.0.4.0) (108). Trimmed reads were then mapped to the *X. maculatus* reference genome (102) using BWA-MEM (v.0.7.12) (109). Depending on the lineage, between 81.0% and 94.5% of reads mapped to the reference genome (mean \pm standard deviation: 87.9% \pm 3.8%). Note that mapping to an alternative reference genome (*Poecilia mexicana*) yielded qualitatively similar results (30), indicating that mapping biases among lineages did not play a major role in shaping analytical outcomes (results not shown).

Identifying focal and background genes

To identify focal genes, we extracted 11 hemoglobin and 1 myoglobin genes (Table 2) using the *X. maculatus* genome annotation file (GTF) (102). For a subset of individuals in each

population, the sequence for each gene was compared to the nr/nt database using BLASTn to confirm that the *X. maculatus* gene was within the set of top hits. For a subset of *P. latipinna* and *P. mexicana* individuals, each gene's sequence was compared to the respective available reference genomes (*P. latipinna* or *P. mexicana*) using BLASTn (Critical E-value: 0.001). The top hit in the respective genome was then compared with BLASTn back against the *X. maculatus* genome to confirm the best hit for each gene. To generate a background set for reconstructing phylogenetic relationships and conducting analyses of gene expression patterns, we also analyzed 171 genes representing functionally important, highly expressed loci for comparison with the focal oxygen transport genes (Table S1₂) (110, 111).

Variant detection and consensus sequence generation

To detect variants and generate a consensus, we used the Genome Analysis Toolkit (GATK, v.3.5) (112) on the mapped reads for indel realignment and variant detection (via the UnifiedGenotyper tool) across the coding regions of all samples simultaneously, following GATK best practices (113, 114). Individuals were genotyped on a per-population basis using the EMIT_ALL_SITES output mode in the UnifiedGenotyper, creating a *.vcf file for each population. A custom script was used to fill positions in each *.vcf file that were missing sequence data with Ns. For each *.vcf file, we used the setGT plugin to set all genotypes to the major allele and then created a consensus sequence across all individuals from each population with the consensus tool, as implemented in BCFtools (v.1.3) (109). The consensus sequences for the coding regions of each gene were combined, resulting in a single sequence file for each gene and population to be used in subsequent analyses. It is important to note that polymorphic sites identified in this manner are not necessarily fixed in a population, and differences between

closely related populations may be due to differences in major allele frequencies (see results for details).

Phylogenetic analysis

To establish a phylogenetic framework for subsequent analyses, we conducted phylogenetic analyses using the consensus sequences from 167 background genes (Table S12; note that four genes were excluded due to alignment issues). Individual genes were aligned using ClustalW (v.2.1) (115). We used jModelTest 2 (v.2.1.10) (116) to determine the best partition scheme based on the most likely model of DNA substitution among 88 candidate models, which was established by evaluating likelihood scores on a fixed BioNJ-JC tree under the Akaike Information Criterion (AIC) (Table S12). Genes were then concatenated and partitioned according to the substitution models indicated by jModelTest and then used in maximum likelihood (ML) analyses using RAxML (v.8.2.9) (117). We ran RAxML analyses under the Rapid Bootstrap Algorithm with 1000 bootstrap replicates and used a thorough maximum likelihood search with each partition assigned its own GTR + Γ + I model. The best scoring ML tree was utilized for subsequent analyses of gene expression variation and molecular evolution. These analyses recovered a robust hypothesis for evolutionary relationships among the focal taxa (bootstrap support generally $\geq 99\%$, Fig. 1) that was consistent with previous phylogenetic studies of the family Poeciliidae (99, 118, 119). The only groups with moderately supported relationships included the two populations of *G. sexradiata* and *G. eurystoma* (bootstrap support 60%, Fig. 1), which have previously been found to represent a complex of closely related and recently diverged species (100).

Evolution of gene expression

To describe variation in gene expression among lineages, we quantified the relative number of RNA-seq reads that mapped to our focal and background genes (measured as fragments per kilobase of transcript per million mapped reads, FPKM) using cufflinks (v.2.2.1) (120) on each sample. FPKM values for each gene were extracted using a custom script, leading to a measurement of gene expression for each individual ($N = 5-6$ per lineage; see Table 1).

Individual-level expression of focal and background genes were then used as dependent variables in Expression Variance and Evolution (EVE) models (121, 122), which implement Ornstein–Uhlenbeck models to conduct phylogenetic analysis of variance (ANOVA) to test for branch-specific shifts in gene expression associated with the colonization of H₂S-rich environments (122). EVE models explicitly test for branch-specific shifts in gene expression by comparing likelihoods associated with an expression shift parameter (θ_i) for a gene being shared between two sets of lineages versus θ_i being significantly different between them (122). We tested for branch-specific expression shifts in two ways: (i) We tested whether colonization of H₂S-rich habitats was consistently associated with gene expression shifts by contrasting θ_i between all sulfidic and all non-sulfidic lineages (i.e., $\theta_i^{\text{sulfidic}} \neq \theta_i^{\text{non-sulfidic}}$). (ii) We tested whether colonization of H₂S-rich habitats was associated with gene expression shifts in specific sulfidic lineages by contrasting θ_i between a foreground lineage (each sulfidic lineage as designated in Table 1) and all other lineages (i.e., $\theta_i^{\text{foreground lineage}} \neq \theta_i^{\text{other lineages}}$).

For statistical analyses, we calculated a likelihood ratio test (LRT $_{\theta}$) contrasting the null hypothesis (θ_i equal between groups) to the alternative hypotheses (θ_i unequal between groups) (122). To minimize issues of multiple testing, we avoided significance testing using χ^2 -tests for each gene as suggested by Rohlf and Nielsen (122). We instead generated empirical

LRT₀ distributions including both oxygen-transport and background genes, deeming shifts in the focal oxygen transport genes significant if their LRT₀ values were in the top 5% of all values.

Quantifying positive selection

To test for positive selection on the focal myoglobin and hemoglobin genes associated with the colonization of H₂S-rich environments, we used branch models as implemented in codeml of the PAML package (v.4.9) (123), which evaluate variation in the rates of non-synonymous to synonymous substitutions (ω) across the phylogeny. We created multispecies codon alignments for each of our focal genes with the “codon” option in PRANK (v.150803) (124). For analysis in codeml, lineages from H₂S-rich habitats were set as foreground branches, and lineages from non-sulfidic habitats were set as background (125). For each gene, we compared a branch model ($\omega_{\text{non-sulfidic}} \neq \omega_{\text{sulfidic}}$) to a null model ($\omega_{\text{non-sulfidic}} = \omega_{\text{sulfidic}}$). *P*-values were generated based on a maximum likelihood ratio test with a χ^2 approximation (126). In addition, we also conducted branch-site tests to evaluate evidence for positive selection on specific branches and codons (126, 127).

We used Protein Variation Effect Analyzer (PROVEAN, v.1.1.3) to test whether non-synonymous mutations in codons with evidence of positive selection are functionally important (128, 129). For PROVEAN analyses, we tested whether an amino acid substitution found in a sulfidic lineage occurs in a highly conserved region of the protein using the protein sequence of the most closely related non-sulfidic reference lineage as our query sequence and the amino acid substitution found in the sulfidic lineage as our variant, applying the default delta alignment score threshold of -2.5 for determination of potential functional effects.

Results

Focal oxygen transport genes

Our analyses recovered a single gene encoding for myoglobin and 11 genes encoding for hemoglobin subunits (Table 2), including six α - and five β -type subunits. Two of the α - (HEMOAA and HEMOAL2) and two of the β -type (HEMOBAL and HEMOBAL2) subunits of hemoglobin exhibited very high levels of gene expression across all taxa, which were orders of magnitude higher than the expression of the other hemoglobin genes (Fig. 2; Table S2₂). These findings are consistent with previous studies on hemoglobin gene evolution documenting widespread duplication of genes that give rise to functionally distinct heme proteins and whose expression varies depending on developmental stage and environmental conditions (130, 131).

Expression variation

Analysis of evolutionary patterns of gene expression with EVE revealed no evidence for significant shifts in gene expression between all sulfidic versus all non-sulfidic lineages (Table 2; Fig. 3). However, the expression of oxygen-transport genes shifted in a subset of sulfidic lineages. In three sulfidic lineages, there was evidence for a significant expression shift in a single gene: *G. eurystoma* shifted in the expression of *HEMOAL*, *L. sulphurophila* in *HEMOBIL*, and *P. mexicana* (Puyacatengo) in *HEMOESA2* (Table 2; Fig. 3). In *P. sulphuraria*, we detected significant expression shifts in five oxygen-transport genes, including myoglobin, the two top-expressed heme genes (*HEMOBAL* and *HEMOAA*), as well as two additional heme genes (*HEMOBIL2* and *HEMOADL*). In all documented cases, significant shifts were associated with increased levels of gene expression relative to other lineages (Fig. 4).

Evidence for positive selection

Analysis of molecular evolution based on branch models revealed evidence for different rates of non-synonymous to synonymous amino acid substitutions in sulfidic lineages ($\omega_{\text{non-sulfidic}} \neq \omega_{\text{sulfidic}}$) for two highly expressed hemoglobin genes (*HEMOAA* and *HEMOBAL2*; Table 3). In addition, branch-site models provided evidence for positive selection on specific codons in *HEMOAA* and *HEMOBAL* (Table 4).

HEMOAA exhibited evidence for positive selection at two codons (positions 73 and 143) with high support (probability >0.95 based on Bayes Empirical Bayes analysis; Fig. 5). Evidence for positive selection at position 73 was driven by a shift from glycine to alanine in the sulfidic lineage of *P. bimaculatus* as well as all sulfidic lineages in the *P. mexicana* species complex (*P. sulphuraria* and *P. mexicana* from the Puyacatengo and Tacotalpa river drainages). Analyses using PROVEAN suggested that these amino acid substitutions likely have neutral effects on protein function (PROVEAN scores between -1.913 and -1.640). The effect at position 143 was driven by sulfidic populations of *P. bimaculatus*, *G. eurystoma*, and *P. mexicana* (Puyacatengo) exhibiting a histidine instead of an arginine in all other lineages. PROVEAN results indicated that changes from arginine to histidine at position 143 have significant functional consequences (PROVEAN scores between -4.479 and -4.398). Note that the sites were fixed in *G. eurystoma*, *P. sulphuraria*, and *P. mexicana* (Tacotalpa); in *P. bimaculatus* and *P. mexicana* (Puyacatengo) the sites were at high frequency (allele frequencies between 0.8 and 0.9) in the sulfidic population.

HEMOBAL exhibited evidence for positive selection at one codon (position 26) with high support (Fig. 6). Codon position 26 is occupied by a proline in a majority of lineages and a glutamine in the others, and both variants occur in sulfidic and non-sulfidic populations.

Evidence for positive selection was primarily driven by a shift toward a glutamine in two sulfidic *P. mexicana* lineages (Tacotalpa: allele fixed; Puyacatengo: allele frequency of 0.9). PROVEAN results indicated that a shift from a proline to a glutamine has significant consequences for the function of heme proteins (PROVEAN score: -5.745).

Discussion

Organisms inhabiting environments with similar sources of selection provide an opportunity to investigate convergence in evolutionary adaptation, particularly when selection is strong, as in environments characterized by extreme physiological conditions. H₂S binds to oxygen transport proteins and drastically impedes their function by reducing their oxygen binding affinity.

Organisms inhabiting H₂S-rich environments are consequently predicted to compensate for the reduced capacity to transport oxygen, potentially leading to repeatable patterns of gene expression variation and molecular evolution. Our analyses of poeciliid fishes in sulfidic environments have revealed evidence for shifts in the expression of and positive selection on oxygen-transport genes. However, repeated changes in gene expression and evidence for positive selection was exceedingly rare and mostly restricted to a small number of sulfide spring lineages. Myoglobin and 7 of 11 hemoglobin genes exhibited evidence for significant up-regulation upon sulfide spring colonization, but all expression shifts were restricted to a single lineage (most of them in *P. sulphuraria*). Similarly, repeated positive selection was only found in *HEMOAA* (two codons) and *HEMOBAL* (one codon), and putatively adaptive amino acid substitutions at these codons were restricted to *P. bimaculatus*, *G. eurystoma*, and lineages within the *P. mexicana* species complex. Hence, neither changes in gene expression nor signatures of relaxed or positive selection were consistently present among all lineages in H₂S-rich environments, and

four lineages inhabiting sulfide springs (*X. hellerii*, *G. holbrooki*, *G. sexradiata*, and *P. latipinna*) exhibited no evidence for significant shifts in the expression of oxygen-transport genes or for positive selection on them. Hence, while first principles may suggest that oxygen transport genes are predictable targets of selection in sulfidic environments and there is indeed lineage-specific evidence supporting this prediction, modulation and modification of oxygen-transport genes are not necessarily repeatable across replicated lineages.

Shared and unique patterns of expression and evolution of oxygen transport genes

As predicted, our results indicated that life in H₂S-rich environments can elicit up-regulation of and drive positive selection on oxygen transport genes. However, few of the documented patterns were shared among evolutionarily replicated lineages, suggesting that they may contribute to the evolution of increased H₂S tolerance but are not required for it. Several non-mutually exclusive hypotheses can potentially explain the lack of consistent, convergent modulations and modifications of oxygen transport genes (see Kaeuffer et al. 2012 for a conceptual overview (52)).

(1) There may be variation in the nature and strength of selection across independent lineages of sulfide spring fish, which could explain the lack of consistency in evolutionary responses. In our analyses, we have treated the presence and absence of H₂S as a dichotomous variable, because all sulfide springs investigated here exhibit H₂S concentrations above what is considered acutely toxic for animals (86). Nonetheless, there is significant variation in H₂S concentrations even among geographically proximate sulfide spring complexes. For example, the Baños del Azufre in Mexico that harbor *P. sulphuraria* and *G. eurystoma* exhibit peak H₂S concentrations in excess of 1000 μM, while

nearby Mogote del Puyacatengo with *G. sexradiata* only reaches low double digits (83, 86, 132). Previous studies in the genera *Gambusia* and *Poecilia* have found that phenotypic divergence between adjacent sulfidic and non-sulfidic populations increased with average H₂S concentrations (133), highlighting the possibility that among-lineage variation in the modulation and modification of oxygen transport genes may be a function of unquantified environmental variation (also see Stuart et al. (134)). In addition, the presence of H₂S may also interact with hypoxia and other environmental factors to drive unique, lineage-specific adaptive solutions across the taxa we examined.

(2) Variation in evolutionary responses among different sulfide spring lineages may be a consequence of variation in the degree of divergence from non-sulfidic ancestors. Some sulfide spring populations (e.g., *P. sulphuraria*, *P. mexicana* from the Tacotalpa river drainage, *L. sulphurophila*, and *G. eurystoma*) exhibit low rates of gene flow with populations from adjacent non-sulfidic habitats (133, 135), and *P. sulphuraria* is considerably more divergent than other sulfidic lineages, having diverged over 200,000 years ago (68). Interestingly, *P. sulphuraria* was the only lineage exhibiting significant up-regulation of multiple oxygen-transport genes, and all of the older lineages were characterized by having at least one amino acid substitution at a codon with evidence for positive selection in *HEMOAA* and *HEMOBAL*. In other lineages (e.g., *P. latipinna*, *G. holbrooki*, *G. sexradiata*, and *X. hellerii*), population genetic differentiation is much lower (133), and they exhibit no evidence for differential expression or positive selection on oxygen transport genes. These observations may point toward a possible role of gene flow in preventing adaptive divergence between adjacent populations in sulfidic and non-sulfidic habitats (136). It is noteworthy though that some young lineages exhibit amino acid

substitutions in *HEMOAA* and *HEMOBAL* (*P. bimaculatus* and *P. mexicana* from the Puyacatengo drainage) and evidence for differential expression of hemoglobin genes (*HEMOESA2* in *P. mexicana* from the Puyacatengo river drainage).

(3) Variation in evolutionary responses among sulfide spring fish lineages may be a consequence of functional redundancy, where multiple molecular modifications lead to equivalent performance of organisms in H₂S-rich habitats. A recent study on birds indicated that high-altitude species consistently evolved hemoglobins with higher oxygen-binding affinity, yet amino acid substitutions underlying variation in oxygen-binding substantially varied among lineages (56). If there are multiple amino acid substitutions with equivalent functional consequences, we would expect widespread positive selection on hemoglobin genes, but not necessarily congruence in amino acid substitutions among lineages exposed to the same sources of selection. This could explain why we see elevated rates of non-synonymous to synonymous amino acid substitutions for *HEMOBAL2*, but no consistent substitutions among lineages. Lineage-specific branch tests indicated evidence for relaxed selection in *G. eurystoma*, *P. sulphuraria*, and *P. mexicana* (Tacotalpa), but potentially relevant amino acid substitutions have occurred at different codon positions (see supplementary Fig. S12), leaving the possibility that non-convergent changes of the same gene might confer similar benefits in presence of H₂S. Patterns of consistent selection on oxygen transport genes—yet at different loci and through different amino acid substitutions—have also been documented in weakly electric fishes exposed to chronic hypoxia (137).

Open questions

Our study uncovered evidence for differential expression of and positive selection on oxygen transport genes of fishes inhabiting H₂S-rich environments, but several key questions remain unaddressed. First and foremost, the functional consequences of the observed expression and amino acid sequence variation in hemoglobin genes remain unknown. Up-regulation of oxygen-transport genes in *P. sulphuraria* and positive selection inferred from branch-site models predominantly occurred in the hemoglobin genes that are consistently highly expressed across all lineages (see Fig. 2), suggesting that putative adaptive modulations and modifications have occurred at loci that are important for the acquisition and distribution of oxygen in adult fish. Assessment of functional consequences of amino acid substitutions at codons with evidence for positive selection indicated that the shift from a proline to a glutamine at codon position 26 of *HEMOBAL* as well as the shift from arginine to histidine at position 143 in *HEMOAA* should impact hemoglobin functionality. In the human homolog of *HEMOAA* (*HBA1*), the substitution of arginine to histidine causes an increase in oxygen binding affinity and a decrease in cooperativity and Bohr effect (138, 139). Thus, future research needs to explicitly test whether and how oxygen-binding affinity of hemoglobin varies among sulfidic and non-sulfidic lineages with evidence for non-synonymous amino acid substitutions. This is also required for assessing potential functional redundancies among different combinations of amino acid substitutions observed among sulfide spring lineages, especially in *HEMOBAL2*. Evaluating oxygen-binding affinities both in presence and absence of H₂S would further provide insights into the relative roles of H₂S and hypoxia in shaping the evolution of hemoglobin genes. If modifications of hemoglobins are an adaptation to H₂S, oxygen-binding affinity should decrease at a greater rate with increasing H₂S concentrations in non-sulfidic than in sulfidic lineages. In contrast, if

hypoxia is the primary source of selection shaping hemoglobin evolution, sulfidic lineages are expected to have hemoglobins with a higher oxygen-binding affinity than non-sulfidic lineages, but the rate of decline in binding-affinity in presence of H₂S should be equal.

It also remains unclear whether variation in oxygen transport gene expression documented here is a consequence of evolutionary change, or whether it merely reflects population-specific exposure histories to ambient environmental conditions. Gene expression in general—and hemoglobin expression specifically—is highly plastic and can be modulated over short periods of time upon exposure to environmental stressors (90, 94, 140, 141). Laboratory experiments using common-garden-reared fish consequently need to test whether the colonization of H₂S-rich environments has resulted in evolved changes in regulatory mechanisms underlying oxygen transport gene expression. Laboratory studies of gene expression variation in two lineages of *P. mexicana* from sulfidic environments have shown that ancestral plasticity plays a minor role in explaining gene expression differences between sulfidic and non-sulfidic populations (30). Instead, differential expression in fish from different habitat types appears to be primarily a consequence of evolved changes in baseline expression (in absence of H₂S) and canalization (loss of expression responses to H₂S exposure in the derived, sulfide spring populations), suggesting that regulatory evolution plays an important role during adaptation to H₂S-rich environments (30). Whether these findings are mirrored in the expression variation of hemoglobin genes across the broad sampling of sulfide spring fish lineages investigated here remains to be tested.

Finally, our study also has no possibility to detect recent gene duplication events that potentially play a role in adaptation to H₂S-rich environments. Focal genes were identified through the inspection of the *X. maculatus* genome (102), and potential hemoglobin copy

variation in specific lineages would therefore go unnoticed. This could affect both our analyses of gene expression variation, because reads from recently duplicated genes would be mapped to the same locus, and our inferences about positive selection, because variation in the amino acid sequences from recently duplicated genes may either be lost during the inference of consensus sequences for each population or artificially combined into the same locus. Gene duplications have played an important role in the evolution of oxygen transport genes. Over broad evolutionary timescales, such duplications have given rise to gene complexes encoding for proteins with different functional properties that are expressed at different life stages or under different environmental conditions (130, 142). It remains unclear, however, whether gene duplications also played a role during microevolutionary changes that could mediate adaptation to particular environmental conditions, and analysis of whole-genome sequences will be required to detect recent gene duplication events in sulfide spring fishes.

Conclusions

The extreme environmental conditions in freshwater sulfide springs with their acutely toxic concentrations of H₂S and widespread hypoxia has led to pronounced patterns of convergent evolution in phenotypic traits. Sulfide spring fishes of the family Poeciliidae consistently exhibit elevated tolerance to H₂S as well as behavioral and morphological modifications that facilitate efficient oxygen acquisition (13, 27, 84, 133, 143). Our knowledge of potentially convergent modifications of the molecular mechanisms underlying tolerance to the extreme environmental conditions remains much more fragmentary, although there appear to be convergent changes of toxicity targets (cytochrome *c* oxidase in the mitochondrial respiratory chain) and physiological pathways involved in enzymatic H₂S detoxification in at least a subset of sulfide spring fish

lineages (22, 68). This study identified another group of functionally important targets of selection in H₂S-rich environments. As predicted by theory, some oxygen transport genes exhibit evidence for shifts in expression and positive selection upon colonization of sulfide springs. Patterns of expression variation and amino acid substitutions were nonetheless highly idiosyncratic among different sulfide spring lineages, indicating that we may be able to predict the targets of selection during adaptation, but not the nature of modifications at those targets (56, 58). Convergent evolution in oxygen-transport genes in response to H₂S is consequently far less prominent as other examples that investigated the evolutionary effects of physiochemical stressors with explicit biochemical consequences (58, 59, 61). The current study also highlights that adaptation to the extreme environmental conditions in sulfide springs likely involves complex changes in the genome, including toxicity targets in the mitochondrial respiratory chain, toxicity targets involved in oxygen transport, and pathways associated with H₂S sequestration and detoxification (13). A key challenge for future work in this and other systems will be to determine whether different targets of selection represent alternative or complementary mechanisms of adaptation, which will require integrative analyses from genomes to fitness across evolutionary replicated lineages exposed to the same sources of selection.

Figures

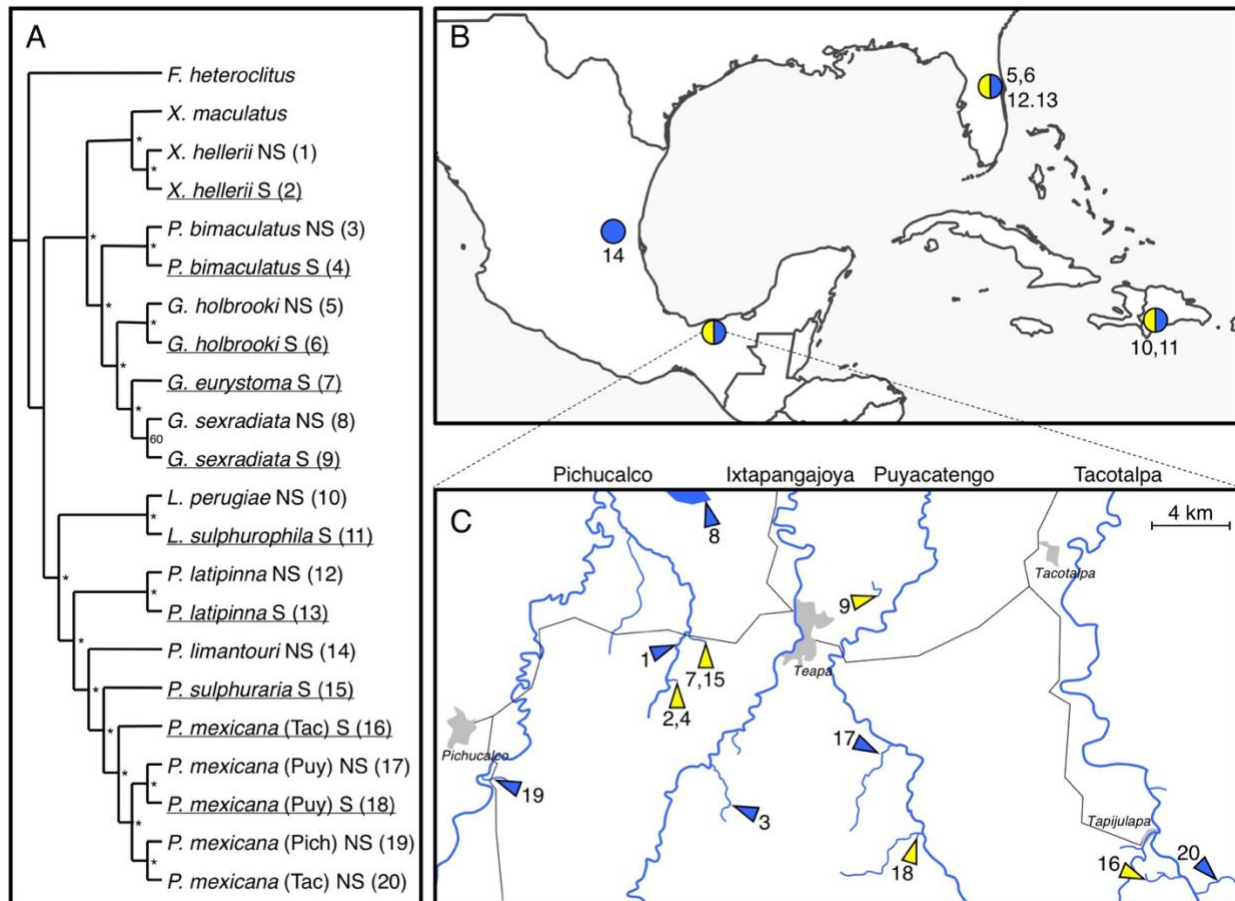


Figure 1-1: Phylogenetic relationships and collection localities of focal lineages of poeciliid fishes that have colonized H₂S-rich environments, along with relevant reference lineages from non-sulfidic habitats. A. Phylogeny of lineages included in analyses of expression variation and evolution of oxygen transport genes. Lineages from H₂S-rich environments (S) are underlined, lineages from non-sulfidic lineages are designated as NS. Asterisks indicate bootstrap support \geq 99%. B. Location of collection sites in the US, Mexico, and the Dominican Republic. C. Detailed view of collection localities in Southern Mexico, which harbors the highest diversity of sulfide spring fishes. Roads (black lines) and major towns (shaded areas) are included for orientation. Note that yellow symbols correspond to sulfidic sites, blue symbols to non-sulfidic sites. Numbers correspond to lineages as listed in Table 1.

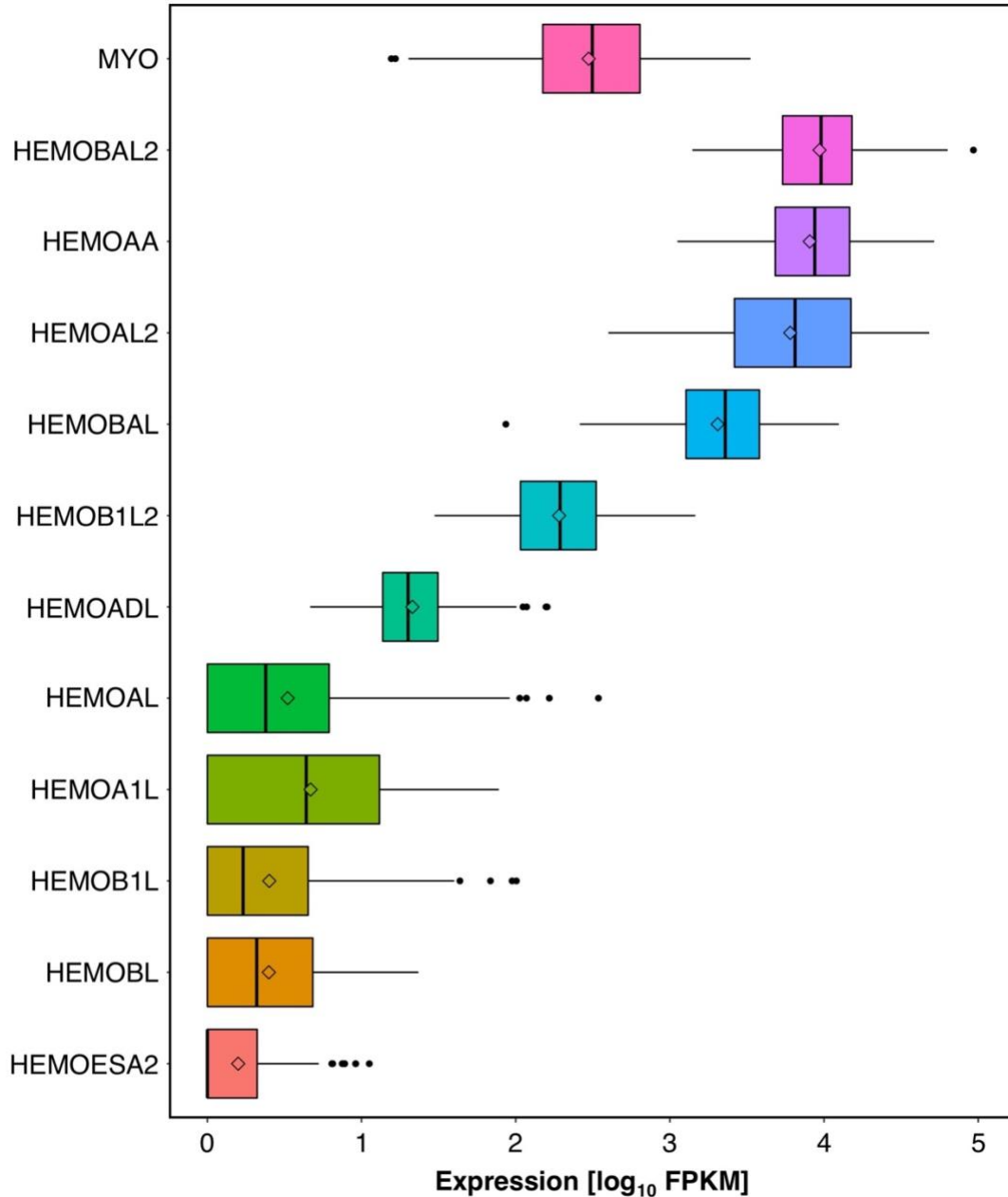


Figure 1-2: Overall expression levels of focal genes across all lineages investigated. Overall expression levels (\log_{10} -transformed) of focal genes (one myoglobin gene and eleven hemoglobin genes) across all lineages investigated. Boxes cover the first through third quartile of the data; vertical black lines indicate the median. Open diamonds indicate the mean for each group, and closed dots indicate outliers.

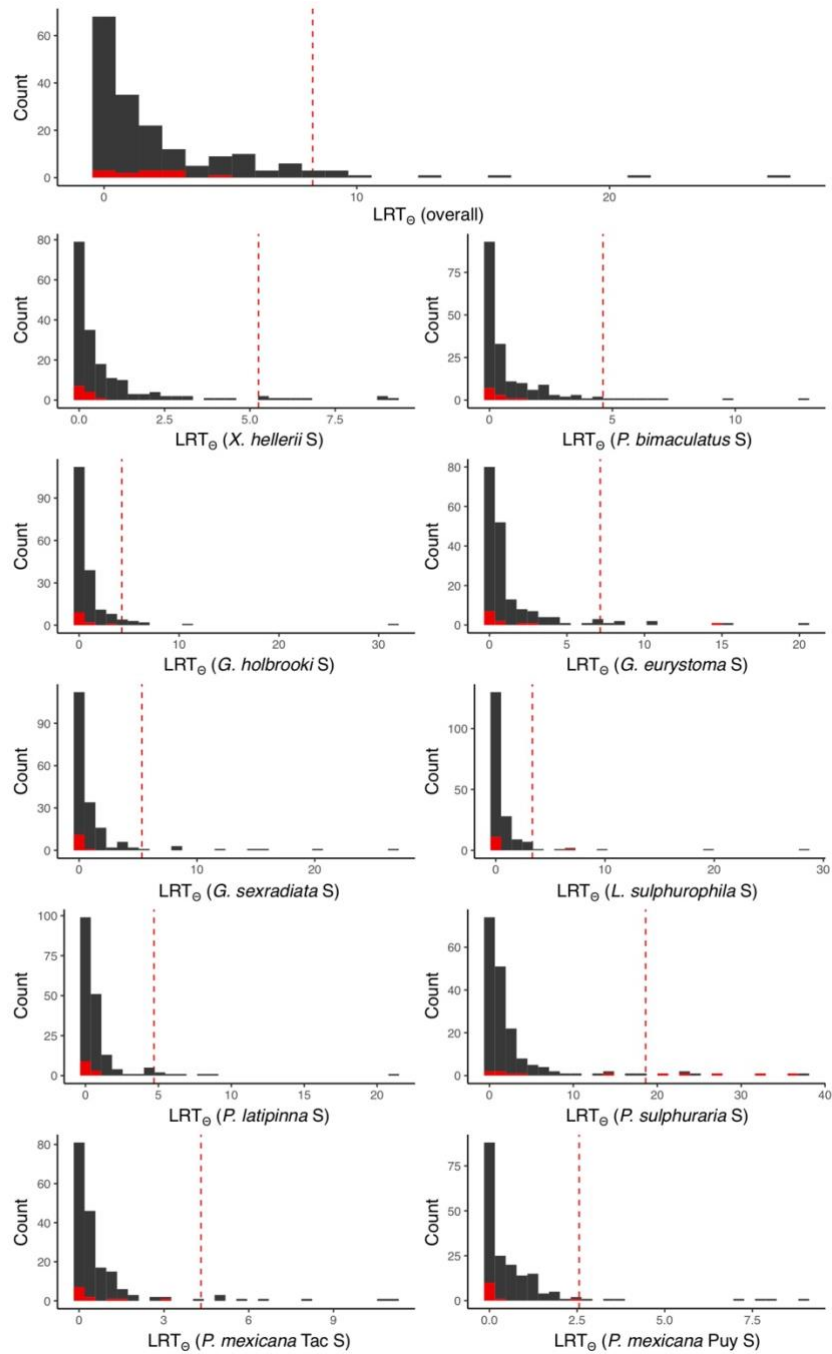


Figure 1-3: Results of EVE analyses testing for gene expression differences between sulfidic and non-sulfidic lineages overall, as well as in specific lineages that have colonized sulfidic environments. Depicted are empirical LRT_{θ} distributions for each comparison, including LRT_{θ} values for background genes (gray) and oxygen-transport genes (red). The vertical red line represents the top 5% cut-off value; i.e., genes with LRT_{θ} values above this line are considered having significant evidence for an expression shift in the focal lineage.

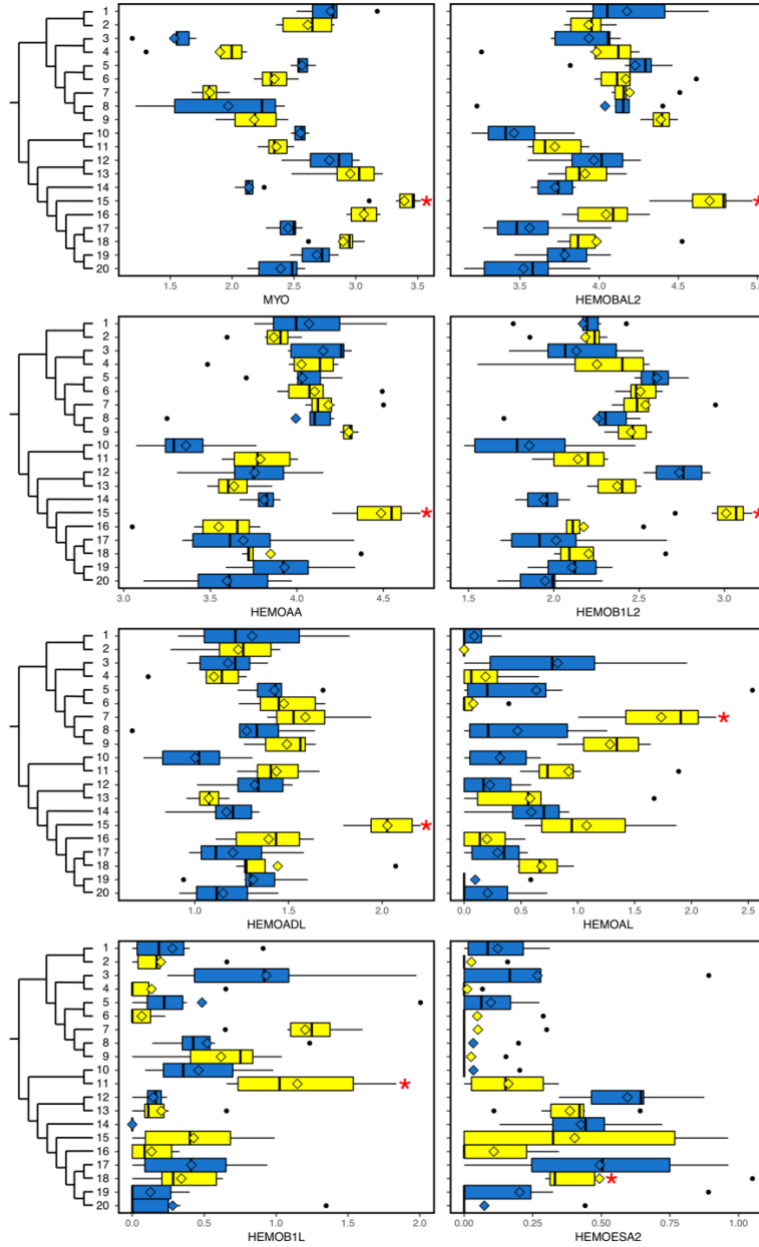


Figure 1-4: Lineage-specific expression variation for oxygen-transport genes with significant evidence for expression shifts associated with the colonization of H₂S-rich environments as established by EVE. Non-sulfidic lineages are in blue, sulfidic lineages in yellow, and lineages with significant expression shifts are highlighted with asterisks (also see Table 2). Boxes cover the first through third quartile of the log₁₀-transformed expression levels of each lineage; vertical black lines indicate the median. Open diamonds indicate the mean for each group, and closed dots indicate outliers. The phylogenetic trees depict the evolutionary relationships across lineages; numbers correspond to lineage IDs in Table 1.

```

X. hellevii NS MSLSGKDKTVVKAFWVKVAPKAAEMGGGALGRMLTAYPQTKTYFSHWSDLSPESAQVKKHGATIMSAIGDAVAKIIDDMPGAMSSELHAFKLRVDPANFRILAHNIIVLVALYFPADFTPEVHVSIDKFLQNLALALSEKYR
X. hellevii S MSLSGKDKTVVKAFWVKVAPKAAEMGGGALGRMLTAYPQTKTYFSHWSDLSPESAQVKKHGATIMSAIGDAVAKIIDDMPGAMSSELHAFKLRVDPANFRILAHNIIVLVALYFPADFTPEVHVSIDKFLQNLALALSEKYR
P. himantodatus NS MSLSGKDKTVVKAFWVKVAPKAAELGGGALGRMLTAYPQTKTYFSHWSDLSPESAQVKKHGATIMLAIGDAIAKIDDLPGALSSELHAFKLRVDPANFRILAHNIIVLVALYFPADFTPEVHVSIDKFLQNLALALSEKYR
P. himantodatus S MSLSGKDKTVVKAFWVKVAPKAAELGGGALGRMLTAYPQTKTYFSHWSDLSPESAQVKKHGATIMLAIGDAIAKIDDLPGALSSELHAFKLRVDPANFRILAHNIIVLVALYFPADFTPEVHVSIDKFLQNLALALSEKYR
G. holbrooki NS MSLSGKDKTVVKAFWVKVAPKAAELGGGALGRMLTAYPQTKTYFSHWSDLSPESAQVKKHGATIMLAIGDAIAKIDDLPGALSSELHAFKLRVDPANFRILAHNIIVLVALYFPADFTPEVHVSIDKFLQNLALALSEKYR
G. holbrooki S MSLSGKDKTVVKAFWVKVAPKAAELGGGALGRMLTAYPQTKTYFSHWSDLSPESAQVKKHGATIMLAIGDAIAKIDDLPGALSSELHAFKLRVDPANFRILAHNIIVLVALYFPADFTPEVHVSIDKFLQNLALALSEKYR
G. eurytoma S MSLSGKDKTVVKAFWVKVAPKAAELGGGALGRMLTAYPQTKTYFSHWSDLSPESAQVKKHGATIMLAIGDAIAKIDDLPGALSSELHAFKLRVDPANFRILAHNIIVLVALYFPADFTPEVHVSIDKFLQNLALALSEKYR
G. secretata NS MSLSGKDKTVVKAFWVKVAPKAAELGGGALGRMLTAYPQTKTYFSHWSDLSPESAQVKKHGATIMLAIGDAIAKIDDLPGALSSELHAFKLRVDPANFRILAHNIIVLVALYFPADFTPEVHVSIDKFLQNLALALSEKYR
G. secretata S MSLSGKDKTVVKAFWVKVAPKAAELGGGALGRMLTAYPQTKTYFSHWSDLSPESAQVKKHGATIMLAIGDAIAKIDDLPGALSSELHAFKLRVDPANFRILAHNIIVLVALYFPADFTPEVHVSIDKFLQNLALALSEKYR
L. perugina NS MSLSGKDKTVVKAFWVKVAPKAAELGGGALGRMLTAYPQTKTYFSHWSDLSPESAQVKKHGATIMLAIGDAIAKIDDLPGALSSELHAFKLRVDPANFRILAHNIIVLVALYFPADFTPEVHVSIDKFLQNLALALSEKYR
L. sulphuriphila S MSLSGKDKTVVKAFWVKVAPKAAELGGGALGRMLTAYPQTKTYFSHWSDLSPESAQVKKHGATIMLAIGDAIAKIDDLPGALSSELHAFKLRVDPANFRILAHNIIVLVALYFPADFTPEVHVSIDKFLQNLALALSEKYR
P. latipinna NS MSLSGKDKTVVKAFWVKVAPKAAELGGGALGRMLTAYPQTKTYFSHWSDLSPESAQVKKHGATIMLAIGDAIAKIDDLPGALSSELHAFKLRVDPANFRILAHNIIVLVALYFPADFTPEVHVSIDKFLQNLALALSEKYR
P. latipinna S MSLSGKDKTVVKAFWVKVAPKAAELGGGALGRMLTAYPQTKTYFSHWSDLSPESAQVKKHGATIMLAIGDAIAKIDDLPGALSSELHAFKLRVDPANFRILAHNIIVLVALYFPADFTPEVHVSIDKFLQNLALALSEKYR
P. limantodatus NS MSLSGKDKTVVKAFWVKVAPKAAELGGGALGRMLTAYPQTKTYFSHWSDLSPESAQVKKHGATIMLAIGDAIAKIDDLPGALSSELHAFKLRVDPANFRILAHNIIVLVALYFPADFTPEVHVSIDKFLQNLALALSEKYR
P. sulphuraria S MSLSGKDKTVVKAFWVKVAPKAAEMGGGALGRMLTAYPQTKTYFSHWSDLSPESAQVKKHGATIMLAIGDAIAKIDDLPGALSSELHAFKLRVDPANFRILAHNIIVLVALYFPADFTPEVHVSIDKFLQNLALALSEKYR
P. mexicana (Tac) S MSLSGKDKTVVKAFWVKVAPKAAEMGGGALGRMLTAYPQTKTYFSHWSDLSPESAQVKKHGATIMLAIGDAIAKIDDLPGALSSELHAFKLRVDPANFRILAHNIIVLVALYFPADFTPEVHVSIDKFLQNLALALSEKYR
P. mexicana (Puy) NS MSLSGKDKTVVKAFWVKVAPKAAELGGGALGRMLTAYPQTKTYFSHWSDLSPESAQVKKHGATIMLAIGDAIAKIDDLPGALSSELHAFKLRVDPANFRILAHNIIVLVALYFPADFTPEVHVSIDKFLQNLALALSEKYR
P. mexicana (Puy) S MSLSGKDKTVVKAFWVKVAPKAAEMGGGALGRMLTAYPQTKTYFSHWSDLSPESAQVKKHGATIMLAIGDAIAKIDDLPGALSSELHAFKLRVDPANFRILAHNIIVLVALYFPADFTPEVHVSIDKFLQNLALALSEKYR
P. mexicana (Pich) NS MSLSGKDKTVVKAFWVKVAPKAAELGGGALGRMLTAYPQTKTYFSHWSDLSPESAQVKKHGATIMLAIGDAIAKIDDLPGALSSELHAFKLRVDPANFRILAHNIIVLVALYFPADFTPEVHVSIDKFLQNLALALSEKYR
P. mexicana (Tac) NS MSLSGKDKTVVKAFWVKVAPKAAELGGGALGRMLTAYPQTKTYFSHWSDLSPESAQVKKHGATIMLAIGDAIAKIDDLPGALSSELHAFKLRVDPANFRILAHNIIVLVALYFPADFTPEVHVSIDKFLQNLALALSEKYR

```

Figure 1-5: Amino acid sequence alignment of HEMOAA, which had significant evidence for selection on specific codons based on a branch-site test in codeml (see Table 4). Highlighted in red are amino acid positions that exhibited evidence for positive selection based on a Bayes Empirical Bayes (BEB) analysis (position 73, probability of 0.996; position 143, probability of 0.989). Amino acid substitutions in sulfidic lineages are highlighted in bold; substitutions with significant functional effects based on Provean analyses are underlined.


```

X. ballerii NS MVEWTDEERKAITTLWGQIDVGEIGPQALTRLLVVYPWTQRHFGAFGNLSTYAAIVGNAKVAQHGKTVMSGLETAVKNMDNIKNAYAKLSVMHSDKLHVDPNFRALAECISVVVAAKFGPTVFTASFQEAWKFLAVVSALGRQYH
X. ballerii S MVEWTDEERKAITTLWGQIDVGEIGPQALTRLLVVYPWTQRHFGAFGNLSTYAAIVGNAKVAQHGKTVMSGLETAVKNMDNIKNAYAKLSVMHSDKLHVDPNFRALAECISVVVAAKFGPTVFTASFQEAWKFLAVVSALGRQYH
P. bimaculatus S MVEWTDEERKAITTLWGQIDVGEIGPQALTRLLVVYPWTQRHFGAFGNLSTYAAIVGNAKVAQHGKTVMSGLETAVKNMDNIKNAYAKLSVMHSDKLHVDPNFRALAECISVVVAAKFGPTVFTASFQEAWKFLAVVSALGRQYH
P. bimaculatus S MVEWTDEERKAITTLWGQIDVGEIGPQALTRLLVVYPWTQRHFGAFGNLSTYAAIVGNAKVAQHGKTVMSGLETAVKNMDNIKNAYAKLSVMHSDKLHVDPNFRALAECISVVVAAKFGPTVFTASFQEAWKFLAVVSALGRQYH
G. boliviroki NS MVEWTDEERKAITTLWGQIDVGEIGPQALTRLLVVYPWTQRHFGAFGNLSTYAAIVGNAKVAQHGKTVMSGLETAVKNMDNIKNAYAKLSVMHSDKLHVDPNFRALAECISVVVAAKFGPTVFTASFQEAWKFLAVVSALGRQYH
G. boliviroki S MVEWTDEERKAITTLWGQIDVGEIGPQALTRLLVVYPWTQRHFGAFGNLSTYAAIVGNAKVAQHGKTVMSGLETAVKNMDNIKNAYAKLSVMHSDKLHVDPNFRALAECISVVVAAKFGPTVFTASFQEAWKFLAVVSALGRQYH
G. erythronema S MVEWTDEERKAITTLWGQIDVGEIGPQALTRLLVVYPWTQRHFGAFGNLSTYAAIVGNAKVAQHGKTVMSGLETAVKNMDNIKNAYAKLSVMHSDKLHVDPNFRALAECISVVVAAKFGPTVFTASFQEAWKFLAVVSALGRQYH
G. erythronema S MVEWTDEERKAITTLWGQIDVGEIGPQALTRLLVVYPWTQRHFGAFGNLSTYAAIVGNAKVAQHGKTVMSGLETAVKNMDNIKNAYAKLSVMHSDKLHVDPNFRALAECISVVVAAKFGPTVFTASFQEAWKFLAVVSALGRQYH
G. serradilata NS MVEWTDEERKAITTLWGQIDVGEIGPQALTRLLVVYPWTQRHFGAFGNLSTYAAIVGNAKVAQHGKTVMSGLETAVKNMDNIKNAYAKLSVMHSDKLHVDPNFRALAECISVVVAAKFGPTVFTASFQEAWKFLAVVSALGRQYH
G. serradilata S MVEWTDEERKAITTLWGQIDVGEIGPQALTRLLVVYPWTQRHFGAFGNLSTYAAIVGNAKVAQHGKTVMSGLETAVKNMDNIKNAYAKLSVMHSDKLHVDPNFRALAECISVVVAAKFGPTVFTASFQEAWKFLAVVSALGRQYH
L. porojana NS MVEWTDEERKAITTLWGQIDVGEIGPQALTRLLVVYPWTQRHFGAFGNLSTYAAIVGNAKVAQHGKTVMSGLETAVKNMDNIKNAYAKLSVMHSDKLHVDPNFRALAECISVVVAAKFGPTVFTASFQEAWKFLAVVSALGRQYH
L. sulpharophila S MVEWTDEERKAITTLWGQIDVGEIGPQALTRLLVVYPWTQRHFGAFGNLSTYAAIVGNAKVAQHGKTVMSGLETAVKNMDNIKNAYAKLSVMHSDKLHVDPNFRALAECISVVVAAKFGPTVFTASFQEAWKFLAVVSALGRQYH
P. latipinna NS MVEWTDEERKAITTLWGQIDVGEIGPQALTRLLVVYPWTQRHFGAFGNLSTYAAIVGNAKVAQHGKTVMSGLETAVKNMDNIKNAYAKLSVMHSDKLHVDPNFRALAECISVVVAAKFGPTVFTASFQEAWKFLAVVSALGRQYH
P. latipinna S MVEWTDEERKAITTLWGQIDVGEIGPQALTRLLVVYPWTQRHFGAFGNLSTYAAIVGNAKVAQHGKTVMSGLETAVKNMDNIKNAYAKLSVMHSDKLHVDPNFRALAECISVVVAAKFGPTVFTASFQEAWKFLAVVSALGRQYH
P. limantouri NS MVEWTDEERKAITTLWGQIDVGEIGPQALTRLLVVYPWTQRHFGAFGNLSTYAAIVGNAKVAQHGKTVMSGLETAVKNMDNIKNAYAKLSVMHSDKLHVDPNFRALAECISVVVAAKFGPTVFTASFQEAWKFLAVVSALGRQYH
P. sulphuraria S MVEWTDEERKAITTLWGQIDVGEIGPQALTRLLVVYPWTQRHFGAFGNLSTYAAIVGNAKVAQHGKTVMSGLETAVKNMDNIKNAYAKLSVMHSDKLHVDPNFRALAECISVVVAAKFGPTVFTASFQEAWKFLAVVSALGRQYH
P. mexicana (Tae) S MVEWTDEERKAITTLWGQIDVGEIGPQALTRLLVVYPWTQRHFGAFGNLSTYAAIVGNAKVAQHGKTVMSGLETAVKNMDNIKNAYAKLSVMHSDKLHVDPNFRALAECISVVVAAKFGPTVFTASFQEAWKFLAVVSALGRQYH
P. mexicana (Puy) NS MVEWTDEERKAITTLWGQIDVGEIGPQALTRLLVVYPWTQRHFGAFGNLSTYAAIVGNAKVAQHGKTVMSGLETAVKNMDNIKNAYAKLSVMHSDKLHVDPNFRALAECISVVVAAKFGPTVFTASFQEAWKFLAVVSALGRQYH
P. mexicana (Puy) S MVEWTDEERKAITTLWGQIDVGEIGPQALTRLLVVYPWTQRHFGAFGNLSTYAAIVGNAKVAQHGKTVMSGLETAVKNMDNIKNAYAKLSVMHSDKLHVDPNFRALAECISVVVAAKFGPTVFTASFQEAWKFLAVVSALGRQYH
P. mexicana (Pich) NS MVEWTDEERKAITTLWGQIDVGEIGPQALTRLLVVYPWTQRHFGAFGNLSTYAAIVGNAKVAQHGKTVMSGLETAVKNMDNIKNAYAKLSVMHSDKLHVDPNFRALAECISVVVAAKFGPTVFTASFQEAWKFLAVVSALGRQYH
P. mexicana (Tae) NS MVEWTDEERKAITTLWGQIDVGEIGPQALTRLLVVYPWTQRHFGAFGNLSTYAAIVGNAKVAQHGKTVMSGLETAVKNMDNIKNAYAKLSVMHSDKLHVDPNFRALAECISVVVAAKFGPTVFTASFQEAWKFLAVVSALGRQYH

```

Figure 1-6: Amino acid sequence alignment of HEMOBAL, which had significant evidence for selection on one codon based on a branch-site test in codeml (see Table 4). Highlighted in red is the amino acid position that exhibited evidence for positive selection based on a Bayes Empirical Bayes (BEB) analysis (position 26, probability of 0.954). Amino acid substitutions in sulfidic lineages are highlighted in bold; substitutions with significant functional effects based on Provean analyses are underlined.

Tables

Table 1-1: List of lineages from sulfidic and non-sulfidic habitats included in this study. The table provides descriptions of the collection localities, information about the presence or absence of H₂S, latitude and longitude, as well as the number of individuals (*N*) collected from each site.

ID	Species	Locality	H₂S	Lat/Long	<i>N</i>
1	<i>Xiphophorus hellerii</i>	Rio El Azufre, west branch, Rio Pichucalco drainage, Chiapas, Mexico	–	17.556/-93.008	6
2	<i>Xiphophorus hellerii</i>	La Gloria springs, Rio Pichucalco drainage, Chiapas, Mexico	+	17.532/-93.015	6
3	<i>Pseudoxiphophorus bimaculatus</i>	Arroyo Pujil, Rio Ixtapangajoya drainage, Chiapas, Mexico	–	17.476/-92.986	6
4	<i>Pseudoxiphophorus bimaculatus</i>	La Gloria springs, Rio Pichucalco drainage, Chiapas, Mexico	+	17.532/-93.015	6
5	<i>Gambusia holbrooki</i>	Mariner's Cove, Lake Monroe, St. Johns River drainage, Florida, USA	–	28.857/-81.239	6
6	<i>Gambusia holbrooki</i>	Green Springs, St. Johns River drainage, Florida, USA	+	28.863/-81.248	6
7	<i>Gambusia eurystoma</i>	Baños del Azufre, Rio Pichucalco drainage, Tabasco, Mexico	+	17.552/-92.999	6
8	<i>Gambusia sexradiata</i>	Laguna Sitio Grande, Rio Ixtapangajoya drainage, Tabasco, Mexico	–	17.677/-92.997	6
9	<i>Gambusia sexradiata</i>	Mogote del Puyacatengo, Rio Puyacatengo drainage, Tabasco, Mexico	+	17.582/-92.900	6
10	<i>Limia perugiae</i>	Stream in Cabral, Rio Yaque del Sur drainage, Barahona, Dominican Republic	–	18.246/-71.223	6
11	<i>Limia sulphurophila</i>	Balnearios La Zurza, Lago Enriquillo basin, Independencia, Dominican Republic	+	18.398/-71.570	6
12	<i>Poecilia latipinna</i>	Mariner's Cove, Lake Monroe, St. Johns River drainage, Florida, USA	–	28.857/-81.239	6
13	<i>Poecilia latipinna</i>	Green Springs, St. Johns River drainage, Florida, USA	+	28.863/-81.248	6
14	<i>Poecilia limantouri</i>	Rio Garces, Rio Panuco drainage, Hidalgo, Mexico	–	20.940/-98.282	6
15	<i>Poecilia sulphuraria</i>	Baños del Azufre, Rio Pichucalco drainage, Tabasco, Mexico	+	17.552/-92.999	6
16	<i>Poecilia mexicana</i>	El Azufre II, Rio Tacotalpa drainage, Tabasco Mexico	+	17.438/-92.775	6

17	<i>Poecilia mexicana</i>	Rio Puyacatengo, Rio Puyacatengo drainage, Tabasco Mexico	-	17.510/-92.914	6
18	<i>Poecilia mexicana</i>	La Lluvia springs, Rio Puyacatengo drainage, Tabasco, Mexico	+	17.464/-92.895	5
19	<i>Poecilia mexicana</i>	Arroyo Rosita, Rio Tacotalpa drainage, Chiapas, Mexico	-	17.485/-93.104	6
20	<i>Poecilia mexicana</i>	Arroyo Bonita, Rio Pichucalco drainage, Tabasco, Mexico	-	17.427/-92.752	6

Table 1-2: List of focal oxygen transport genes investigated in this study, including eleven hemoglobin genes and one myoglobin gene. The table includes the gene ID from the *X. maculatus* reference genome annotation file (XM ID), the accession ID, percent sequence similarity, and *E*-value from the top BLAST hit in Swiss-Prot. The table also contains the results of branch tests that evaluated shifts in gene expression associated with the colonization of H₂S-rich habitats as implemented in EVE. We list the likelihood ratio test statistic (LRT_{θ}) for all sulfidic lineages combined (overall) as well as for each sulfidic lineage individually. Genes with evidence for divergence in expression are highlighted in bold.

Gene	XM ID	Accession	% similarity	<i>E</i> -value	Overall	Xhel (2)	Pbim (4)	Ghol (6)	Geur (7)	Gsex (9)	Lsul (11)	Plat (13)	Psul (15)	Pmex (Tac) (16)	Pmex (Puy) (18)
HEMOA1L	005809044.2	P02008	49	1.40E-44	0.000	0.000	0.000	0.000	0.000	0.000	0.000	0.000	0.000	0.000	0.000
HEMOAA	005816937.1	P69905	55.2	1.80E-48	1.532	0.000	0.000	0.000	0.000	0.000	0.000	0.000	20.987	0.000	0.000
HEMOADL	005815125.2	P02008	52.9	1.30E-47	3.035	0.172	0.186	0.040	0.527	0.042	0.000	0.323	36.268	0.000	0.083
HEMOAL	014474961.1	P02008	58.9	2.00E-36	1.561	0.000	0.031	0.043	14.501	0.030	0.112	0.000	0.728	0.000	0.000
HEMOAL2	005809047.2	P69905	53.8	7.90E-47	3.064	0.000	0.000	0.000	0.000	0.000	0.000	0.000	14.289	0.000	0.000
HEMOB1L	005815126.1	P69891	50.7	8.40E-49	0.023	0.330	0.640	0.642	3.119	0.072	6.696	0.254	0.023	0.158	0.055
HEMOB1L2	005809045.2	P02100	43.8	3.80E-41	1.308	0.242	0.031	0.085	0.326	0.013	0.299	0.011	27.709	0.235	0.121
HEMOBAL	005816936.2	P02100	52.7	9.60E-51	0.000	0.480	0.245	2.954	2.107	0.664	0.250	1.043	3.998	2.892	0.130

HEMOBAL2	005809046.1	P02100	50.7	7.70E-50	2.550	0.000	0.000	0.000	0.000	0.000	0.000	0.000	0.000	32.787	0.000	0.000
HEMOBL	005809043.1	P02100	46.3	1.10E-43	4.297	0.059	1.111	0.945	0.322	0.010	0.014	0.634	0.945	1.111	0.063	
HEMOESA2	005809048.1	P02008	52.8	1.30E-45	1.155	0.188	0.410	0.156	0.163	0.240	0.045	0.030	2.280	0.459	2.559	
MYO	005797508.1	P02144	43.2	1.00E-32	1.832	0.015	0.876	0.277	0.675	0.405	0.267	0.887	23.503	1.549	0.316	

Table 1-3: Results of branch tests evaluating differences in non-synonymous to synonymous amino acid substitution rates (ω) between non-sulfidic and sulfidic lineages. Branch test models ($\omega_{NS} \neq \omega_S$) were evaluated against a null model ($\omega_{NS} = \omega_S$) using a likelihood ratio test, and we present the log-likelihoods ($\ln L$) for each model, the test statistic ($2\Delta \ln L$), and the corresponding P -value. In addition, we provide ω of the null model or separate estimates of ω for non-sulfidic and sulfidic lineages, depending on which model was supported. Genes with evidence for $\omega_{NS} \neq \omega_S$ are highlighted in bold.

Gene	$\ln L_{null}$	$\ln L_{branch}$	$2\Delta \ln L$	P	ω_{null}	ω_{NS}	ω_S
HEMOA1L	-258.0	-256.4	3.195	0.074	0.228		
HEMOAA	-1154.1	-1151.0	6.023	0.014		0.252	0.818
HEMOADL	-676.5	-676.5	0.000	0.998	0.036		
HEMOAL2	-994.8	-993.7	2.130	0.144	0.599		
HEMOAL	-15.3	-15.3	0.000	1.000	1.000		
HEMOB1L2	-853.5	-853.4	0.253	0.615	0.183		
HEMOB1L	-425.9	-425.7	0.255	0.613	0.109		
HEMOBAL2	-819.4	-817.2	4.415	0.036		0.153	0.565
HEMOBAL	-941.3	-941.4	0.209	0.648	0.327		
HEMOESA2	-1.4	-1.4	0.000	1.000	1.000		
MYO	-813.2	-812.2	1.825	0.177	0.152		

Table 1-4: Results of branch-site tests evaluating positive selection on specific codon between sulfidic and non-sulfidic lineages. Branch-site models were evaluated against a null model using a likelihood ratio test, and we present the log-likelihoods ($\ln L$) for each model, the test statistic ($2\Delta\ln L$), and the corresponding P -value. Genes with evidence for significant branch-site models are highlighted in bold.

Gene	$\ln L_{null}$	$\ln L_{branch-site}$	$2\Delta\ln L$	P
HEMOA1L	-868.3	-868.2	0.248	0.619
HEMOAA	-1123.6	-1115.8	15.424	<0.001
HEMOADL	-673.3	-673.3	0.000	0.998
HEMOAL2	-972.8	-970.9	3.745	0.053
HEMOAL	-620.5	-620.5	0.000	1.000
HEMOB1L2	-848.0	-848.0	0.000	1.000
HEMOB1L	-669.3	-669.3	0.000	1.000
HEMOBAL2	-806.0	-805.5	0.823	0.364
HEMOBAL	-919.6	-913.3	12.692	<0.001
HEMOBL	-1046.6	-1046.4	0.511	0.475
HEMOESA2	-1021.7	-1021.5	0.425	0.514
MYO	-813.2	-813.2	0.000	1.000

Chapter 2 - Convergent evolution of conserved mitochondrial pathways underlies repeated adaptation to extreme environments

Ryan Greenway†, Nick Barts†, Chaturika Henpita†, Anthony P. Brown, Lenin Arias Rodriguez, Carlos M. Rodríguez Peña, Sabine Arndt, Gigi Y. Lau, Michael P. Murphy, Lei Wu, Dingbo Lin, Jennifer H. Shaw‡, Joanna L. Kelley‡ & Michael Tobler‡

†Shared first authorship

‡Co-corresponding authors

Abstract

Extreme environments test the limits of life; yet, some organisms thrive in harsh conditions. Extremophile lineages inspire questions about how organisms can tolerate physiochemical stressors and whether the repeated colonization of extreme environments is facilitated by predictable and repeatable evolutionary innovations. We identified the mechanistic basis underlying convergent evolution of tolerance to hydrogen sulfide (H₂S)—a toxicant that impairs mitochondrial function—across evolutionarily independent lineages of a fish (*Poecilia mexicana*, Poeciliidae) from H₂S-rich springs. Using comparative biochemical and physiological analyses, we found that mitochondrial function is maintained in the presence of H₂S in sulfide spring *P. mexicana* but not ancestral lineages from nonsulfidic habitats due to convergent adaptations in the primary toxicity target and a major detoxification enzyme. Genome-wide local ancestry analyses indicated that convergent evolution of increased H₂S tolerance in different populations is likely caused by a combination of selection on standing genetic variation and de novo mutations. On a macroevolutionary scale, H₂S tolerance in 10 independent lineages of sulfide spring fishes across multiple genera of Poeciliidae is correlated with the convergent modification

and expression changes in genes associated with H₂S toxicity and detoxification. Our results demonstrate that the modification of highly conserved physiological pathways associated with essential mitochondrial processes mediates tolerance to physiochemical stress. In addition, the same pathways, genes, and—in some instances—codons are implicated in H₂S adaptation in lineages that span 40 million years of evolution.

*Published as: Greenway, R., Barts, N., Henpita, C., et al. (2020). Convergent evolution of conserved mitochondrial pathways underlies repeated adaptation to extreme environments.

Proceedings of the National Academy of Sciences: 202004223.

Introduction

Stephen J. Gould made a strong case for the importance of contingency in evolution, famously quipping that replaying the “tape of life” would lead to different outcomes every time (144). But despite the unpredictability of mutations, the effects of genetic drift, and other historical contingencies, convergent evolution of phenotypic traits and their underlying genes is common, indicating that natural selection sometimes finds repeatable and predictable solutions to shared evolutionary challenges (145, 146). A major challenge that remains is the identification of the ecological, genetic, and functional factors that might determine the repeatability and predictability of evolutionary outcomes (52).

Mitochondria and their genomes provide a fascinating model to ask questions about the predictability of evolution for two reasons: (i) Mitochondrial genomes were historically thought to be a prime example of contingency evolution, because alternative genetic variants were assumed to be selectively neutral (147). This paradigm has been shifting though, with mounting

evidence that mitochondria—and genes encoded in the mitochondrial genome—can play important roles in adaptation, especially in the context of physiochemical stress (148). (ii) Mitochondria are critical for the cellular function of eukaryotes (149). Their function is dependent on the gene products from two genomes, the mitochondrial and the nuclear (150), which interact to ultimately shape whole-organism performance. Despite extensive characterization of allelic variation in mitochondrial genomes, it often remains unclear how variation in genes that contribute to mitochondrial function translates to variation in physiological and organismal function. Furthermore, it is not known whether exposure to similar selective regimes may cause convergent modifications of mitochondrial genomes and emergent biochemical and physiological functions in evolutionarily independent lineages.

Extreme environments that represent novel ecological niches are natural experiments to address questions about mechanisms underlying mitochondrial adaptations and illuminate the predictability of adaptive evolution of mitochondria. Among the most extreme freshwater ecosystems are springs with high levels of hydrogen sulfide (H₂S), a potent respiratory toxicant lethal to metazoans due to its inhibition of mitochondrial ATP production (151). Multiple lineages of livebearing fishes (Poeciliidae) have colonized H₂S-rich springs throughout the Americas and independently evolved tolerance to sustained H₂S concentrations orders of magnitude higher than those encountered by ancestral lineages in nonsulfidic habitats (152). Here, we identify the molecular basis of an evolutionary innovation that facilitated the independent colonization of extreme environments (increased H₂S tolerance) and ask if the underlying mechanisms have evolved in convergence in disparate lineages of livebearing fishes.

H₂S toxicity and detoxification are associated with highly conserved physiological pathways in mitochondria (Figure 1A) (153, 154), providing *a priori* predictions about the potential

molecular mechanisms underlying adaptation to this strong source of selection. Toxic effects of H₂S result from binding to and inhibition of cytochrome c oxidase (COX) in the oxidative phosphorylation (OxPhos) pathway, which contains subunits encoded in both the nuclear and the mitochondrial genomes (155). Animal cells can also detoxify low concentrations of endogenously produced H₂S via the mitochondrial sulfide:quinone oxidoreductase (SQR) pathway, which is linked to OxPhos but entirely encoded in the nuclear genome (156). We have previously shown that genes associated with both pathways are under divergent selection and differentially expressed between fish populations in sulfidic and nonsulfidic habitats (152). These include nuclear and mitochondrial genes encoding subunits of the direct toxicity target (COX) and the nuclear gene encoding the enzyme mediating the first step of detoxification (SQR) (152). Tolerance to H₂S may therefore be mediated by resistance (modification of toxicity targets that reduce the negative impact of H₂S), regulation (modification of physiological pathways that maintain H₂S homeostasis), or both (151).

Based on these previous results, we hypothesized that the repeated modification of enzymes in the OxPhos and SQR pathways in *P. mexicana* populations from sulfidic habitats leads to an increased ability to maintain mitochondrial function in the presence of H₂S. In the present study, we consequently used a series of *in vivo* and *in vitro* assays to identify the functional consequences of modifications to the OxPhos and SQR pathways in evolutionarily independent population pairs of *P. mexicana* from adjacent sulfidic and nonsulfidic habitats that are situated in different river drainages. In addition, we hypothesized that convergent molecular modifications in the same pathways underlie the convergent evolution of H₂S tolerance across different lineages of poeciliid fishes. Hence, we also used phylogenetic comparative analyses of

gene expression and analyses of molecular evolution to detect patterns of molecular convergence in 10 lineages of sulfide spring poeciliids and ancestors from nonsulfidic habitats.

Results and Discussion

Sulfide spring P. mexicana exhibit a resistant toxicity target

If resistance is the primary mechanism of tolerance, we would predict that COX function is maintained in the presence of H₂S in fish from sulfidic populations, but not those from nonsulfidic populations. Quantification of COX function indicated that enzyme activity generally declined with increasing H₂S concentrations, but this decline was reduced in populations from sulfidic habitats (Figure 1B; habitat × H₂S: $P < 0.001$, Table S3). Even though the drainage of origin was not retained as an explanatory variable in statistical models (SI Appendix, Table S2), COX activity in one H₂S-tolerant population (Tac) declined just as in nonsulfidic populations (Figure 1B). The other two *P. mexicana* populations from sulfidic habitats (Puy and Pich) maintained significant COX activity even at the highest H₂S concentrations, which should reduce the negative impact of H₂S on cellular respiration. These results are consistent with previous analyses (157) and indicate that resistance may contribute to H₂S tolerance in some populations, but cannot explain the repeated evolution of H₂S tolerance by itself.

Sulfide spring P. mexicana can regulate mitochondrial H₂S through increased detoxification

We also tested whether tolerant and intolerant populations differ in their ability to detoxify H₂S by conducting enzyme activity assays of SQR. Activity of SQR was significantly higher in mitochondria from sulfidic populations at intermediate and high H₂S concentrations (Figure 1C;

habitat \times H₂S: $P < 0.001$ in SI Appendix, Table S5), likely helping fish from sulfidic habitats to maintain H₂S homeostasis during environmental exposure. To test this prediction *in vivo*, we used a novel mitochondria-specific H₂S-probe (MitoA) that allows for the monitoring of relative H₂S levels inside the mitochondria of living organisms (158). We measured mitochondrial H₂S concentrations in this manner using laboratory-reared fish that were exposed to varying levels of environmental H₂S. Because laboratory-reared fish were not available for the population pair from Pich, only two population pairs were used for this analysis. Overall, mitochondrial H₂S concentrations increased with environmental exposure ($P = 0.001$) and was higher in fish from non-sulfidic habitats ($P < 0.001$ in SI Appendix, Table S7). H₂S concentrations in mitochondria isolated from livers (Figure 1D) and other organs (SI Appendix, Figure S2) of fish from nonsulfidic habitats increased above control levels at all exposure concentrations. In contrast, mitochondrial H₂S concentrations in isolates of fish from sulfidic populations did not usually exceed control levels and remained lower than levels in fish from nonsulfidic habitats. Together, these results indicate that populations of *P. mexicana* from sulfidic habitats can detoxify H₂S at higher rates and thus regulate mitochondrial H₂S upon environmental exposure.

Sulfide spring P. mexicana can maintain mitochondrial function in presence of H₂S

Modification of the OxPhos and SQR pathways in *P. mexicana* suggests that mitochondrial adaptations are key to the evolution of H₂S tolerance. Therefore, mitochondrial function of fish from sulfidic habitats should be maintained upon exposure to H₂S. We tested this hypothesis by quantifying different aspects of mitochondrial function (basal respiration, maximal respiration, and spare respiratory capacity) along a gradient of H₂S concentrations using an *ex vivo* coupling assay. As expected, all aspects of mitochondrial function generally declined with increasing H₂S

(Figures 1E; SI Appendix, S3-S5). Comparison of mitochondrial function between adjacent populations in sulfidic and nonsulfidic habitats indicated no differences in basal respiration (SI Appendix, Figure S3). However, individuals from sulfidic populations were able to maintain maximal respiration and spare respiratory capacity at higher levels compared to individuals from nonsulfidic habitats of the same river drainage (Figure 1E), even though the magnitude of difference and the shape of response curves varied (SI Appendix; significant drainage \times habitat interactions in Tables S10 & S12, Figures S4-S5). These findings indicate that mitochondria of H₂S-tolerant individuals continue to produce ATP in the presence of a potent inhibitor that reduces mitochondrial function in ancestral lineages.

Overall, our quantitative analyses indicate clear patterns of convergence in functional physiological traits associated with H₂S tolerance. Nonetheless, further inspection of the results also reveals lineage-specific patterns (especially in H₂S-dependent COX activity and mitochondrial respiration), indicating that evolutionary responses across lineages are similar but not necessarily identical. These idiosyncrasies are consistent with the results of previous comparative transcriptome analyses, which revealed a large number of genes that are under selection or differentially expressed in just a subset of lineages in addition to genes that are consistently differentially expressed and under selection across all lineages (72, 106, 159). Based on their functions, the OxPhos and SQR pathways undoubtedly include some major-effect genes influencing H₂S tolerance in different populations of *P. mexicana*, but tolerance—as an emergent physiological trait—is a complex trait impacted by other genes as well. In the future, quantitative genetic analyses will be required to understand how other loci contribute to tolerance within each lineage, and how population-specific patterns of genetic differentiation might shape variation in functional physiology evident in our data.

Convergence among P. mexicana populations is shaped by selection on de novo mutations and standing genetic variation

The convergent evolution of H₂S tolerance in *P. mexicana* begs questions about the origin of adaptive alleles (55). At microevolutionary scales, convergence may be a consequence of the repeated assembly of related alleles into different genomic backgrounds, either through selection on standing genetic variation or introgression (160, 161). However, the epitome of convergent evolution is, arguably, the independent origin of adaptive mutations at the same locus that lead to consistent functional outcomes (162). To identify convergence at a genomic level, we re-sequenced whole genomes of multiple *P. mexicana* individuals from sulfidic and nonsulfidic habitats. Analyzing phylogenetic relationship among *P. mexicana* populations (with *P. reticulata* as an outgroup) using 13,390,303 single nucleotide polymorphisms (SNPs) distributed across the genome confirmed three independent colonization events of sulfide springs and distinct evolutionary trajectories for sulfide spring populations in different drainages (Figure 2A), as inferred by previous studies (163). If adaptive alleles arose separately through *de novo* mutation in each sulfide spring population, we would expect that putative adaptive alleles mirror these relationships, as previously documented for H₂S-resistant alleles in mitochondrial *COX* subunits (157). However, patterns of divergence (SI Appendix, Figure S6) and local ancestry were highly variable across the genome. Classifying local patterns of genetic similarity using a Hidden Markov Model and a self-organizing map allowed us to identify genomic regions in which ancestry patterns deviate from the genome-wide consensus, including multiple regions with a strong signal of clustering by ecotype (sulfidic vs. nonsulfidic populations). Such clustering by ecotype occurred in less than 1 % of the genome (SI Appendix, Figure S7), but included genomic regions encoding key genes associated with H₂S detoxification (e.g., *SQR* and *ETHE1*; Figure

2B; SI Appendix, Dataset S2). Clustering by ecotype indicates a monophyletic origin of putatively adaptive alleles at these loci that are shared across independent lineages of sulfide spring *P. mexicana* as a consequence of selection on standing genetic variation or introgression (164), although the latter scenario is less likely considering the geographic barriers and strong survival selection against migrants from sulfidic to nonsulfidic habitats (135). Consequently, multiple mechanisms—not just selection on *de novo* mutations (72)—played a role in the convergent evolution of H₂S-tolerance in *P. mexicana*.

Convergent modifications of toxicity targets and detoxification pathways are evident at macroevolutionary scales

While selection on standing genetic variation and introgression can contribute to convergent evolution at microevolutionary scales, adaptive alleles are unlikely to be shared among lineages at macroevolutionary scales due to high phylogenetic and geographic distances separating gene pools (165). Absence of convergence in molecular mechanisms at broader phylogenetic scales might indicate the importance of contingency in evolution, as asserted by Gould (146). In contrast, the presence of convergence would indicate that fundamental constraints limit the number of solutions for a functional problem (166).

We used phylogenetic comparative analyses of gene expression and analyses of molecular evolution to detect patterns of molecular convergence in 10 lineages of sulfide spring poeciliids and ancestors in nonsulfidic habitats (Figure S1). This included members of five genera that span over 40 million years of divergence and occur in different biogeographic contexts (SI Appendix, Figure S1). We found evidence for convergence in both gene expression and sequence evolution. Variation in overall gene expression was strongly influenced by phylogenetic relationships

(Figure 3A). However, 186 genes exhibited significant evidence for convergent expression shifts in sulfide spring fishes (Figure 3B; SI Appendix, Dataset S3), segregating lineages based on habitat type of origin, irrespective of phylogenetic relationships (Figure 3C). The only outlier was *Limia sulphurophila*, which clustered with nonsulfidic lineages despite significant expression differences with its sister, *L. perugiae*. Functional annotation indicated that genes with convergent expression shifts were enriched for biological processes associated with H₂S detoxification (SQR pathway, Figure 3D), the processing of sulfur compounds, and H₂S toxicity targets in OxPhos (SI Appendix, Figure S8, Table S14).

We also identified 11 genes with elevated nonsynonymous to synonymous substitution rates across the phylogeny, including three mitochondrial genes that encode subunits of H₂S's toxicity target (*COX1* and *COX3*) and OxPhos complex III (*CYTB*; Dataset S4). Most amino acid substitutions in *COX1* and *COX3* occurred in a lineage-specific fashion, but convergent substitutions across clades occurred at six codons in *COX1* and two codons in *COX3* (Figure 4). These findings suggest that modifications of H₂S toxicity targets and detoxification pathways are not only critical in the evolution of H₂S tolerance in *P. mexicana*, but they have evolved in convergence in other lineages that were exposed to the same source of selection.

Conclusions

We capitalized on past evolutionary genetics studies that compared *P. mexicana* populations from sulfidic and nonsulfidic environments (152) to test hypotheses about functional ramifications of genetic differences and their impact on organismal performance. As predicted, we found that the repeated evolution of H₂S tolerance in independent *P. mexicana* populations is mediated both by modifications of a direct toxicity target (causing increased resistance to H₂S)

and a pathway involved in detoxification (causing an increased ability to regulate mitochondrial H₂S). Similar modifications to COX and SQR have been hypothesized to mediate H₂S adaptation in other groups of organisms (67, 71, 167), but the evolutionary context and the consequences for mitochondrial function in these cases remained unknown. Overall, our analyses indicated that closely related populations can exhibit substantial differences in what we assume to be highly conserved physiological pathways associated with the function of mitochondria. Modification of mitochondrial processes consequently can be critical in mediating adaptation to different environmental conditions at microevolutionary scales, underscoring the long overlooked role of mitochondria in adaptive evolution (148).

Our comparative transcriptome analyses across a broader sampling of sulfide spring fishes further indicated that colonization of novel niches with extreme environmental conditions can arise through the convergent modification of conserved physiological pathways. The convergent evolution of high H₂S tolerance across species is the result of repeated and predicted modifications of the same physiological pathways, genes, and—in some instances—codons associated with mitochondrial function. This convergence at multiple levels of biological organization is likely a consequence of constraint, because the explicit biochemical and physiological consequences of H₂S limit the ways organisms can cope with its toxicity (60, 168). Due to these constraints, molecular convergence is not only evident at microevolutionary scales, where selection can repeatedly assemble related alleles into different genomic backgrounds, but also at macroevolutionary scales including lineages separated by over 40 million years of evolution.

That said, there is an inordinate amount of genetic and gene expression variation that seemingly varies idiosyncratically across different lineages. In comparative analyses of highly

quantitative traits (such as H₂S tolerance), there is an inherent bias to emphasize the importance of shared modifications in adaptation, while we tend to dismiss lineage-specific patterns as noise. But how lineage-specific genetic and gene expression variation interacts with molecular mechanisms that have evolved in convergence remains largely unknown for most study systems. So, if we replayed the tape of life, the same characters may make an appearance in the same setting, but the overall plots may still unfold in very different ways when many characters are part of the story.

Methods

Background and hypotheses

The overall goals of our study were to test hypotheses about the mechanistic basis of H₂S tolerance in evolutionarily replicated populations of *Poecilia mexicana* and about potential signatures of convergent evolution in sulfide spring fishes across the family Poeciliidae. *Poecilia mexicana* has been a model for the study of adaptation to H₂S-rich environments (152). This species is widely distributed in Mexico and Central America, inhabiting a wide range of freshwater habitats (99, 169). In southern Mexico, this species has also colonized H₂S-rich springs in four different river drainages of the Rio Grijalva basin (including the Rios Tacotalpa, Puyacatengo, Ixtapangajoya, and Pichucalco; see Figure S1). Colonization of springs has occurred independently, providing evolutionarily replicated population pairs in sulfidic and nonsulfidic habitats (83, 163). Sulfide spring populations are locally adapted and differ from ancestral populations in adjacent nonsulfidic habitats in a number of physiological, morphological, behavioral, and life-history traits (83, 86, 170). Most importantly, sulfide spring populations can tolerate H₂S concentrations that are orders of magnitudes higher than what is

considered lethal for most metazoans, while ancestral populations are susceptible to the toxic effects of H₂S over short periods of time (83, 135), indicating strong survival selection that impacts fitness across small spatial scales. In addition, sulfide spring populations are reproductively isolated from adjacent populations in nonsulfidic water, with low levels of gene flow and high genetic differentiation despite small spatial scales (in some instances <100 m) and an absence of physical barriers that prevent fish movement (135). Reproductive isolation is in part mediated by natural and sexual selection against migrants (135, 171).

Comparative genomic and transcriptomic analyses of *P. mexicana* populations from sulfidic and nonsulfidic habitats have provided insights into mechanisms that potentially underlie tolerance to toxic levels of H₂S (106, 159, 164, 172). Collectively, these studies have indicated that modification of mitochondrial function may be critical in mediating adaptation to H₂S. Mitochondrial modifications may impact H₂S tolerance through two mechanisms, resistance and regulation (151). Resistance involves modification of the direct toxicity target (cytochrome c oxidase, COX) of H₂S and other components of the oxidative phosphorylation pathway (OxPhos). Regulation involves modification of physiological pathways associated with the maintenance of mitochondrial H₂S concentrations; most notably the mitochondrial sulfide:quinone oxidoreductase (SQR) pathway. Past analyses have provided evidence for both resistance and regulation, as multiple components of the OxPhos and SQR pathways exhibit evidence for selection and/or heritable changes in gene regulation (106, 159, 164, 172). However, the functional ramifications of amino acid substitutions and gene expression changes remain largely unknown.

Here, we hypothesized that the repeated modification of enzymes in the OxPhos and SQR pathways in *P. mexicana* populations from sulfidic habitats leads to an increased ability to

maintain mitochondrial function in the presence of H₂S. We tested this hypothesis through multiple, complementary analyses:

1. Modification of COX—the primary toxicity target in OxPhos—is predicted to make the enzyme more resistant to the effects of H₂S. Previous analyses have already found evidence for this prediction in some *P. mexicana* populations (157). We followed up on this study and quantified COX activity across a broad range of H₂S concentrations in multiple populations of *P. mexicana* from sulfidic and nonsulfidic habitats (see Section 2).
2. Modification of SQR—the first step in enzymatic H₂S oxidation—is predicted to increase the rate of H₂S detoxification. We tested this prediction by conducting enzyme activity assays, quantifying the rate at which H₂S is oxidized by SQR in multiple populations of *P. mexicana* from sulfidic and nonsulfidic habitats (see Section 2).
3. If regulation of mitochondrial H₂S is a primary mechanism of H₂S tolerance, *P. mexicana* from sulfidic habitats should be able to maintain low endogenous H₂S concentrations upon environmental exposure, whereas endogenous concentrations should increase in individuals from nonsulfidic habitats. We tested this prediction by experimentally exposing laboratory-reared individuals of *P. mexicana* to environmental H₂S and quantifying endogenous H₂S where it matters—in the mitochondria—using a novel mitochondria-targeted probe (MitoA) that can be deployed to measure H₂S *in vivo* (see Section 3).
4. If regulation of endogenous H₂S is a primary mechanism of H₂S tolerance, mitochondrial function should be maintained in the presence of H₂S even in sulfide

spring populations that do not exhibit an H₂S-resistant COX. We tested this prediction by quantifying mitochondrial respiration across multiple *P. mexicana* populations in presence and absence of H₂S *in vitro* (see Section 4).

5. We also asked whether adaptive alleles in *P. mexicana* from different sulfidic populations rose to high frequency through selection on standing genetic variation, or whether adaptive alleles arose independently in different sulfide spring populations through *de novo* mutations. To do so, we sequenced whole genomes of multiple *P. mexicana* populations to conduct local ancestry analyses (see Section 5).

Overall, our analyses in *P. mexicana* revealed that some sulfide spring populations have adaptive modifications to COX, an increased SQR activity, a higher capacity in maintaining low endogenous H₂S concentration upon environmental exposure, and an ability to maintain mitochondrial respiration in presence of H₂S irrespective of the presence of an H₂S-resistant toxicity target. Adaptive alleles at some loci (e.g., COX) arose independently in different populations, while there is also evidence for selection on standing genetic variation (e.g., genes associated with detoxification). Based on these findings, we asked whether other species that successfully colonized H₂S-rich habitats exhibit convergent modifications of genes associated with H₂S toxicity and detoxification. This was possible because sulfide springs are widely distributed across the globe (173), and species of the family Poeciliidae are among the few metazoans that have colonized and adapted to these extreme environments (152). Collecting species from multiple genera allowed for the investigation of mechanisms underlying the evolution of H₂S tolerance across broad phylogenetic scales (over 40 million years of divergence among lineages) and in different ecological and biogeographical contexts (Figure S1).

We hypothesized that convergent molecular modifications underlie the convergent evolution of H₂S tolerance across different lineages of poeciliid fishes. We sequenced transcriptomes of five to six individuals from each of 10 independent lineages of sulfide spring fishes—as well as closely related lineages from nonsulfidic habitats—to test the following predictions (see Section 6):

6. Genes associated with H₂S toxicity and detoxification should exhibit repeated changes of gene expression upon colonization of H₂S-rich habitats. We used phylogenetic comparative analyses to identify genes with convergent expression shifts in sulfide spring fishes.
7. Genes associated with H₂S toxicity and detoxification should exhibit evidence for positive selection upon colonization of H₂S-rich habitats. We used analyses of molecular evolution to identify convergent targets of selection in sulfide spring fishes.

Note that all procedures used were approved by the Institutional Animal Care and Use Committees at Kansas State University (protocol #3418, 3473, 3581, 3886, 3992) and Oklahoma State University (protocol #1015, 1102). All statistical analyses were conducted in R version 3.6.1 (174) unless otherwise stated.

Enzyme activity assays

Sample procurement

We collected fish from three population pairs of *Poecilia mexicana* from the Tacotalpa (Tac), Puyacatengo (Puy), and Pichucalco (Pich) drainages in Mexico, each including an H₂S-tolerant and ancestral, intolerant population (Table S1). All fish were collected using a seine (2 × 5 m, 3

mm mesh size), immediately euthanized, and livers were extracted. Liver tissues were immediately frozen in liquid nitrogen and stored at -80° C upon return to Kansas State University.

Cytochrome c oxidase (COX) activity

Preparation of reagents and chemicals

All chemicals used to make the mitochondrial isolation buffer, incubation buffer, and substrates were purchased from Sigma-Aldrich (St. Louis, MO, USA), and solutions were made following the methods of previously published studies on OxPhos enzyme activity (167, 175, 176). The mitochondrial isolation buffer was prepared with 140 mM KCl, 10mM EDTA, 5mM MgCl₂, 20mM Hepes, and 2% bovine serum albumin (pH 7.3). Mitochondrial pellets were resuspended in an isotonic solution containing 100 mM KCl, 25 mM K₂HPO₄, and 5 mM MgCl₂ (pH 7.4). The reaction solution consisted of 25 mM K₂HPO₄, 5 mM MgCl₂, 2.5 mg/ml BSA, 0.6 mM lauryl maltoside, and 50 μM reduced cytochrome c (175). H₂S was prepared with 1 mM Na₂S·9 H₂O and DDW purged of oxygen via bubbling of nitrogen under anoxic conditions. All solutions were prepared daily.

Isolation of mitochondria

For the isolation of mitochondria, 60 mg of liver tissue was placed directly into 500 μl of ice-cold mitochondrial isolation buffer and homogenized using a Dounce homogenizer (DWK Life Sciences, Millville, NJ, USA). An additional 500 μl of buffer was added to the sample prior to centrifugation. Homogenates were centrifuged at 600 g for 5 minutes at 4° C, and the supernatant was transferred to a new tube and centrifuged again at 9000 g for 5 minutes at 4° C. The pellet

was resuspended in 500 μ l of isotonic solution. 75 μ l of the sample was taken to measure the total protein concentration (μ g/ml) by using the BCA Assay reagent (Thermo Scientific Pierce, Rockford, IL, USA).

Measuring COX activity

COX activity was assayed using a 96-well plate spectrometer (BioTek Instruments Inc., Winooski, VT, USA), which allows for the measurement of change in absorbance of a reaction solution at different wavelengths and environmental parameters. Activity of COX is quantified following a decrease in absorbance at 550 nm resulting from the protein's oxidation of reduced cytochrome c (175, 176). Samples were assayed across a gradient of H₂S concentrations between 0 and 0.9 μ M in quadruplicate. Oxidation of cytochrome c was measured for 3 minutes at 11-second intervals and 25° C.

Statistical analyses

Variation in COX activity was analyzed using linear mixed-effects models as implemented in the LME4 package (177). Habitat type of origin (sulfidic or nonsulfidic) and drainage were used as factors, H₂S concentration as a covariate, and sample ID was designated as a random effect. Alternative models were assessed by using Akaike Information Criteria with finite sample correction (AIC_c) (178). Besides the model with the lowest AIC_c score, alternative models with Δ AIC_c < 2 were considered equally supported (179).

Sulfide:quinone oxireductase (SQR) activity

Preparation of reagents and solutions

All chemicals used to make the mitochondrial isolation buffer, incubation buffer, and substrates were purchased from Sigma-Aldrich (St. Louis, MO, USA), and solutions were made following the methods of Hildebrandt and Grieshaber (167). The mitochondrial isolation buffer was prepared with 250 mM sucrose, 10 mM triethanolamine, 1 mM EGTA, 2 mM K₂HPO₄, 2 mM KH₂PO₄, and double distilled water (DDW) at pH 7.4. Incubation buffer was prepared with 250 mM sucrose, 10 mM triethanolamine, 1 mM EGTA, 2 mM K₂HPO₄, 2 mM KH₂PO₄, 5 mM MgCl₂, and DDW at pH 7.4. The reaction solution consisted of 20 mM Tris-HCl (pH 8.0) and the substrates 2 mM KCN, 100 μM decyl-ubiquinone, and 1 mM H₂S. H₂S was prepared with 1 mM Na₂S·9 H₂O and DDW purged of oxygen via bubbling of nitrogen under anoxic conditions. Except for the H₂S solution, which were prepared fresh daily, all solutions were stored at 4° C until used.

Isolation of mitochondria

To isolate mitochondria, 60 mg of liver tissue was placed directly into 500 μl ice-cold isolation buffer. Liver samples were homogenized on ice using a Dounce homogenizer (DWK Life Sciences, Millville, NJ, USA). Homogenates were centrifuged at 600 g for 10 minutes at 4° C, and the supernatant of each sample was again centrifuged at 9000 g for 20 minutes at 4° C. The resulting pellets were then resuspended in 500 ml ice-cold incubation buffer. 75 μl of the sample was taken to measure the total protein concentration (μg/ml) by using the BCA Assay reagent (Thermo Scientific Pierce, Rockford, IL, USA).

Measuring SQR activity

SQR activity was assayed using a 96-well plate spectrometer (BioTek Instruments Inc., Winooski, VT, USA). SQR activity was quantified following the reduction of decyl-ubiquinone. This reaction is cyanide-dependent in the absence of thioredoxin and sulfite, requiring the addition of KCN to the reaction mixture (180). Each reaction consisted of 2 mM KCN, 20 mM Tris-HCl, 100 μ g/ml mitochondrial protein, decyl-ubiquinone, and H₂S. Samples were assayed across a gradient of H₂S concentrations (0, 10, 30, 50, 80, and 100 μ M) in duplicate. Reduction of decyl-ubiquinone was followed at 285 nm for 5 minutes using 50-second intervals at 25° C (167, 181).

Statistical analyses

Variation in SQR activity was analyzed using linear mixed-effects models as implemented in the LME4 package (177). Habitat type of origin (sulfidic or nonsulfidic) and drainage were used as factors, H₂S concentration as a covariate, and sample ID was designated as a random effect. Alternative models were assessed by using Akaike Information Criteria with finite sample correction (AIC_c) (178). Besides the model with the lowest AIC_c score, alternative models with Δ AIC_c < 2 were considered equally supported (179).

In vivo measurement of endogenous H₂S with MitoA

Sample procurement

Fish used in this portion of the study were common-garden-raised F1 individuals from two population pairs in Mexico, Rios Puyacatengo (Puy) and Tacotalpa (Tac). Fish of the third population pair (Rio Pichucalco, Pich) were not available in the laboratory, because they are

difficult to transport and maintain in aquaria. *Poecilia mexicana* were housed in 38-l tanks and maintained at 26° C with a 12h:12h light:dark cycle. Fish were fed *ad libitum* each day using commercial fish food and starved 24 h prior to experiments.

Preparation of reagents and solutions

The MitoA compounds (MitoA, MitoN, d₁₅-MitoA, and d₁₅-MitoN) used to quantify endogenous sulfide in this study were synthesized as previously described (158). A 10 mM stock solution of each MitoA compound was prepared with 200 proof ethanol. 60% acetonitrile was prepared with acetonitrile (Honeywell Research Chemicals, Mexico City, MX) and HPLC-grade water. H₂S solutions (0, 1, 3, 4, and 5 mM) were prepared as described above.

MitoA injection and H₂S exposure

To detect changes in endogenous H₂S upon environmental exposure, we used MitoA, a mitochondrial specific probe that is capable of detecting H₂S *in vivo* (158, 182). In brief, this probe is shown to readily accumulate within mitochondria due to its unique chemical structure, and upon binding to H₂S, it is converted to MitoN. MitoA and MitoN can then be quantified using tandem mass spectrometry, which allows for the analysis of change in H₂S concentration within specific tissues and whole organisms (158). Methods described in the following section were specifically developed for *P. mexicana* (182).

On the day of each experiment, the 10 mM MitoA stock solution was diluted in phosphate-buffered saline (Sigma-Aldrich, St. Louis, MO, USA). Each fish was briefly anaesthetized using MS-222 (Sigma-Aldrich, St. Louis, MO, USA), restrained using a wet paper towel, and 8 nmol of MitoA in a volume of 50 µl was injected into the peritoneum using an insulin syringe with a

31-G needle (Becton, Dickinson and Company, Franklin Lakes, NJ, USA). Immediately after injection, each fish was placed into a 1-l container holding 250 mL of aerated water situated in a 25° C water bath and allowed to acclimate for 1 hour prior to the start of the trial. After acclimation, each container was sealed, and peristaltic pumps were used to provide a continuous supply of the designated H₂S solution at a rate of 150 ml/h (107). Experimental exposures lasted 5 hours, when the final H₂S concentrations were measured and fish were euthanized.

Environmental H₂S concentrations were measured using a methylene blue assay (Hach Company, Loveland, CO, USA). Gill, liver, brain, and muscle tissues were sampled from fish and flash frozen in liquid nitrogen. Tissue samples were stored at -80° C until further analysis.

Extraction of MitoA and MitoN from tissues and LC-MS/MS analysis

The methods for extraction of MitoA and MitoN followed previous protocols established for poeciliid fish (182). Tissues were weighed, placed into tubes containing 210 µl of a 60% acetonitrile solution spiked with internal standards, and underwent two separate homogenizations using a bead homogenizer. Between homogenizations, samples were centrifuged at 16000 g for 10 minutes, and supernatants were collected. The supernatant was incubated at 4° C for 30 minutes to precipitate proteins before being recentrifuged. Supernatants were then loaded onto 96-well Millipore Multiscreen filter plates (44 µm pore size) and centrifuged at 1100 g for 10 minutes. Filtrates were added to new collection tubes, dried using a SpeedVac vacuum concentrator, and stored until LC-MS/MS analysis.

LC-MS/MS analysis of tissue samples relied on the same methods used in Arndt et al. (158). Standard curves were generated using known amounts of MitoA and MitoN to calculate concentrations of each compound inside tissues, and the peak area of MitoA, MitoN, and

standards were quantified using MASSLYNX version 4.1 (Waters Corporation, Milford, MA, USA).

Statistical analyses

Since we were interested in how endogenous H₂S concentrations in different organs change upon environmental exposure, MitoN/MitoA ratios were standardized to the mean ratio of each organ and population. Variation in standardized MitoN/MitoA ratios was then analyzed using linear mixed-effects models as implemented in the LME4 package (177). Habitat type of origin (sulfidic or nonsulfidic), drainage, and H₂S concentration were used as predictor variables. Organ type and individual ID were designated as random effects. Alternative models were assessed by using Akaike Information Criteria with finite sample correction (AIC_c) (178). Besides the model with the lowest AIC_c score, alternative models with $\Delta\text{AIC}_c < 2$ were considered equally supported (179).

Mitochondrial Function

Sample procurement

This portion of the study focused on three sulfidic/nonsulfidic population pairs of *Poecilia mexicana* complex from the Rios Tacotalpa, Puyacatengo, and Pichucalco drainages in Mexico (Table S1). Fish were collected in their natural habitats using seines, transported to the laboratory at Oklahoma State University, and used for experiments within a few weeks of their capture.

Preparation of reagents and solutions

All chemicals that used to make mitochondrial isolation buffer (MSHE+BSA), mitochondrial assay solution (MAS, 3X) and substrates were purchased from Sigma-Aldrich (St. Louis, MO, USA). MSHE+BSA was prepared with 70 mM sucrose, 210 mM mannitol, 5 mM HEPES, 1 mM EGTA, 0.5% (w/v) fatty acid-free bovine serum albumin (BSA), and DDW. MAS, 3X was prepared with 210 mM sucrose, 660 mM mannitol, 30 mM KH_2PO_4 , 15 mM MgCl_2 , 6 mM HEPES, 3 mM EGTA, 0.6% (w/v) fatty acid free BSA, and DDW. 3X MAS was then diluted to make 1X MAS, which was used for the preparation of substrates, ADP, and respiration reagents. As substrates, 0.5 M succinate, 0.5 M malate, 0.5 M pyruvate, and 40 mM ADP were prepared with DDW. As respiration reagents, 10 μM oligomycin, 10 μM antimycin A/rotenone mix, and 3 μM FCCP [carbonyl cyanide 4-(trifluoromethoxy)-phenylhydrazone] (Seahorse XF Cell Mito Stress Test Kit, Santa Clara, CA, USA) were prepared with 1X MAS. All reagents and solutions were adjusted to pH 7.2 with potassium hydroxide. Except for the respiration reagents, which were prepared fresh on the day of each experiment, solutions were stored at 4° C until used.

Isolation of mitochondria

To isolate mitochondria, fish were euthanized and dissected to isolate livers, which were added to 500 μl MSHE+BSA and stored on ice. Due to the small size of the study species, livers from multiple individuals were pooled to obtain at least 60 mg of tissue, which provided a sufficient amount of mitochondria to run one coupling assay (see below). Liver samples were homogenized on ice with a Bio-Gen PRO200 (PRO Scientific, Oxford, CT, USA) for 10 seconds at the lowest speed, and then 500 μl MSHE+BSA were added to each homogenate. Homogenates were centrifuged at 600 g for 5 minutes at 4° C, and the filtered supernatant of each sample was again

centrifuged at 5000 g for 5 minutes at 4° C. The resulting pellets were then resuspended in 1 ml 1X MAS. 100 µl of the sample was taken to measure the total protein concentration (mg/ml) by using the BCA Assay reagent (Thermo Scientific Pierce, Rockford, IL, USA).

Mitochondrial coupling assay

Mitochondrial function was assayed using a Seahorse XFe96 Extracellular Flux Analyzer (Agilent Technologies, Santa Clara, CA, USA), which allows for the quantification of oxygen consumption rates (OCR) of isolated mitochondria in 96-well plates (183). Energy demand and substrate availability for mitochondria can be tightly controlled in this setup through the sequential addition of compounds that either stimulate or inhibit components of the electron transport chain: the addition of ADP stimulates oxygen consumption, oligomycin blocks ATP synthase, FCCP uncouples oxygen consumption from ATP synthesis, and antimycin A and rotenone block mitochondrial complexes I and III, respectively. Measuring mitochondrial OCR in presence of these different compounds during a coupling assay allows for the quantification of a variety of mitochondrial functions (184), and we measured basal respiration, maximal respiration, and spare capacity as indicators of mitochondrial function across a range of H₂S concentrations.

Prior to a coupling assay, the XFe96 sensor cartridge was pre-hydrated with calibrant solution (200 µl per well) overnight in a non-CO₂ 370c incubator. ADP, oligomycin, FCCP, and antimycin A/rotenone solutions (XF Cell Mito Stress Test Kit; Agilent Technologies) were then loaded into the four injection ports at the sensor cartridge for calibration. Meanwhile mitochondrial solution was added to each well of a 96-well plate (4 mg mitochondria per well) along with substrates (succinate, malate, and pyruvate) and 1X MAS. To test how mitochondrial

function was affected by the presence of H₂S, sodium hydrosulfide (NaSH) was added directly to each well as H₂S donor, just before a plate was placed in the analyzer. Overall, OCRs were measured at up to seven different doses of H₂S (5, 15, 30, 50, 60, 80 and 90 μM) along with a nonsulfidic control (0 μM). After the addition of H₂S, coupling assays were conducted following the manufacturer's protocols. Each isolate was measured across a range of H₂S concentrations, but tissue limitations prevented that all isolates were measured across all concentrations. All assays were run in triplicates, and OCR measurements were normalized by protein content.

Statistical analyses

To compare responses in mitochondrial function to H₂S between sulfidic and nonsulfidic populations, we employed drug response analysis. Separate n-parameter logistic regressions were fit for each mitochondrial isolate with the metrics of mitochondrial function (basal respiration, maximal respiration, and spare capacity) as dependent variables and H₂S concentration as independent variable, using the NPLR package (185). Based on regression models, AUC was estimated based on Simpson's rule, where higher AUC values represent an increased ability to maintain mitochondrial function in the presence of H₂S. AUC values inferred for different mitochondrial isolates were then used as a dependent variable in linear models using the STATS package (174). Alternative models were assessed by using Akaike Information Criteria with finite sample correction (AIC_c) (178). Besides the model with the lowest AIC_c score, alternative models with $\Delta AIC_c < 2$ were considered equally supported (179).

Comparative genomics and local ancestry analysis

To test hypotheses about the origin of adaptive alleles, we re-analyzed data from Brown et al. (164) (NCBI short-read archive BioProject no. PRJNA473350) and used the raw reads from the guppy genome NCBI short-read archive accession no. SRR1171024 (186). Detailed methods about sample collection, library preparation, whole-genome sequencing, and single-nucleotide polymorphism (SNP) calling and filtering can be found there, and we provide a summary of general approaches here.

Sample procurement

We collected one individual each from all sites known to harbor H₂S-tolerant populations of the *P. mexicana* species complex ($N=5$) as well as adjacent nonsulfidic habitats ($N=5$; see Table S1 for details). Specimens were sacrificed on site, and muscle tissue was isolated and preserved in 96% ethanol.

DNA extraction, library preparation, and sequencing

A MagAttract High Molecular Weight DNA extraction kit was used to extract DNA, and the amount of extracted DNA was quantified with a Qubit fluorometer. Library preparation was completed using an Illumina's TruSeq DNA PCR-Free LT Library Preparation Kit. DNA was sheared using a Covaris M220 with a 550-bp insert size. Quantitative polymerase chain reaction (qPCR) with the KAPA Library Quantification kit for Illumina Sequencing Platforms was used for determining pooling amounts. Two equimolar pools of the libraries were created using the estimated concentrations from the qPCR. Libraries were then sequenced on an Illumina HiSeq 2500 platform at the Washington State University Genomics Core with paired-end, 100 bp runs.

Mapping and variant calling

Reads were mapped to the *Xiphophorus maculatus* reference genome [RefSeq accession number: GCF_000241075.1 (102)] using the BWA-MEM algorithm from BWA version 0.7.12-r1039 (187). SNPs were then called on a per-individual basis in the Genome Analysis Toolkit (GATK v. 3.5) with the EMIT_ALL_SITES option in the UnifiedGenotyper (112-114). Individual vcfs were merged with vcfmerge (vcftools version 0.1.15) (188). Filtering in GATK was conducted with the recommended filters $QD < 2.0$, $FS > 60.0$, $MQ < 40.0$, $MQRankSum < -12.5$, and $ReadPosRankSum < -8.0$. Additional filtering with vcftools retained only biallelic sites (--min-alleles 2 and --max-alleles 2), with at least 10 reads supporting the call (--minDP 10), quality scores greater than 30 (--minQ 30), and less than 10% missing data (--max-missing 0.9).

Shared ancestry analysis

To identify outliers between sulfidic and nonsulfidic populations, we first calculated F_{ST} between the sulfidic and nonsulfidic samples, treating the two as separate groups. We also identified shared ancestry among lineages using Saguario (189), which uses a combination of a Hidden Markov Model and a self-organizing map to build ‘cacti’ (matrices of pairwise genetic distance between samples) that describe phylogenetic relationships among samples in specific genomic regions. Saguario builds an initial cactus (topology) based on the entire genome, then iteratively hypothesizes a new cactus for regions of the genome that do not fit the initial cactus. The process is iterated a user-defined number of times, and a new cactus is hypothesized in each iteration. To run Saguario, our vcf was converted into the hidden Markov model format using the VCF2HMMFeature command within Saguario (189). Saguario was executed for 29 iterations, which resulted in 30 cacti describing local ancestry patterns for segments of the genome.

Comparative Transcriptomics

Sample procurement

We collected specimens from multiple lineages of poeciliid fishes that have independently colonized H₂S-rich springs in the United States, Mexico, and the island of Hispaniola, as well as from geographically and phylogenetically proximate lineages in nonsulfidic habitats. This approach led to sets of closely related lineages found in sulfidic and nonsulfidic habitats, including populations of *Poecilia latipinna* and *Gambusia holbrooki* in Florida; populations of the *Poecilia mexicana* species complex (including *Poecilia mexicana*, *Poecilia sulphuraria*, and *Poecilia limantouri*) (99), the *Gambusia sexradiata* species complex (including *G. sexradiata* and *Gambusia eurystoma*) (100), *Pseudoxiphophorus bimaculatus*, and *Xiphophorus hellerii* in Mexico; as well as populations of the *Limia perugiae* species complex (*L. perugiae* and *Limia sulphurophila*) (101) in the Dominican Republic (see Table S1 for localities and habitat associations of specific lineages). All fish were caught using a seine (2 × 5 meters; 3 mm mesh size). Immediately upon capture, adult females ($N=5-6$ per site; Table S1) were euthanized, and the gills were extracted from both sides of the body using sterilized scissors and forceps. Tissues were then preserved in RNAlater (Ambion Inc.) for subsequent analysis in the laboratory. We focused on gill tissues, because they are in direct contact with the toxic environment (151), mediate a variety of physiological processes involved in the maintenance of homeostasis (104, 105), and exhibit strong transcriptional responses upon exposure to H₂S (106, 107). Note that data for some lineages of the *P. mexicana* species complex were reanalyzed from a previous study [GenBank BioProject accession number: PRJNA290391 (106)].

RNA extraction, cDNA library preparation, and sequencing

The general protocols for RNA extraction, library preparation and sequencing of all new samples followed procedures previously employed for *Poecilia* (106, 190). In brief, 10-30 mg of gill tissues from each individual were sealed in a Covaris TT1 TissueTube (Covaris, Inc., Woburn, MA, USA), frozen in liquid nitrogen, and pulverized. Total RNA was extracted from pulverized tissue using the NucleoSpin RNA kit (Machery-Nagel, Düren, Germany) following the manufacturer's protocol. mRNA isolation and cDNA library preparation were conducted using the NEBNext Poly(A) mRNA Magnetic Isolation Module (New England Biolabs, Inc., Ipswich, MA, USA) and NEBNext Ultra Directional RNA Library Prep Kit for Illumina (New England Biolabs, Inc., Ipswich, MA, USA) following the manufacturers' protocol with minor modifications. All cDNA libraries were individually barcoded, quantified using Qubit and an Agilent 2100 Bioanalyzer High Sensitivity DNA chip, and pooled in sets of 11-12 samples based on nanomolar concentrations. Samples were split into pools such that samples from different species and habitat types were sequenced together. There was no evidence for significant lane effects. Libraries were sequenced on an Illumina HiSeq 2500 with paired-end 101 base pair (bp) reads at the Washington State University Spokane Genomics Core. Due to low coverage, some samples were re-sequenced, and reads from separate runs were combined for each sample for data analysis.

Mapping and annotation

All raw RNA-seq reads were sorted by barcode and trimmed twice (quality 0 to remove adapters, followed by quality 24) using Trimalore! version 0.4.0 (108). Trimmed reads for all 118 individuals were mapped to the *Poecilia mexicana* reference genome [RefSeq accession number:

GCF_001443325.1 (191)] with an appended mitochondrial genome (GenBank Accession Number: KC992998.1) using BWA-MEM version 0.7.12 (192). An average of $92.6 \pm 3.6\%$ of reads mapped across all individuals (Table S13). We annotated genes from the *P. mexicana* reference genome by extracting the longest transcript per gene (using the perl script gff2fasta.pl¹) and comparing them to the entries in the human SWISSPROT database (critical E-value 0.001; access date 04/15/2017) using BLASTx (193). We retained the top BLAST hit for each gene based on the top high-scoring segment pair.

Phylogenetic analyses

We used a phylogenetic framework established in a previous study (24) for subsequent analyses. In brief, we created lineage specific consensus sequences from 167 random genes, which were then aligned using ClustalW version 2.1 (115). Besides the focal lineages (Table S1), the alignment included sequences from *Fundulus heteroclitus* [GenBank accession number: JXMV00000000.1 (103)], which was used as an outgroup. We used jModelTest 2 version 2.1.10 (116) to determine the best partition scheme based on the most likely model of DNA substitution among 88 candidate models. Genes were then concatenated and partitioned according to the substitution models indicated by jModelTest and then used in Maximum Likelihood analyses using RAxML version 8.2.9 (117). We ran RAxML analyses under the Rapid Bootstrap Algorithm with 1,000 bootstrap replicates and used a thorough maximum likelihood (ML) search with each partition assigned its own GTR + Γ + I model. These analyses recovered a robust hypothesis for evolutionary relationships among the focal taxa (bootstrap support generally $\geq 99\%$) that was consistent with previous phylogenetic studies of the family Poeciliidae (99, 118,

¹ Available from https://github.com/ISUgenomics/common_scripts/blob/master/gff2fasta.pl

119). The only groups with moderately supported relationships included the two populations of *G. sexradiata* and *G. eurystoma* (bootstrap support 60%), which have previously been found to represent a complex of closely related and recently diverged species (100). The best scoring ML tree was utilized for subsequent analyses of gene expression variation and molecular evolution.

Analysis of gene expression

We used cufflinks version 2.2.1 (120) to quantify the number of RNA-seq reads mapped (measured as fragments per kilobase of transcript per million mapped reads, FPKM) to each gene in the *P. mexicana* reference genome for each individual. We then removed genes that did not have at least two FPKM in 70 or more individuals across all species. We subsequently focused our expression analyses on the remaining 5,000 genes with the highest average FPKM among all individuals. A total of 4,538 genes from this focal set (91%) had an annotation based on the human SWISSPROT database, including in 3,764 unique entries as some *P. mexicana* genes matched to the same human gene (see Datasets S3-4).

Since pairwise comparisons of gene expression across a broad phylogenetic sampling can be problematic (194), we used a phylogenetic comparative approach for analyzing gene expression variation to explicitly account for the effects of evolutionary relationships. Specifically, we used individual-level expression data as dependent variables in Expression Variance and Evolution (EVE) models that identify genes exhibiting convergent shifts in expression upon the colonization of sulfidic habitats based on the phylogenetic hypothesis described above (195, 196). EVE models implement an extended Ornstein-Uhlenbeck process that incorporates within-species expression variance to test for branch-specific shifts in gene expression by comparing likelihoods that an expression parameter (θ_i) for a given gene is shared between two groups of

lineages versus θ_i for that gene being significantly different between the groups (195). We designated branches associated with lineages from sulfidic habitats as one group and those associated with nonsulfidic lineages as another group and then contrasted θ_i for each gene between these two groups. For each gene, we employed a likelihood ratio test (LRT_{θ}) contrasting the null hypothesis ($\theta_{\text{sulfidic}} = \theta_{\text{nonsulfidic}}$) to the alternative hypothesis ($\theta_{\text{sulfidic}} \neq \theta_{\text{nonsulfidic}}$) using a χ^2 distribution to assess statistical significance (195). To account for multiple testing, we calculated FDR adjusted P -values using the Benjamini-Hochberg procedure (197). To explore the biological functions of genes with evidence for convergent expression shifts upon the colonization of sulfide springs (Dataset S3), we used a Gene Ontology (GO) enrichment analysis (198) as implemented in GOrilla [p -value threshold: 0.0001, accessed 03/07/2019 (199)]. The transcriptome wide annotation set served as the reference set, and a total of 3,711 unique SWISSPROT annotations were associated with a term in the GO database.

While we use gene expression variation to detect patterns of convergent evolution, we acknowledge that gene expression patterns are notoriously plastic, and organismal responses to physicochemical stressors occur at multiple hierarchical levels, including short-term acclimatization, developmental plasticity, genetic variation, and their interactions (200). Comparisons of gene expression between H_2S -tolerant and non-tolerant populations of *P. mexicana* have indicated a heritable basis underlying gene expression responses to H_2S exposure, indicating that population differences are not a mere consequence of the environmental exposure history (172). However, our comparative data does not allow us to disentangle potential effects of plasticity in response to H_2S exposure and genetic differences among sulfidic and nonsulfidic lineages. Even if mechanisms underlying gene expression variation differ among lineages,

identifying sets of genes that are repeatedly recruited in H₂S responses still provides insights into the role of convergence in H₂S adaptation.

Analyses of molecular evolution

To identify genes with potential structural or functional changes in lineages from sulfidic habitats, we analyzed patterns of molecular evolution in 4,467 protein coding genes included in the analysis of gene expression. We first used the Genome Analysis Toolkit (GATK) version 3.5 (112) to realign mapped reads around indels (using the RealignerTargetCreator and IndelRealigner tools) and detect variants (using the UnifiedGenotyper tool) following GATK best practices (201, 202). Individuals were genotyped on a per-lineage basis with the EMIT_ALL_SITES output mode in the UnifiedGenotyper, creating a vcf file for each lineage. A custom pipeline was used to fill positions lacking sequence data in each vcf file with Ns. We used the setGT plugin of BCFtools version 1.3 (203) to designate the genotype at all variable sites as the major allele in each population vcf file. The coordinates for the coding sequences (CDS) were determined based on the *P. mexicana* gene annotation file (GTF) and subsequently used with the consensus tool in BCFtools to create population-specific consensus sequences across all individuals for each population. The consensus sequences for all exons of a gene were then concatenated, producing a single protein-coding sequence for each gene and lineage. The nucleotide sequences for all populations were aligned using the corresponding amino acid sequence with translatorX (204), which implements the MAFFT progressive alignment method (205), ultimately resulting in an in-frame multispecies alignment for each gene. Phylogenetic trees were constructed for each gene using a maximum likelihood approach implemented with the DNAML program in PHYLIP version 3.696 (206).

To identify genes under positive selection in sulfide spring lineages, we used branch models implemented in the program codeml from the PAML package version 4.9a (123). Branch models in codeml estimate variation in the rates of synonymous to synonymous substitutions (ω) for each codon in an alignment across branches in a phylogeny. We supplied codeml with the in-frame multispecies alignment and maximum likelihood tree (gene tree) for each of our focal genes, designating lineages from sulfidic habitats as foreground branches and lineages from nonsulfidic habitats as background branches in the tree file to test for shifts in ω between foreground and background branches. Specifically, we compared a two-ratio branch model, calculating separate ω values for the foreground and background groups (*i.e.*, sulfidic and nonsulfidic lineages) designated in the tree file (M2; model = 2, NSsites = 0), against a null model with a single ω estimated for the tree (M0; model = 0, NSsites = 0) for each gene. We assessed significance using a likelihood-ratio test, calculating the test statistic as two times the difference between the log-likelihood of the branch model and the-log likelihood of the null model, with *P*-values calculated from a X^2 approximation (207). To account for multiple testing, we calculated FDR adjusted *P*-values using the Benjamini-Hochberg procedure (see above) . Genes with evidence for positive selection across sulfidic lineages were used in a GO enrichment analysis, as described above (see Gene expression analysis).

Figures

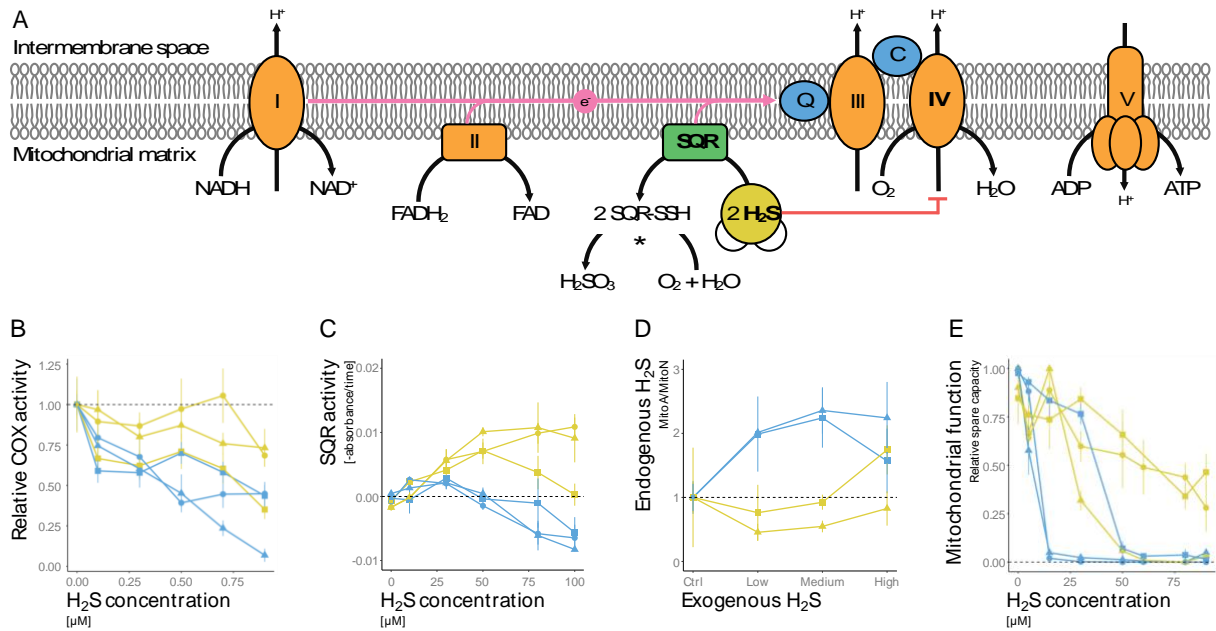


Figure 2-1: **A.** Physiological pathways associated with H₂S toxicity and detoxification are located in the inner mitochondrial membrane. H₂S inhibits OxPhos (orange enzymes) by binding to COX (Complex IV). H₂S can be detoxified through the nuclear-encoded SQR (green enzyme) and additional enzymes (indicated by asterisks). **B.** Relative activity of COX upon H₂S exposure, which was primarily explained by an interaction between habitat type of origin and ambient H₂S concentration (Tables S2-S3). **C.** Activity of SQR as a function of H₂S concentration, which was explained by an interaction between habitat type of origin and H₂S concentration (Tables S4-S5). **D.** Relative change in mitochondrial H₂S concentrations in the liver of live fish exposed to different levels of environmental H₂S. Variation in mitochondrial H₂S levels were explained by habitat type of origin and exogenous H₂S concentration (Tables S6-S7). **E.** Relative spare respiratory capacity of isolated liver mitochondria at different levels of H₂S. The interaction between habitat type of origin and drainage of origin best explained variation in spare respiratory capacity (Tables S11-S12). For all graphs, yellow colors denote *P. mexicana* from H₂S-rich

habitats, blue from nonsulfidic habitats. Symbols stand for populations from different river drainages (■: Tac; ▲: Puy; ●: Pich; see Figure S1).

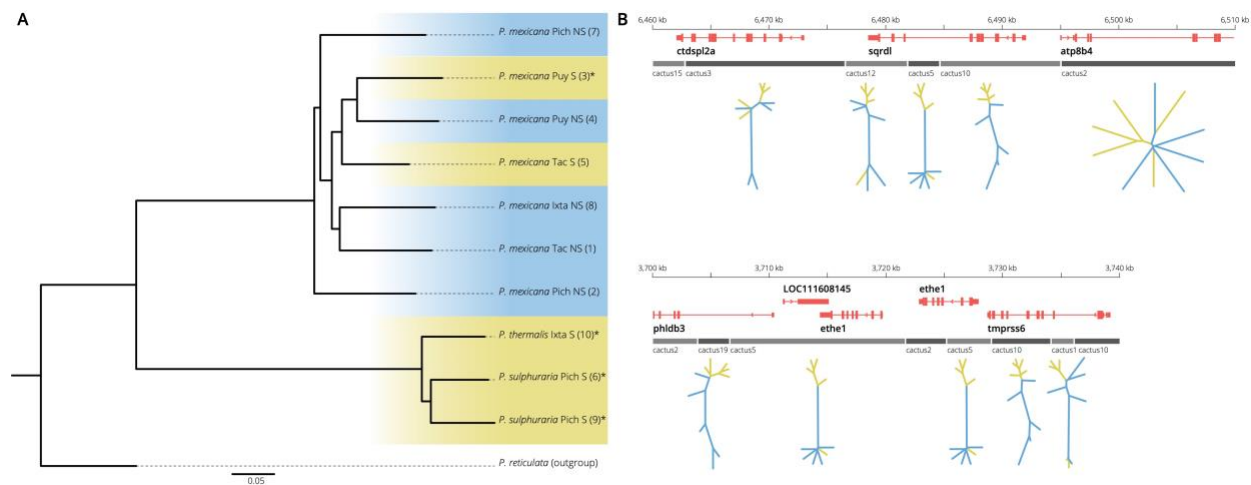


Figure 2-2: **A.** Phylogeny of different population in the *P. mexicana* species complex (with *P. reticulata* as an outgroup) based on genome-wide SNPs. Colors indicate sulfidic (yellow) and nonsulfidic (blue) lineages. **B.** Local ancestry patterns around genes encoding two enzymes involved in H₂S detoxification, *SQR* and *ETHE1*. Gray bars represent the local ancestry pattern (cactus) associated with each region. Unrooted trees represent local ancestry relationships, with sulfidic lineages colored in yellow and nonsulfidic lineages in blue. Cacti 10 and 19 show clear clustering by ecotype. In cacti 1, 5, and 12, four of five sulfidic individuals cluster together.

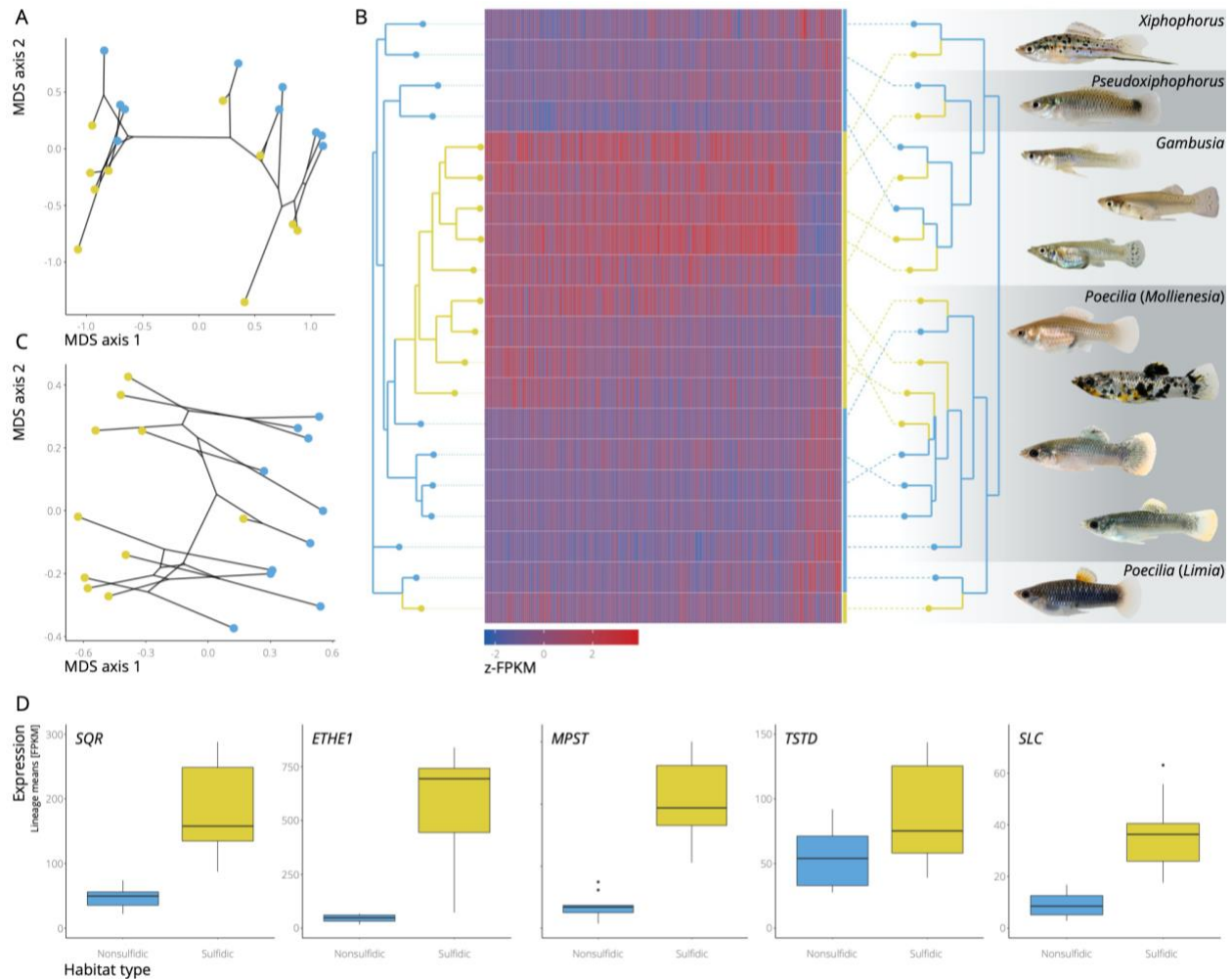


Figure 2-3: **A.** Multidimensional scaling (MDS) plot of overall gene expression patterns across 20 lineages of poeciliid fishes. Black lines represent phylogenetic relationships among lineages; color represents habitat type of origin (yellow: sulfidic; blue: nonsulfidic). **B.** Expression variation of 186 genes with evidence for convergent expression shifts (z -transformed FPKM). Colors represent expression levels as indicated by the scale. The neighbor-joining tree on the left organizes species based on expression similarity. The cladogram on the right shows the phylogenetic relationship among lineages. Pictures on the side are examples of sulfide spring fishes (from top to bottom): *X. hellerii*, *P. bimaculatus*, *G. holbrooki*, *G. sexradiata*, *G. eurystoma*, *P. latipinna*, *P. sulphuraria* (Pich), *P. mexicana* (Tac), *P. mexicana* (Puy), and *L.*

sulphurophila. **C.** MDS plot of the expression of 186 genes with evidence for convergent expression shifts. **D.** Boxplot with mean expression levels of different components of the SQR pathway across lineages from sulfidic (yellow) and nonsulfidic (blue) habitats.

Chapter 3 - Molecular consequences of metabolic function: Does genetic variation predict physiological differences?

Nick Barts, Chathurika Henpita, G. Alex Keithline, Lenin Arias-Rodriguez, Jennifer Shaw, and Michael Tobler

Abstract

Identifying the mechanisms underlying physiological adaptation remains an important task for the field of comparative physiology, as it can be difficult to infer the functional consequences of genetic variation. One way to identify if genetic variation shapes physiological function is to test for functional variation across biological scales. In this study, we leveraged pre-existing data that outlines genetic variation in oxidative phosphorylation (OxPhos) and sulfide detoxification genes in sulfide-tolerant and intolerant populations of *Poecilia mexicana* to test if modification at the genetic level shaped biochemical, mitochondrial, and organismal metabolic performance.

Analyses of OxPhos enzyme activity in lab-reared individuals revealed variation in activity was largely driven by H₂S and drainage of origin, while variation in detoxification enzyme activity was driven by H₂S and habitat. Mitochondrial respiration from wild-caught individuals measured under control conditions mirrored genetic variation in cytochrome c oxidase (COX), but these patterns were not reflected in whole organismal respiration data. Additionally, sulfide-tolerant populations were able to maintain aerobic respiration at lower levels of dissolved oxygen.

Overall, we find that although there is clear evidence for selection at the molecular level within metabolic pathways, these patterns of variation dissolve at higher levels of organization, and we

hypothesize that this is largely driven by the complex integration and regulation of physiological pathways.

Introduction

A fundamental goal of comparative physiology is to integrate data across temporal and biological scales to elucidate the mechanisms underlying the functional diversity of organisms (38). Until recently, this goal proved difficult to achieve when investigating the mechanisms of physiological adaptation in non-model organisms. Through powerful comparative approaches and innovations in technology, the field has begun to disentangle the mechanisms underlying adaptation in diverse systems, allowing scientists to experimentally address the grand challenges of comparative physiology outlined by Mykles and colleagues (209, 210). These grand challenges were identified as 1) the vertical integration of data collected across biological levels of organization to elucidate how genetic variation shapes physiological processes, 2) the horizontal integration of analyses that compare physiological processes across populations and species inhabiting similar ecosystems, and 3) the temporal integration of physiological processes during evolutionary change. In addition, they highlight the need for integrative and comparative studies to explore the predictability of variation both within organisms and ecosystems (209). Studies have addressed these challenges in diverse systems and ecological contexts, including host-microbiome interactions (211), regulation of molting in crustaceans (212, 213), and the plastic responses of gene expression and physiology in response to warming in polar organisms (214). These studies have highlighted the complexity of physiological responses organisms exhibit in response to stress and identified modifications of energy metabolism as a common theme in physiological adaptation regardless of ecological context (215, 216). This may be

unsurprising, as energy metabolism is a necessary biological process, and genetic variation within metabolic pathways has been frequently identified (217). A major question is how genetic variation in metabolic pathways contributes to functional variation across levels of organization and, if it does, how this variation mediates adaptation to diverse environmental conditions.

Aerobic metabolism is a fundamental biological process that underlies much of organismal form and function. Metabolic pathways are necessary to sustain fitness-related processes, such as growth, reproduction, and maintenance of homeostasis in response to environmental perturbation (218-220), and it can influence an organism's ability to tolerate novel and persistent stressors (221, 222). Indeed, selection on metabolic pathways in response to environmental stress has facilitated the evolution of adaptations in cellular and organismal physiologies and behaviors (218, 223-228). Much evidence for adaptation in metabolic pathways relates to alterations of the mitochondria's ability to modulate energy production (224). Mitochondria house the machinery necessary to conduct oxidative phosphorylation (OxPhos), the biochemical process that produces the majority of ATP in eukaryotic cells (229). Four of five enzymatic complexes in OxPhos are composed of subunits encoded in both the mitochondrial and nuclear genomes, and variation in either genome can result in changes in respiratory function of mitochondria (230, 231). Genetic variation of OxPhos complexes is well documented across many taxa, and some mitochondrial genes are frequently used as genetic barcodes to identify species (232). However, little is known about the functional ramifications that result from this variability (233-235).

The difficulty in understanding how genetic variation in metabolic processes leads to functional differences in metabolic performance lies in the interactive nature of metabolism (236, 237). Metabolic physiology is the result of complex interactions between biochemical, regulatory, and physiological systems (237-242). To address the role of metabolism in

adaptation, it is necessary to consider how metabolic processes function across biochemical and physiological systems as a function of genetic variation (217, 235, 236). Given the complexity of metabolic phenotypes, it is possible that variation at lower levels of organization is lost at the organismal level due to multiple regulatory steps, and vertical integration of data is necessary to identify these patterns (209, 218). Additionally, organisms inhabiting similar environmental conditions may adopt alternative evolutionary strategies to overcome environmental stress, and the horizontal integration of data collected from multiple, evolutionarily-independent lineages allows scientists to parse out patterns of evolution to identify whether evolution may be predictable or not (209).

Extreme environments provide ideal systems to explore the mechanisms that underlie biochemical and physiological adaptation (10, 11), including metabolism (243). The physiochemical stressors that characterize these habitats create unique challenges that organisms must overcome to persist, and their clear selective regimes enable hypothesis-driven tests that explore the influence of stressors across biological levels of organization (12, 244). Additionally, the existence of ancestral forms inhabiting environments lacking these stressors allow for powerful comparisons that assist in the identification of mechanisms mediating tolerance to stress. Consequently, extreme environments and the organisms that inhabit them provide unique opportunities to advance the field of comparative physiology.

Among the most extreme aquatic environments are habitats rich in hydrogen sulfide (H_2S), including deep sea hydrothermal vents, coastal salt marshes, and freshwater springs (14). H_2S is a naturally occurring compound that can be generated both by geochemical and biochemical processes (245). In aquatic habitats, H_2S readily reacts with available oxygen, resulting in low levels of dissolved oxygen available to organisms (18). Additionally, H_2S is a cellular toxicant

capable of inhibiting aerobic respiration. The primary toxic effect of H₂S is due to its binding to cytochrome *c* oxidase (COX), the fourth complex of OxPhos, which prevents the continued transport of electrons and disrupts aerobic ATP production (16, 66). Due to the importance of H₂S in the energy metabolism of ancient organisms (246), many organisms are equipped to combat H₂S toxicity at low levels via the sulfide:quinone oxidoreductase (SQR) pathway (19). SQR serves as the first step in H₂S detoxification, and oxidation of H₂S provides electrons that are fed into the electron transport chain, directly influencing mitochondrial respiration (19-21). Given the physiological constraints H₂S imposes on organisms, it is likely that modifications of both mitochondrial metabolic and detoxification pathways play pivotal roles in survival under toxic conditions.

Across Latin America, freshwater fishes within the family Poeciliidae have successfully colonized H₂S-rich springs on at least ten occasions (23, 24). Within this family, *Poecilia mexicana*, the Atlantic molly, has served as a model for exploring the diverse mechanisms that facilitate life in sulfidic habitats across biological levels of organization (13, 22, 25). *Poecilia mexicana* has independently colonized H₂S-rich springs in three river drainages of the Río Grijalva basin in Southern Mexico, and adjacent sulfide-tolerant and intolerant populations are phenotypically distinct and genetically isolated, exhibiting only low levels of gene flow (27, 33, 34, 84). Previous work has identified genomic and physiological modifications of important metabolic pathways, including OxPhos and associated H₂S detoxification pathways (22, 24, 68). Genes associated with H₂S detoxification were consistently upregulated in wild-caught populations of *P. mexicana*, and OxPhos complexes exhibited varying patterns of expression and evidence for positive selection (22). Components of Complexes I and II were consistently downregulated in sulfide-tolerant fish, and genomic analyses revealed amino acid substitutions in

cox1 and cox3, subunits of COX, in the sulfidic populations from the Puyacatengo and Pichucalco drainages, but not fish from the Tacotalpa drainage (22, 34, 68). Recent studies have begun to document that genetic variation in these pathways has functional ramifications. In particular, SQR activity was found to be greater in sulfide-tolerant lineages, and this is correlated with increased ability to regulate internal H₂S concentrations upon environmental exposure (36). COX activity was found to be unaffected by the presence of H₂S in lineages that exhibit evidence for positive selection on COX subunits, but was not maintained in Tacotalpa fish, just like in ancestral lineages (36, 68). Additionally, sulfide-tolerant populations are able to maintain mitochondrial respiration in presence of H₂S, indicating that these functional differences may have continuous effects across levels of biological organization (36). Importantly, these studies have identified that the mitochondrial metabolic and detoxification pathways are integral components of adaptation to H₂S-rich habitats. However, it is unclear if the genetic consequences of these key adaptations influence other aspects of metabolic function (247).

The goal of this study was to assess the consequences of genetic variation on the function of mitochondrial and organismal metabolism using the grand challenges of comparative physiology as a guiding framework. We conducted a series of experiments on two focal sulfide-spring lineages of *P. mexicana* that differ in their mitochondrial physiology, the Puyacatengo (Puy) and Tacotalpa (Tac), to address the following questions: 1) Does previously documented genetic (248) variation of OxPhos complexes and SQR (36, 68) influence enzyme activity in the presence of H₂S? 2) Do differences in enzymatic function result in measurable differences of mitochondrial respiration? 3) Does variation at lower levels of organization shape organismal metabolic function? Ultimately, we tested if evidence of genetic variation in metabolic pathways

has consistent effects on physiological processes at higher levels of biological organization and if patterns of variation are similar across different populations.

Methods

Study sites and fish care

P. mexicana were collected from four sites near the city of Teapa, Tabasco, Mexico in summers 2015 and 2017. Focal sulfide-tolerant and adjacent intolerant populations were collected from two tributaries of the Río Grijalva (Ríos Tacotalpa and Puyacatengo) located at the foothills of the Sierra Madre Occidental mountain range. Fish were caught with a seine (2 m x 5 m, 3 mm mesh size). Upon arrival to Kansas State University, fish were placed into 38 L aquaria with aerated, non-sulfidic water maintained at 26 °C with a 12 h light:dark cycle. All cellular and organismal respiration experiments were conducted on wild-caught fish, while enzyme assays were conducted on tissues collected from F1 individuals. Fish were fed *ad libitum* each day using commercial fish food and starved 24 hours prior to experimentation.

Measuring activity of OxPhos and detoxification enzymes

Populations of *P. mexicana* exhibit both convergent and divergent patterns of gene expression and positive selection of OxPhos complexes and SQR, and a goal of this study is to characterize functional differences in enzyme activity as a product of that genetic variation. Specific predictions for each enzyme are detailed in Table 1. Additionally, we wanted to characterize if functional differences observed in the COX and SQR activity of wild-caught fish are maintained in lab-reared individuals. We predict that given the evidence of selection on both enzyme complexes, patterns of activity would remain the same as those seen in wild individuals.

Isolation of mitochondria

Fish were euthanized, and liver tissue was immediately dissected, frozen in liquid nitrogen, and stored at -80°C until the day of the assay. Due to size limitations of *P. mexicana*, liver samples were pooled to achieve a mass of at least 60 mg, which is known to provide a sufficient amount of mitochondria for activity assays (36). On the day of the experiment, pooled liver samples were placed into 500 μl of ice-cold isolation buffer. For oxidative phosphorylation enzymes, the buffer consisted of 140 mM KCl, 10mM ethylenediaminetetraacetic acid (EDTA), 5mM MgCl_2 , 20mM HEPES, and 2% bovine serum albumin (BSA) adjusted to pH 7.3. For SQR, the buffer consisted of 250 mM sucrose, 10 mM triethanolamine, 1 mM EGTA, 2 mM K_2HPO_4 , 2 mM KH_2PO_4 , and double distilled water (DDW) adjusted to pH 7.4. Tissues were homogenized using a Dounce homogenizer (DWK Life Sciences, Millville, NJ, USA) before adding an additional 500 μl of buffer (20, 36, 37, 249). Tissue homogenates were centrifuged at 600 g for 5 minutes at 4°C , and the supernatant was collected and transferred to a new tube before being centrifuged again at 9000 g for 5 minutes at 4°C . The supernatant was removed and the mitochondrial pellet was resuspended in 500 μl of either isotonic (100 mM KCl, 25 mM K_2HPO_4 , and 5 mM MgCl_2 adjusted to pH 7.4; Complexes III and IV), hypotonic (25 mM K_2HPO_4 and 5 mM MgCl_2 adjusted to pH 7.4; Complexes I and II), or incubation (250 mM sucrose, 10 mM triethanolamine, 1 mM EGTA, 2 mM K_2HPO_4 , 2 mM KH_2PO_4 , 5 mM MgCl_2 , and double distilled water (DDW) adjusted to pH 7.4) medium (20, 37). Each sample underwent three freeze-thaw cycles prior to measuring total protein content using a BCA Assay (Thermo Scientific Pierce, Rockford, IL, USA).

Measurement of enzyme activity

All measurements were conducted using previously established protocols (20, 37, 249). Activity was measured at 25°C using a 96-well plate spectrophotometer at 11 s intervals (BioTek Instruments Inc., Winooski, VT, USA). Samples were measured across a gradient of H₂S concentrations (oxidative phosphorylation: 0-0.9 μM; SQR: 0-90 μM). All assays were measured in triplicate and background rates were subtracted from experimental data. To calculate activities of oxidative phosphorylation enzymes, we calculated the change in absorbance and used millimolar extinction coefficients of 6.22 mM⁻¹ cm⁻¹ for nicotinamide adenine dinucleotide (NADH), 19.1 mM⁻¹ cm⁻¹ for dichlorophenol indophenol (DCPIP), and 29.5 mM⁻¹ cm⁻¹ for cytochrome c. To calculate activity of SQR, we calculated the change in absorbance over the course of the reaction only.

Activity of Complex I was quantified following an increase in absorbance at 600 nm resulting from the protein's oxidation of NADH and reduction of DCPIP. The assay buffer consisted of 25 mM K₂HPO₄, 25 μM DCPIP, 65 μM ubiquinone-2, 0.2 mM NADH, 2 μg/mL antimycin, 2 mM KCN, and 2 μg/mL rotenone. Complex II activity was quantified following a decrease in absorbance at 600 nm resulting from the oxidation of ubiquinone and the reduction of DCPIP. The assay buffer consisted of 25 mM K₂HPO₄, 25 μM DCPIP, 65 μM ubiquinone-2, 20 mM succinate, 2 μg/mL antimycin, and 2 mM KCN. Activity of Complex III was quantified following the increase in absorbance that results from the reduction of cytochrome c. The assay buffer consisted of 25 mM K₂HPO₄, 5 mM MgCl₂, 2.5 mg/mL BSA, 0.6 mM lauryl maltoside, 35 μM reduced ubiquinol-2, 50 μM oxidized cytochrome c, 2 μg/mL rotenone, 2 mM KCN, and 2 μg/mL antimycin A. Complex IV activity was quantified following the decrease in absorbance that results from the oxidation of cytochrome c. The assay buffer consisted of of 25 mM

K₂HPO₄, 5 mM MgCl₂, 2.5 mg/ml BSA, 0.6 mM lauryl maltoside, and 50 μM reduced cytochrome c. SQR activity was quantified following the reduction of decyl-ubiquinone. Each reaction consisted of 2 mM KCN, 20 mM Tris-HCl, 100 μg/ml mitochondrial protein, decyl-ubiquinone, and H₂S.

Mitochondrial respiration

Aerobic respiration occurs within mitochondria as a function of OxPhos, and therefore, we predicted that differences in enzyme activity of OxPhos enzymes would have consequences on mitochondrial respiratory function. Specifically, we predicted that PuyS individuals would exhibit increased respiratory costs under control conditions due to genetic variation that has led to a sulfide-resistant COX. Analyses of mitochondrial respiration under non-sulfidic, normoxic conditions were conducted on previously published data investigating the relative effects of H₂S exposure on mitochondrial respiration, and more specific information on the methods used to isolate and measure mitochondria function is detailed there (Greenway et al., 2020).

Isolation of mitochondria

To isolate mitochondria, fish were euthanized and dissected to isolate livers, which were added to 500 μl MSHE-BSA (70 mM sucrose, 210 mM mannitol, 5 mM HEPES, 1 mM EGTA, 0.5% (w/v) fatty acid-free BSA, and DDW) and stored on ice. Liver samples were homogenized on ice with a Bio-Gen PRO200 (PRO Scientific, Oxford, CT, USA) for 10 s at the lowest speed prior to the addition of 500 μl MSHE-BSA to each homogenate. Homogenates were centrifuged at 600 g for 5 minutes at 4 °C, and the filtered supernatant was centrifuged for an additional 5 minutes at 5000 g. The mitochondrial pellets were resuspended in 1 ml 1X MAS (210 mM sucrose, 660

mM mannitol, 30 mM KH₂PO₄, 15 mM MgCl₂, 6 mM HEPES, 3 mM EGTA, 0.6% (w/v) fatty acid free BSA, and DDW). Total protein concentration was measured using 100 µl of each sample using a BCA Assay Reagent (Thermo Scientific Pierce, Rockford, IL, USA) taken prior to measuring mitochondrial respiration.

Mitochondrial coupling assay

Mitochondrial respiration (measured as oxygen consumption rates; OCR) was assayed using a Seahorse XFe96 Extracellular Flux Analyzer (Agilent Technologies, Santa Clara, CA, USA)(250). This method allows for the tight control of substrate availability necessary to measure basal and maximal respiration, as well as spare respiratory capacity (251). The Xfe96 cartridge was calibrated prior to each assay by pre-hydrating with calibrant solution and incubating at 37°C overnight. ADP (40 mM), oligomycin (10 µM), FCCP (3 µM), and antimycin A/rotenone mix (10 µM) were loaded into the injection ports of the sensor cartridge, and mitochondrial solution (4 mg mitochondria per well) was added to each of 96 wells along with the substrates succinate, malate, and pyruvate (all 0.5 M) and 1X MAS. Coupling assays were run in triplicate and measurements were normalized by protein content.

Whole organism performance

It has been demonstrated that mitochondrial phenotypes may influence organismal phenotypes, such as metabolic function under different thermal scenarios and starvation resistance (236, 252). Therefore, we predicted that variation in mitochondrial respiration would result in observable differences in whole organismal metabolism. In particular, we predicted that PuyS would have a reduced aerobic scope (AS), either due to an increased standard metabolic rate (SMR) or

increased maximum metabolic rate (MMR). More generally, we predicted that SMR and MMR would be reduced in sulfide-tolerant populations due to the results of previous research and potential costs of limiting in an oxygen-limited environment (31, 32). Additionally, we tested the resilience of aerobic metabolic function under hypoxia to determine if local adaptation to H₂S-rich environments resulted in the increased ability to maintain aerobic metabolism under oxygen stress.

Measuring aerobic scope

Oxygen consumption rates (MO₂; mg O₂ g⁻¹ h⁻¹) were measured using intermittent flow respirometry and methods previously established for measuring respiration in small fishes (253-256). MO₂ measurements were used to calculate SMR, MMR, and AS for N = 10 fish per population. A four-chambered intermittent flow respirometer (Loligo Systems, Tjele, Denmark) was used to measure metabolic rates (256). Respirometry chambers were housed inside a circulating water bath held at 24 °C, and a submersible pump was used to continuously provide aerated water to the water bath from a reservoir tank (≥95% O₂ saturation). A four-chambered oxygen meter with fiber-optic mini sensors allowed for continuous measurements of oxygen consumption over the course of the experiment. Oxygen sensors were calibrated each week following manufacturer's protocol. To account for background respiration, one chamber remained empty and the slope was subtracted from the experimental measurements (254). The respirometry chambers and water bath were cleaned with bleach after each use to minimize background respiration overall.

Fish mass and standard length were collected prior to introduction the respirometer. Individual fish were placed inside 90 mL cylindrical respirometry chambers and allowed to

acclimate for at least one hour prior to the start of the experiment. Each chamber was connected to a flush pump that circulated water from the water bath into the chamber during open, flush circuits and a recirculating pump that circulated water within the chamber during closed, measurement circuits. These circuits were controlled by AutoResp software (Loligo Systems, Tjele, Denmark), and consisted of 120 s flush, 20 s wait, and 480 s measurement periods. Oxygen measurements were collected every second, and resting measures of metabolism were collected overnight for approximately 14 hours total (253, 256). MO_2 was calculated from the slope of the reduction of oxygen content (kPa) over time (h). SMR was calculated as the average of the 10 lowest MO_2 values collected over this 14 h period.

MMR measurements were collected upon completion of the 14 h resting period. To elicit MMR, fish were removed from the respirometer one at a time and placed into a circular arena containing water of the same oxygen content and temperature as the water bath (253, 254). Fish were chased using the handle of a dipnet in the arena until they exhibited exhaustion, which we defined as the onset of burst swimming as opposed to sustained swimming, or until 10 minutes had passed (253, 256). Fish were immediately returned to the respirometry chamber to quantify MMR. We used the average of the three highest values obtained following reintroduction to calculate MMR (254). AS was calculated as the absolute difference between MMR and SMR (254, 257).

Measurement of critical oxygen tension

The critical oxygen tension of *P. mexicana* was measured following similar protocols to that described above for calculating SMR and those described in a recent investigation in the hypoxia tolerance of fish from the family Fundulidae (258). Fish were housed inside the respirometry

chambers for 14 h to establish SMR under normoxia prior to initiation of a progressive stepwise hypoxia protocol (258). Using nitrogen gas to establish hypoxia, we decreased oxygen concentrations by 0.5 mg O₂ L⁻¹ every 20 minutes, allowing for two measurements at each concentration. MO₂ was calculated for each fish until loss of equilibrium was reached.

Statistical analyses

Variation in absolute and normalized oxidative phosphorylation enzyme and absolute variation of SQR activity was analyzed using linear mixed-effects models as performed in the LME4 package in R v. 4.0.2 (36, 259). Absolute measures of enzyme activity were analyzed to identify the natural magnitude of variation in activity under control conditions, while normalized activity was necessary to measure relative change in function as a response to H₂S. Drainage and habitat type of origin (sulfidic or nonsulfidic streams) were used as factors, H₂S concentration as a covariate, and sample ID was assigned as a random effect. Similarly, we used linear mixed-effects models to analyze mitochondrial respiration, whole organismal respiration, and critical oxygen tension with drainage and habitat type of origin used as factors and sample ID as a random effect (259). Data for SMR, MMR, and AS were ln-transformed prior to analyses to meet assumptions of normality. To calculate P_{crit}, we (1) plotted the relationship between environmental oxygen concentration (mg O₂ L⁻¹) and MO₂ (mg O₂ g⁻¹ h⁻¹), (2) detected the environmental oxygen concentration and MO₂ at the breakpoint in the plot using the ‘segmented’ package in R (260), and (3) calculated the significance of the breakpoint using a Davies test with 95% confidence intervals (261). MO₂ values obtained at environmental O₂ concentrations above 6.0 mg O₂ L⁻¹ were excluded from these analyses as they are likely not representative of SMR MO₂ values (262). A model selection approach was used by assessing alternative models using

Akaike Information Criteria with finite sample correction (AICc) (263). Models with a $\Delta\text{AICc} \leq 2$ were considered equally supported (263).

Results

OxPhos and SQR enzyme activity

We found that absolute enzyme activity under control conditions did not significantly differ across drainages or habitats, indicating that under non-stressful environments there are no significant differences in enzyme activity across populations. However, we did document significant variation in relative enzyme activity between habitats and drainages in response to the presence of H₂S (Table 2). Model selection identified that the three-way interaction of drainage \times habitat \times H₂S concentration best described the relative activity of Complexes I and II (Table 2, Figure 1A, B). Activity in both enzymes increased when compared to the control, which contradicts our prediction that activity in these complexes should decrease in response to H₂S (Table 1). Interestingly, we observed an increase in Complex II activity until H₂S concentrations exceeded 0.3 μM , at which point Puy populations continued to increase in activity with PuyS having the highest activity overall. This suggests that at least for Complex II, Puy populations exhibit higher activities than Tac populations in response to H₂S exposure.

Complex III activity was best explained by the model including a drainage \times H₂S concentration interaction (Table 2). At 0.5 μM H₂S, Tac and Puy lineages begin to separate in activity, at which point Tac populations exhibit higher activity of Complex III than Puy populations (Figure 1C). Activities of Tac populations match our prediction that Complex III activity may increase in the presence of H₂S, whereas Puy populations appear to respond to a milder degree and actually decrease or maintain Complex III activity over time.

Relative activity of Complex IV was best explained by the models containing H₂S concentration and H₂S concentration + drainage effects (Table 2). Complex IV activity was consistently highest in PuyS except at 0.3 μM in which both Puy populations exhibited higher activity than the Tac populations (Figure 1D). Despite this pattern, models did not indicate an effect of habitat, and therefore, our predictions that COX activity is maintained higher in PuyS over all other populations was not met.

SQR activity varied across H₂S concentrations and between sulfidic and non-sulfidic populations, and the model was best supported by H₂S and habitat + H₂S (Table 2). Activity gradually increased in all individuals, as predicted by the detoxification function of SQR; however, activity was higher in sulfide-tolerant populations at most concentrations (Figure 2). Therefore, SQR activity observed in our study matches our predictions and corroborates differences in SQR activity identified in a previous study (36). Overall, our results reveal the idiosyncratic effects of H₂S exposure on OxPhos enzyme activity, highlighting functional differences between both drainages and habitats.

Mitochondrial respiration

Population differences in basal and maximal respiratory capacity were measured in the mitochondria of wild-caught fish, and spare respiratory capacity was calculated using these two values. Results indicated a habitat × drainage effect for all three measures, in which PuyS consistently exhibited higher mitochondrial respiration (Table 3; Figure 3 A-C).

Whole organism metabolism

We used intermittent-flow respirometry to measure differences in the standard and maximal metabolic rates of wild-caught fish, and these values were used to calculate aerobic scope. Our hypotheses and predictions were not supported by the model selection results, which indicated that the null model best fit the variation observed in all three metrics despite a tendency for higher SMR values exhibited by PuyS (Table 4; Figure 3 D-F).

We predicted that sulfide-tolerant populations would have a lower P_{crit} value due to the hypoxic conditions these organisms inhabit, and our analyses support our hypothesis and prediction (Table 4). The highest supported model indicated a habitat effect on P_{crit} , and the values of P_{crit} are significantly lower in sulfide-tolerant fishes (Figure 4). This suggests that despite the unequal differences in mitochondrial respiratory function, organismal performance and the ability to maintain aerobic respiration in the presence of low oxygen conditions do not differ across tolerant populations of *P. mexicana*.

Discussion

Investigations into the mechanisms mediating adaptation often infer functional differences based on genetic and transcriptomic data (264). However, not all genetic variation leads to functional variation at higher levels of biological organization (39), necessitating multi-level studies to identify consequences for organismal function and mechanisms of adaptation (38, 209). We tested the consequences of known genetic variation (22, 30, 34, 36, 68) on enzymatic, mitochondrial, and organismal metabolic function in sulfide-tolerant and intolerant *P. mexicana* from two evolutionarily independent lineages. Physiological function across levels of organization exhibited population-specific variation. In particular, the activity of different

OxPhos complexes differed between habitat types, drainages, and across H₂S concentrations, but the observed patterns did not necessarily match a priori predictions. Additionally, functional differences in mitochondrial respiratory function that were not mirrored in whole organismal data. This study highlights that we cannot make generalizations about function across levels of organization or across populations inhabiting similar environmental conditions. Additionally, although particular physiological pathways may be predictable targets of selection under environmental constraints, the ways in which these processes are modified may be highly variable.

Variation in OxPhos and detoxification enzyme activity across populations and H₂S exposure

Investigations into the molecular mechanisms underlying H₂S tolerance in *P. mexicana* have identified both OxPhos and the SQR pathway as important processes mediating adaptation (22, 34, 68), and both Complex IV of OxPhos and SQR exhibit functional variation across sulfide spring populations, possibly as a result of genetic variation (36). Although our study did not identify among-population variation in any of the enzymes tested under control conditions (absolute enzyme activity in the absence of sulfide), our investigation did document variation in relative enzyme activity in response to H₂S concentrations. Interestingly, COX activity in lab-reared individuals differed across drainages instead of habitats, indicating that despite known genetic variation, PuyS fish did not exhibit an H₂S-tolerant COX (36, 68). One possibility is a lack of statistical power within our data, since the general trend of PuyS retaining higher activity in presence of H₂S is still evident. *Poecilia mexicana* are small fish, and pooling of individual livers is required to obtain enough mitochondria for enzyme activity analyses, making obtaining

large sample sizes challenging in this system. Alternatively, some putative adaptations may be context-dependent (265, 266). For example, it is possible that the role of COX in aerobic energy production may make functional resilience in the presence of H₂S costly to maintain in absence of sulfide, and different isoforms of COX subunits may be expressed under environmental conditions (267). Future investigations should use extended acclimation periods of common-garden-raised individuals to determine potential environmental effects on COX assembly and activity.

Wild populations of TacS and PuyS individuals exhibit evidence of positive selection, heritable upregulation of detoxification genes, and functional differences in SQR activity, and these functional differences were mirrored in our analyses (30, 34, 36). Lab-reared sulfide-tolerant populations generally exhibited higher SQR activities as H₂S concentrations increased, indicating similar functional differences found in wild-caught fish. Given the near ubiquitous identification of SQR as an important factor mitigating H₂S toxicity (19, 20, 36), its increased ability to oxidize H₂S may have important functional consequences for OxPhos function. Oxidation of H₂S by SQR introduces additional electrons into the ETC, which may result in stoichiometric imbalances if Complexes I and II continue to introduce electrons and/or if Complex III does not increase oxidation of ubiquinone (21, 246, 268, 269). Therefore, organisms may have to regulate the function of other OxPhos complexes in the presence of H₂S, a process underexplored in natural populations of sulfide-tolerant organisms.

Complexes I and II initiate the first steps of the electron transport chain by oxidizing NADH and FADH₂, respectively. Under normal circumstances, these electrons are used to reduce ubiquinone and ultimately generate the electrochemical gradient necessary to produce ATP aerobically. Given their function, we predicted that Complexes I and II would exhibit no

differences or decreased activity in the presence of H₂S and that their activity would be lower in sulfide-tolerant lineages to offset the potential imbalance caused by electrons derived from H₂S oxidation (Table 1). Contrary to our predictions, both enzymes increased activity as a response to H₂S, although the degree to which they increased activity varied between drainages and habitats. Patterns of activity indicated that Tac populations have higher Complex I activity and lower Complex II activity at higher levels of H₂S exposure when compared to Puy (Figure 1 A, C). Intriguingly, Complexes I and II can work in reverse when exposed to H₂S, transferring excess electrons back to their substrates when COX is blocked (270, 271). When complexes I and II operate in the opposite direction, they consequently assist in sulfide oxidation and no longer compete with SQR for the addition of electrons into the transport chain (272). This process begets an interesting question: does the increased activity of these enzymes potentially facilitate reverse electron flow that may be adaptive in the presence of H₂S? Future research investigating the redox state of organisms tolerant of and exposed to high concentrations of H₂S should consequently test for this as a possible explanation. Alternatively, the substrate used to measure activity of Complexes I and II (DCPIP) is reactive with H₂S, which may explain observed increases in activity. However, we controlled for background rates of substrate depletion in our analyses, suggesting this is unlikely the case.

A potential consequence of the identified increases in activity of Complexes I and II and SQR is an abundance of electrons within the ETC when H₂S concentrations are high, which may necessitate an increase in the reduction of quinone to maintain stoichiometric balance (272). Relative activity of Complex III exhibited drainage-specific differences similar to that of Complex I, in which activity was higher in Tac populations than in Puy populations (Figure 1E). These results suggest that Tac populations may rely on increased reductive capabilities of

Complex III to a greater extent than Puy population. Overall, our results suggest that there are two potential mechanisms that protect mitochondrial function in the presence of H₂S, 1) reverse electron flow may occur at either Complex I or II to decrease flow of electrons into the ETC, and 2) Complex III may increase activity to more efficiently reduce cytochrome c, which provides a mechanisms to temporarily store electrons until it can be oxidized by COX (269). Future studies need to investigate whether these observed lineage-specific patterns in activity conduct either of these functions and further validate if differences exist between lineages.

Overall, these data highlight the complexity of metabolism at the molecular level. OxPhos enzyme activity most often exhibited drainage specific differences, suggesting that independent lineages of *P. mexicana* may have evolved different biochemical mechanisms in coping with exposure to H₂S, perhaps due to random change or environmental variation across drainages. Additionally, findings from this study suggest that putatively adaptive physiological differences observed in wild-caught populations may be environmentally dependent given that genetic variation in natural populations known to influence COX activity did not appear to provide a significant difference in the ability of lab-reared individuals to maintain COX function, and this has important implications for inferences made in laboratory studies.

Mitochondrial and organismal respiration

Given the absence of significant variation in absolute enzyme activity under control conditions in all OxPhos complexes, one may predict that respiration should not differ among populations at either the mitochondrial or organismal levels. We hypothesized that observed variation in mitochondrial respiration and COX function in the presence of H₂S may have functional consequences on respiration under normoxic, non-sulfidic conditions (36). Interestingly, despite

a lack of variation in OxPhos enzyme activity under control conditions, PuyS mitochondria exhibited higher basal, maximal, and, spare respiratory capacity under normoxic conditions. Generally, increased basal respiration may be considered costly due to increased costs of maintaining basic functions; however, with concomitant increases in maximal respiratory rates, these costs can be offset (273, 274). This indicates that increased basal respiration does not come at a cost of decreased mitochondrial efficiency, and the increased spare respiratory capacity suggests an increase in the ability to generate ATP in PuyS cells (275).

Modification of mitochondrial respiratory function may have consequences on organismal respiration and has been identified as the basis for adaptive variation in aerobic performance in mice adapted to high altitudes (276). In our examination, differences in mitochondrial respiration were not reflected at the organismal level, although SMR in PuyS trended towards higher rates than the other populations. This suggests that the mitochondrial phenotypes may not necessarily influence organismal metabolic performance. Previous investigations into the metabolism of sulfide-tolerant *P. mexicana* identified reductions in routine metabolic rate (RMR), generally described as the energy used to perform normal levels of activity (32). In the context of our data, this may suggest that sulfide-tolerant *P. mexicana* reduce activity to conserve energy, modifying behavioral phenotypes as opposed to metabolic phenotypes (277).

Maintenance of aerobic respiration under environmental stress

Sulfidic springs are not only rich in H₂S but are also characterized by chronic hypoxia due to the molecule's reactivity with dissolved oxygen in the water. Adaptation to chronic hypoxia and mito-toxic stress did not confer any significant differences in whole organism metabolism under normoxic conditions. However, the ability of sulfide-tolerant populations of *P. mexicana* to

maintain aerobic respiration under periods of hypoxia was higher when compared to sulfide-intolerant populations (Figure 4). The results of this experiment matched our predictions, as we identified that fish inhabiting H₂S-rich springs could maintain aerobic respiration at lower levels of oxygen, and therefore had a lower P_{crit} . These differences cannot necessarily be explained by the functional variation we quantified for other components and are likely the result of other aspects of organismal biology we did not assess.

Organismal adaptations to hypoxia are largely the result of modifications within the oxygen transport cascade, which includes morphological (278-280), behavioral (281, 282), physiological (283, 284), and biochemical traits (226, 278, 285-288). Fish inhabiting sulfidic springs have larger heads and gills, which has been hypothesized to facilitate an increased ability to acquire oxygen from the hypoxic environment and shown to increase ventilation capacity (27, 28). Additionally, sulfide spring fishes exhibit aquatic surface respiration, a behavior that maximizes oxygen obtained from their environment (29); however, this likely did not influence the results of our experiment due to the design of the intermittent-flow respirometer. There is also evidence for modification of oxygen transport proteins in some sulfide-tolerant poeciliids, which may confer an increased hypoxia tolerance (24). Although there are many alternative mechanisms that may facilitate our observed differences in metabolism under hypoxia, it is also possible that OxPhos activity does play a pivotal role. Investigations into the hypoxia tolerance of bar-headed geese, locusts, and marine sculpins have identified molecular evolution and functional modifications of COX in populations experiencing chronic hypoxia (278, 288, 289). Indeed, it was found that marine sculpins with higher hypoxia tolerance, determined by lower P_{crit} values, possessed COX proteins with a higher affinity for oxygen. Therefore, future work investigating aerobic metabolic adaptations to hypoxia in this system should include measures of biochemical

and mitochondrial performance along a gradient of hypoxia and H₂S, including oxygen-binding affinities of COX, activities of all OxPhos complexes, and mitochondrial respiration.

Additionally, future work should strive to measure organismal metabolism in the presence of H₂S, although this remains a challenging endeavor due to the toxic effects of H₂S in closed systems and the competitive consumption of oxygen between organisms and H₂S (14).

Conclusions

Overall, our data provides two main conclusions when considering the evolution of physiological traits: 1) the consequences of genetic variation on physiological function may not be evident at all levels of organization, and scientists must take care when making inferences from any one set of data, and 2) although physiological processes may be predictable targets of selection, the ways in which these pathways are modified may not be repeatable across environments. These conclusions are derived from the vertical and horizontal integration of data between two lineages of sulfide-tolerant and intolerance *P. mexicana*, in which we found drainage-specific differences in enzyme activity, population-specific variation in mitochondrial respiration, and habitat-specific differences in maintenance of aerobic respiration under hypoxia. These data provide further support that generalizations about physiological adaptation cannot be inferred when assessing any one set of data at either micro- or macroevolutionary scales (38, 39). Future work investigating the predictability and repeatability of physiological adaptation must consider the complex nature of these phenotypes, as regulatory and environmental effects may be fundamental drivers of patterns observed in putatively adaptive traits in nature.

Figures

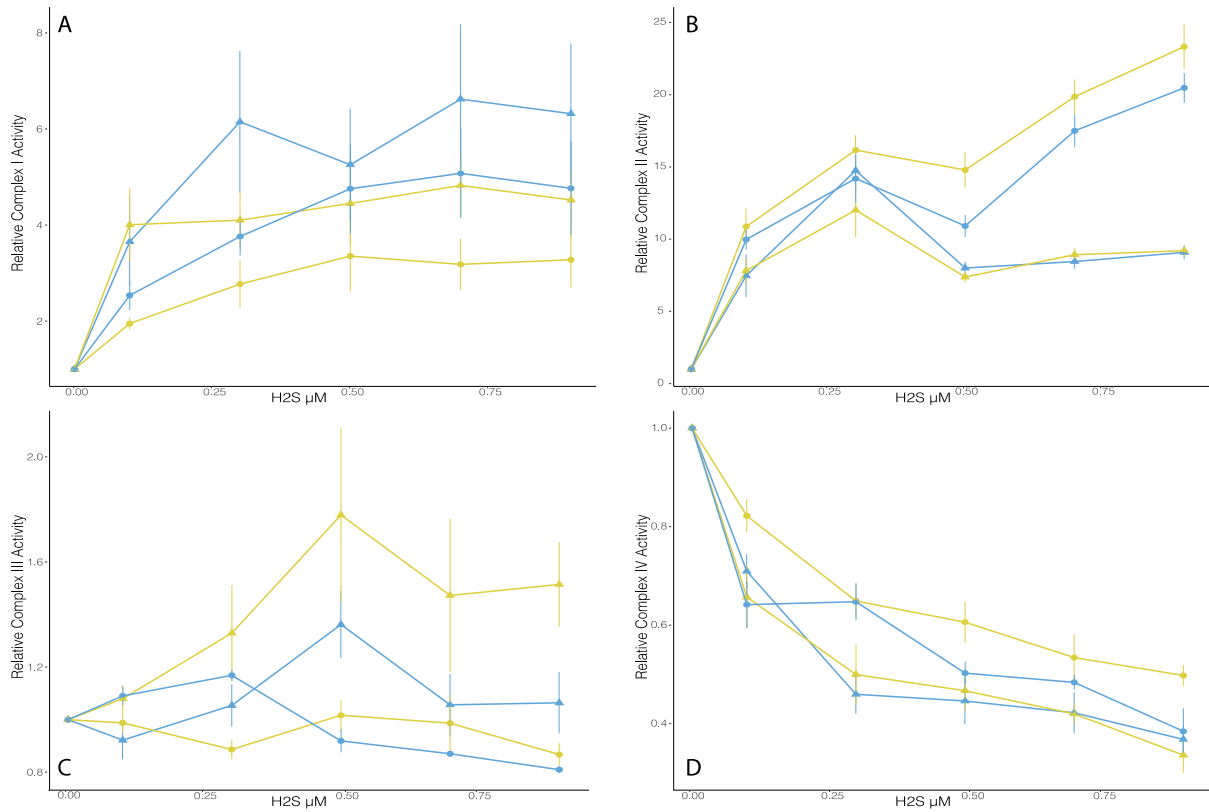


Figure 3-1: Relative enzyme activity of OxPhos enzymes from sulfide-tolerant (yellow) and intolerant (blue) populations of *Poecilia mexicana* from two independent lineages (▲: Tac; ●: Puy). **A:** Relative activity of Complex I along a gradient of H₂S exposure was best explained by the interaction between habitat of origin, drainage of origin, and H₂S concentration (Table 3-2). **B:** The relative enzyme activity of Complex II was primarily explained by the three-way interaction between habitat of origin, drainage of origin, and ambient H₂S concentration (Table 3-2). **C:** Complex III activity was best explained by the two-way interaction between drainage of origin and H₂S (Table 3-2). **D:** The relative activity of Complex IV (COX) was primarily explained by both H₂S and an additive effect of H₂S and drainage of origin (Table 3-2). For all graphs, each point indicates the population mean ± standard error.

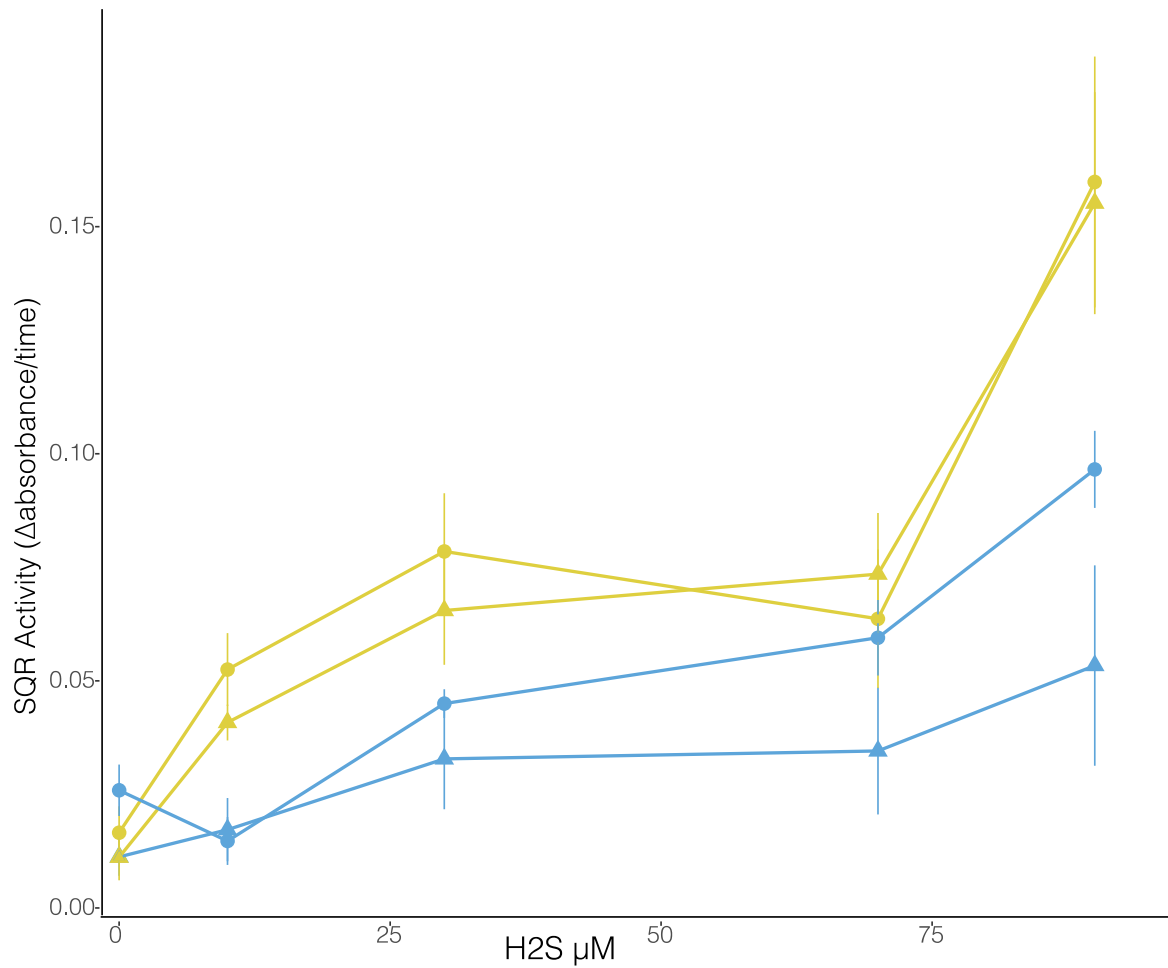


Figure 3-2: SQR enzyme activity in sulfide-tolerant (yellow) and intolerant (blue) populations of *P. mexicana* from two independent drainages (▲: Tac; ●: Puy). SQR activity was best explained by ambient H₂S and an additive effect of habitat of origin and H₂S concentration (Table 3-2). Each point indicates the population mean \pm standard error.

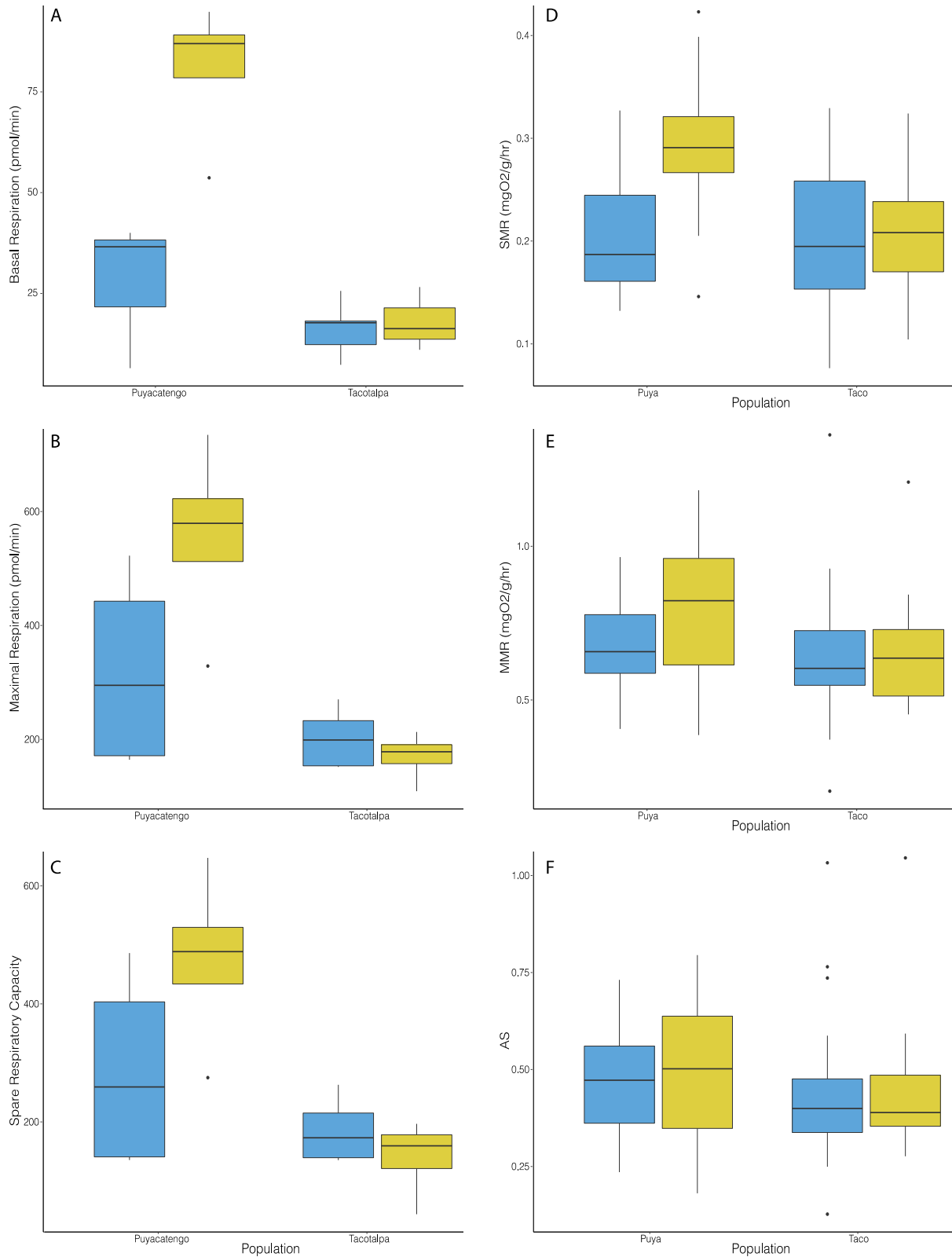


Figure 3-3: Measures of mitochondrial (A-C) and organismal (D-F) respiration collected from sulfide-tolerant (yellow) and intolerant (blue) populations of *P. mexicana* from two independent drainages (Puyacatengo and Tacotalpa). Boxes cover the first through third quartile of the data;

horizontal black lines indicate the median; vertical lines indicate the 10th and 90th percentiles. **A.** Variation in the basal respiration of mitochondria was best explained by an interaction between habitat of origin and drainage of origin (Table 3-3). **B.** Measures of maximal mitochondrial respiration indicated variation was best explained by a two-way interaction between habitat of origin and drainage of origin (Table 3-3). **C.** Spare respiratory capacity, which is the difference between maximal and basal respiration rates, exhibited similar patterns of variation explained by the interaction between habitat and drainage of origin (Table 3-3). **D.** No variation was observed in standard metabolic rate (Table 3-4). **E.** Maximum metabolic rate did not exhibit any variation across habitats or drainages and was best explained by the null model (Table 3-4). **F.** Absolute aerobic scope, which is the difference between standard and maximum metabolic rates, was best explained by the null model (Table 3-4).

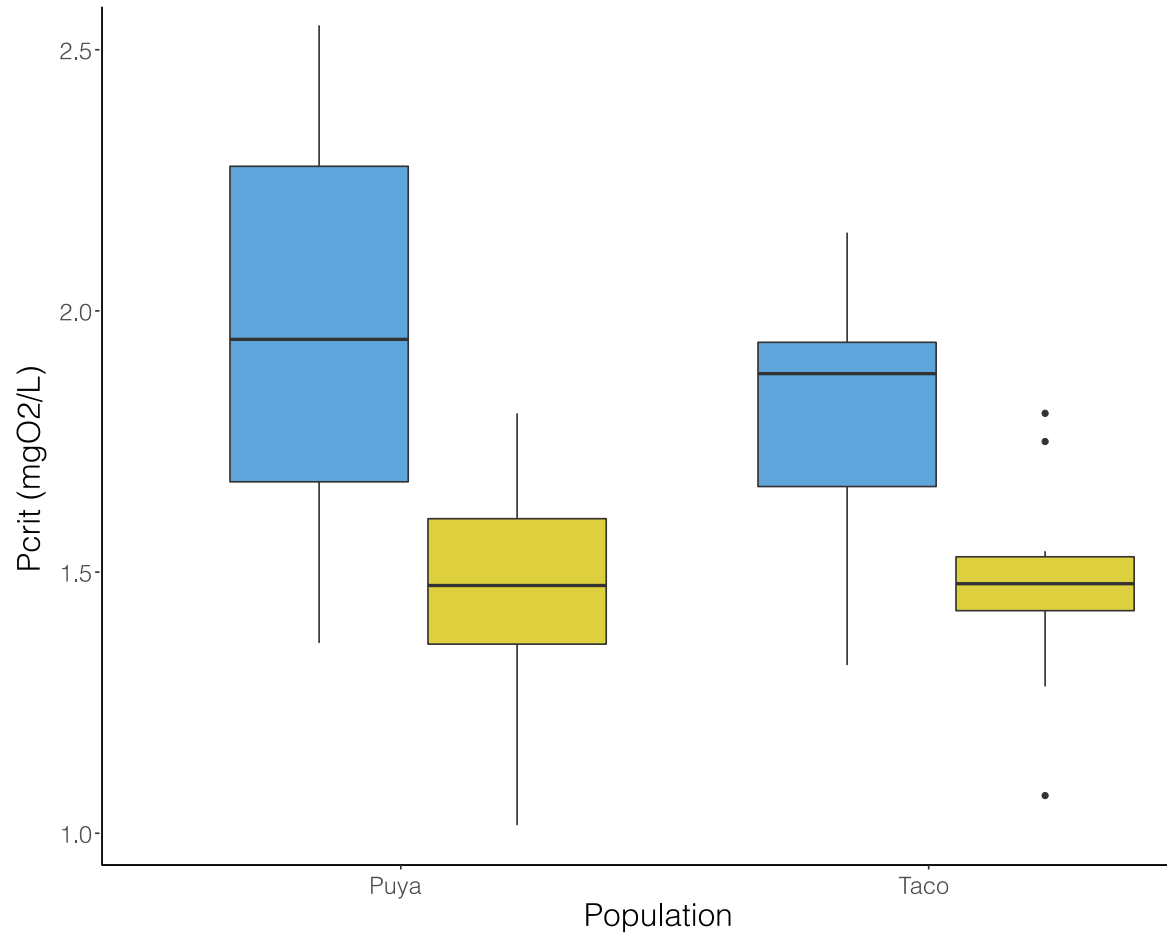


Figure 3-4: Critical oxygen tension (P_{crit}) of sulfide-tolerant (yellow) and intolerant (blue) populations of *P. mexicana*. Boxes cover the first through third quartile of the data; horizontal black lines indicate the median; vertical lines indicate the 10th and 90th percentiles. Habitat of origin primarily explained the variation observed in P_{crit} (Table 3-4).

Tables

Table 3-1: Predictions for the plasticity of OxPhos enzyme activity in the presence of H₂S and the evolution of enzyme activity in sulfide-tolerant lineages of *Poecilia mexicana* based on biochemical studies of OxPhos function and previously collected data from wild-caught individuals.

Complex	Predictions: changes in enzyme activity in response to H ₂ S	Predictions: differences in enzyme activity between populations
CI	<p>Data: Complex I transfers electrons from NADH to ubiquinone, introducing electrons into the electron transport chain (ETC) (268, 269). Although there is no evidence for direct effects of H₂S on enzyme activity, there is evidence for the induction of reverse electron flow at Complex I under H₂S toxicity (290).</p> <p>Predictions: Due to no direct interactions between H₂S and Complex I, one prediction is that activity will not change in response to H₂S. Alternatively, due to the additional inputs of electrons into the ETC via oxidation of H₂S by SQR, Complex I activity may decrease to maintain balance of electrons entering the system.</p>	<p>Data: The activity of Complex I has not been measured in <i>Poecilia mexicana</i>.</p> <p>Predictions: Due to the competing additions of electrons into the ETC by Complex I and SQR, reductions in enzyme activity may be expected in sulfide-tolerant fish.</p>
CII	<p>Data: Complex II transfers electrons from FADH₂ to ubiquinone (268, 269). Similarly to Complex I, there is no direct interaction between H₂S and the enzyme. Reverse electron flow at Complex II can be induced when the ubiquinone pool</p>	<p>Data: The activity of Complex II has not been measured in <i>Poecilia mexicana</i>.</p>

	<p>becomes over-reduced with electrons (271).</p> <p>Predictions: Enzyme activity may not be affected by H₂S due to no direct interactions. Alternatively, activity of Complex II may decrease to limit competitive additions of electrons into the ETC, similarly to predicted reductions in Complex I activity.</p>	<p>Predictions: Due to the competitive addition of electrons into the ETC with SQR, reductions in enzyme activity may be expected.</p>
CIII	<p>Data: Complex III reduces cytochrome c by oxidizing ubiquinone, which helps maintain the redox balance of the mitochondrial ETC (269, 272). Complex III does not directly interact with H₂S.</p> <p>Prediction: Activity of Complex III may not be influenced by the presence of H₂S. Alternatively, Complex III Activity may increase to offset the increased input of electrons into the ETC.</p>	<p>Data: Complex III activity has not been assessed in <i>Poecilia mexicana</i>.</p> <p>Prediction: Complex III activity is predicted to be higher in sulfide-tolerant populations due to the increased input of electrons into the ETC by SQR.</p>
CIV	<p>Data: Complex IV oxidizes cytochrome c and transfers electrons to oxygen molecules to generate water (269). Its activity is directly inhibited by H₂S toxicity (16, 272).</p> <p>Prediction: Complex IV activity should decrease as H₂S concentrations increase.</p>	<p>Data: Wild-caught PuyS fish exhibit the ability to maintain Complex IV activity in the presence of H₂S, while TacS and sulfide-intolerant populations suffer from decreases in activity as H₂S concentrations increase (36, 68).</p> <p>Prediction: PuyS fish will maintain a higher Complex IV activity in the</p>

		presence of H ₂ S than all other populations.
SQR	<p>Data: SQR catalyzes H₂S detoxification by oxidizing the molecule (246). Previous research indicates SQR activity is higher in the presence of H₂S in sulfide-tolerant animals (20).</p> <p>Prediction: We predict SQR activity will increase as H₂S concentrations increase.</p>	<p>Data: SQR activity is higher in wild-caught sulfide-tolerant populations of <i>Poecilia mexicana</i>, and activity increases in these populations as H₂S increases (14).</p> <p>Prediction: We predict SQR activity will be higher in sulfide-tolerant populations and that activity will increase as H₂S increases.</p>

Table 3-2: Results of mixed-effect linear models analyzing absolute variation of OxPhos enzyme activity under control conditions and relative activity under H2S exposure. Models are ordered based on $\Delta AICc$ values. Models in bold exhibit a $\Delta AICc < 2$.

Enzyme	Data	Models	$\Delta AICc$	df	Weight
CI	Absolute	Null: (1 ID)	0.0	3	0.8726
		Drainage + (1 ID)	4.1	4	0.1101
		Habitat + (1 ID)	8.0	4	0.0161
		Habitat + Drainage + (1 ID)	13.0	5	0.0013
		Habitat * Drainage + (1 ID)	23.2	6	<0.001
	Relative	Habitat * Drainage * H2S + (1 ID)	0.0	10	0.651
		Habitat * H2S + (1 ID)	2.1	6	0.233
		Habitat + Drainage + H2S + (1 ID)	5.5	6	0.041
		Drainage * H2S + (1 ID)	6.5	6	0.025
		Drainage + H2S + (1 ID)	6.6	5	0.024
		Habitat + H2S + (1 ID)	7.3	5	0.017
		H2S + (1 ID)	8.3	4	0.010
		Habitat * Drainage + (1 ID)	59.1	6	<0.001
		Habitat + Drainage + (1 ID)	59.3	5	<0.001
		Drainage + (1 ID)	60.4	4	<0.001
Habitat + (1 ID)	61.1	4	<0.001		
Null: (1 ID)	62.2	3			
CII	Absolute	Null: (1 ID)	0.0	3	0.9935
		Drainage + (1 ID)	10.7	4	0.0046
		Habitat + (1 ID)	12.6	4	0.0019
		Habitat + Drainage + (1 ID)	24.4	5	<0.001
		Habitat * Drainage + (1 ID)	37.2	6	<0.001
	Relative	Habitat * Drainage * H2S + (1 ID)	0.0	10	0.975
		Drainage * H2S + (1 ID)	7.3	6	0.025
		Habitat + Drainage + H2S + (1 ID)	36.8	6	<0.001
		Drainage + H2S + (1 ID)	37.0	5	<0.001
		Habitat * H2S + (1 ID)	56.8	6	<0.001
		Habitat + H2S + (1 ID)	58.8	5	<0.001
		H2S + (1 ID)	59.6	4	<0.001
		Habitat * Drainage + (1 ID)	90.0	6	<0.001
		Habitat + Drainage + (1 ID)	92.3	5	<0.001
		Drainage + (1 ID)	92.7	4	<0.001
Habitat + (1 ID)	109.8	4	<0.001		
Null: (1 ID)	110.6	3	<0.001		
CIII	Absolute	Null: (1 ID)	0.0	3	0.9899
		Drainage + (1 ID)	10.3	4	0.0056

		Habitat + (1 ID)	10.8	4	0.0044
		Habitat + Drainage + (1 ID)	21.9	5	<0.001
		Habitat * Drainage + (1 ID)	31.9	6	<0.001
	Relative	Drainage * H2S + (1 ID)	0.0	6	0.8788
		Habitat * Drainage * H2S + (1 ID)	4.1	10	0.1103
		Drainage + (1 ID)	10.6	4	.0045
		Null: (1 ID)	11.0	3	.0036
		Habitat + Drainage + (1 ID)	13.8	5	0.001
		Drainage + H2S + (1 ID)	14.2	5	<0.001
		Habitat + (1 ID)	14.3	4	<0.001
		H2S + (1 ID)	14.6	4	<0.001
		Habitat * Drainage + (1 ID)	15.0	6	<0.001
		Habitat * H2S + (1 ID)	16.3	6	<0.001
		Habitat + Drainage + H2S + (1 ID)	17.5	6	<0.001
		Habitat + H2S + (1 ID)	18	5	<0.001
CIV	Absolute	Null: (1 ID)	0.0	3	0.9893
		Drainage + (1 ID)	9.2	4	0.0098
		Habitat + (1 ID)	13.9	4	<0.001
		Habitat + Drainage + (1 ID)	24.9	5	<0.001
		Habitat * Drainage + (1 ID)	40.6	6	<0.001
	Relative	H2S + (1 ID)	0.0	4	0.5490
		Drainage + H2S + (1 ID)	0.8	5	0.3712
		Drainage * H2S + (1 ID)	5.6	6	0.0336
		Habitat + H2S + (1 ID)	6.1	5	0.0263
		Habitat + Drainage + H2S + (1 ID)	6.8	6	0.0182
		Habitat * H2S + (1 ID)	11.6	6	0.0016
		Habitat * Drainage * H2S + (1 ID)	26.1	10	<0.001
		Null: (1 ID)	101.7	3	<0.001
		Drainage + (1 ID)	104.9	4	<0.001
Habitat + (1 ID)	107.6	4	<0.001		
Habitat + Drainage + (1 ID)	110.8	5	<0.001		
Habitat * Drainage + (1 ID)	115.3	6	<0.001		
SQR		H2S + (1 ID)	0.0	4	0.5439
		Habitat + H2S + (1 ID)	0.5	5	0.4280
		Habitat * H2S + (1 ID)	7.2	6	0.0150
		Drainage + H2S + (1 ID)	8.6	5	0.0074
		Habitat + Drainage + H2S + (1 ID)	9.1	6	0.0057
		Drainage * H2S + (1 ID)	26.1	6	<0.001
		Null: (1 ID)	35.3	3	<0.001
		Habitat + (1 ID)	36.1	4	<0.001
		Drainage + (1 ID)	44.1	4	<0.001

	Habitat + Drainage + (1 ID)	45.1	5	<0.001
	Habitat * Drainage + (1 ID)	52.8	6	<0.001
	Habitat * Drainage * H2S + (1 ID)	55.7	10	<0.001

Table 3-3: Results of mixed-effect linear models analyzing variation in basal respiration, maximal respiration, and spare respiratory capacity of mitochondria. Models are ordered based on ΔAICc values. Models in bold exhibit a $\Delta\text{AICc} < 2$.

Respiration	Models	ΔAICc	df	Weight
Basal	habitat*drainage + (1 ID)	0.0	6	.9984
	habitat + drainage + (1 ID)	13.0	5	.0015
	drainage + (1 ID)	18.4	4	<0.001
	habitat + (1 ID)	25.1	4	<0.001
	Null: (1 ID)	31.4	3	<0.001
Maximal	habitat*drainage + (1 ID)	0.0	6	0.998
	habitat + drainage + (1 ID)	12.4	5	.002
	drainage + (1 ID)	21.1	4	<0.001
	habitat + (1 ID)	25.5	3	<0.001
	Null: (1 ID)	34.5	3	<0.001
Spare Capacity	habitat*drainage + (1 ID)	0.0	6	.9970
	habitat + drainage + (1 ID)	11.7	5	.0029
	drainage + (1 ID)	19.8	4	<0.001
	habitat + (1 ID)	23.4	4	<0.001
	Null: (1 ID)	32.1	3	<0.001

Table 3-4: Results of mixed-effect linear models analyzing variation in the standard metabolic rate, maximum metabolic rate, absolute aerobic scope, and critical oxygen tension of whole fish. Models are ordered based on $\Delta AICc$ values. Models in bold exhibit a $\Delta AIC < 2$.

Respiration	Models	$\Delta AICc$	df	Weight
Standard	Null: (1 ID)	0.0	3	0.743
	habitat + (1 ID)	2.6	4	0.201
	drainage + (1 ID)	7.4	6	0.019
	habitat + drainage + (1 ID)	7.4	6	0.019
	habitat * drainage + (1 ID)	7.4	6	0.019
Maximum	Null: (1 ID)	0.0	3	0.8843
	habitat + (1 ID)	4.2	4	0.1075
	drainage + (1 ID)	11.6	6	0.0027
	habitat + drainage + (1 ID)	11.6	6	0.0027
	habitat * drainage + (1 ID)	11.6	6	0.0027
Aerobic Scope	Null: (1 ID)	0.0	3	1
	habitat + (1 ID)	25.1	4	<0.001
	drainage + (1 ID)	33.1	6	<0.001
	habitat + drainage + (1 ID)	33.1	6	<0.001
	habitat * drainage + (1 ID)	33.1	6	<.001
Pcrit	habitat + (1 ID)	0.0	4	0.467
	Null: (1 ID)	0.7	3	0.336
	habitat + drainage + (1 ID)	3.2	5	0.096
	drainage + (1 ID)	3.5	4	0.082
	habitat * drainage + (1 ID)	6.4	6	0.019

Chapter 4 - The role of plasticity in facilitating the colonization of extreme environments

Nick Barts, Shawn Trojan, Nichole Nieves, Lenin Arias-Rodriguez, Joanna Kelley, and Michi Tobler

Abstract

Abstract

Identifying the mechanisms and traits that allow organisms to colonize and persist under novel environmental conditions remains a key challenge in biology. There are three theoretical mechanisms that facilitate the ability of species to invade and adapt to the presence of novel stressors: 1) organisms may rapidly evolve post-colonization as a result of natural selection acting on pre-existing genetic variation, 2) a trait evolved for one function in the original environment may be co-opted for a new function under novel conditions (exaptation), and 3) a trait adaptive in the original environmental context facilitates persistence in another without changing function (pre-adaptation). Using a comparative transcriptomics approach, we quantified adaptive and maladaptive plasticity to infer the potential roles of pre-adaptation and post-colonization evolution in facilitating colonization of extreme environments rich in hydrogen sulfide (H₂S) by ancestral, sulfide-intolerant species that differ in their colonization success. Expression variation indicated that all species respond plastically to H₂S exposure, but in largely unique ways. We also found evidence for adaptive plasticity in all species, regardless of colonization success, but only a few of these genes were shared among successful colonizing species. By far, evidence of maladaptive plasticity outnumbered evidence of adaptive plasticity

in our dataset. Overall, the findings of this study suggest that pre-adaptation in key pathways may initially facilitate colonization of H₂S-rich habitats, but post-colonization evolution, potentially potentiated by maladaptive plasticity, is necessary to persist upon exposure to extreme environmental conditions.

Introduction

A primary objective of evolutionary biology is to identify the origin of putatively adaptive traits, a difficult task due to our inability to go back in time and identify singularly important events in evolutionary history (40, 41). Although originally considered a strictly evolutionary problem, identifying the mechanisms underlying the ability of species to adapt to novel environmental conditions is becoming an increasingly relevant question for many fields of biology, as human impacts are causing rapid environmental change and unprecedented mobility of species around the globe (46, 291-293). Invasion biology is a growing field that seeks to understand the mechanisms driving invasion success, and recent research in this field has documented the important role evolution plays in determining what species are capable of invading novel habitats (46, 294). A unifying goal driving research in both of these fields is to determine the origins of adaptive traits that facilitate persistence in the presence of novel stressors (46, 295).

Evolutionary biologists have identified three primary mechanisms that facilitate the persistence of species exposed to novel environmental conditions (41, 291, 296, 297): 1) natural selection acts on pre-existing genetic variation, ultimately resulting in evolutionary novelty (post-colonization evolution) (42, 298-301), 2) a trait previously evolved for particular function under one selective regime is co-opted for a new function in another context (exaptation) (291, 296, 302-306), and 3) a trait that is adaptive in an ancestral environment facilitates colonization

of a novel habitat without changing its initial function (pre-adaptation) (46). Rapid post-introduction evolution has been the primary focus of much recent research, documenting the ability of species to quickly evolve upon exposure to a novel selection regime, such as modifying morphology (307-309), physiology (42, 44, 45), and life history (300, 310). Exaptations are thought to be an important factor generating evolutionary novelty (291, 306), and examples of historical exaptations include the co-opted function of dinosaur feathers from thermoregulation to flight. Pre-adaptations are traits that are adaptive in an ancestral environment—but unlike exaptations—retain the same function and facilitate the colonization of a novel, derived habitat (46, 311). The concept of pre-adaptation is most often invoked when examining traits that facilitate invasion into non-native ranges by a species that threatens native organisms, and identification of these traits may allow scientists to predict which species are capable of becoming invasive (297, 311-314). However, few studies have assessed the role of pre-adaptations in facilitating colonization of novel environments characterized by harsh conditions and naturally low biodiversity (43-45).

Decades of research into the pre-adaptive mechanisms facilitating the invasion success of species into non-native ranges has provided a framework for identifying potential pre-adaptations in other contexts. Traits that increase competitive ability (313, 315-317) or reproductive capability (318-320) are frequently identified as pre-adaptive traits in invasive plant species, and these traits can also rapidly evolve in populations recently introduced to novel environments (42, 298, 310). The ability to plasticly respond to changing environmental conditions has also been suggested to play an important role in pre-adaptation, as organisms that are capable of modulating phenotypes may be more apt to survive under a wider range of environmental contexts (312, 314, 321). Specific examples include the plasticity of morphology

(322, 323), physiology (324-326), and gene expression (327-329) as potential candidates for pre-adaptations in diverse species encountering natural and anthropogenic stress. To identify potentially adaptive traits, most experiments compare species within common-garden environments or in the native environmental setting, which allows for the identification of trait differences among species but makes it difficult to infer whether these traits were truly able to facilitate invasion (319, 330). Alternatively, studies compared invasive and non-invasive species within the introduced range, but this fails to identify if “invasive traits” are the product of rapid adaptation or pre-adaptation to the environment (319, 330). Finally, a challenge in identifying pre-adaptations may be the lack of suitable ancestors for comparisons, as making comparisons across broad phylogenetic scales may introduce substantial variance into analyses (319, 330). Therefore, it is critically important to identify systems in which closely related species or populations within their native range differ in their capabilities to colonize a particular novel habitat when addressing questions concerning the role of pre-adaptation in facilitating colonization of new environments.

Extreme environments and the organisms inhabiting them provide ideal systems to explore the evolutionary origins of adaptive traits and the role of pre-adaptations in facilitating colonization of novel habitats. Extreme environments are characterized by physiochemical stressors that are lethal to most organisms, and these conditions serve as an ecological filter determining what species are capable of persisting in these habitats (10, 12, 331, 332). Selection regimes in extreme environments have predictable consequences on biochemical and physiological function of organisms, allowing for the development of *a priori* hypotheses about mechanisms mediating tolerance and adaptation (12, 244). Comparative analyses of species living in ancestral, non-extreme environments that vary in their success to colonize extreme habitat patches allow us to

identify specific trait that enable some species to colonize these habitats. In particular, extremophile fishes may serve as excellent models for investigating pre-adaptations due to the presence of replicated, independent colonization of extreme habitats and easily identifiable ancestral, non-extremophile lineages (10).

Freshwater springs rich in hydrogen sulfide (H₂S) are among the most extreme aquatic environments (14). H₂S is a naturally occurring respiratory toxin that is lethal to most organisms at micromolar concentrations due to its inhibitory effects on aerobic respiration (66). The molecule readily and reversibly binds to cytochrome c oxidase (COX; Complex IV of the mitochondrial respiratory chain), which results in the inability to establish the electrochemical gradient necessary for generating ATP aerobically (16, 66). Most organisms are also equipped with the capacity to detoxify H₂S at low levels of exposure via the sulfide:quinone oxidoreductase (SQR) pathways (19, 20, 246). Both the primary toxicity target (COX) and the primary mode of detoxification (SQR) are found within the mitochondria and play important roles in cellular metabolism, making them ideal candidates as predictable targets of selection in these environments. Indeed, investigations into organisms inhabiting these naturally toxic habitats have identified increased detoxification ability as a near ubiquitous trait associated with adaptation to H₂S-rich conditions (19-21, 248), and some organisms exhibit modifications of both aerobic and anaerobic metabolism as well (22, 68, 248). Poeciliid fishes across Latin America have served as a system to explore questions concerning adaptation to H₂S-rich springs (23, 24, 248). Macroevolutionary comparisons of gene expression and molecular evolution have revealed that oxygen binding proteins, oxidative phosphorylation complexes, and sulfide detoxification enzymes are predictable and frequent targets of selection in sulfide-tolerant lineages of livebearing fishes (248). In particular, the sulfide spring systems in Southern Mexico

have served as a focus for studying adaptation to H₂S across levels of organization (13, 22, 84). These springs are located within three river drainages of the Rio Grijalva and geographically adjacent to ancestral, non-sulfidic habitats (25, 27). Poeciliids from four genera (*Gambusia*, *Poecilia*, *Pseudoxiphophorus*, and *Xiphophorus*) have successfully colonized these habitats, are among the only vertebrate species known to inhabit such springs, and may have diverged from ancestral populations as recently as 500 years ago (23, 33). The ancestral environments are characterized by much higher biodiversity (34 species within 11 families) than the sulfidic springs (six species within two families) despite the little to no physical barriers preventing dispersal into sulfide springs (23). This begets the question: why are only some species from non-sulfidic environments capable of colonizing sulfidic habitats repeatedly? Is it possible that some species may have pre-adaptations that facilitate colonization, such as the ability to plastically regulate mechanisms mediating H₂S tolerance?

Using a controlled H₂S exposure experiment and comparative transcriptomics, we sought to address the following questions: 1) How does gene expression change upon exposure to H₂S within each lineage, and can we identify shared responses within among all species, and 2) Do patterns of adaptive and maladaptive plasticity differ between successful and unsuccessful lineages? Comparative transcriptomics approaches are an ideal method to assess the potential roles of pre-adaptation and post-colonization evolution in sulfide spring colonization and persistence. First of all, transcriptome sequencing has allowed for the identification of adaptive gene expression differences between locally adapted populations in sulfidic and nonsulfidic habitats (22, 30), providing a reference set of putatively optimal levels of gene expression. Using H₂S-exposure experiments in conjunction with transcriptomic profiling allows for the quantification of H₂S responses in individuals from non-adapted populations that can then be

compared to the reference set (Figure 1). In theory, there are four potential categories of responses: (1) A particular gene may not be differentially expressed between locally adapted populations (i.e., it is not in the reference set), but it may be differentially regulated upon H₂S exposure in individual from sulfide-intolerant populations (Figure 1A). This would be an example of maladaptive plasticity, where differential expression is a symptom of loss of homeostasis associated with H₂S toxicity. In this case, we would predict post-colonization selection against H₂S-induced plasticity in gene expression. (2) A particular gene may be differentially expressed between locally adapted populations (i.e., it is in the reference set), but it may be differentially regulated in the opposite direction upon H₂S exposure in individuals from non-adapted populations (Figure 1B). This is another form of maladaptive plasticity, and we would predict post-colonization selection evolution of gene regulation to match optimal patterns. (3) A particular gene may be differentially expressed between locally adapted populations (i.e., it is in the reference set), but it may not be differentially regulated upon H₂S exposure in individuals from non-adapted populations (Figure 1B). This would be an example of lack of plasticity, and we would predict post-colonization evolution of gene regulation. (4) Last but not least, a particular gene may be differentially expressed between locally adapted populations (i.e., it is in the reference set), and it may be differentially regulated in the same direction upon H₂S exposure in individuals from non-adapted populations (Figure 1B). In this case, the plastic response matches the adaptive response, providing an example of pre-adaptation. The central hypothesis of this paper is that the ancestors of lineages that have successfully colonized sulfide springs exhibit at least some adaptive plasticity (green box in Figure 1), whereas lineages that have not successfully colonized sulfide spring primarily lack H₂S-inducibility in relevant genes or exhibit maladaptive plasticity (red box in Figure 1).

Methods

Study sites and fish collection

We collected fish from freshwater habitats within four tributaries of the Río Grijalva located in the foothills of the Sierra Madre Occidental mountain range near the city of Teapa, Tabasco, Mexico (23, 26, 27). We collected nine fish species (N = 4 successful colonizing species from the family Poeciliidae and 5 unsuccessful colonizing species from the families Characidae, Cichlidae, and Poeciliidae ; Table 1) by seine (2 m x 5 m, 3 mm mesh size), transferred them to insulated coolers containing water from their respective sites, and brought them to a nearby field station. Fish were acclimated to laboratory conditions in species-specific tanks for at least 18 hours and were not fed prior to conducting the experiment.

H₂S exposure

To test for plastic responses of gene expression in response to H₂S exposure, we conducted a series of H₂S exposure trials (27). Prior to each experiment, we prepared a 5 mM H₂S stock solution by dissolving 5 mg sodium sulfite (Na₂SO₃) and 1.204 g sodium sulfide nonahydrate (Na₂S • 9H₂O) into 1 L water deoxygenated with nitrogen gas (30, 333). Fish were placed into individual 1 L plastic chambers containing 150 mL water from the holding tanks and allowed to acclimate to the chamber for at least 10 minutes. At the start of the experiment, 15 mL of either H₂S solution or control water was added to the chamber at 20-minute intervals using a syringe until fish lost equilibrium (LOE) or 8 hours had passed. Once we observed LOE or the trial period ended, we recorded the time and euthanized the fish before dissecting gill tissue. We also measured the H₂S concentration within the experimental chamber. Gill tissues were stored in 2

mL of RNAlater (Ambion, Inc.). H₂S concentrations were determined using a methylene blue assay (Hach Company, Loveland, CO, USA).

RNA isolation and cDNA library preparation

RNA extraction, library preparation, and sequencing were conducted using previously employed procedures (22, 24, 30). In brief, total RNA was extracted from 10-30 mg of pulverized gill tissues ($N = 3-6$ individuals per species) using a NucleoSpin RNA kit (Macherey-Nagel GmbH & Co. KG, Düren, Germany) following the manufacturer's protocol. mRNA isolation and cDNA library preparation were conducted using the NEBNext Poly(A) mRNA Magnetic Isolation Module and the NEBNext Ultra Directional RNA Library Prep Kit for Illumina (New England Biolabs, Inc. Ipswich, MA, USA) using a modified version of the manufacturer's protocol (30). Libraries were assigned unique barcodes and their qualities were assessed using an Agilent Bioanalyzer High Sensitivity DNA chip prior to sequencing. Barcoded libraries were pooled based on nanomolar concentrations and sequenced on an Illumina NovaSeq S4 with paired-end 100 base pair (bp) reads at MedGenome, Inc. (San Francisco, CA, USA). Due to low coverage, some samples were re-sequenced.

Transcriptome assembly and gene annotation

The transcriptomes consisted of over 5.1 billion reads (Table 2). Raw RNA-seq reads were trimmed twice using TrimGalore!, and these trimmed reads were then mapped to one of three reference genomes (Poeciliidae: *Xiphophorus maculatus*-male-5.0, GenBank accession number GCA_002775205.2, Cichlidae: *Archocentrus centrarchus* nuclear genome, GenBank accession number GCA_007364275.2 and *Amphilophus citrinellus* mitochondrial genome, BioProject

PRJNA242721; and Characidae: *Astyanax-mexicanus*-2.0, Genbank accession number GCA_000372685.2) using BWA-MEM (109). 95.87% \pm 2.55% of trimmed reads successfully aligned to the reference genomes (Table 2). We functionally annotated genes from the reference genomes by extracting a representative transcript for each gene using the perl script gff2fasta.pl and identifying the top match for each gene in the SWISSPROT database using BLASTx (critical E-value 0.001) (193). Each gene was annotated using the top BLAST hit against the human SWISSPROT database. We then used STRINGTIE to quantify the number of reads mapped to each gene in the reference genome for each individual and used the provided python script to generate a read counts matrix (334, 335).

To make comparisons across species that were mapped to different reference genomes, we used OrthoFinder to identify orthologous genes across the different reference genomes (336, 337). To generate an orthogroup counts matrix, we aligned gene counts matrix with the OrthoFinder output file containing orthogroups and their associated protein IDs. To account for the many-to-one mapping that may occur when identifying orthogroups, we averaged counts by the number of individuals within each species and treatment. For final analyses, we only retained orthogroups that were expressed in all individuals (cpm > 0). We then visualized expression patterns in the 6,275 orthogroups identified between samples exposed to H₂S and controls with multidimensional scaling (MDS) using Euclidian distances based on normalized count data to identify and remove outliers.

Quantifying expression of orthogroups

To identify differentially expressed genes, we used generalized linear models (GLMs) on normalized read counts as documented in the Bioconductor package edgeR in R (338). We then

used glmFit to fit a negative binomial GLM to each gene based on tagwise dispersion estimates and a design matrix describing comparisons between control and H₂S-exposed individuals of each species. To assess statistical significance, we used the GLM likelihood ratio test as implemented by the glmLRT function in edgeR with a false discovery rate of <0.05 based on the Benjamini-Hochberg correction (197).

Differences in gene expression upon H₂S exposure have previously been identified in lab-reared sulfidic *Poecilia mexicana* (22), but no experiments have analyzed transcriptome wide differences in expression in non-sulfidic populations or species. To characterize the transcriptional responses associated with H₂S toxicity, we compared gene expression variation between H₂S exposed and unexposed individuals within the same species to identify species-specific responses. Additionally, we were interested in assessing if H₂S exposure resulted in general responses within the same genes, so we intersected the expression profiles of all species to document if any genes were universally expressed in the same direction.

We assume that gene expression plasticity may serve as a pre-adaptation if the direction of expression is shared between sulfide tolerant and intolerant species. To test this, we quantified adaptive plasticity in our data set by intersecting the transcriptional profiles of our freshwater species with previously collected data on three sulfidic populations of *Poecilia mexicana* collected in the wild to identify any overlap (22). In addition to quantifying adaptive plasticity across lineages separately, we also intersected the lists of candidate pre-adaptations of only successful colonizers, only unsuccessful colonizers, and all lineages to identify if successful ancestors shared a greater number of pre-adaptations. Similarly, we quantified the number of genes exhibiting maladaptive plasticity and lack of plasticity within each species (Figure 1).

Results and discussion

Species-specific responses to H₂S exposure

We assessed variation in orthogroup expression to identify the physiological pathways that respond to H₂S exposure in populations of fish that have never been exposed to H₂S, including some ancestors of lineages that have successfully colonized H₂S-rich habitats and lineages that have not. We predicted that H₂S exposure would elicit transcriptional responses in all species, and given H₂S's direct effects on the SQR and OXPHOS pathways that are highly conserved among species, we expected similar overall gene expression changes. Indeed, we identified significant orthogroup expression responses in all species, and depending on the species, between 346 and 4,122 of 6275 orthogroups were differentially expressed between exposed and non-exposed individuals (Table 3). However, the patterns of expression change in response to H₂S exposure were highly idiosyncratic and species-specific, both in in direction and magnitude (Figure 2). Although species-specific responses to stress are common (339, 340), the toxic effects of H₂S exposure impose specific constraints on biochemical and physiological function (13-15), and different lineages of poeciliids adapted to H₂S exhibit strong patterns of convergence in gene expression (24, 248). Hence, our analyses suggest that convergent evolution among sulfide spring fishes is not likely the result of shared responses to H₂S in ancestral populations, but instead natural selection must have acted on the idiosyncratic variation among lineages to produce similar H₂S-tolerant phenotypes post-colonization.

The toxic effects of H₂S impose predictable constraints on physiological function due to the inhibition of both oxygen transport (17, 24) and oxidative phosphorylation (16, 68, 248) and induces predictable upregulation of detoxification pathways (248, 341). These physiological pathways are highly conserved across vertebrates (246), and therefore, we predicted that

exposure to H₂S would likely result in shared expression of these key pathways. However, when we intersected the gene expression profiles of all species, we only uncovered 7 genes that were consistently upregulated in response to H₂S exposure (Table 4). These genes were primarily associated with cell cycle regulation. BTG-3, GADD45A, and DDIT4L are all involved in regulating the cell cycle, and previous studies have identified that overexpression of BTG-3 and GADD45A prevents cells from entering S-phase (342). Expression of DDIT4L inhibits cell growth by regulating the TOR signaling pathway and has been suggested to regulate hypoxia-induced apoptosis (343). In that same regard, TNFRSF10A is the receptor of the cytotoxic ligand TRAIL (344), and the interaction with TRAIL triggers a cellular cascade that initiates function of caspases, including CASP7, which mediate apoptosis (345, 346). Consistent differential expression of these cell cycle regulators suggest that ancestral populations are largely incapable of coping with extended exposure to H₂S, and a slow-down of cell proliferation and an increase in apoptosis are likely just a symptom of H₂S's toxicity. Beyond that, H₂S-intolerant species largely respond to H₂S toxicity in unique ways, starkly contrasting with the patterns of convergence that emerge after post-colonization evolution.

Adaptive plasticity as evidence for pre-adaptation to H₂S-rich environments

Pre-adaptations are traits that evolved within one environmental context and facilitate success in non-native range while retaining the same function (46). We hypothesized that adaptive plasticity of gene expression in key physiological pathways may represent pre-adaptations that initially allowed some species of poeciliids to colonize H₂S-rich environments in Southern Mexico. The mechanisms underlying adaptation to H₂S-rich environments are well characterized in poeciliids (22, 30, 34, 248), and macroevolutionary investigations of gene expression have

identified sulfide detoxification, aerobic and anaerobic metabolism, and oxygen transport as key components of expression variation in these systems (248). Hence, we predicted that evidence of adaptive plasticity, and therefore evidence of pre-adaptation, would most likely exist in genes associated within these pathways. We also expected to find adaptive plasticity disproportionately in lineages that have colonized H₂S-rich springs compared to lineages that have not. However, our analyses indicated that adaptive plasticity is relatively rare. All species—regardless of whether they colonize sulfide spring or not—exhibited evidence for adaptive plasticity in 11-57 genes, which only represented about 3% of differentially expressed genes in each lineage (Table 3, Figure 3).

We were interested in identifying any genes that might exhibit adaptive plasticity in the ancestors of successful colonizers but not lineages that never colonized sulfide springs. Indeed, we identified nine unique orthogroups that were shared among the ancestors of successful colonizers (Table 5), including some key H₂S response genes. For example, ETHE1 encodes a sulfur dioxygenase that mediates the second step of H₂S detoxification within the SQR pathways (290). This gene is ubiquitously upregulated in sulfide-tolerant poeciliids and is hypothesized to play an important role in adaptation to sulfide-rich environments (22, 34, 248, 290, 347). Along the same lines, we identified adaptive plasticity of HIGD1A, which encodes a subunit of COX, the primary toxicity target of H₂S (348). Upregulation of this subunit under H₂S conditions suggests that it may facilitate some functional benefit to mitochondria under mitotoxic or hypoxic conditions, as this gene has been shown to minimize cellular damage and apoptosis under hypoxia (348). Upregulation of ETHE1 and HIGD1A suggests that pathways known to be critically important aspects of H₂S tolerance may have initially been physiologically flexible in ancestral populations of successful colonizers and therefore assisted in the original colonization

of these habitats. In addition to modification of detoxification and oxidative phosphorylation pathways, upregulation of orthogroups containing genes known for hypoxia responses were also identified. ELGN2 and ELGN3 both encode prolyl hydroxylases which play important roles in oxygen sensing and regulating the expression of hypoxia-inducible factors (HIFs) (349).

Interestingly, none of the adaptively plastic orthogroups were shared by all species, or by species that have never successfully colonize sulfide springs. We had predicted that orthogroups including genes that encode for oxidative phosphorylation or sulfide detoxification enzymes would respond to H₂S exposure in successful colonizing lineages, and potentially in the unsuccessful lineages as well given the conserved nature of these key pathways. Paradoxically, we observed that none of the successful ancestors exhibited adaptive plasticity of SQR, while the orthogroup including this gene exhibited adaptive plasticity in *Astyanax aeneus* and *Heterophallus milleri*, two species from different families that have never successfully colonized H₂S-rich habitats. Additionally, these two species and the cichlid *Trichromis salvani* exhibited adaptive plasticity of the orthogroup including ETHE1, which is adaptively expressed across all successful lineages. *A. aeneus*, *T. salvani*, and *Belonesox belizanus* also exhibited adaptive plasticity of the orthogroup encoding HIGD1A. Additionally, some lineages of both successful and unsuccessful colonizing species exhibited adaptive plasticity in orthogroups including genes encoding for glutathione reductase (GSR), a mitochondrial protein that mitigates oxidative stress.

Based on the patterns of shared adaptive plasticity among lineages, we cannot conclude that the degree of adaptive plasticity in gene expression was the primary determinant of colonization success across the lineages investigated. Clearly, phylogenetic distance among our focal species likely played a role in the degree of overlap we observed, with higher levels of overlap in successful colonizers (which are all poeciliids) and no overlap among unsuccessful lineages

(which include species from three different families). Along this vein, we identified two genes with adaptive plasticity across all poeciliids (ALDOC and SLC16A1). Both of these genes are involved in anaerobic metabolism (350, 351) and encode for fructose-bisphosphate aldolase and monocarboxylate transporter 1, respectively. Fructose-bisphosphate aldolase is a glycolytic enzyme (350) and the monocarboxylate transporter plays a necessary role in transporting molecules such as pyruvate and lactate (351, 352), which are substrates involved in glycolysis and gluconeogenesis (353). Given the disruptive effects H₂S has on aerobic metabolism and the hypoxic conditions that generally co-occur with H₂S conditions (14, 18), it is likely that modification of anaerobic metabolism is one of the many solutions organisms have adopted to withstand H₂S exposure (13).

The presence of adaptive plasticity in key genes associated with H₂S and hypoxia raises the question of why such plasticity arose to begin with. Although it is unlikely that any of our study populations have been exposed to chronic H₂S or hypoxia based on our sampling locations, we cannot exclude the possibility that they are exposed to these stressors intermittently. Poeciliids in particular are known for inhabiting marginal habitats (354-356), and during periods of drought and receding water levels, they may become isolated in small pools or ponds with adverse environmental conditions (356, 357). Particularly at night, when oxygen levels plummet, anoxic conditions in aquatic sediments can actually facilitate the biotic production of H₂S (358, 359), which can be released when the sediment is disturbed. H₂S- and hypoxia-induced plasticity in gene expression may facilitate survival of such intermittent H₂S exposures, and adaptive plasticity in these genes may ultimately have helped to mitigate H₂S toxicity during the colonization of sulfide springs. Considering that some degree of adaptive plasticity in key pathways is found in all species and not just lineages that successfully colonized H₂S-rich

habitats, our results suggest that pre-adaptation mediated by adaptive plasticity in gene expression cannot explain what species are capable of colonization of H₂S-rich habitats.

Maladaptive plasticity and post-colonization evolution

Given that we found relatively few genes exhibiting adaptive plasticity, we were interested in assessing the degree to which species demonstrate either maladaptive plasticity or a lack of plasticity, as these two mechanisms may have implications for post-colonization evolution. Previous investigations have suggested that the presence of plasticity, both adaptive and maladaptive, may facilitate rapid adaptation (360). Interestingly, we identified that ancestors of successful colonizers trend towards a larger number of orthogroups exhibiting maladaptive plasticity (Table 3; Figure 3). The role of plasticity in facilitating evolution is controversial, as it has often thought to constrain evolution (361); however, multiple studies investigating the role of plasticity in facilitating evolution to novel conditions has shown that maladaptive plasticity may potentiate rapid adaptation post-colonization (360, 362). One such study found that guppies (*Poecilia reticulata*) from high predation habitats introduced to low predation environments evolved similar gene expression patterns to guppies native to low predation streams and that these genes exhibit maladaptive plasticity in guppies from high predation environments exposed to low predation conditions (360). Maladaptive plasticity may therefore facilitate post-colonization adaptation by increasing the strength of selection. We additionally found that a lack of plasticity was highest, although not significant, in lineages that have no colonized H₂S-rich habitats. A lack of plasticity may prevent species from responding to an environmental stressor, and therefore limit the ability of selection to act on that trait (363). A key difference between lineages that have successfully colonized sulfide springs and those that have not may therefore

be the ability to modulate gene expression in response to an external stimulus. Having the regulatory machinery to modulate gene expression as opposed to lacking a plastic response may therefore facilitate colonization of novel environments, even if plastic responses are initially maladaptive (360, 364). Overall, our results suggest that adaptive plasticity in key pathways may facilitate initial colonization of H₂S-rich habitats and serve as a pre-adaptive mechanism, but post-colonization adaptation, possibly potentiated by maladaptive plasticity, also plays a critical role in the colonization of novel environments.

Future considerations

Our study identified evidence of both adaptive and maladaptive plasticity, and both of these mechanisms may potentially facilitate the colonization of and adaptation to sulfidic habitats. It is important to highlight, however, that gene expression variation does not necessarily confer functional consequences (38, 39), and future investigations considering the mechanisms that allowed some species of poeciliids to repeatedly colonize H₂S-rich environments should measure the biochemical and physiological differences that exist between successful and unsuccessful colonizers, as was done in Chapters 2 and 3. Additionally, there are other at different levels of biological organization that may also determine what species can persist in sulfide springs. Poeciliids are live-bearing fishes, meaning that embryonic development occurs internally, largely shielded from external stressors (356). This reproductive strategy may minimize the negative consequences of H₂S toxicity on the development of offspring and may explain why poeciliids have successfully colonized H₂S-rich springs in Southern Mexico more than any other family (365, 366).

Although livebearing may be a successful strategy to persisting in sulfidic habitats, it is evident that not all species of livebearers are capable of colonizing them. Therefore, an additional consideration may be differences in behavior. Sulfide-adapted fishes exhibit a behavior known as aquatic surface respiration (ASR), in which fish skim the surface of the water to maximize oxygen availability (29, 281). This behavior has largely been unexplored in the freshwater populations included in our study, and the onset of ASR in response to H₂S may similarly be a pre-adaptation facilitating success in the environments. Future studies should consider these traits when investigating the mechanisms underlying species-specific differences in tolerating chronic H₂S exposure.

Conclusions

The primary goal of this study was to identify potential mechanisms facilitating colonization of H₂S-rich springs in Southern Mexico. Collectively, our comparative transcriptomic analyses revealed idiosyncratic responses to H₂S exposure across species, indicating that sulfide-intolerant organisms largely employ unique regulatory mechanisms in response to H₂S toxicity. This result is intriguing, as it highlights that exposing organisms to similar stressors, even those that impose specific biochemical and physiological constraints, may not result in the obvious identification of coping mechanisms. Additionally, we successfully identified nine genes that exhibited adaptive plasticity across all poeciliids and seven genes uniquely shared by successful ancestors, some of which were present in pathways predicted to facilitate adaptation to H₂S. This finding suggests that adaptive plasticity in key pathways may represent pre-adaptations that initially facilitated the ability of some species to colonize H₂S-rich environments. Given that all species exhibited some degree of adaptive plasticity, however, it is likely not enough to facilitate persistence upon

exposure to novel conditions. Our assessment of plasticity indicated that ancestors of successful colonizing lineages exhibited a larger number of orthogroups responding to H₂S exposure in a maladaptive fashion. Given the previously indicated role of maladaptive plasticity potentiating evolution, it is possible that this phenomenon plays an important role in determining what species can persist upon invading novel environments. These results have implications for considering the evolutionary origins of putatively adaptive traits in locally adapted populations, and our findings may suggest that plasticity per se, whether adaptive or maladaptive, may ultimately be a pre-adaptation facilitating colonization of extreme environments.

Figures

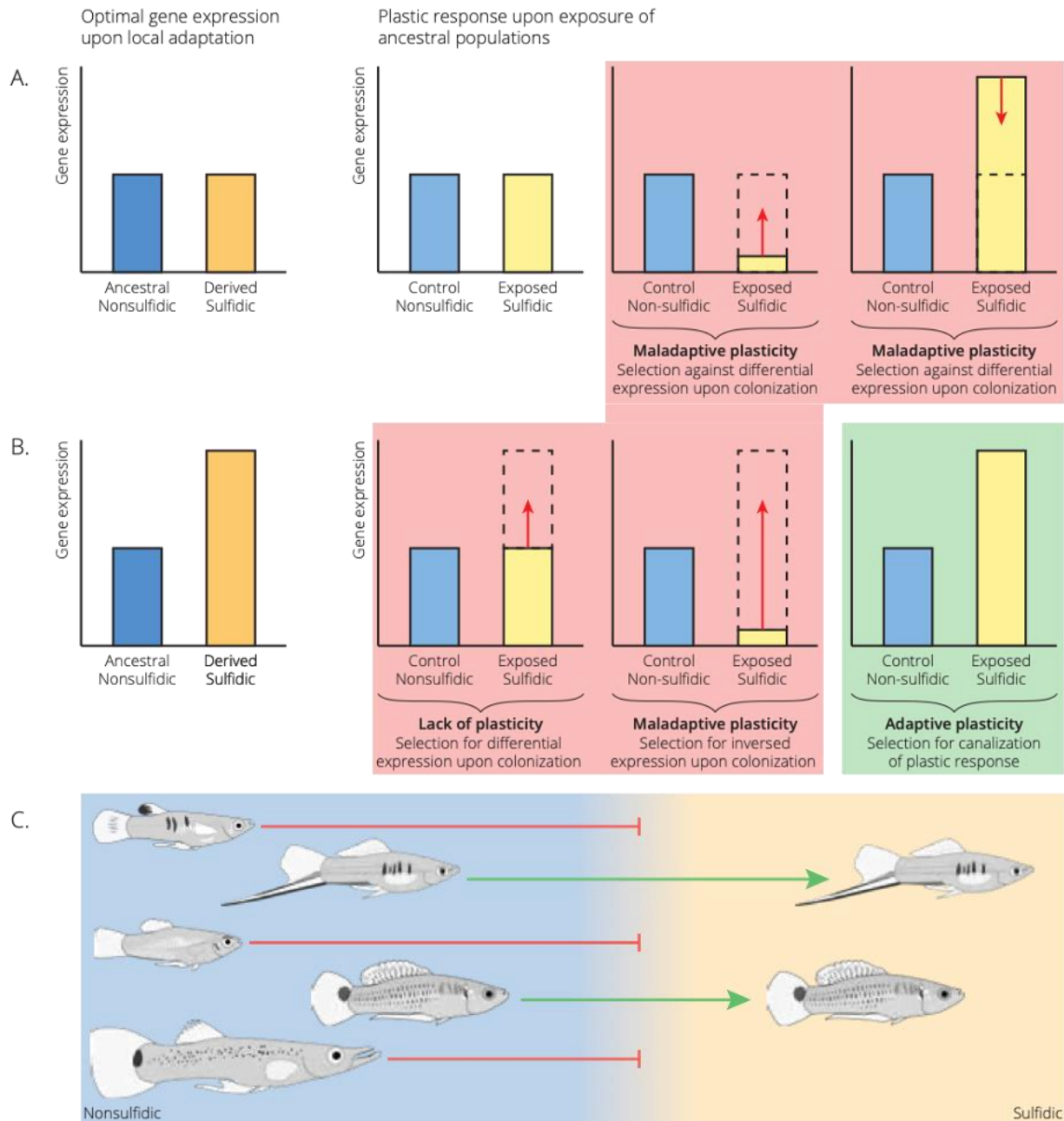


Figure 4-1: Conceptual framework detailing the three potential categories of gene expression responses to H₂S exposure in ancestral populations of fish compared to locally adapted populations of sulfide-tolerant *Poecilia mexicana* (optimal expression levels). A. In this scenario, optimal gene expression does not differ between ancestral and derived populations. Upon exposure to H₂S, these genes may exhibit no plasticity and remain equal in expression, or they may exhibit maladaptive plasticity in freshwater populations due to the presence of expression variation that is lacking in locally adapted populations. B. This scenario considers that there are

expression differences between ancestral and derived populations. Under these conditions, we can identify evidence of adaptive plasticity if exposure to H₂S results in similar expression profiles between freshwater ancestors and locally adapted sulfide-tolerant populations. Alternatively, we can identify a lack of plasticity, in which gene expression does not change upon exposure to H₂S, or maladaptive plasticity, in which plasticity drives expression variation in the opposite direction predicted by patterns observed in adapted populations. C. A visualization of our predicted results, in which species with a derived sulfidic ecotype will exhibit evidence for adaptive plasticity (green arrows), while species that did not successfully colonize sulfide springs will exhibit for a lack of plasticity or maladaptive plasticity (red lines).

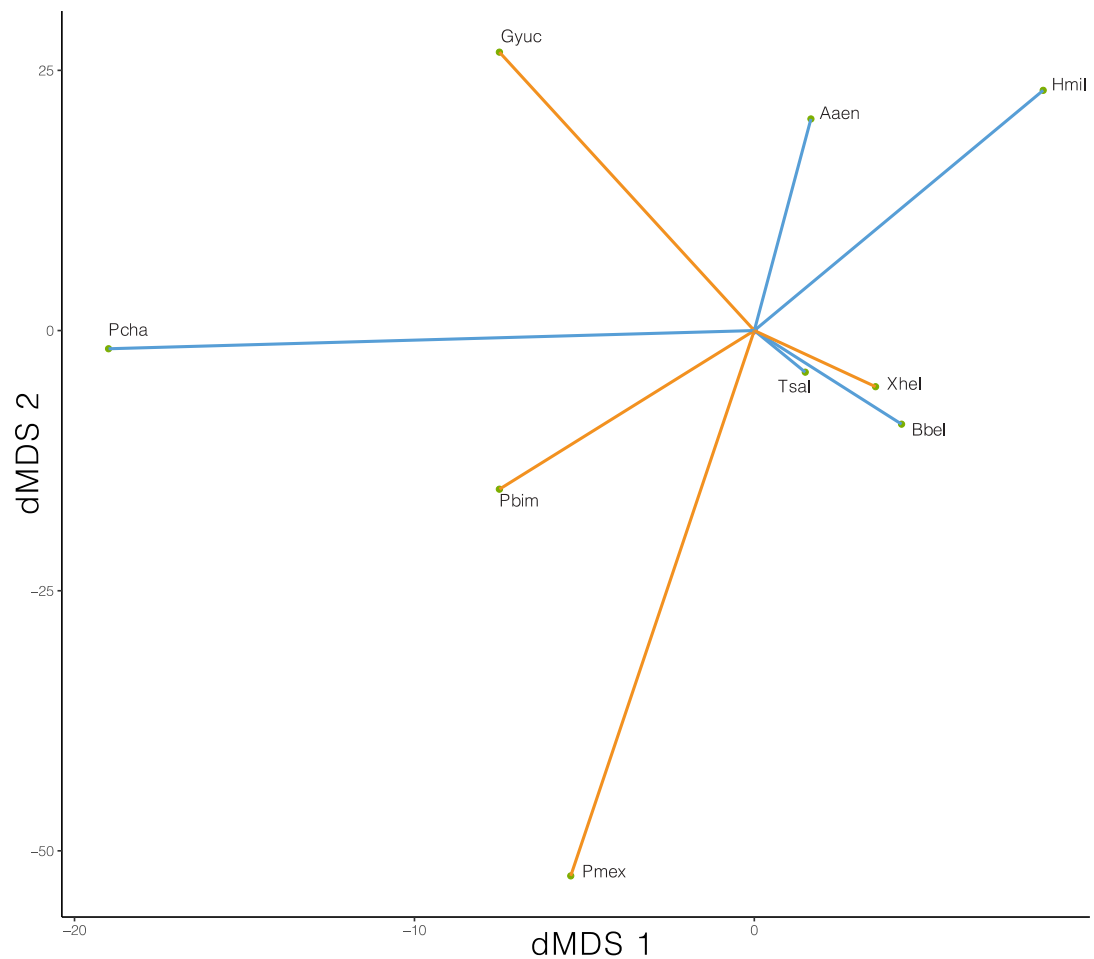


Figure 4-2: MDS plot visualizing the high degree of lineage-specific transcriptional responses upon exposure to H₂S. The center point represents expression under control conditions, and each outward point represents the lineage-specific expression profile upon exposure. Unsuccessful species are represented by blue lines and successful species are represented by orange lines.

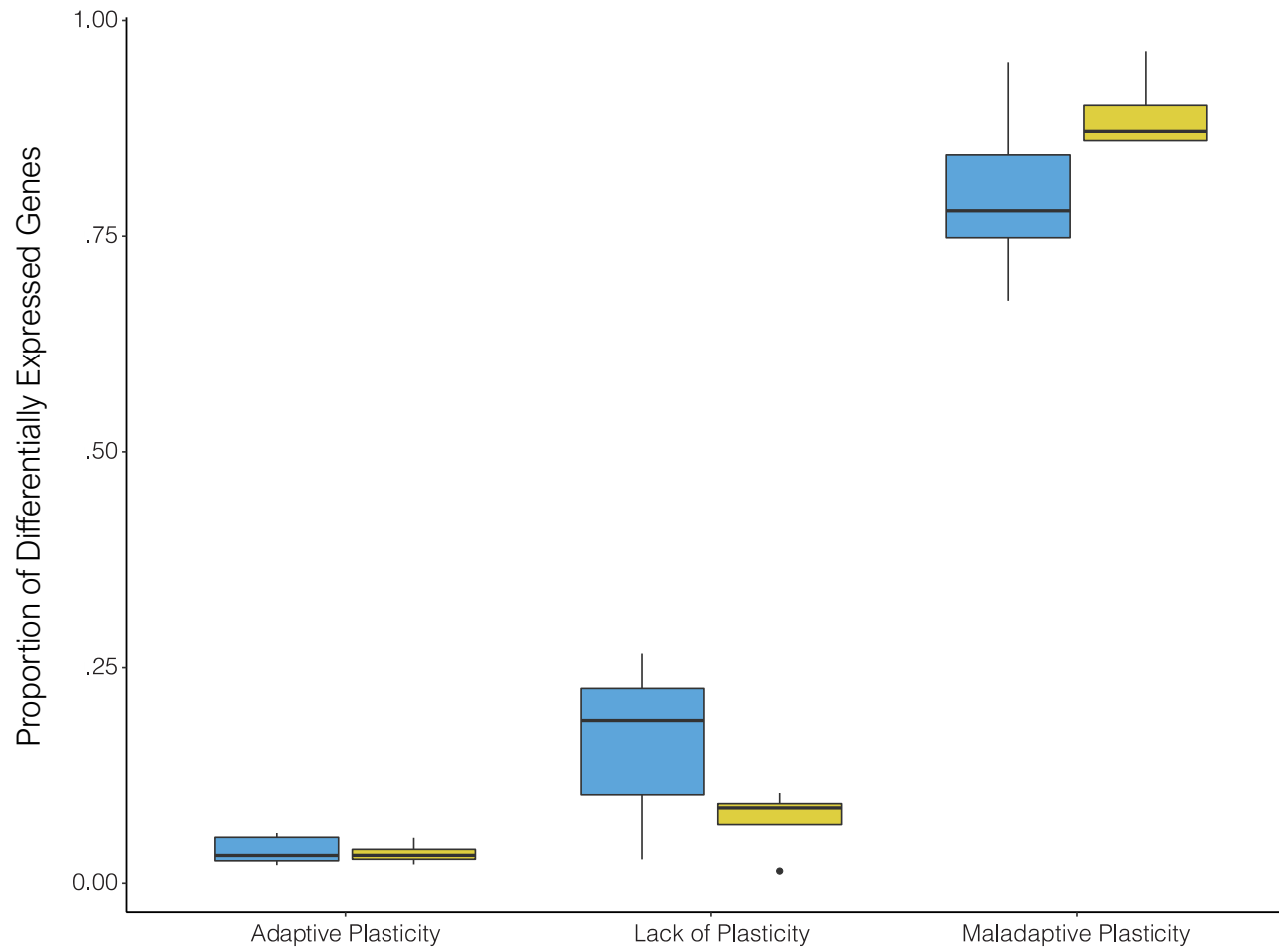


Figure 4-3: Relative gene expression patterns within the three potential categories of plasticity. Blue boxes indicate unsuccessful colonizing species and yellow boxes indicate successful colonizing species. There was no statistically significant difference across measures of plasticity.

Tables

Table 4-1: List containing the species name, family, colonizing success, and sample size for each treatment used for comparative transcriptomics analyses.

Species	Family	Colonizing success	Control	H ₂ S-exposed
<i>Astyanax aeneus</i>	Characidae	Unsuccessful	6	6
<i>Trichromis salvini</i>	Cichlidae	Unsuccessful	6	3
<i>Belonesox belizanus</i>	Poeciliidae	Unsuccessful	3	3
<i>Heterophallus millerii</i>	Poeciliidae	Unsuccessful	6	4
<i>Priapella chamulae</i>	Poeciliidae	Unsuccessful	4	4
<i>Gambusia yucatana</i>	Poeciliidae	Successful	4	4
<i>Poecilia mexicana</i>	Poeciliidae	Successful	5	5
<i>Pseudoxiphophorus bimaculatus</i>	Poeciliidae	Successful	4	4
<i>Xiphophorus helleri</i>	Poeciliidae	Successful	5	6

Table 4-2: Descriptive sequencing and mapping statistics for each species and treatment. All numbers represent means (\pm standard deviation).

Group	Total Reads	Trimmed Reads – qual0	Trimmed Reads – qual24	Aligned Reads	Mapping Percentage
Astyanax Control	80788324 \pm 14576879	80141591 \pm 14603500	78956854 \pm 14430324	72774879 \pm 11363999	96.1 \pm 2.1
Astyanax H ₂ S	764670823 \pm 3552833	75276491 \pm 3731700	74073503 \pm 3711382	71676267 \pm 3600784	96.8 \pm 0.5
Belonesox Control	64302211 \pm 5378899	63409811 \pm 5133154	62598876 \pm 4821089	59838285 \pm 4773934	95.6 \pm 0.6
Belonesox H ₂ S	57487151 \pm 7562020	55802496 \pm 7246645	54858263 \pm 7034340	52736996 \pm 6847929	96.1 \pm 1.3
Gambusia Control	51330015 \pm 5953872	50449801 \pm 6113401	49688865 \pm 5941736	46437281 \pm 5806907	93.3 \pm 2.1
Gambusia H ₂ S	54869144 \pm 10216895	47443534 \pm 9671819	46569141 \pm 9454108	44868870 \pm 9036461	96.5 \pm 1.2
Heterophallus Control	76305500 \pm 4384828	73854825 \pm 5115829	72729284 \pm 5019379	68835247 \pm 4352462	93.6 \pm 1.4
Heterophallus H ₂ S	56969361 \pm 10736935	56516846 \pm 10785908	55833937 \pm 10778227	52885683 \pm 10360607	94.5 \pm 1.0
Priapella Control	34069417 \pm 9282375	72010847 \pm 19295689	71404470 \pm 19256457	68818771 \pm 18335316	96.7 \pm 0.8
Priapella H ₂ S	60537878 \pm 13850800	55555938 \pm 11011082	54679104 \pm 10948617	53436780 \pm 10845465	97.6 \pm 0.6
Pseudoxiphophorus Control	72749767 \pm 19260486	33241031 \pm 8728539	32700512 \pm 8614739	31351498 \pm 8137045	96.0 \pm 1.3
Pseudoxiphophorus H ₂ S	55808343 \pm 11038382	59375592 \pm 13505391	58297614 \pm 13314030	57093254 \pm 13373885	96.9 \pm 1.0
Poecilia Control	52450618 \pm 10689815	51800492 \pm 23942323	51163904 \pm 10670398	47320669 \pm 9766502	92.7 \pm 0.9
Poecilia H ₂ S	47925337 \pm 7123448	45200206 \pm 6062726	44559001 \pm 6048905	42219191 \pm 5933922	94.4 \pm 1.8
Trichromis Control	59406863 \pm 6673359	58942021 \pm 6763091	58109635 \pm 6645983	56789045 \pm 6505901	97.7 \pm 0.4
Trichromis H ₂ S	61883467 \pm 1964067	60489739 \pm 3190347	59583514 \pm 3233988	57616357 \pm 3788295	96.5 \pm 4.0
Xiphophorus Control	50807222 \pm 9478287	50214277 \pm 9509542	49515566 \pm 9394782	46769483 \pm 8951468	94.9 \pm 2.7
Xiphophorus H ₂ S	51491461 \pm 6033110	51162984 \pm 6078926	50414958 \pm 5975091	49819741 \pm 5888080	98.8 \pm 0.4

Table 4-3: Comparisons between control and H₂S exposed individuals within species were used to identify lineage-specific and universal trends of orthogroup expression plasticity induced by H₂S toxicity. Additionally, comparisons between the expression profiles of exposed individuals and wild-caught sulfidic *Poecilia mexicana* were used to identify patterns of plasticity. For each species, we provide the number of up and downregulated orthogroups and the number of orthogroups exhibiting adaptive, maladaptive, or a lack of plasticity. Underlined values indicate the number of shared orthogroups within the group comparisons.

Species	Upregulated	Downregulated	Adaptive Plasticity	Maladaptive Plasticity	Lack of Plasticity
Successful ancestors	<u>142</u>	<u>36</u>	<u>9</u>	<u>111</u>	<u>4</u>
<u>Family: Poeciliidae</u>					
<i>Gambusia yucatanana</i>	2131	1991	57	2545	37
<i>Poecilia mexicana</i>	726	305	41	672	68
<i>Pseudoxiphophorus bimaculatus</i>	698	534	26	773	78
<i>Xiphophorus maculatus</i>	667	465	28	695	85
Unsuccessful ancestors	<u>18</u>	<u>0</u>	<u>0</u>	<u>14</u>	<u>1</u>
<u>Family: Poeciliidae</u>	<u>35</u>	<u>0</u>	<u>2</u>	<u>22</u>	<u>14</u>
<i>Belonesox belizanus</i>	210	136	18	208	82
<i>Heterophallus millerii</i>	550	432	38	605	74
<i>Priapella chamulae</i>	407	91	11	318	96
<u>Family: Characidae</u>					
<i>Astyanax aeneus</i>	1374	1122	34	1554	45
<u>Family: Cichlidae</u>					
<i>Trichromis salvini</i>	372	84	12	293	71

Table 4-4: List of universally upregulated genes in successful and unsuccessful ancestors. Included are the orthogroup ID, the accession number associated with the top BLAST hit, the gene name, the protein name, and the E-value.

Orthogroup	Accession	Gene	Protein	E-value
OG0014278	Q14201	BTG3	Protein BTG3	6.00E-34
OG0005154	P01100	FOS	Proto-oncogene c-Fos	3.00E-18
OG0011131	P24522	GADD45A	Growth arrest and DNA damage-inducible protein GADD45 alpha	1.00E-74
OG0009808	Q96D03	DDIT4L	DNA damage-inducible transcript 4-like protein	2.00E-18
OG0009898	P55210	P55210	Caspase-7	1.00E-34
OG0012992	O00220	TNFRSF10A	Tumor necrosis factor receptor superfamily member 10A	2.00E-07

Table 4-5: List of candidate pre-adaptations as identified in the comparison of differential expression patterns in successful and adaptive groups. Included are the orthogroup ID, the accession number associated with the top BLAST hit, the gene name, the protein name, the directionality of expression, and the E-value.

Orthogroup ID	Accession	Gene	Protein	Expression	E-value
OG0008849	P53985	SLC16A1	Monocarboxylate transporter 1	↑	0
OG0010253	Q96KS0	EGLN2	Egl nine homolog 2	↑	4.00E-127
OG0009986	Q16831	UPP1	Uridine phosphorylase 1	↑	1.00E-140
OG0012407	Q9Y241	HIGD1A	HIG1 domain family member 1A, mitochondrial	↑	3.00E-37
OG0013308	Q9H6Z9	EGLN3	Egl nine homolog 3	↑	4.00E-117
OG0005897	O95571	ETHE1	Persulfide dioxygenase ETHE1, mitochondrial	↑	5.00E-97
OG0010180	P09972	ALDOC	Fructose-bisphosphate aldolase C	↑	0
OG0008004	P55017	SLC12A3	Solute carrier family 12 member 3	↓	0
OG0016575	P58743	SLC26A5	Prestin	↑	0

Chapter 5 - Synthesis

The predictability of biological processes

Evolution's predictability is a point of contention within the field of biology, in part due to an argument originally introduced by Stephen J. Gould who famously stated that "replaying the tape of life" would result in any number of possibilities, ultimately limiting our ability to predict evolutionary outcomes (144). In contrast to Gould's idea of evolutionary contingency, Simon Conway Morris firmly believed in evolutionary determinism, an idea based on the belief that the laws of the chemical and physical world restrict evolution's potential and drive organisms towards similar phenotypes in response to similar environmental pressures (166). Indeed, evidence for convergent evolution is nearly ubiquitous in nature and is found across wide phylogenetic and environmental scales (7, 24, 49). Examples of convergent evolution include the evolution of hemoglobin function in high altitude organisms (56), the loss of eyes in cave-dwelling animals (367), and the similarity in morphology of particular ecomorphs of *Anolis* lizards (49, 368, 369). As demonstrated by the previous examples, it appears that convergence of physiological and ecological function is quite common in nature; however, the genetic architectures underlying these traits tend to exhibit less evidence of convergence (1, 5, 248). This begets the question when and under what circumstances can we predict evolution at the molecular level? And similarly, is our ability to predict evolutionary patterns shaped by our ability to predict the functional aspects of phenotypes across levels of organization? These two questions were the focal points of my doctoral research, and the four chapters provided in this dissertation build upon one another to understand the relationships between predicting evolution and predicting the consequences of genetic variation on physiological function across levels of organization.

The role of environment in predicting evolutionary outcomes

In Chapters 1 and 2, I explored the ability to predict evolutionary outcomes in 10 lineages of fishes found in environments rich in hydrogen sulfide (H₂S). In these studies, we hypothesized that evolutionary predictability is influenced by the constraints that environments impose on organismal function. In environments that impose strong sources of selection with clear consequences for key physiological pathways, we predicted that evolution across all levels of organization would be easier to predict given that the number of solutions to overcome environmental challenges would be limited. Indeed, we found evidence for predictable evolutionary change in three physiological pathways known to be directly influenced by the presence of H₂S (24, 248). Oxygen transport proteins, such as hemoglobin, and cytochrome c oxidase (COX) are toxicity targets of H₂S and are ultimately rendered ineffective upon binding with the molecule (15, 16, 370). We were able to identify convergent modifications of amino acid composition in both of these targets, indicating that these fundamentally important pathways are predictable targets of selection in H₂S-rich environments, at least at the molecular level (24, 248). We additionally identified a nearly ubiquitous upregulation of sulfide detoxification genes, encoding for enzymes such as sulfide:quinone oxidoreductase (SQR), in sulfide-tolerant lineages, suggesting that detoxification may be a predictably important component of adaptation to these toxic habitats (248). In *Poecilia mexicana*, we found that the genetic variation identified in COX and SQR correlated with differences in physiology, suggesting that genetic variation had predictable consequences on physiological function (248). We hypothesize that our ability to detect evolutionary predictability in this system is related to Conway Morris' argument that chemical and physical laws may ultimately drive organisms to the same solution to overcome a

shared evolutionary problem (166). This phenomenon is not unique to sulfide springs, and patterns of evolution's predictability at multiple biological scales may likely be found in other environments that impose specific and direct constraints on organismal function (58, 60, 61). What may be unique to our analyses of evolution in response to H₂S is that this molecule interferes with highly conserved pathways, such as oxidative phosphorylation and H₂S detoxification, which may have perpetuated our ability to identify patterns of molecular predictability (248).

Broadly, it may be that evolution does not follow predictable patterns in most populations or species (or physiological systems) due to the complexity of the natural world. Environments rarely impose a single source of selection, and it is possible that the interaction between multiple sources of selection may influence evolutionary outcomes even when it appears organisms are exposed to similar selective regimes (52). Additionally, the genetic architecture of distinct evolutionary lineages may influence evolution's ability to drive populations to the same adaptive peaks, and this may similarly be shaped by the environment of ancestral populations or possibly by different mutations occurring in the same or different genes (52). In Chapter 4, I investigated whether plasticity within the pathways underlying adaptation outlined in Chapters 1 and 2 was a pre-adaptation that facilitated colonization of these environments by certain species. I found that responses to H₂S exposure in all species studied was largely lineage-specific, even in the direct ancestors of sulfide-tolerant populations. These individuals shared a number of differentially expressed orthogroups, but largely our results suggest that these lineages evolved similar phenotypes despite their original variable responses. Additionally, we identified that all successful and unsuccessful colonizing species exhibited both adaptive and maladaptive plasticity, which in itself is not surprising (361, 364). However, we found that successful

colonizing species possessed higher numbers of orthogroups characterized as maladaptively plastic when compared to known adaptive responses. This suggests that plasticity itself may be a pre-adaptation that assists in initial invasion of novel habitats, but post-colonization evolution likely influences which species can persist. Previous research has found that maladaptive responses may result in rapid adaptation by providing selection a trait to act upon and drive traits towards an adaptive peak (362, 371). This study further builds upon that literature, providing evidence that the presence of plasticity, whether adaptive or maladaptive, may facilitate adaptation to novel environments. Additionally, it sheds light onto the predictability of both evolution and phenotype. Each lineage exhibited largely unique responses to H₂S exposure despite the fact that organismal tolerance of H₂S are largely similar within successful and unsuccessful groups independently. When considering adaptive plasticity, all successful colonizing species shared transcriptional responses in 9 genes within physiological pathways predicted to be important for adaptation to sulfidic environments, such as H₂S detoxification, aerobic and anaerobic metabolism, and ion transport. Although unshared, these genes and others within these pathways were also found in unsuccessful colonizing species. Therefore, it may be that we can predict what phenotypes play important roles in adaptation, but the way selection acts on the architecture underlying these phenotypes may be more difficult to predict.

Predicting the consequences of phenotypic variation

In Chapter 3, I particularly focused on our ability to predict physiological function as a consequence of variation across biological scales. Scientists frequently invoke that the observation of variation at lower levels of organization, such as genotypic differences in mitochondrial genomes, necessitates functional differences at the organismal levels. However,

there is much evidence to suggest that this is not always the case (38, 39). In these counter-arguments, it is found that genetic variation does not necessarily equal functional variation, but fewer studies have assessed how variation in function influences phenotypes as they scale up in biological organization. I particularly focused on metabolism, given that our previous analyses have indicated variation in key components of the oxidative phosphorylation pathway (22, 30, 34, 68, 248). In addition, previous studies have documented that sulfide tolerant and intolerant fishes differ in their routine metabolic rates (32). I found that variation at any level of organization does not necessitate similar variation within the same phenotype across biological scales. Despite evidence for genetic and gene expression variation in all four complexes of the oxidative phosphorylation pathway (22, 34, 164, 248), I did not find evidence of functional variation in these enzymes. This may be due to the use of lab-reared individuals for this portion of the study, and patterns of variation may be different for wild-caught individuals. Nonetheless, I found that mitochondrial function did significantly differ across populations, such that one lineage that is known to have a sulfide-resistant COX also exhibited higher mitochondrial respiration rates. This variation disappeared at the organismal level, in which all populations exhibited similar metabolic rates under control conditions, which was surprising given that increased mitochondrial respiratory function is thought to improve aerobic performance (275). It is known that under periods of stress, cryptic variation of phenotypes may be revealed (372-374), which we found to be true when looking at organismal respiration in the presence of hypoxia, in which there was a clear separation between the hypoxia tolerance of sulfide tolerant and intolerant fishes. This suggests that although we are able to predict what pathways selection may act on, our ability to predict the functional ramifications of evolutionary modifications may be relatively low. This is likely particularly true for physiological phenotypes, which are inherently

complex given that they are often the result of interacting pathways (375). Metabolism is a broad physiological phenotype that is composed of interactions between oxidative phosphorylation, anaerobic respiration, oxygen transport, and many other pathways (376). Modifications of any of these pathways may influence how phenotypes are observed at higher levels of organization. Therefore, although the predictable outcomes of evolution are of particular interest to evolutionary biologists as they may explain how the natural world limits evolutionary potential, the unpredictable outcomes may be equally important as we consider how organismal phenotypes are shaped by evolution.

Convergent and nonconvergent patterns of evolution

My dissertation largely considered the predictability of biological processes by exploring convergent evolution in lineages of sulfide tolerant fishes. Convergence is regularly cited as a prime example for the deterministic nature of evolution (47, 48, 52); however, it is known that even when evidence of convergence is found, organisms inhabiting similar environments still show some degree of lineage-specific variation (7, 52). This nonconvergence is sometimes discarded as noise clouding the larger picture, but it is possible that these unpredictable components may provide fundamental insights into how evolution operates in the natural world (52). My research found evidence for evolutionary convergence in the sulfide detoxification, oxidative phosphorylation, and oxygen transport pathways in response to chronic exposure to H₂S across biological levels (24, 248). This convergence may represent the deterministic nature of evolution when organisms are exposed to selective regimes that constrain function of necessary biological processes (166), such as aerobic metabolism. However, these shared mechanisms likely do not compose the only adaptive possibilities as evidenced by the large

number of nonconvergent variation we identified across lineages (248). Although organisms may evolve similar solutions to the same environmental challenge, either due to constraints or similar genetic background, unique adaptations may still surface due to differences in evolutionary history or random mutation (52). In respect to the sulfur system, perhaps modification of detoxification pathways, which exhibits near ubiquitous upregulation in all sulfide tolerant fishes included in our studies (248), was an initial pre-requisite to persist, and modification of alternative pathways, such as oxidative phosphorylation or oxygen transport, may have occurred due to random change. Although there is evidence of convergent modification of these pathways, molecular evolution was not observed in all sulfide tolerant lineages and may therefore represent random evolutionary modifications (52). Is it possible that modification of H₂S detoxification, which directly interacts with oxidative phosphorylation, in conjunction with the environmental constraints experienced in sulfidic springs resulted in the unique evolutionary trajectories of each species to often reach similar phenotypic outcomes? Are the pathways that exhibit lineage-specific variation predictable? Are they related to the hypothesized initial modification of SQR? I believe that exploring these differences may shed insights into how evolutionary and phenotypic predictability relate to one another and provide novel insights into the mechanisms regulating adaptive evolution.

Appendix A - Molecular evolution and expression of oxygen transport genes in livebearing fishes (Poeciliidae) from hydrogen sulfide rich springs

Appendix A Figures

```

X. helleri NS MVEWTD AERTAI STLWSNIDVGEIGPQALSRLLVFPWTRQRYFFTFGDLSTPAAIAANFKVAQHGTKVMGGLAVKNDMDNIKNAYAKLSVMHSEKLVHPDNDNFRVLAECITVVVAAKFGPSVFTAGFQEAQKFLAVVVSALGRQYH
X. helleri S MVEWTD AERTAI STLWSNIDVGEIGPQALSRLLVFPWTRQRYFFTFGDLSTPAAIAANFKVAQHGTKVMGGLAVKNDMDNIKNAYAKLSVMHSEKLVHPDNDNFRVLAECITVVVAAKFGPSVFTAGFQEAQKFLAVVVSALGRQYH
P. bimaculata NS MVEWTD AERTAI STLWSNIDVGEIGPQALSRLLVFPWTRQRYFFTFGDLSTPAAIAANFKVAQHGTKVMGGLAVKNDMDNIKNAYAKLSVMHSEKLVHPDNDNFRVLAECITVVVAAKFGPSVFTAGFQEAQKFLAVVVSALGRQYH
P. bimaculata S MVEWTD AERTAI STLWSNIDVGEIGPQALSRLLVFPWTRQRYFFTFGDLSTPAAIAANFKVAQHGTKVMGGLAVKNDMDNIKNAYAKLSVMHSEKLVHPDNDNFRVLAECITVVVAAKFGPSVFTAGFQEAQKFLAVVVSALGRQYH
G. holbrooki NS MVEWTD AERTAI STLWSNIDVGEIGPQALSRLLVFPWTRQRYFFTFGDLSTPAAIAANFKVAQHGTKVMGGLAVKNDMDNIKNAYAKLSVMHSEKLVHPDNDNFRVLAECITVVVAAKFGPSVFTAGFQEAQKFLAVVVSALGRQYH
G. holbrooki S MVEWTD AERTAI STLWSNIDVGEIGPQALSRLLVFPWTRQRYFFTFGDLSTPAAIAANFKVAQHGTKVMGGLAVKNDMDNIKNAYAKLSVMHSEKLVHPDNDNFRVLAECITVVVAAKFGPSVFTAGFQEAQKFLAVVVSALGRQYH
G. eurystoma S MVEWTD AERTAI STLWSNIDVGEIGPQALSRLLVFPWTRQRYFFTFGDLSTPAAIAANFKVAQHGTKVMGGLAVKNDMDNIKNAYAKLSVMHSEKLVHPDNDNFRVLAECITVVVAAKFGPSVFTAGFQEAQKFLAVVVSALGRQYH
G. eurystoma NS MVEWTD AERTAI STLWSNIDVGEIGPQALSRLLVFPWTRQRYFFTFGDLSTPAAIAANFKVAQHGTKVMGGLAVKNDMDNIKNAYAKLSVMHSEKLVHPDNDNFRVLAECITVVVAAKFGPSVFTAGFQEAQKFLAVVVSALGRQYH
G. secretulata S MVEWTD AERTAI STLWSNIDVGEIGPQALSRLLVFPWTRQRYFFTFGDLSTPAAIAANFKVAQHGTKVMGGLAVKNDMDNIKNAYAKLSVMHSEKLVHPDNDNFRVLAECITVVVAAKFGPSVFTAGFQEAQKFLAVVVSALGRQYH
L. paraguayana NS MVEWTD AERTAI STLWSNIDVGEIGPQALSRLLVFPWTRQRYFFTFGDLSTPAAIAANFKVAQHGTKVMGGLAVKNDMDNIKNAYAKLSVMHSEKLVHPDNDNFRVLAECITVVVAAKFGPSVFTAGFQEAQKFLAVVVSALGRQYH
L. sulphuriphila S MVEWTD AERTAI STLWSNIDVGEIGPQALSRLLVFPWTRQRYFFTFGDLSTPAAIAANFKVAQHGTKVMGGLAVKNDMDNIKNAYAKLSVMHSEKLVHPDNDNFRVLAECITVVVAAKFGPSVFTAGFQEAQKFLAVVVSALGRQYH
P. latipinna NS MVEWTD AERTAI STLWSNIDVGEIGPQALSRLLVFPWTRQRYFFTFGDLSTPAAIAANFKVAQHGTKVMGGLAVKNDMDNIKNAYAKLSVMHSEKLVHPDNDNFRVLAECITVVVAAKFGPSVFTAGFQEAQKFLAVVVSALGRQYH
P. latipinna S MVEWTD AERTAI STLWSNIDVGEIGPQALSRLLVFPWTRQRYFFTFGDLSTPAAIAANFKVAQHGTKVMGGLAVKNDMDNIKNAYAKLSVMHSEKLVHPDNDNFRVLAECITVVVAAKFGPSVFTAGFQEAQKFLAVVVSALGRQYH
P. limantouri NS MVEWTD AERTAI STLWSNIDVGEIGPQALSRLLVFPWTRQRYFFTFGDLSTPAAIAANFKVAQHGTKVMGGLAVKNDMDNIKNAYAKLSVMHSEKLVHPDNDNFRVLAECITVVVAAKFGPSVFTAGFQEAQKFLAVVVSALGRQYH
P. sulphuraria S MVEWTD AERTAI STLWSNIDVGEIGPQALSRLLVFPWTRQRYFFTFGDLSTPAAIAANFKVAQHGTKVMGGLAVKNDMDNIKNAYAKLSVMHSEKLVHPDNDNFRVLAECITVVVAAKFGPSVFTAGFQEAQKFLAVVVSALGRQYH
P. mexicana (Tac) S MVEWTD AERTAI STLWSNIDVGEIGPQALSRLLVFPWTRQRYFFTFGDLSTPAAIAANFKVAQHGTKVMGGLAVKNDMDNIKNAYAKLSVMHSEKLVHPDNDNFRVLAECITVVVAAKFGPSVFTAGFQEAQKFLAVVVSALGRQYH
P. mexicana (Puy) NS MVEWTD AERTAI STLWSNIDVGEIGPQALSRLLVFPWTRQRYFFTFGDLSTPAAIAANFKVAQHGTKVMGGLAVKNDMDNIKNAYAKLSVMHSEKLVHPDNDNFRVLAECITVVVAAKFGPSVFTAGFQEAQKFLAVVVSALGRQYH
P. mexicana (Pich) NS MVEWTD AERTAI STLWSNIDVGEIGPQALSRLLVFPWTRQRYFFTFGDLSTPAAIAANFKVAQHGTKVMGGLAVKNDMDNIKNAYAKLSVMHSEKLVHPDNDNFRVLAECITVVVAAKFGPSVFTAGFQEAQKFLAVVVSALGRQYH
P. mexicana (Tac) NS MVEWTD AERTAI STLWSNIDVGEIGPQALSRLLVFPWTRQRYFFTFGDLSTPAAIAANFKVAQHGTKVMGGLAVKNDMDNIKNAYAKLSVMHSEKLVHPDNDNFRVLAECITVVVAAKFGPSVFTAGFQEAQKFLAVVVSALGRQYH

```

Figure A1: Amino acid sequence alignment of HEMOBAL2, which exhibited ω s was higher than ω NS, but no evidence for a significant a branch-site test (see Table 4). Branch tests with a single lineage in the foreground revealed significantly elevated values of ω for *G. eurystoma*, *P. sulphuraria*, and *P. mexicana* (Tacotalpa) (results not shown), which all exhibit amino acid substitutions at unique codon positions (highlighted in red).

Appendix A Tables

Table A1. List of background genes used for phylogenetic analyses and to estimate expression variation for EVE analyses. The table includes the gene ID from the *X. maculatus* reference genome annotation file (XM ID), the number of base pairs included in phylogenetic analyses, and the best supported model based on analyses of jModelTest. Note that genes with an asterisk were excluded from phylogenetic analyses due to alignment problems.

Gene	XM ID	Length (bp)	Model
AADAT	005807238.2	1278	HKY+G
ABCD3	014475225.1	1980	GTR+I+ G
ABHD10	005797896.2	870	HKY+G
ABHD11	014474520.1	1077	HKY+G
ABHD112	005813987.1	954	HKY+G
ACADS	005811490.2	1368	GTR+I+ G
ACSL5	005794720.1	2064	K80+I+ G
ACSS2	005801880.1	2070	GTR+G
ACTC1	005806151.1	1131	SYM+I+ G
ADSL	005811732.2	1449	GTR+G
ALAS2	005808942.2	2349	HKY+I+ G
ALDH1L2	005808146.1	3375	GTR+I+ G
ALDH2	005816457.1	1877	HKY+G
AMACR	005798702.1	1212	GTR+G
ANXA2	014475428.1	1017	HKY+G
ARMC4	014475557.1	2637	GTR+I+ G
AURKAIP1	014474989.1	636	HKY+G
CASP8	005797663.1	2091	HKY+G
CCT3	005805489.1	1623	GTR+I+ G
CCT7	005799601.1	2082	GTR+I+ G
CGA	005801281.1	375	K80+G
Chaperonin	005816344.1	1737	GTR+I+ G
CLIC4	005799133.2	756	GTR+G
CLYBL	014468401.1	1086	GTR+G
COMT	005813825.2	792	HKY+G
COPA	005796554.1	3861	GTR+I+ G
CPSF1	005809367.1	4464	GTR+I+ G
CPSF4	005808808.1	798	GTR+G
CSTF3	005813724.1	2560	GTR+G
CTSD	005808104.1	1206	GTR+I+ G
CTSZ	005804262.2	909	GTR+G

CYP11B1	014473016.1	1626	HKY+I+ G
CYP27A1	014468470.1	1554	HKY+I+ G
DAZAP2	005815697.2	507	HKY+I
DDOST	005805756.2	1401	SYM+G
DDX19A	005797975.2	1467	GTR+G
DDX27	005812949.1	3246	GTR+G
DDX55	005815541.2	1770	GTR+I+ G
ECH1	005796846.2	933	HKY+G
ECHS1	005813416.2	1122	GTR+I
ECI2	005796012.2	1212	HKY+G
ECT2	005816235.1	3072	HKY+I+ G
EEF1A1P1	005805749.1	1386	GTR+I+ G
EEF2	005797097.1	2577	GTR+G
EIF2S3	005812701.2	1497	GTR+G
ENDOG	014470985.1	903	HKY+G
FAM36A	005816157.2	444	K80+I
FOXRED1	005809315.1	1713	GTR+G
G6PD	005801747.2	1543	GTR+G
GAC	005807371.1	1842	GTR+I+ G
GAPDH	005798762.2	1002	GTR+G
GCG	005808066.2	807	HKY+G
GK	005807820.1	2184	GTR+I+ G
GLE1	005803874.2	2190	GTR+G
GLRX	005814739.2	318	K80+G
GLRX2	005800858.2	741	GTR+I
GTPBP3	014469449.1	1563	HKY+I+ G
HADHB	005803415.1	1422	HKY+G
HDAC1	005799138.2	1467	GTR+G
HDAC3	005813186.2	1287	GTR+G
HIGD1A	005809444.2	279	HKY+G
HK1	005804231.1	3930	GTR+G
HSP90AB1	005803118.1	2181	GTR+I+ G
HSPB7	005805755.2	468	K80+G
HSPE1	005816343.1	297	K80+G
HTRA2	005801130.2	1344	GTR+G
IDH3B	005808461.1	1578	GTR+G
IGSF8	005796988.1	1905	HKY+I+ G
IMMT	005816057.1	2529	GTR+G
KARS	005810419.1	1734	GTR+G
L2HGDH	005799262.1	1344	GTR+G
LDHB	014473567.1	1002	GTR+G
LOC10223 1964*	005809220.1		
MCEE	005812538.2	519	HKY+G
MCM2	005808547.1	2703	GTR+G

MCM7	014469884.1	2703	GTR+I+ G
ME1	005798064.2	1863	GTR+G
METTL17	005796597.2	1395	GTR+G
MICU1	005810989.2	1452	GTR+I+ G
MMAB	005804029.2	690	HKY+G
MR1	005807674.1	1068	K80+I+ G
MRPL30	005798047.2	480	HKY+G
MRPL42	005797188.2	435	K80+G
MRPL52	005807216.2	384	HKY+G
MRPS2	005797990.2	807	HKY+I
MRPS25	005801682.2	516	HKY+G
MRPS9	005802575.2	1149	HKY+G
MTERF2*	005803267.1		
MTX2	005816134.1	861	GTR+G
NARS	005813657.2	1701	GTR+I+ G
NDC80	014476171.1	2643	GTR+G
NFYC	005797337.2	1119	GTR+G
NME1	005811683.1	456	SYM+I+ G
NOP56	005815162.1	1686	GTR+G
ODC1	005799115.2	1380	SYM+G
OGDH	005806877.1	3432	GTR+I+ G
OGG1	005801686.2	1203	HKY+G
OPA3	005810552.2	468	HKY+G
OXCT1	005795042.2	1584	GTR+G
PABPC1	005797394.1	1905	GTR+G
PANK2	005806844.2	1299	GTR+G
PDK2	005815972.2	1227	GTR+G
PDSS2	005798304.2	1158	HKY+G
PGK1	014474319.1	1257	GTR+I+ G
PGS1	005794622.1	1647	HKY+G
PKD2	005797595.2	2685	GTR+G
PLRG1	005810225.2	1947	GTR+G
POLR1A	014471940.1	5073	GTR+I+ G
POLR2D	005808231.2	558	HKY+I
PPIE	005799140.2	906	GTR+G
PPIF	005794591.2	582	K80+G
PRDX5	005800759.2	573	GTR+I
PRODH	005810076.2	1884	GTR+I+ G
PRODH2	005810843.1	1896	GTR+G
PRPF3	014473017.1	2091	GTR+G
PRTFDC1	005796013.2	675	K80+G
PSMC6	005806032.2	1170	GTR+G
PSPC1	005810205.2	1683	GTR+G
PTS	014473362.1	492	GTR+G
PYCR1	005801446.2	972	GTR+G
RAE1	005800637.1	1110	GTR+I+ G

RFC5	005803838.2	1008	GTR+G
RPL13A	005801275.1	615	GTR+I+ G
RPL24	005798066.1	471	GTR+I
RPL28	005798660.1	414	GTR+I+ G
RPL3	005810301.1	1800	HKY+I+ G
RPL35	005814550.1	369	GTR+G
RPL7	005797870.1	738	GTR+I+ G
RPL8	005802986.1	771	GTR+I+ G
RPS11*	005796715.2		
RPS15	NM_0012863 09.1	435	HKY+I+ G
RPS18	005804726.1	456	GTR+G
RPS4XP21	005806410.1	789	GTR+I+ G
RPS5	005796424.1	609	HKY+I+ G
SEPT4Iso2	005801071.1	1869	HKY+G
SEPT4Iso3	005801071.1	1497	GTR+I+ G
SFXN3	005801574.1	969	GTR+G
SHMT1	005808810.1	1449	GTR+G
SKP1	005807193.2	489	GTR+G
SLC25A14	005800355.1	1278	K80+G
SLC25A22 *	005806958.1		
SLC25A27	005804585.2	858	GTR+G
SLC25A4	005807138.1	897	GTR+I+ G
SLC30A6	014471433.1	1405	HKY+G
SLC35D1	005817323.1	972	GTR+I
SLIRP	005797730.1	330	K80+G
SRP68	005797485.2	2514	GTR+G
STAR	005808973.1	858	GTR+I+ G
STOML2	014473560.1	1077	GTR+G
STXBP3	005805216.2	1782	GTR+I+ G
SUCLA2	005811324.1	1401	GTR+I+ G
TATDN3	005799224.2	834	K80+I+ G
TBP	005804211.2	924	GTR+G
TDRKH	005811695.2	1752	GTR+G
TIMM9	005812066.1	267	K80
TRAP1	005809292.1	2148	GTR+G
TRIAP1	005813844.1	222	F81
TRNT1	005808484.2	1275	GTR+G
TXN2	005802800.1	510	HKY+I
TXNRD1	005807810.2	1803	GTR+I+ G

U2AF1	005812217.2	684	GTR+I+ G
UCP1	014476189.1	915	GTR+I+ G
UFD1L	005794850.2	936	GTR+G
VAMP8	005802151.1	372	HKY+G
VARS	014468686.1	5490	GTR+G
VPS18	005808318.1	2949	GTR+G
WEE1	005807460.2	1869	GTR+G
YBX1	005800098.1	897	GTR+I+ G
YME1L1	014474304.1	2184	GTR+G
YWHAQ	005805652.1	732	GTR+I
ZBED5	014475757.1	4365	HKY+G

Table A2: Descriptive statistics (mean FPKM \pm standard error) of expression levels across species for all oxygen-transport genes.

Lineage	MYO	HEMOBAL2	HEMOAA	HEMOAL2	HEMOBAL	HEMOB1L2	HEMOADL	HEMOAL	HEMOA1L	HEMOB1L	HEMOBL	HEMOESA2
<i>X. hellerii</i> NS	706.2 \pm 109.8	19980.9 \pm 3662.0	14392.8 \pm 2511.5	9635.8 \pm 2598.3	2718.1 \pm 735.8	161.3 \pm 56.5	26.4 \pm 7.0	0.3 \pm 15.0	43.7 \pm 4.3	1.6 \pm 5.8	7.9 \pm 1.4	0.4 \pm 0.7
<i>X. hellerii</i> S	452.1 \pm 109.8	8910.2 \pm 3662.0	7696.4 \pm 2511.5	4740.2 \pm 2598.3	1809.5 \pm 735.8	159.8 \pm 56.5	17.8 \pm 7.0	0 \pm 15.0	15.4 \pm 4.3	0.8 \pm 5.8	2.2 \pm 1.4	0.1 \pm 0.7
<i>P. bimaculatus</i> NS	35.6 \pm 120.3	9389.4 \pm 4011.5	15124.1 \pm 2751.2	10164.7 \pm 2846.3	2815.0 \pm 806.1	165.3 \pm 61.9	15.1 \pm 7.6	21.8 \pm 16.5	6.8 \pm 4.7	22.9 \pm 6.3	0.1 \pm 1.6	1.6 \pm 0.8
<i>P. bimaculatus</i> S	91.2 \pm 109.8	11883.7 \pm 3662.0	12207.1 \pm 2511.5	10546.4 \pm 2598.3	3479.0 \pm 735.8	228.0 \pm 56.5	12.6 \pm 7.0	0.9 \pm 15.0	0.6 \pm 4.3	0.6 \pm 5.8	0.0 \pm 1.4	0.0 \pm 0.7
<i>G. holbrooki</i> NS	370.5 \pm 109.8	18534.1 \pm 3662.0	11579.9 \pm 2511.5	17786.9 \pm 2598.3	4859.3 \pm 735.8	414.8 \pm 56.5	27.1 \pm 7.0	58.5 \pm 15.0	45.0 \pm 4.3	17.2 \pm 5.8	2.3 \pm 1.4	0.3 \pm 0.7
<i>G. holbrooki</i> S	228.5 \pm 109.8	17101.3 \pm 3662.0	14280.9 \pm 2511.5	12793.4 \pm 2598.3	5098.4 \pm 735.8	329.4 \pm 56.5	31.3 \pm 7.0	0.3 \pm 15.0	33.8 \pm 4.3	0.2 \pm 5.8	0.2 \pm 1.4	0.2 \pm 0.7
<i>G. eurystoma</i> S	66.9 \pm 109.8	16652.4 \pm 3662.0	16322.7 \pm 2511.5	15752.5 \pm 2598.3	4759.0 \pm 735.8	389.5 \pm 56.5	42.3 \pm 7.0	79.1 \pm 15.0	9.9 \pm 4.3	18.5 \pm 5.8	4.5 \pm 1.4	0.2 \pm 0.7
<i>G. sexradiata</i> NS	147.0 \pm 109.8	13914.2 \pm 3662.0	11977.2 \pm 2511.5	10680.3 \pm 2598.3	3104.0 \pm 735.8	206.3 \pm 56.5	22.0 \pm 7.0	5.2 \pm 15.0	4.6 \pm 4.3	3.9 \pm 5.8	5.0 \pm 1.4	0.1 \pm 0.7
<i>G. sexradiata</i> S	167.7 \pm 109.8	24894.6 \pm 3662.0	20033.6 \pm 2511.5	20174.1 \pm 2598.3	3912.8 735.8	290.8 \pm 56.5	31.6 \pm 7.0	22.9 \pm 15.0	12.8 \pm 4.3	4.4 \pm 5.8	3.2 \pm 1.4	0.1 \pm 0.7
<i>L. perugiae</i> NS	358.3 \pm 109.8	3323.4 \pm 3662.0	2639.4 \pm 2511.5	1925.4 \pm 2598.3	1153.2 \pm 735.8	103.5 \pm 56.5	10.2 \pm 7.0	1.5 \pm 15.0	0.3 \pm 4.3	2.9 \pm 5.8	0.4 \pm 1.4	0.1 \pm 0.7
<i>L. sulphurophila</i> S	233.3 \pm 109.8	5641.9 \pm 3662.0	6652.4 \pm 2511.5	3208.6 \pm 2598.3	3493.6 \pm 735.8	148.2 \pm 56.5	28.0 \pm 7.0	16.7 \pm 15.0	3.4 \pm 4.3	23.2 \pm 5.8	3.2 \pm 1.4	0.5 \pm 0.7
<i>P. latipinna</i> NS	690.4 \pm 109.8	10642.7 \pm 3662.0	6816.8 \pm 2511.5	11654.8 \pm 2598.3	2562.5 \pm 735.8	576.8 \pm 56.5	21.5 \pm 7.0	1 \pm 15.0	6.6 \pm 4.3	0.4 \pm 5.8	9.4 \pm 1.4	3.3 \pm 0.7
<i>P. latipinna</i> S	1038.4 \pm 109.8	8831.7 \pm 3662.0	4533.5 \pm 2511.5	10953.2 \pm 2598.3	1375.3 \pm 735.8	243.8 \pm 56.5	11.1 \pm 7.0	9.2 \pm 15.0	5.9 \pm 4.3	0.8 \pm 5.8	0.7 \pm 1.4	1.6 \pm 0.7
<i>P. limantouri</i> NS	138.0 \pm 109.8	5455.8 \pm 3662.0	6563.3 \pm 2511.5	3978.8 \pm 2598.3	2143.9 \pm 735.8	89.1 \pm 56.5	14.8 \pm 7.0	3.9 \pm 15.0	0.3 \pm 4.3	0.0 \pm 5.8	0.2 \pm 1.4	1.9 \pm 0.7
<i>P. sulphuraria</i> S	2581.5 \pm 109.8	55517.8 \pm 3662.0	33158.6 \pm 2511.5	32174.9 \pm 2598.3	5442.8 \pm 735.8	1081.1 \pm 56.5	111.5 \pm 7.0	21.7 \pm 15.0	1.5 \pm 4.3	2.8 \pm 5.8	0.2 \pm 1.4	2.8 \pm 0.7
<i>P. mexicana</i> (Tac) S	1199.2 \pm 109.8	12240.6 \pm 3662.0	4051.7 \pm 2511.5	8390.6 \pm 2598.3	490.3 \pm 735.8	161.5 \pm 56.5	26.3 \pm 7.0	0.8 15.0	0.5 \pm 4.3	0.4 \pm 5.8	0.0 \pm 1.4	0.4 \pm 0.7
<i>P. mexicana</i> (Puy) NS	289.8 \pm 109.8	4567.2 \pm 3662.0	7030.5 \pm 2511.5	1788.5 \pm 2598.3	1625.4 \pm 735.8	146.3 \pm 56.5	17.4 \pm 7.0	1.2 \pm 15.0	0.0 \pm 4.3	2.5 \pm 5.8	5.0 \pm 1.4	3.1 \pm 0.7
<i>P. mexicana</i> (Puy) S	833.0 \pm 120.3	12445.7 \pm 4011.5	8878.2 \pm 2751.2	7522.9 \pm 2846.3	2248.9 \pm 806.1	190.5 \pm 61.9	38.1 \pm 7.6	4.3 \pm 16.5	10.7 \pm 4.7	1.5 \pm 6.3	2.2 \pm 1.6	3.1 \pm 0.8
<i>P. mexicana</i> (Pich) NS	506.9 \pm 109.8	6718.5 \pm 3662.0	9995.3 \pm 2511.5	1724.2 \pm 2598.3	1734.0 \pm 735.8	137.8 \pm 56.5	21.7 \pm 7.0	0.5 \pm 15.0	0.6 \pm 4.3	0.5 \pm 5.8	8.0 \pm 1.4	1.3 \pm 0.7
<i>P. mexicana</i> (Tac) NS	267.3 \pm 109.8	4056.4 \pm 3662.0	4825.4 \pm 2511.5	1103.2 \pm 2598.3	815.1 \pm 735.8	98.1 \pm 56.5	14.5 \pm 7.0	1.1 \pm 15.0	3.9 \pm 4.3	3.7 \pm 5.8	3.0 \pm 1.4	0.3 \pm 0.7

Appendix B - Convergent evolution of conserved mitochondrial pathways underlies repeated adaptation to extreme environments

Appendix B Figures

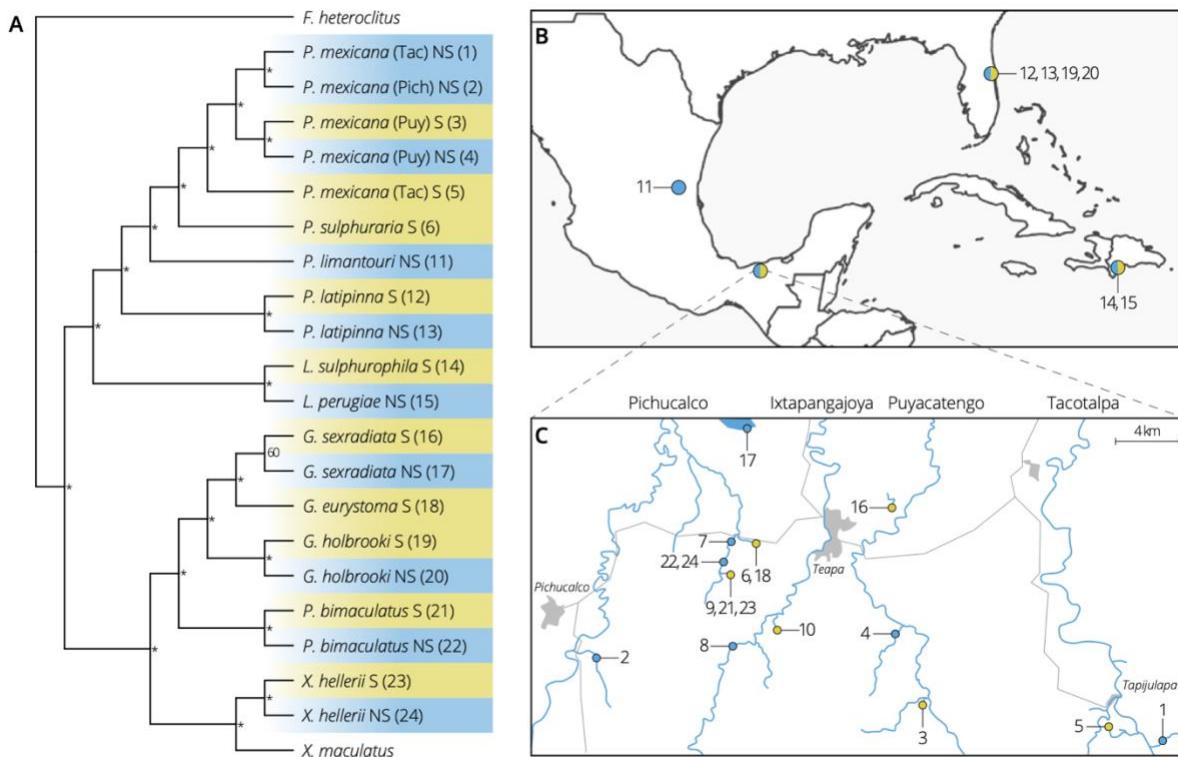


Figure B1. Overview of the phylogenetic relationships and distribution of lineages investigated in the comparative transcriptomics portion of this study. **A.** Phylogenetic tree of different sulfidic (S, underlined) and nonsulfidic lineages (NS), with *Fundulus heteroclitus* as outgroup. Asterisks indicate bootstrap support >0.99. **B.** Map depicting the collection locations of sulfide spring (yellow) and reference (blue) lineages. **C.** Detailed view of collection localities in southern Mexico; this map also includes sample sites from the comparative genomics analysis. Lineages included are numbered corresponding to Table S1. Black lines in panel C indicate major roads and gray shadings the location of major towns that have been added for orientation.

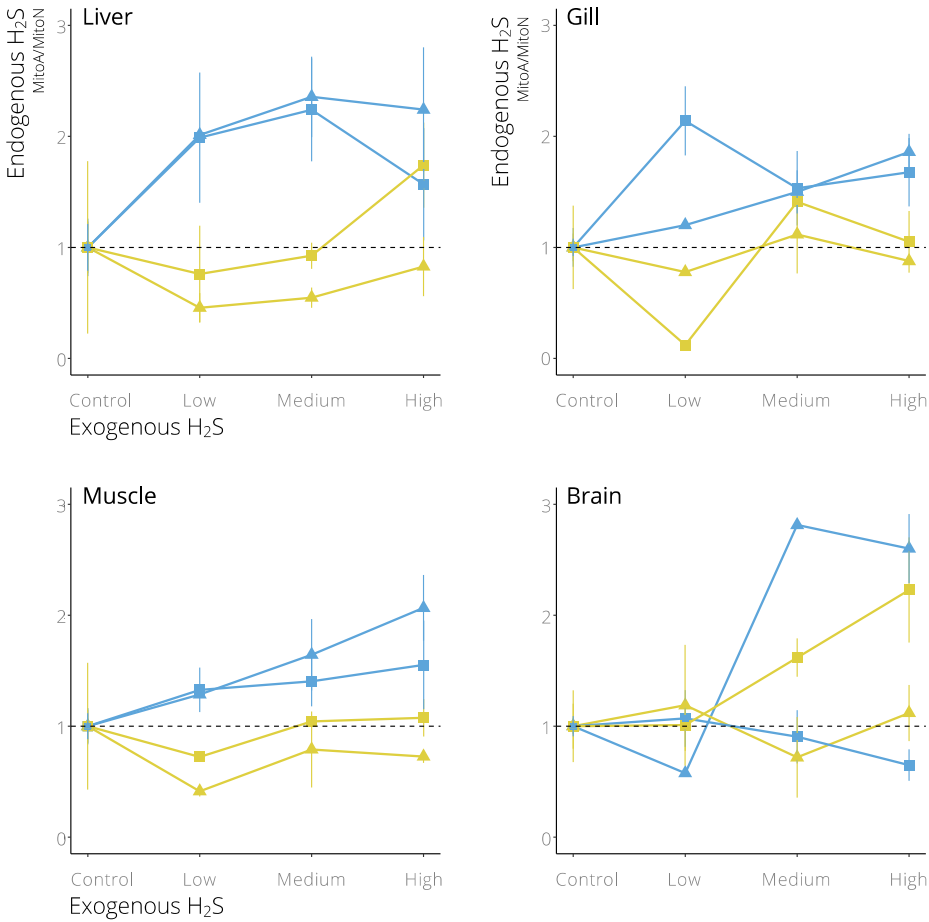


Figure B2. Relative change in endogenous H₂S concentrations of live fish exposed to different levels of environmental H₂S, as quantified in different organs. For all graphs, yellow colors denote *P. mexicana* from sulfidic habitats, blue from nonsulfidic habitats. Symbols stand for populations from different river drainages (■: Tac; ▲: Puy). The results indicate that exposure to exogenous H₂S leads to increases in endogenous H₂S in fish from nonsulfidic environments. In contrast, fish from sulfidic environments have an increased ability to maintain low H₂S endogenous concentrations upon exposure. These general trends are evident peripheral (gill) as well as internal organs (liver and muscle). However, these general patterns are much less clear in the brain, where there were no clear differences between sulfidic and nonsulfidic populations.

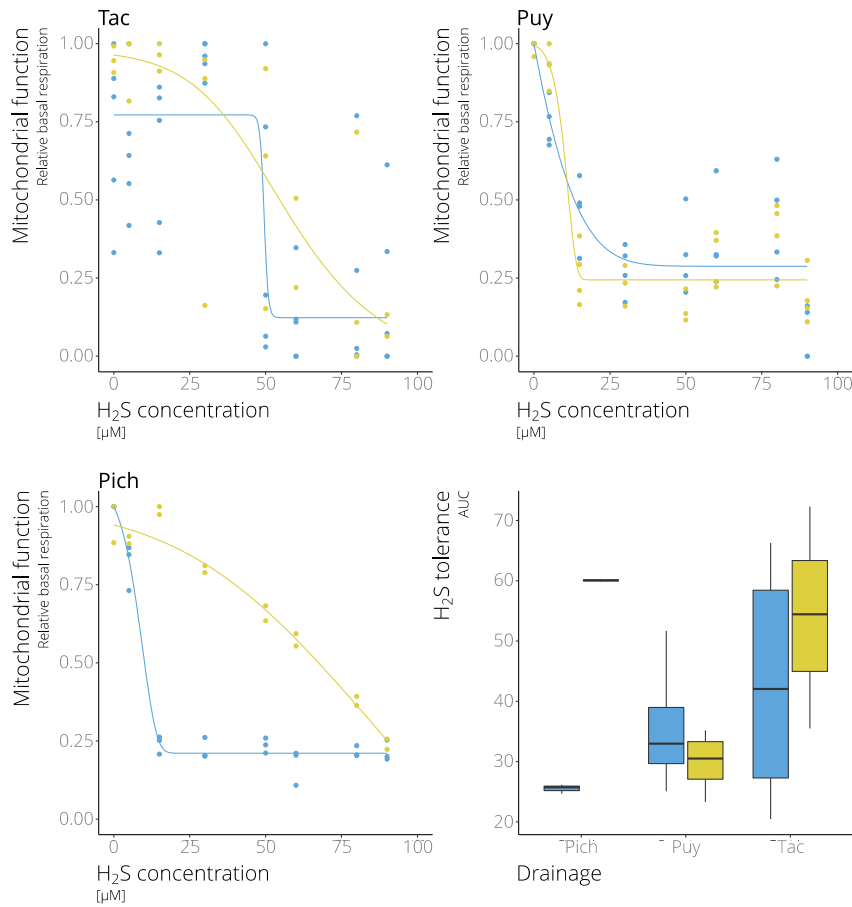


Figure B3. Dose response curves for basal mitochondrial respiration in sulfidic (yellow) and nonsulfidic (blue) populations of *P. mexicana* from different river drainages. Boxplots indicate levels of H₂S tolerance (area under the curve, AUC) across populations. Variation in basal respiration was not related to any of the predictor variable (Table S8).

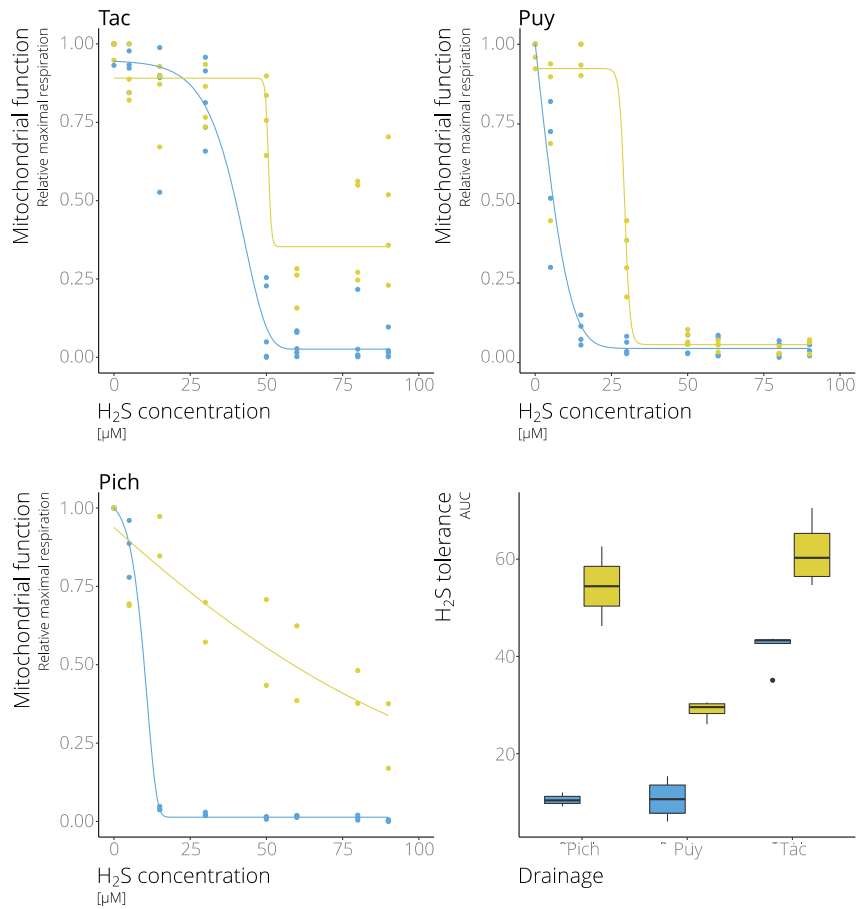


Figure B4. Dose response curves for maximal mitochondrial respiration in sulfidic (yellow) and nonsulfidic (blue) populations of *P. mexicana* from different river drainages. Boxplots indicate levels of H₂S tolerance (area under the curve, AUC) across populations. The interaction between habitat type of origin and drainage of origin best explained variation in maximal respiration (Tables S9-S10).

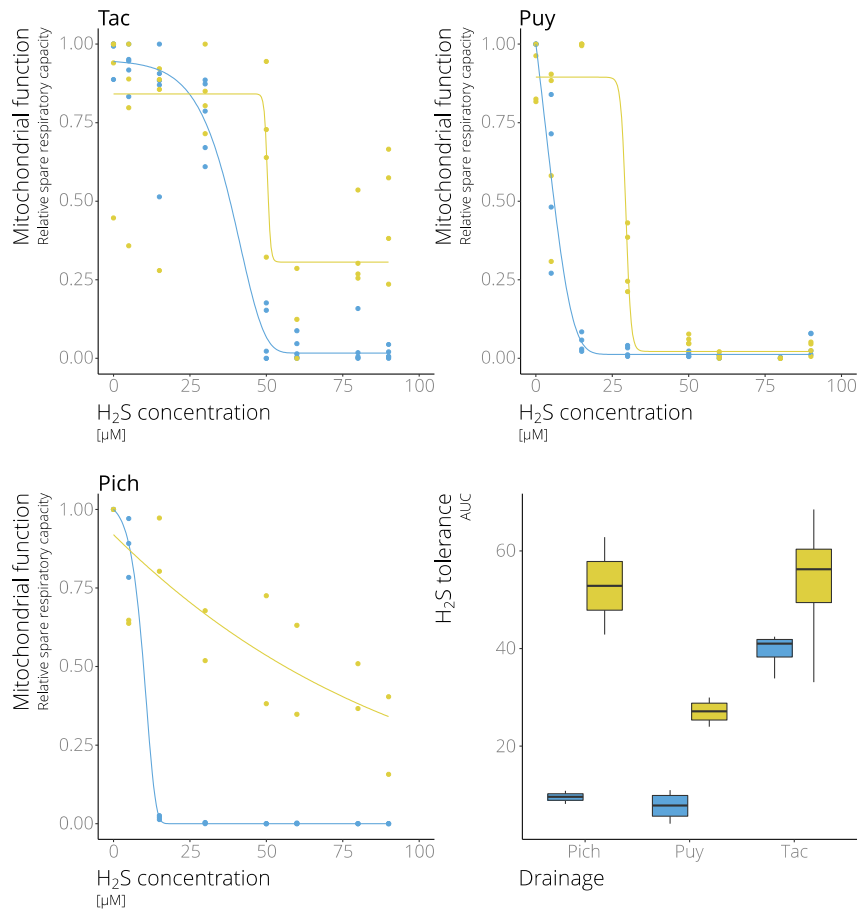


Figure B5. Dose response curves for spare respiratory capacity in sulfidic (yellow) and nonsulfidic populations (blue) of *P. mexicana* from different river drainages. Boxplots indicate levels of H₂S tolerance (area under the curve, AUC) across populations. The interaction between habitat type of origin and drainage of origin best explained variation in spare respiratory capacity (Tables S11-S12).

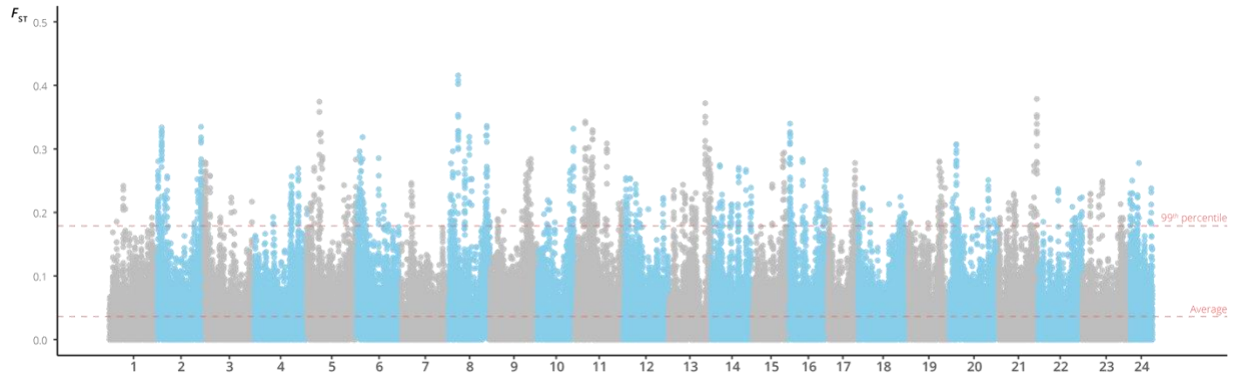


Figure B6. There is significant variation in local ancestry patterns across the genome of populations in the *P. mexicana* complex, as indicated by elevated F_{ST} -values between sulfidic and nonsulfidic populations (see Dataset S1 for details).

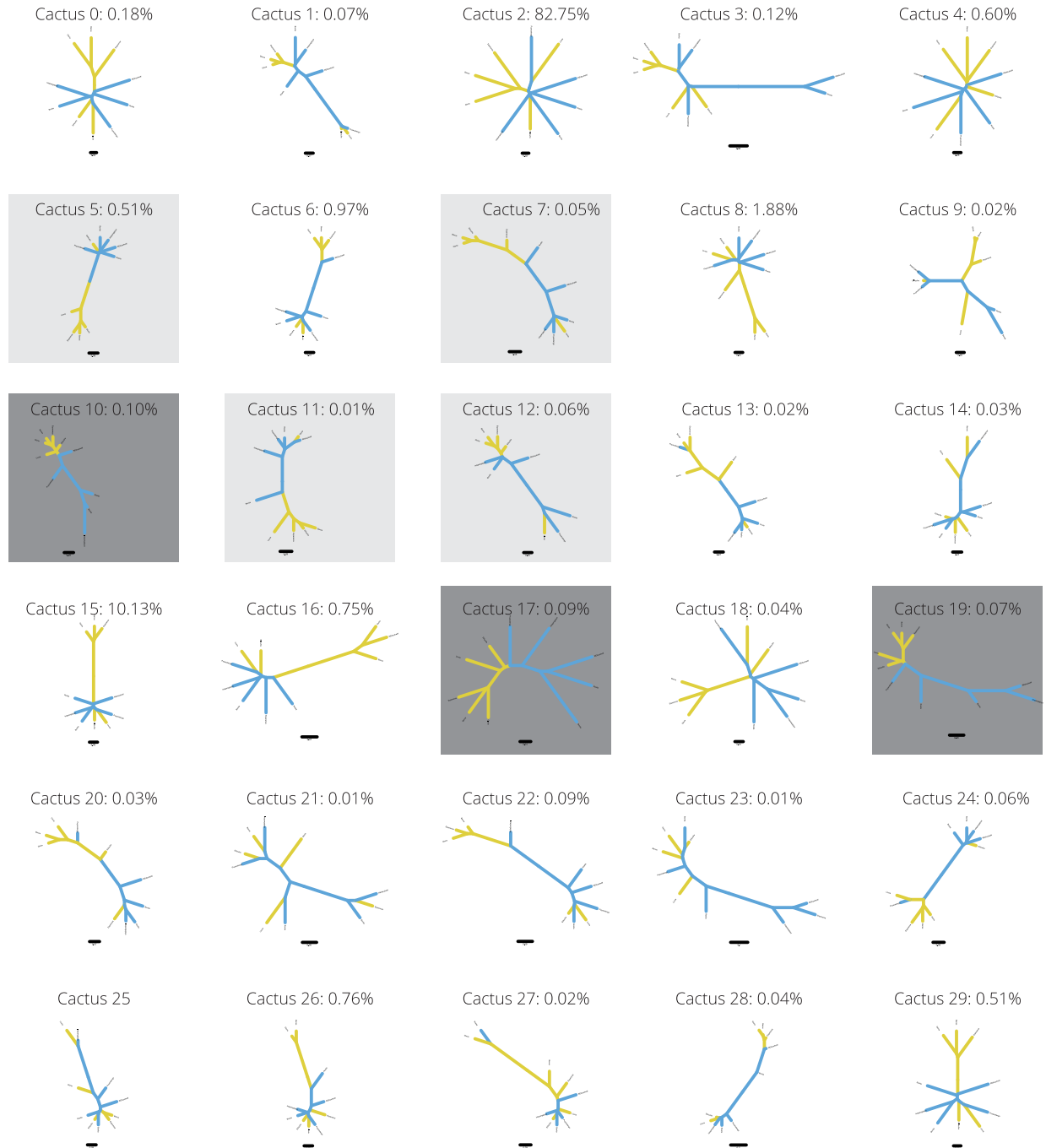


Figure B7. All 30 local topologies (cacti) hypothesized by Saguaro across the genome, including the percentage of the genome each cactus covered (lineages from sulfidic habitats are colored in yellow, those from non-sulfidic habitats in blue). Cacti 2 and 15 together covered over 90 % of the genome. Cacti 10, 17, and 19 (highlighted with dark gray boxes) exhibited strong clustering by ecotype, indicating monophyletic origin of putatively adaptive alleles. Cacti 5, 7, 11, and 12 (highlighted with light gray boxes) show clustering of four (out of five) sulfidic ecotypes. Assignment of genes to different cacti can be found in Dataset S2.

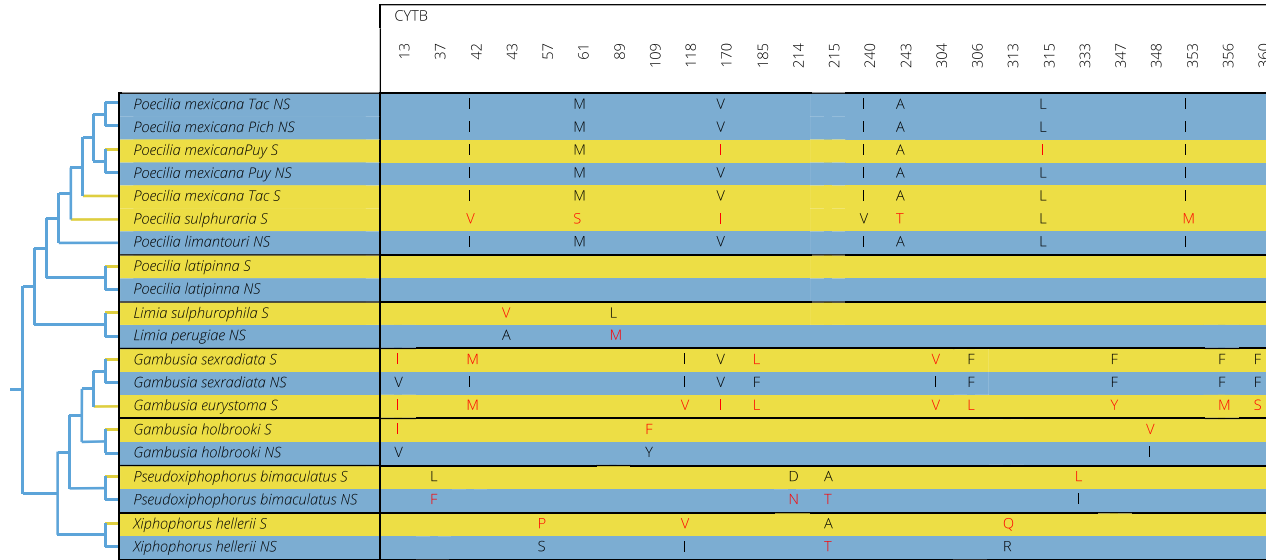


Figure B9. Amino acid differences in *CYTb* between lineages from sulfidic (yellow) and nonsulfidic (blue) habitats. Derived amino acids are shown in red. Bold letters indicate codons with convergent amino acid substitutions in different clades (separated by black horizontal lines) of sulfide spring fishes (codons 13, 118, and 170).

Appendix B Tables

Table B1. List of lineages from sulfidic and nonsulfidic habitats included in this study. The table provides descriptions of the collection localities, information about the presence or absence of H₂S, latitude and longitude (Lat/Long), as well as the sample sizes for the quantification of SQR activity (N_{SQR} ; number of biological replicates, each tested across multiple concentrations), endogenous H₂S concentrations (N_{mitoA} ; number of individuals with multiple tissues analyzed for each), mitochondrial function (N_{resp} ; number of biological replicates, each tested across multiple concentrations), comparative genomics (N_{genomics}), as well as transcriptomics (N_{RNAseq} ; number of individuals).

ID	Species	Locality	H ₂ S	Lat/Long	N_{SQR}	N_{mitoA}	N_{resp}	N_{genomics}	N_{RNAseq}
1	<i>Poecilia mexicana</i>	Arroyo Bonita, Rio Tacotalpa drainage, Tabasco, MX	–	17.427/-92.752	18	14	5	1	6
2	<i>Poecilia mexicana</i>	Arroyo Rosita, Rio Pichucalco drainage, Chiapas, MX	–	17.485/-93.104	12		3	1	6
3	<i>Poecilia mexicana</i>	La Lluvia springs, Rio Puyacatengo drainage, Tabasco, MX	+	17.464/-92.895	18	16	4	1	5
4	<i>Poecilia mexicana</i>	Rio Puyacatengo, Rio Puyacatengo drainage, Tabasco, MX	–	17.510/-92.914	12	16	4	1	6
5	<i>Poecilia mexicana</i>	El Azufre, Rio Tacotalpa drainage, Tabasco, MX	+	17.438/-92.775	24	14	4	1	5
6	<i>Poecilia sulphuraria</i>	Baños del Azufre, Rio Pichucalco drainage, Tabasco, MX	+	17.552/-92.999	24		2	1	6
7	<i>Poecilia mexicana</i>	Rio El Azufre, west branch, Rio Pichucalco drainage, Chiapas, MX	-	17.556/-93.008				1	
8	<i>Poecilia mexicana</i>	Rio Ixtapangajoya, Rio Ixtapangajoya drainage, Chiapas, MX	-	17.495/-92.998				1	
9	<i>Poecilia sulphuraria</i>	La Gloria springs, Rio Pichucalco drainage, Chiapas, MX	+	17.532/-93.015				1	
10	<i>Poecilia thermalis</i>	La Esperanza springs, Rio Ixtapangajoya drainage, Tabasco, MX	+	17.511/-92.983				1	
11	<i>Poecilia limantouri</i>	Rio Garces, Rio Panuco drainage, Hidalgo, MX	–	20.940/-98.282					6
12	<i>Poecilia latipinna</i>	Green Springs, St. Johns River drainage, Florida, USA	+	28.863/-81.248					6
13	<i>Poecilia latipinna</i>	Mariner's Cove, Lake Monroe, St. Johns River drainage, Florida, USA	–	28.857/-81.239					6
14	<i>Limia sulphurophila</i>	Balnearios La Zurza, Lago Enriqueillo basin, Independencia, DR	+	18.398/-71.570					6
15	<i>Limia perugiae</i>	Stream in Cabral, Rio Yaque del Sur drainage, Barahona, DR	–	18.246/-71.223					6
16	<i>Gambusia sexradiata</i>	Mogote del Puyacatengo, Rio Puyacatengo drainage, Tabasco, MX	+	17.582/-92.900					6
17	<i>Gambusia sexradiata</i>	Laguna Sitio Grande, Rio Ixtapangajoya drainage, Tabasco, MX	–	17.677/-92.997					6
18	<i>Gambusia eurystoma</i>	Baños del Azufre, Rio Pichucalco drainage, Tabasco, MX	+	17.552/-92.999					6
19	<i>Gambusia holbrooki</i>	Green Springs, St. Johns River drainage, Florida, USA	+	28.863/-81.248					6
20	<i>Gambusia holbrooki</i>	Mariner's Cove, Lake Monroe, St. Johns River drainage, Florida, USA	–	28.857/-81.239					6
21	<i>Pseudoxiphophorus bimaculatus</i>	La Gloria springs, Rio Pichucalco drainage, Chiapas, MX	+	17.532/-93.015					6
22	<i>Pseudoxiphophorus bimaculatus</i>	Arroyo Pujil, Rio Ixtapangajoya drainage, Chiapas, MX	–	17.476/-92.986					6
23	<i>Xiphophorus hellerii</i>	La Gloria springs, Rio Pichucalco drainage, Chiapas, MX	+	17.532/-93.015					6
24	<i>Xiphophorus hellerii</i>	Rio El Azufre, west branch, Rio Pichucalco drainage, Chiapas, MX	–	17.556/-93.008					6

Table B2. Results of mixed-effect linear models analyzing variation in COX activity. Models are ordered based on ΔAICc values. The null model included biological replicate ID as a random factor. Only one model (bold) exhibited $\Delta\text{AICc} < 2$.

Model	Terms	AICc	ΔAICc	df	Weight
m8	Habitat \times H₂S + (1 ID)	-30.8	0.0	6	0.988
m5	Habitat + H ₂ S + (1 ID)	-21.0	9.8	5	0.007
m11	Habitat \times Drainage \times H ₂ S + (1 ID)	-18.9	11.9	14	0.003
m3	H ₂ S + (1 ID)	-18.6	12.3	4	0.002
m10	Habitat + Drainage + H ₂ S + (1 ID)	-11.8	19.0	7	<0.001
m6	Drainage + H ₂ S + (1 ID)	-10.0	20.9	6	<0.001
m9	Drainage \times H ₂ S + (1 ID)	-5.3	25.5	8	<0.001
m1	Habitat + (1 ID)	45.1	76.0	4	<0.001
null	(1 ID)	47.6	78.4	3	<0.001
m4	Habitat + Drainage + (1 ID)	54.2	85.1	6	<0.001
m2	Drainage + (1 ID)	56.1	87.0	5	<0.001
m7	Habitat \times Drainage + (1 ID)	58.6	89.4	8	<0.001

Table B3. Results of the top mixed-effect linear model analyzing variation in COX activity (m8, Table S2).

Predictors	Estimates	CI	P
(Intercept)	0.8698	0.7567 – 0.9830	<0.001
Habitat	0.0749	-0.0887 – 0.2385	0.369
H ₂ S	-0.6545	-0.7774 – -0.5317	<0.001
Habitat \times H ₂ S	0.3612	0.1836 – 0.5388	<0.001
Random Effects			
σ^2	0.03		
τ_{00-ID}	0.03		
ICC	0.49		
N_{ID}	23		
Observations	138		
Marginal R ₂	0.417		
Conditional R ₂	0.700		

Table B4. Results of mixed-effect linear models analyzing variation in SQR activity. Models are ordered based on ΔAICc values. The null model included biological replicate ID as a random factor. Only one model (bold) exhibited $\Delta\text{AICc} < 2$.

Model	Terms	AICc	ΔAICc	df	Weight
m8	Habitat \times H₂S + (1 ID)	-817.8	0.0	6	0.752
m1	Habitat + (1 ID)	-815.5	2.3	4	0.239
null	(1 ID)	-808.8	9.0	3	0.009
m5	Habitat + H ₂ S + (1 ID)	-795.5	22.3	5	<0.001
m4	Habitat + Drainage + (1 ID)	-789.0	28.8	6	<0.001
m3	H ₂ S + (1 ID)	-788.7	29.1	4	<0.001
m2	Drainage + (1 ID)	-784.4	33.3	5	<0.001
m10	Habitat + Drainage + H ₂ S + (1 ID)	-768.9	48.9	7	<0.001
m7	Habitat \times Drainage + (1 ID)	-766.7	51.1	8	<0.001
m6	Drainage + H ₂ S + (1 ID)	-764.2	53.6	6	<0.001
m9	Drainage \times H ₂ S + (1 ID)	-727.3	90.4	8	<0.001
m11	Habitat \times Drainage \times H ₂ S + (1 ID)	-706.4	111.4	14	<0.001

Table B5. Results of the top mixed-effect linear model analyzing variation in SQR activity (m8, Table S4).

Predictors	Estimates	CI	P
(Intercept)	0.0019	-0.0001 – 0.0040	0.060
Habitat	-0.0011	-0.0037 – 0.0015	0.421
H ₂ S	-0.0001	-0.0001 – 0.0000	<0.001
Habitat × H ₂ S	0.0002	0.0001 – 0.0002	<0.001
Random Effects			
σ ₂	0.00		
τ _{00-ID}	0.00		
ICC	0.10		
N _{ID}	19		
Observations	108		
Marginal R ₂	0.513		
Conditional R ₂	0.563		

Table B6. Results of mixed-effect linear models analyzing variation in relative mitochondrial H₂S concentrations (MitoN/MitoA). Models are ordered based on ΔAIC_c values. The null model included individual ID and organ type as random factors. Only one model (bold) exhibited ΔAIC_c < 2.

Model	Terms	AIC _c	ΔAIC _c	df	Weight
m4	H₂S + Habitat + (1 ID) + (1 Organ)	510.1	0.0	6	0.594
m2	Habitat + (1 ID) + (1 Organ)	513.7	3.6	5	0.100
m7	H ₂ S × Habitat + (1 ID) + (1 Organ)	514.0	3.9	7	0.086
m9	Habitat × Drainage + (1 ID) + (1 Organ)	514.2	4.1	7	0.076
m10	H ₂ S + Habitat + Drainage + (1 ID) + (1 Organ)	514.4	4.3	7	0.069
m11	H ₂ S × Habitat × Drainage + (1 ID) + (1 Organ)	514.8	4.7	11	0.058
m6	Habitat + Drainage + (1 ID) + (1 Organ)	517.9	7.8	6	0.012
m1	H ₂ S + (1 ID) + (1 Organ)	519.8	9.7	5	0.005
null	(1 ID) + (1 Organ)	522.9	12.8	4	0.001
m5	H ₂ S + Drainage + (1 ID) + (1 Organ)	523.8	13.7	6	<0.001
m3	Drainage + (1 ID) + (1 Organ)	526.8	16.7	5	<0.001
m8	H ₂ S × Drainage + (1 ID) + (1 Organ)	528.0	17.9	7	<0.001

Table B7. Results of the top mixed-effect linear model analyzing variation in relative endogenous H₂S concentrations activity (m4, Table S6).

Predictors	Estimates	CI	P
(Intercept)	1.2580	0.9922 – 1.5238	<0.001
H ₂ S	0.1812	0.0706 – 0.2917	0.001
Habitat	-0.5064	-0.7563 – -0.2566	<0.001
Random Effects			
σ ₂	0.48		
τ _{00-ID}	0.11		
τ _{00-Organ}	0.01		
ICC	0.19		
N _{ID}	60		
N _{Organ}	4		
Observations	216		
Marginal R ₂	0.160		
Conditional R ₂	0.318		

Table B8. Results of linear models analyzing variation in basal mitochondrial respiration. Models are ordered based on ΔAICc values. The null model only included the intercept. Even through m2 exhibited $\Delta\text{AICc} < 2$, the null model was best supported overall.

Model	Terms	AICc	ΔAICc	df	Weight
null	1	180.2	0.0	2	0.453
m2	1 + Habitat	181.4	1.2	3	0.248
m1	1 + Drainage	182.4	2.3	4	0.146
m3	1 + Drainage + Habitat	183.4	3.2	5	0.091
m4	1 + Drainage \times Habitat	184.2	4.0	7	0.062

Table B9. Results of linear models analyzing variation in maximal mitochondrial respiration. Models are ordered based on ΔAICc values. The null model only included the intercept. Only one model (bold) exhibited $\Delta\text{AICc} < 2$.

Model	Terms	AICc	ΔAICc	df	Weight
m4	1 + Drainage \times Habitat	148.8	0.0	7	0.996
m3	1 + Drainage + Habitat	159.9	11.1	5	0.004
m1	1 + Drainage	188.7	39.9	4	<0.001
m2	1 + Habitat	191.1	42.3	3	<0.001
null	1	198.1	49.3	2	<0.001

Table B10. Results of the top linear model analyzing variation in maximal mitochondrial respiration (m4, Table S9).

Factor	SS	df	<i>F</i>	<i>P</i>
(Intercept)	333.1	1	13.015	0.002
Drainage	2803.7	2	54.782	<0.001
Habitat	2313.6	1	90.412	<0.001
Drainage \times Habitat	578.2	2	11.298	0.001
Residuals	409.4	16		

Table B11. Results of linear models analyzing variation in spare respiratory capacity. Models are ordered based on ΔAICc values. The null model only included the intercept. Only one model (bold) exhibited $\Delta\text{AICc} < 2$.

Model	Terms	AICc	ΔAICc	df	Weight
m4	1 + Drainage \times Habitat	167.5	0.0	7	0.870
m3	1 + Drainage + Habitat	171.3	3.8	5	0.130
m1	1 + Drainage	189.3	21.8	4	<0.001
m2	1 + Habitat	190.9	23.4	3	<0.001
null	1	196.6	29.0	2	<0.001

Table B12. Results of the top linear model analyzing variation in spare respiratory capacity (m4, Table S11).

Factor	SS	df	<i>F</i>	<i>P</i>
(Intercept)	273.7	1	4.552	0.049
Drainage	2808.1	2	23.351	<0.001
Habitat	2249.4	1	37.410	<0.001
Drainage \times Habitat	698.1	2	5.805	0.013
Residuals	962.0	16		

Table B13. Descriptive statistics for Illumina sequencing reads used for comparative transcriptome analyses of poeciliids from sulfidic and nonsulfidic environments. For each lineage, the table lists the average number of reads per individual after trimming for quality, the average number of reads that mapped to the reference genome, and the average proportion of reads that mapped to the reference genome. Error margins are provided in the form of standard errors. Lineages included are numbered corresponding to Table S1.

ID	Species	H ₂ S	N	Reads	Mapped reads	Percent mapped
1	<i>Poecilia mexicana</i> Tac	–	6	13,179,072 ± 782,269	12,615,832 ± 758,991	0.957 ± 0.004
2	<i>Poecilia mexicana</i> Pich	–	6	11,945,216 ± 1,160,788	11,296,904 ± 1,105,644	0.945 ± 0.005
3	<i>Poecilia mexicana</i> Puy	+	5	20,161,962 ± 2,212,689	18,735,621 ± 2,096,062	0.928 ± 0.007
4	<i>Poecilia mexicana</i> Puy	–	6	19,700,214 ± 1,865,276	18,355,384 ± 1,774,642	0.931 ± 0.007
5	<i>Poecilia mexicana</i> Tac	+	6	14,400,204 ± 2,690,186	13,807,309 ± 2,592,441	0.958 ± 0.003
6	<i>Poecilia sulphuraria</i> Pich	+	6	12,267,262 ± 1,644,534	11,740,414 ± 1,577,010	0.957 ± 0.002
11	<i>Poecilia limantouri</i>	–	6	26,586,625 ± 9,141,136	25,188,316 ± 8,720,553	0.946 ± 0.004
12	<i>Poecilia latipinna</i>	+	6	43,960,656 ± 7,696,566	42,661,324 ± 7,443,424	0.971 ± 0.001
13	<i>Poecilia latipinna</i>	–	6	28,591,830 ± 2,092,989	27,606,064 ± 2,013,339	0.966 ± 0.001
14	<i>Limia sulphurophila</i>	+	6	26,523,621 ± 3,993,393	25,311,603 ± 3,807,545	0.955 ± 0.002
15	<i>Limia perugiae</i>	–	6	26,579,863 ± 3,206,613	25,109,831 ± 3,062,313	0.944 ± 0.003
16	<i>Gambusia sexradiata</i>	+	6	31,896,270 ± 4,598,187	28,595,855 ± 4,024,693	0.900 ± 0.010
17	<i>Gambusia sexradiata</i>	–	6	35,598,499 ± 0,503,441	29,867,961 ± 8,007,416	0.874 ± 0.028
18	<i>Gambusia eurystoma</i>	+	6	19,514,414 ± 4,021,075	16,883,905 ± 3,364,767	0.870 ± 0.006
19	<i>Gambusia holbrooki</i>	+	6	29,612,503 ± 5,887,338	26,944,912 ± 5,401,728	0.909 ± 0.003
20	<i>Gambusia holbrooki</i>	–	6	35,914,764 ± 8,032,747	32,308,042 ± 7,135,952	0.903 ± 0.004
21	<i>Pseudoxiphophorus bimaculatus</i>	+	6	39,545,078 ± 6,735,006	36,031,145 ± 6,142,661	0.910 ± 0.002
22	<i>Pseudoxiphophorus bimaculatus</i>	–	6	35,243,934 ± 7,309,241	32,539,388 ± 6,787,986	0.922 ± 0.001
23	<i>Xiphophorus hellerii</i>	+	6	29,296,035 ± 5,042,914	26,660,330 ± 4,574,585	0.911 ± 0.004
24	<i>Xiphophorus hellerii</i>	–	6	30,761,274 ± 6,214,700	28,144,578 ± 5,721,047	0.914 ± 0.003

Table B14. Gene Ontology terms for genes exhibiting convergent shifts toward higher expression in sulfide spring fishes that had evidence for significant enrichment (after FDR correction). Provided are the GO term identification number, a description of each GO term, *P*-value associated with the enrichment, false-discovery rate (*q*), the level of enrichment, the total number of genes in the reference set (*N*), the total number of genes with a specific GO term in the reference set (*B*), the number of genes in the target set (*n*), and the number of genes in the intersection (*b*). We also provide a list of all upregulated genes associated with each GO term. Note that there was no evidence for enrichment in genes exhibiting convergent shifts toward lower expression in sulfide spring fishes. Enrichment of upregulated genes included biological processes associated with sulfide detoxification as well as sulfur metabolism and transport, mitochondrial function and energy metabolism, as well as protein synthesis and disassembly, which are indirectly affected by the presence of H₂S (151).

GO Term	Description	<i>P</i>	<i>q</i>	Enrichment	<i>N</i>	<i>B</i>	<i>n</i>	<i>b</i>	Genes
GO:0070221	Sulfide oxidation; using sulfide:quinone oxidoreductase	2.30E-06	2.00E-03	25.43	3713	4	146	4	SQRDL: sulfide quinone reductase-like (yeast); SLC25A10: solute carrier family 25 (mt carrier; dicarboxylate transporter); member 10; ETHE1: ethylmalonic encephalopathy 1; TSTD1: thiosulfate sulfurtransferase (rhodanese)-like domain containing 1
GO:0019418	Sulfide oxidation	2.30E-06	2.18E-03	25.43	3713	4	146	4	SQRDL: sulfide quinone reductase-like (yeast); SLC25A10: solute carrier family 25 (mt carrier; dicarboxylate transporter); member 10; TSTD1: thiosulfate sulfurtransferase (rhodanese)-like domain containing 1; ETHE1: ethylmalonic encephalopathy 1
GO:0070813	Hydrogen sulfide metabolic process	1.11E-05	7.76E-03	20.35	3713	5	146	4	SQRDL: sulfide quinone reductase-like (yeast); CBS: cystathionine-beta-synthase; MPST: mercaptopyruvate sulfurtransferase; ETHE1: ethylmalonic encephalopathy 1
GO:0000098	Sulfur amino acid catabolic process	7.32E-05	3.83E-02	14.53	3713	7	146	4	CDO1: cysteine dioxygenase type 1; GADL1: glutamate decarboxylase-like 1; CBS: cystathionine-beta-synthase; MPST: mercaptopyruvate sulfurtransferase
GO:0006534	Cysteine metabolic process	9.74E-06	7.27E-03	14.13	3713	9	146	5	CDO1: cysteine dioxygenase type 1; GCLM: glutamate-cysteine ligase; modifier subunit; CBS: cystathionine-beta-synthase; GCLC: glutamate-cysteine ligase; catalytic subunit; MPST: mercaptopyruvate sulfurtransferase
GO:0000096	Sulfur amino acid metabolic process	6.35E-06	5.10E-03	8.9	3713	20	146	7	CDO1: cysteine dioxygenase type 1; GCLM: glutamate-cysteine ligase; modifier subunit; GADL1: glutamate decarboxylase-like 1; MUT: methylmalonyl coa mutase; GCLC: glutamate-cysteine ligase; catalytic subunit; CBS: cystathionine-beta-synthase; MPST: mercaptopyruvate sulfurtransferase
GO:0070125	Mitochondrial translational elongation	2.50E-08	6.54E-05	5.28	3713	77	146	16	MRPL22: mt ribosomal protein l22; MRPL2: mt ribosomal protein l2; MRPL9: mt ribosomal protein l9; TUFM: tu translation elongation factor; mt; MRPL10: mt ribosomal protein l10; MRPS2: mt ribosomal protein s2; MRPS26: mt ribosomal protein s26; MRPS9: mt ribosomal protein s9; MRPS6: mt ribosomal protein s6; DAP3: death associated protein 3; MRPL27: mt ribosomal protein l27; MRPS11: mt ribosomal protein s11; MRPL38: mt ribosomal protein l38; MRP63: mt ribosomal protein 63; MRPL21: mt ribosomal protein l21; MRPL3: mt ribosomal protein l3
GO:0070126	Mitochondrial translational termination	1.00E-07	2.10E-04	5.16	3713	74	146	15	MRPL22: mt ribosomal protein l22; MRPL2: mt ribosomal protein l2; MRPL9: mt ribosomal protein l9; MRPL10: mt ribosomal protein l10; MRPS2: mt ribosomal protein s2; MRPS26: mt ribosomal protein s26; MRPS9: mt ribosomal protein s9; MRPS6: mt ribosomal protein s6; DAP3: death associated protein 3; MRPL27: mt ribosomal protein l27; MRPS11: mt ribosomal protein s11; MRPL38: mt ribosomal protein l38; MRP63: mt ribosomal protein 63; MRPL21: mt ribosomal protein l21; MRPL3: mt ribosomal protein l3
GO:0006415	Translational termination	2.50E-07	4.36E-04	4.83	3713	79	146	15	MRPL22: mt ribosomal protein l22; MRPL2: mt ribosomal protein l2; MRPL9: mt ribosomal protein l9; MRPL10: mt ribosomal protein l10; MRPS2: mt ribosomal protein s2; MRPS26: mt ribosomal protein s26; MRPS9: mt ribosomal protein s9; MRPS6: mt ribosomal protein s6; DAP3: death associated protein 3; MRPL27: mt ribosomal protein l27; MRPS11: mt ribosomal protein s11; MRPL38: mt ribosomal protein l38; MRP63: mt ribosomal protein 63; MRPL21: mt ribosomal protein l21; MRPL3: mt ribosomal protein l3

GO Term	Description	<i>P</i>	<i>q</i>	Enrichment	<i>N</i>	<i>B</i>	<i>n</i>	<i>b</i>	Genes
GO:0006414	Translational elongation	3.47E-07	5.18E-04	4.42	3713	92	146	16	MRPL22: mt ribosomal protein l22; MRPL2: mt ribosomal protein l2; MRPL9: mt ribosomal protein l9; TUFM: tu translation elongation factor; mt; MRPL10: mt ribosomal protein l10; MRPS2: mt ribosomal protein s2; MRPS26: mt ribosomal protein s26; MRPS9: mt ribosomal protein s9; MRPS6: mt ribosomal protein s6; DAP3: death associated protein 3; MRPL27: mt ribosomal protein l27; MRPS11: mt ribosomal protein s11; MRPL38: mt ribosomal protein l38; MRP63: mt ribosomal protein 63; MRPL21: mt ribosomal protein l21; MRPL3: mt ribosomal protein l3
GO:0006790	Sulfur compound metabolic process	7.01E-09	3.66E-05	4.31	3713	124	146	21	PAPSS2: 3'-phosphoadenosine 5'-phosphosulfate synthase 2; GADL1: glutamate decarboxylase-like 1; GSR: glutathione reductase; B3GNT3: udp-glcnac:betagal beta-1;3-n-acetylglucosaminyltransferase 3; MUT: methylmalonyl coa mutase; SUCLG2: succinate-coa ligase; gdp-forming; beta subunit; GALNS: galactosamine (n-acetyl)-6-sulfate sulfatase; ETHE1: ethylmalonic encephalopathy 1; TSTD1: thiosulfate sulfurtransferase (rhodanese)-like domain containing 1; CDO1: cysteine dioxygenase type 1; SQRD1: sulfide quinone reductase-like (yeast); SLC25A1: solute carrier family 25 (mt carrier; citrate transporter); member 1; GCLM: glutamate-cysteine ligase; modifier subunit; CBS: cystathionine-beta-synthase; GCLC: glutamate-cysteine ligase; catalytic subunit; MPST: mercaptopyruvate sulfurtransferase; SLC25A10: solute carrier family 25 (mt carrier; dicarboxylate transporter); member 10; G6PD: glucose-6-phosphate dehydrogenase; GSTO1: glutathione s-transferase omega 1; MGST1: microsomal glutathione s-transferase 1; HSPA9: heat shock 70kda protein 9 (mortalin)
GO:0043624	Cellular protein complex disassembly	1.46E-06	1.91E-03	4.24	3713	90	146	15	MRPL22: mt ribosomal protein l22; MRPL2: mt ribosomal protein l2; MRPL9: mt ribosomal protein l9; MRPL10: mt ribosomal protein l10; MRPS2: mt ribosomal protein s2; MRPS26: mt ribosomal protein s26; MRPS9: mt ribosomal protein s9; MRPS6: mt ribosomal protein s6; DAP3: death associated protein 3; MRPL27: mt ribosomal protein l27; MRPS11: mt ribosomal protein s11; MRPL38: mt ribosomal protein l38; MRP63: mt ribosomal protein 63; MRPL21: mt ribosomal protein l21; MRPL3: mt ribosomal protein l3
GO:0022904	Respiratory electron transport chain	1.55E-05	1.01E-02	3.98	3713	83	146	13	UQCRC2: ubiquinol-cytochrome c reductase core protein ii; UQCRFS1: ubiquinol-cytochrome c reductase; rieske iron-sulfur polypeptide 1; COX4I1: cytochrome c oxidase subunit iv isoform 1; NDUFA9: nadh dehydrogenase (ubiquinone) 1 alpha subcomplex; 9; 39kda; NDUFA10: nadh dehydrogenase (ubiquinone) 1 alpha subcomplex; 10; 42kda; NDUFC2-KCTD14: ndufc2-kctd14 readthrough; COX10: cytochrome c oxidase assembly homolog 10 (yeast); COX4I2: cytochrome c oxidase subunit iv isoform 2 (lung); AIFM2: apoptosis-inducing factor; mt-associated; 2; COX7B: cytochrome c oxidase subunit viib; NDUFV1: nadh dehydrogenase (ubiquinone) flavoprotein 1; 51kda; NDUFS2: nadh dehydrogenase (ubiquinone) fe-s protein 2; 49kda (nadh-coenzyme q reductase); ETFA: electron-transfer-flavoprotein; alpha polypeptide
GO:0032984	Protein-containing complex disassembly	1.47E-06	1.71E-03	3.6	3713	127	146	18	MRPL22: mt ribosomal protein l22; MRPL2: mt ribosomal protein l2; MRPL9: mt ribosomal protein l9; MRPL10: mt ribosomal protein l10; MRPS2: mt ribosomal protein s2; MRPS26: mt ribosomal protein s26; CHMP2A: charged multivesicular body protein 2a; MTIF2: mt translational initiation factor 2; CHMP5: charged multivesicular body protein 5; MRPS9: mt ribosomal protein s9; MRPS6: mt ribosomal protein s6; DAP3: death associated protein 3; MRPS11: mt ribosomal protein s11; MRPL27: mt ribosomal protein l27; MRPL38: mt ribosomal protein l38; MRP63: mt ribosomal protein 63; MRPL21: mt ribosomal protein l21; MRPL3: mt ribosomal protein l3
GO:0022900	Electron transport chain	3.27E-05	1.90E-02	3.32	3713	115	146	15	UQCRC2: ubiquinol-cytochrome c reductase core protein ii; UQCRFS1: ubiquinol-cytochrome c reductase; rieske iron-sulfur polypeptide 1; GSR: glutathione reductase; COX4I1: cytochrome c oxidase subunit iv isoform 1; NDUFA9: nadh dehydrogenase (ubiquinone) 1 alpha subcomplex; 9; 39kda; NDUFA10: nadh dehydrogenase (ubiquinone) 1 alpha subcomplex; 10; 42kda; NDUFC2-KCTD14: ndufc2-kctd14 readthrough; RDH16: retinol dehydrogenase 16 (all-trans); COX10: cytochrome c oxidase assembly homolog 10 (yeast); COX4I2: cytochrome c oxidase subunit iv isoform 2 (lung); AIFM2: apoptosis-inducing factor; mt-associated; 2; NDUFV1: nadh dehydrogenase (ubiquinone) flavoprotein 1; 51kda; COX7B: cytochrome c oxidase subunit viib; NDUFS2: nadh dehydrogenase (ubiquinone) fe-s protein 2; 49kda (nadh-coenzyme q reductase); ETFA: electron-transfer-flavoprotein; alpha polypeptide

GO Term	Description	P	q	Enrichment	N	B	n	b	Genes
GO:0051186	Cofactor metabolic process	1.51E-06	1.57E-03	3.07	3713	182	146	22	PGK1: phosphoglycerate kinase 1; HK1: hexokinase 1; TPI1: triosephosphate isomerase 1; GSR: glutathione reductase; MUT: methylmalonyl coa mutase; SUCLG2: succinate-coa ligase; gdp-forming; beta subunit; NDUFA9: nadh dehydrogenase (ubiquinone) 1 alpha subcomplex; 9; 39kda; ETHE1: ethylmalonic encephalopathy 1; COQ7: coenzyme q7 homolog; ubiquinone (yeast); SLC25A1: solute carrier family 25 (mt carrier; citrate transporter); member 1; ABCB6: atp-binding cassette; sub-family b (mdr/tap); member 6; COX10: cytochrome c oxidase assembly homolog 10 (yeast); GCLM: glutamate-cysteine ligase; modifier subunit; PRDX1: peroxiredoxin 1; BLVRB: biliverdin reductase b (flavin reductase (nadph)); MMADHC: methylmalonic aciduria (cobalamin deficiency) cblid type; with homocystinuria; TALDO1: transaldolase 1; GCLC: glutamate-cysteine ligase; catalytic subunit; G6PD: glucose-6-phosphate dehydrogenase; GSTO1: glutathione s-transferase omega 1; MGST1: microsomal glutathione s-transferase 1; HSPA9: heat shock 70kda protein 9 (mortalin)
GO:0055114	Oxidation-reduction process	2.20E-10	2.29E-06	2.98	3713	324	146	38	UQCRC2: ubiquinol-cytochrome c reductase core protein ii; PGK1: phosphoglycerate kinase 1; ACAA2: acetyl-coa acyltransferase 2; TPI1: triosephosphate isomerase 1; UQCRFS1: ubiquinol-cytochrome c reductase; rieske iron-sulfur polypeptide 1; GSR: glutathione reductase; COX4I1: cytochrome c oxidase subunit iv isoform 1; TSTD1: thiosulfate sulfurtransferase (rhodanese)-like domain containing 1; CDO1: cysteine dioxygenase type 1; SQRDL: sulfide quinone reductase-like (yeast); COQ7: coenzyme q7 homolog; ubiquinone (yeast); COX10: cytochrome c oxidase assembly homolog 10 (yeast); SCP2: sterol carrier protein 2; COX4I2: cytochrome c oxidase subunit iv isoform 2 (lung); COX7B: cytochrome c oxidase subunit viib; GSTO1: glutathione s-transferase omega 1; TXN: thioredoxin; ETFA: electron-transfer-flavoprotein; alpha polypeptide; DHRS1: dehydrogenase/reductase (sdr family) member 1; HK1: hexokinase 1; HCCS: holocytochrome c synthase; NDUFA9: nadh dehydrogenase (ubiquinone) 1 alpha subcomplex; 9; 39kda; NDUFA10: nadh dehydrogenase (ubiquinone) 1 alpha subcomplex; 10; 42kda; HIGD1A: hig1 hypoxia inducible domain family; member 1a; NDUFC2-KCTD14: ndufc2-kctd14 readthrough; ETHE1: ethylmalonic encephalopathy 1; RDH16: retinol dehydrogenase 16 (all-trans); PRDX1: peroxiredoxin 1; BLVRB: biliverdin reductase b (flavin reductase (nadph)); RDH13: retinol dehydrogenase 13 (all-trans/9-cis); CBS: cystathionine-beta-synthase; AIFM2: apoptosis-inducing factor; mt-associated; 2; NDUFV1: nadh dehydrogenase (ubiquinone) flavoprotein 1; 51kda; SLC25A10: solute carrier family 25 (mt carrier; dicarboxylate transporter); member 10; NDUFS2: nadh dehydrogenase (ubiquinone) fe-s protein 2; 49kda (nadh-coenzyme q reductase); MGST1: microsomal glutathione s-transferase 1; G6PD: glucose-6-phosphate dehydrogenase; DHRS13: dehydrogenase/reductase (sdr family) member 13
GO:0022411	Cellular component disassembly	2.88E-05	1.77E-02	2.83	3713	171	146	19	MRPL22: mt ribosomal protein l22; MRPL2: mt ribosomal protein l2; MRPL9: mt ribosomal protein l9; MRPL10: mt ribosomal protein l10; MRPS2: mt ribosomal protein s2; CTSV: cathepsin v; MRPS26: mt ribosomal protein s26; CHMP2A: charged multivesicular body protein 2a; MTIF2: mt translational initiation factor 2; CHMP5: charged multivesicular body protein 5; MRPS9: mt ribosomal protein s9; MRPS6: mt ribosomal protein s6; DAP3: death associated protein 3; MRPS11: mt ribosomal protein s11; MRPL27: mt ribosomal protein l27; MRPL38: mt ribosomal protein l38; MRP63: mt ribosomal protein 63; MRPL21: mt ribosomal protein l21; MRPL3: mt ribosomal protein l3
GO:0006091	Generation of precursor metabolites and energy	5.65E-05	3.10E-02	2.61	3713	195	146	20	UQCRC2: ubiquinol-cytochrome c reductase core protein ii; GBAS: glioblastoma amplified sequence; PGK1: phosphoglycerate kinase 1; HK1: hexokinase 1; TPI1: triosephosphate isomerase 1; UQCRFS1: ubiquinol-cytochrome c reductase; rieske iron-sulfur polypeptide 1; GSR: glutathione reductase; COX4I1: cytochrome c oxidase subunit iv isoform 1; NDUFA9: nadh dehydrogenase (ubiquinone) 1 alpha subcomplex; 9; 39kda; NDUFA10: nadh dehydrogenase (ubiquinone) 1 alpha subcomplex; 10; 42kda; NDUFC2-KCTD14: ndufc2-kctd14 readthrough; RDH16: retinol dehydrogenase 16 (all-trans); COX10: cytochrome c oxidase assembly homolog 10 (yeast); ATP5F1: atp synthase; h+ transporting; mt fo complex; subunit b1; COX4I2: cytochrome c oxidase subunit iv isoform 2 (lung); AIFM2: apoptosis-inducing factor; mt-associated; 2; NDUFV1: nadh dehydrogenase (ubiquinone) flavoprotein 1; 51kda; COX7B: cytochrome c oxidase subunit viib; NDUFS2: nadh dehydrogenase (ubiquinone) fe-s protein 2; 49kda (nadh-coenzyme q reductase); ETFA: electron-transfer-flavoprotein; alpha polypeptide

GO Term	Description	<i>P</i>	<i>q</i>	Enrichment	<i>N</i>	<i>B</i>	<i>n</i>	<i>b</i>	Genes
GO:0044281	Small molecule metabolic process	1.48E-08	5.15E-05	2.28	3713	512	146	46	UQCRC2: ubiquinol-cytochrome c reductase core protein ii; PGK1: phosphoglycerate kinase 1; PAPSS2: 3'-phosphoadenosine 5'-phosphosulfate synthase 2; ACAA2: acetyl-coa acyltransferase 2; GADL1: glutamate decarboxylase-like 1; TPI1: triosephosphate isomerase 1; LTA4H: leukotriene a4 hydrolase; GSR: glutathione reductase; SUCLG2: succinate-coa ligase; gdp-forming; beta subunit; MFN1: mitofusin 1; GALNS: galactosamine (n-acetyl)-6-sulfate sulfatase; CDO1: cysteine dioxygenase type 1; COQ7: coenzyme q7 homolog; ubiquinone (yeast); OSBPL1A: oxysterol binding protein-like 1a; PDK3: pyruvate dehydrogenase kinase; isozyme 3; GCLM: glutamate-cysteine ligase; modifier subunit; SCP2: sterol carrier protein 2; MMADHC: methylmalonic aciduria (cobalamin deficiency) cbl d type; with homocystinuria; SLC16A1: solute carrier family 16 (monocarboxylate transporter); member 1; TALDO1: transaldolase 1; GCLC: glutamate-cysteine ligase; catalytic subunit; LDLRAP1: low density lipoprotein receptor adaptor protein 1; FARSA: phenylalanyl-trna synthetase; alpha subunit; GSTO1: glutathione s-transferase omega 1; TXN: thioredoxin; ETFA: electron-transfer-flavoprotein; alpha polypeptide; GBAS: glioblastoma amplified sequence; HK1: hexokinase 1; TMEM55B: transmembrane protein 55b; B3GNT3: udp-glcna:betagal beta-1,3-n-acetylglucosaminyltransferase 3; MUT: methylmalonyl coa mutase; ATP6V1A: atpase; h+ transporting; lysosomal 70kda; v1 subunit a; NDUFA9: nadh dehydrogenase (ubiquinone) 1 alpha subcomplex; 9; 39kda; GIMAP7: gtpase; imap family member 7; QARS: glutaminyl-trna synthetase; SLC25A1: solute carrier family 25 (mt carrier; citrate transporter); member 1; RDH16: retinol dehydrogenase 16 (all-trans); EPRS: glutamyl-prolyl-trna synthetase; PFKFB4: 6-phosphofructo-2-kinase/fructose-2,6-biphosphatase 4; ATP5F1: atp synthase; h+ transporting; mt fo complex; subunit b1; FH: fumarate hydratase; RDH13: retinol dehydrogenase 13 (all-trans/9-cis); CBS: cystathionine-beta-synthase; MPST: mercaptopyruvate sulfurtransferase; SLC25A10: solute carrier family 25 (mt carrier; dicarboxylate transporter); member 10; G6PD: glucose-6-phosphate dehydrogenase

Appendix C - The role of plasticity in facilitating colonization of extreme environments

Appendix C Tables

Table C1: List of identified orthogroups and the summary statistics for each species and treatment. Additionally includes information on whether genes were up-(1) or down-(-1) regulated and whether they exhibited adaptive, maladaptive, or a lack of plasticity. Due to the large size, the table is provided in a separate excel spreadsheet titled “C1 – Overall Results.csv”

References

1. Losos JB. CONVERGENCE, ADAPTATION, AND CONSTRAINT. *Evolution; international journal of organic evolution*. 2011;65(7):1827-40.
2. Dalziel AC, Laporte M, Rougeux C, Guderley H, Bernatchez L. Convergence in organ size but not energy metabolism enzyme activities among wild Lake Whitefish (*Coregonus clupeaformis*) species pairs. *Molecular ecology*. 2017;26(1):225-44.
3. Conte GL, Arnegard ME, Peichel CL, Schluter D. The probability of genetic parallelism and convergence in natural populations. *Proceedings Biological sciences*. 2012;279(1749):5039-47.
4. Elmer KR, Meyer A. Adaptation in the age of ecological genomics: insights from parallelism and convergence. *Trends in ecology & evolution*. 2011;26(6):298-306.
5. Rosenblum EB, Parent CE, Brandt EE. The molecular basis of phenotypic convergence. *Annual Review of Ecology, Evolution, and Systematics*. 2014;45:203-26.
6. Vermeij GJ. Historical contingency and the purported uniqueness of evolutionary innovations. *Proceedings of the National Academy of Sciences*. 2006;103(6):1804-9.
7. Landry L, Bernatchez L. Role of epibenthic resource opportunities in the parallel evolution of lake whitefish species pairs (*Coregonus* sp.). *Journal of evolutionary biology*. 2010;23(12):2602-13.
8. Winemiller KO, Kelso-Winemiller LC, Brenkert AL. Ecomorphological diversification and convergence in fluvial cichlid fishes. *Ecomorphology of fishes: Springer*; 1995. p. 235-61.
9. Wilkens H, Strecker U. Convergent evolution of the cavefish *Astyanax* (Characidae, Teleostei): genetic evidence from reduced eye-size and pigmentation. *Biological Journal of the Linnean Society*. 2003;80(4):545-54.
10. Waterman TH. The evolutionary challenges of extreme environments (Part 1). *The Journal of experimental zoology*. 1999;285(4):326-59.
11. Bell E. *Life at extremes : environments, organisms, and strategies for survival: CAB International*; 2012. 554- p.
12. Plath M, Tobler M, Riesch R. *Extremophile fishes: An Integrative Synthesis Springer International Publishing*; 2015. p. 279-96.

13. Tobler M, Kelley JL, Plath M, Riesch R. Extreme environments and the origins of biodiversity: Adaptation and speciation in sulphide spring fishes. *Molecular ecology*. 2018;27(4):843-59.
14. Tobler M, Passow CN, Greenway R, Kelley JL, Shaw JH. The Evolutionary Ecology of Animals Inhabiting Hydrogen Sulfide–Rich Environments. *Annual Review of Ecology, Evolution, and Systematics*. 2016;47(1):239-62.
15. Bagarinao T. Sulfide as an environmental factor and toxicant: tolerance and adaptations in aquatic organisms. *Aquatic Toxicology*. 1992;24(1):21-62.
16. Cooper CE, Brown GC. The inhibition of mitochondrial cytochrome oxidase by the gases carbon monoxide, nitric oxide, hydrogen cyanide and hydrogen sulfide: Chemical mechanism and physiological significance. 2008. p. 533-9.
17. Park CM, Nagel R, Blumberg W, Peisach J, Magliozzo R. Sulfhemoglobin. Properties of partially sulfurated tetramers. *Journal of Biological Chemistry*. 1986;261(19):8805-10.
18. Chen KY, Morris JC. Kinetics of Oxidation of Aqueous Sulfide by O₂. *Environmental Science and Technology*. 1972;6(6):529-37.
19. Theissen U, Hoffmeister M, Grieshaber M, Martin W. Single Eubacterial Origin of Eukaryotic Sulfide:Quinone Oxidoreductase, a Mitochondrial Enzyme Conserved from the Early Evolution of Eukaryotes During Anoxic and Sulfidic Times. *Molecular Biology and Evolution*. 2003;20(9):1564-74.
20. Hildebrandt TM, Grieshaber MK. Three enzymatic activities catalyze the oxidation of sulfide to thiosulfate in mammalian and invertebrate mitochondria. *FEBS Journal*. 2008;275(13):3352-61.
21. Jackson MR, Melideo SL, Jorns MS. Human sulfide:Quinone oxidoreductase catalyzes the first step in hydrogen sulfide metabolism and produces a sulfane sulfur metabolite. *Biochemistry*. 2012;51(34):6804-15.
22. Kelley JL, Arias-Rodriguez L, Patacsil Martin D, Yee M-C, Bustamante CD, Tobler M. Mechanisms Underlying Adaptation to Life in Hydrogen Sulfide–Rich Environments. *Molecular Biology and Evolution*. 2016;33(6):1419-34.
23. Greenway R, Arias-Rodriguez L, Diaz P, Tobler M. Patterns of Macroinvertebrate and Fish Diversity in Freshwater Sulphide Springs. *Diversity*. 2014;6(3):597-632.

24. Barts N, Greenway R, Passow CN, Arias-Rodriguez L, Kelley JL, Tobler M. Molecular evolution and expression of oxygen transport genes in livebearing fishes (Poeciliidae) from hydrogen sulfide rich springs. *Genome*. 2018;61(4):273-86.
25. Tobler M, DeWitt TJ, Schlupp I, García de León FJ, Herrmann R, Feulner PGD, et al. Toxic hydrogen sulfide and dark caves: phenotypic and genetic divergence across two abiotic environmental gradients in *Poecilia mexicana*. *Evolution; international journal of organic evolution*. 2008;62(10):2643-59.
26. Palacios M, Arias-Rodriguez L, Plath M, Eifert C, Lerp H, Lamboj A, et al. The Rediscovery of a Long Described Species Reveals Additional Complexity in Speciation Patterns of Poeciliid Fishes in Sulfide Springs. *PloS one*. 2013;8(8):e71069.
27. Tobler M, Palacios M, Chapman LJ, Mitrofanov I, Bierbach D, Plath M, et al. EVOLUTION IN EXTREME ENVIRONMENTS: REPLICATED PHENOTYPIC DIFFERENTIATION IN LIVEBEARING FISH INHABITING SULFIDIC SPRINGS. *Evolution; international journal of organic evolution*. 2011;65(8):2213-28.
28. Camarillo H, Arias Rodriguez L, Tobler M. Functional consequences of phenotypic variation between locally adapted populations: Swimming performance and ventilation in extremophile fish. *Journal of evolutionary biology*. 2020;33(4):512-23.
29. Plath M, Tobler M, Riesch R, García de León FJ, Giere O, Schlupp I. Survival in an extreme habitat: the roles of behaviour and energy limitation. *Die Naturwissenschaften*. 2007;94(12):991-6.
30. Passow CN, Henpita C, Shaw JH, Quackenbush CR, Warren WC, Scharl M, et al. The roles of plasticity and evolutionary change in shaping gene expression variation in natural populations of extremophile fish. *Molecular ecology*. 2017;26(22):6384-99.
31. Passow CN, Greenway R, Arias-Rodriguez L, Jeyasingh PD, Tobler M. Reduction of Energetic Demands through Modification of Body Size and Routine Metabolic Rates in Extremophile Fish. *Physiological and Biochemical Zoology*. 2015;88(4):371-83.
32. Passow CN, Arias-Rodriguez L, Tobler M. Convergent evolution of reduced energy demands in extremophile fish. *PloS one*. 2017;12(10):e0186935.
33. Brown AP, Greenway R, Morgan S, Quackenbush CR, Giordani L, Arias-Rodriguez L, et al. Genome-scale data reveal that endemic *Poecilia* populations from small sulphidic springs display no evidence of inbreeding. *Molecular ecology*. 2017;26(19):4920-34.

34. Brown AP, Arias-Rodriguez L, Yee M-C, Tobler M, Kelley JL. Concordant Changes in Gene Expression and Nucleotides Underlie Independent Adaptation to Hydrogen-Sulfide-Rich Environments. *Genome Biology and Evolution*. 2018;10(11):2867-81.
35. Völkel S, Berenbrink M. Sulphaemoglobin formation in fish: a comparison between the haemoglobin of the sulphide-sensitive rainbow trout (*Oncorhynchus Mykiss*) and of the sulphide-tolerant common carp (*Cyprinus Carpio*). *The Journal of experimental biology*. 2000;203(Pt 6):1047-58.
36. Greenway R, Barts N, Henpita C, Brown AP, Rodriguez LA, Rodríguez Peña CM, et al. Convergent evolution of conserved mitochondrial pathways underlies repeated adaptation to extreme environments. *bioRxiv*. 2020:2020.02.24.959916-2020.02.24.
37. Dalziel AC, Martin N, Laporte M, Guderley H, Bernatchez L. Adaptation and acclimation of aerobic exercise physiology in Lake Whitefish ecotypes (*Coregonus clupeaformis*). *Evolution; international journal of organic evolution*. 2015;69(8):2167-86.
38. Dalziel AC, Laporte M, Guderley H, Bernatchez L. Do differences in the activities of carbohydrate metabolism enzymes between Lake Whitefish ecotypes match predictions from transcriptomic studies? *Comparative Biochemistry and Physiology Part B: Biochemistry and Molecular Biology*. 2018;224:138-49.
39. Diz AP, MartÍNez-FernÁNdez M, RolÁN-Alvarez E. Proteomics in evolutionary ecology: linking the genotype with the phenotype. *Molecular ecology*. 2012;21(5):1060-80.
40. Charlesworth D, Barton NH, Charlesworth B. The sources of adaptive variation. *Proceedings of the Royal Society B: Biological Sciences*. 2017;284(1855):20162864.
41. Darwin C. *The different forms of flowers on plants of the same species*: D. Appleton and Company; 1897.
42. Lee CE, Remfert JL, Gelembiuk GW. Evolution of Physiological Tolerance and Performance During Freshwater Invasions¹. *Integrative and comparative biology*. 2003;43(3):439-49.
43. Lee CE, Gelembiuk GW. Evolutionary origins of invasive populations. *Evolutionary Applications*. 2008;1(3):427-48.
44. Lee CE. RAPID AND REPEATED INVASIONS OF FRESH WATER BY THE COPEPOD EURYTEMORA AFFINIS. *Evolution; international journal of organic evolution*. 1999;53(5):1423-34.

45. Lee CE. Evolutionary mechanisms of habitat invasions, using the copepod *Eurytemora affinis* as a model system. *Evolutionary Applications*. 2016;9(1):248-70.
46. Hufbauer RA, Facon B, Ravigné V, Turgeon J, Foucaud J, Lee CE, et al. Anthropogenically induced adaptation to invade (AIAI): contemporary adaptation to human-altered habitats within the native range can promote invasions. *Evolutionary Applications*. 2012;5(1):89-101.
47. Endler JA. *Natural selection in the wild*. Princeton, NJ: Princeton University Press; 1986.
48. Schluter D. *The Ecology of Adaptive Radiation*. Oxford: Oxford University Press; 2000.
49. Losos JB, Ricklefs RE. Adaptation and diversification on islands. *Nature*. 2009;457(7231):830-6.
50. Winemiller KO, Kelsowinemiller LC, Brenkert AL. Ecomorphological Diversification and Convergence in Fluvial Cichlid Fishes. *Environmental Biology of Fishes*. 1995;44(1-3):235-61.
51. Gould SJ, Lewontin RC. The spandrels of San Marco and the panglossian paradigm: a critique of the adaptationist programme. *Proceedings of the Royal Society B*. 1979;205:581-98.
52. Kaeuffer R, Peichel CL, Bolnick DI, Hendry AP. Parallel and nonparallel aspects of ecological, phenotypic, and genetic divergence across replicate population pairs of lake and stream stickleback. *Evolution; international journal of organic evolution*. 2012;66:402-18.
53. DeWitt TJ, Scheiner S. *Phenotypic plasticity: Functional and conceptual approaches*. Oxford: Oxford University Press; 2004.
54. Blount ZD, Borland CZ, Lenski RE. Historical contingency and the evolution of a key innovation in an experimental population of *Escherichia coli*. *Proceedings of the National Academy of Sciences USA*. 2008;105(23):7899-906.
55. Stern DL. The genetic causes of convergent evolution. *Nature Reviews Genetics*. 2013;14:751-64.
56. Natarajan C, Hoffmann FG, Weber RE, Fago A, Witt CC, Storz JF. Predictable convergence in hemoglobin function has unpredictable molecular underpinnings. *Science*. 2016;354:336-9.
57. Culumber ZW, Tobler M. Ecological divergence and conservatism: spatiotemporal patterns of niche evolution in a genus of livebearing fishes (Poeciliidae: *Xiphophorus*). *BMC Evolutionary Biology*. 2016;16:44.
58. Reid NM, Prostou DA, Clark BW, Warren WC, Colbourne JK, Shaw JR, et al. The genomic landscape of rapid repeated evolutionary adaptation to toxic pollution in wild fish. *Science*. 2016;354:1305-8.

59. Dobler S, Dalla S, Wagschal V, Agrawal AA. Community-wide convergent evolution in insect adaptation to toxic cardenolides by substitutions in the Na,K-ATPase. *Proceedings of the National Academy of Sciences USA*. 2012;109:13040-5.
60. Feldman CR, Brodie Jr. ED, Brodie III ED, Pfrender ME. Constraint shapes convergence in tetrodotoxin-resistant sodium channels of snakes. *Proceedings of the National Academy of Sciences USA*. 2012;109:4556-61.
61. Tarvin RD, Santos JC, O'Connell LA, Zakon HH, Cannatella DC. Convergent substitutions in a sodium channel suggests multiple origins of toxin resistance in poison frogs. *Molecular Biology and Evolution*. 2016;33:1068-81.
62. Fukuto JM, Carrington SJ, Tantillo DJ, Harrison JG, Ignarro LJ, Freeman BA, et al. Small molecule signaling agents: the integrated chemistry and biochemistry of nitrogen oxides, oxides of carbon, dioxygen, hydrogen sulfide, and their derived species. *Chemical Research in Toxicology*. 2012;25:769-93.
63. Kabil O, Banerjee R. Redox biochemistry of hydrogen sulfide. *Journal of Biological Chemistry*. 2010;285:21903-7.
64. Khan AA. Biochemical effects of hydrogen sulfide toxicity. In: Prior M, Roth S, Green F, Hulbert W, Reiffenstein R, editors. *Proceedings of the international conference on hydrogen sulfide toxicity*, Banff, Alberta, Canada, June 18-21, 1989. Edmonton: Sulfide Research Network; 1990. p. 79-89.
65. Bagarinao T, Vetter RD. Sulfide-hemoglobin interactions in the sulfide-tolerant salt marsh resident, the California killifish *Fundulus parvipinnis*. *Journal of Comparative Physiology B*. 1992;162:614-24.
66. Beauchamp RO, Bus JS, Popp JA, Boreiko CJ, Andjelkovich DA, Leber P. A critical review of the literature on hydrogen sulfide toxicity. *Critical Reviews in Toxicology*. 1984;13(1):25-97.
67. Martin NM, Maricle BR. Species-specific enzymatic tolerance of sulfide toxicity in plant roots. *Plant Physiology and Biochemistry*. 2015;88:36-41.
68. Pfenninger M, Lerp H, Tobler M, Passow C, Kelley JL, Funke E, et al. Parallel evolution of cox genes in H₂S-tolerant fish as key adaptation to a toxic environment. *Nature Communications*. 2014;5.

69. Huang J, Zhang L, Li J, Shi X, Zhang Z. Proposed function of alternative oxidase in mitochondrial sulphide oxidation detoxification in the Echiuran worm, *Urechis unicinctus*. *Journal of the Marine Biological Association*. 2013;93:2145-54.
70. Liu X, Zhang Z, Ma X, Li X, Zhou D, Gao B, et al. Sulfide exposure results in enhanced sqp transcription through upregulating the expression and activation of HSF1 in echiuran worm *Urechis unicinctus*. *Aquatic Toxicology*. 2016;170:229-39.
71. Ma Y-B, Zhang Z-F, Shao M-Y, Kang K-H, Shi X-L, Dong Y-P, et al. Response of sulfide-quinone oxireductase to sulfide exposure in the echiuran worm *Urechis unicinctus*. *Marine Biotechnology*. 2012;14:245-51.
72. Pfenninger M, Patel S, Arias-Rodriguez L, Feldmeyer B, Riesch R, Plath M. Unique evolutionary trajectories in repeated adaptation to hydrogen sulphide-toxic habitats of a neotropical fish (*Poecilia mexicana*). *Molecular ecology*. 2015;24:5446-59.
73. Olson KR. The therapeutic potential of hydrogen sulfide: separating hype from hope. *American Journal of Physiology-Regulatory, Integrative and Comparative Physiology*. 2011;301:R297-312.
74. Pietri R, Roman-Morales E, Lopez-Garriga J. Hydrogen sulfide and heme proteins: knowledge and mysteries. *Antioxidants & Redox Signaling*. 2011;15:393-404.
75. Grieshaber MK, Völkel S. Animal adaptations for tolerance and exploitation of poisonous sulfide. *Annual Review of Physiology*. 1998;60:33-53.
76. Evans SV, Sishta BP, Mauk AG, Brayer GD. Three-dimensional structure of cyanomet-sulfmyoglobin C. *Proceedings of the National Academy of Sciences USA*. 1994;91:4723-6.
77. Johnson EA. The reversion to haemoglobin of sulphhaemoglobin and its coordination derivatives. *Biochimica Et Biophysica Acta*. 1970;207:30-40.
78. Flores JF, Fisher CR, Carney SL, Green BN, Freytag JK, Schaeffer SW, et al. Sulfide binding is mediated by zinc ions discovered in the crystal structure of a hydrothermal vent tubeworm hemoglobin. *Proceedings of the National Academy of Sciences USA*. 2005;102:2713-8.
79. Kraus DW, Wittenberg JB. Hemoglobins of the *Lucina pectinata*/bacteria symbiosis: 1. Molecular properties, kinetics and equilibria of reactions with ligands. *Journal of Biological Chemistry*. 1990;265:16043-53.

80. Zal F, Leize E, Lallier FH, Toulmond A, Van Dorsselaer A, Childress JJ. S-sulfohemoglobin and disulfide exchange: the mechanisms of sulfide binding by *Riftia pachyptila* hemoglobins. Proceedings of the National Academy of Sciences USA. 1998;95:8997-9002.
81. Hourdez S, Weber RE, Green BN, Kenney JM, Fisher CR. Respiratory adaptations in a deep-sea oribiniid polychaete from Gulf of Mexico brine pool NR-1: metabolic rates and hemoglobin structure/function relationships. Journal of Experimental Biology. 2002;205:1669-81.
82. Riesch R, Tobler M, Plath M. Hydrogen sulfide-toxic habitats. In: Riesch R, Tobler M, Plath M, editors. Extremophile Fishes: Ecology, Evolution, and Physiology of Teleosts in Extreme Environments. Heidelberg, Germany: Springer; 2015. p. 137-59.
83. Tobler M, Palacios M, Chapman LJ, Mitrofanov I, Bierbach D, Plath M, et al. Evolution in extreme environments: replicated phenotypic differentiation in livebearing fish inhabiting sulfidic springs. Evolution; international journal of organic evolution. 2011;65:2213-28.
84. Tobler M, Hastings L. Convergent Patterns of Body Shape Differentiation in Four Different Clades of Poeciliid Fishes Inhabiting Sulfide Springs. Evolutionary Biology. 2011;38(4):412-21.
85. Riesch R, Schlupp I, Langerhans RB, Plath M. Shared and unique patterns of embryo development in extremophile poeciliids. PloS one. 2011;6(11):e27377.
86. Riesch R, Plath M, Schlupp I, Tobler M, Langerhans RB. Colonization of toxic springs drives predictable life-history shift in livebearing fishes (Poeciliidae). Ecology Letters. 2014;17:65-71.
87. Riesch R, Reznick DN, Plath M, Schlupp I. Sex-specific local life-history adaptation in surface- and cave-dwelling Atlantic mollies (*Poecilia mexicana*). Scientific reports. 2016;6:22968.
88. Plath M, Pfenninger M, Lerp H, Riesch R, Eschenbrenner C, Slattery PA, et al. Genetic differentiation and selection against migrants in evolutionarily replicated extreme environments. Evolution; international journal of organic evolution. 2013;67(9):2647-61.
89. Vitvitsky V, Kabil O, Banerjee R. High turnover rates for hydrogen sulfide allow for rapid regulation of its tissue concentrations. Antioxid Redox Signal. 2012;17(1):22-31.
90. Roesner A, Hankeln T, Burmester T. Hypoxia induces a complex response of globin expression in zebrafish (*Danio rerio*). Journal of Experimental Biology. 2006;209(11):2129-37.

91. Fraser J, de Mello LV, Ward D, Rees HH, Williams DR, Fang YC, et al. Hypoxia-inducible myoglobin expression in nonmuscle tissues. *Proceedings of the National Academy of Sciences of the United States of America*. 2006;103(8):2977-81.
92. Richards JG. Metabolic and molecular responses of fish to hypoxia. In: Richards JG, Farrell AP, Brauner CJ, editors. *Hypoxia*. London: Academic Press; 2009. p. 443-85.
93. van der Meer DL, Van Den Thillart G, Witte F, de Bakker MA, Besser J, Richardson MK, et al. Gene expression profiling of the long-term adaptive response to hypoxia in the gills of adult zebrafish. *American Journal of Physiology - Integrative and Comparative Physiology*. 2005;289:1512-9.
94. Wawrowski A, Gerlach F, Hankeln T, Burmester T. Changes of globin expression in the Japanese medaka (*Oryzias latipes*) in response to acute and chronic hypoxia. *Journal of Comparative Physiology B*. 2011;181:199-208.
95. Storz JF, Scott GR, Cheviron ZA. Phenotypic plasticity and genetic adaptation to high-altitude hypoxia in vertebrates. *Journal of Experimental Biology*. 2010;213:4125-36.
96. Weber RE. High-altitude adaptations in vertebrate hemoglobins. *Respiration Physiology and Neurobiology*. 2007;158:132-42.
97. Weber RE, Fago A. Functional adaptation and its molecular basis in vertebrate hemoglobins, neuroglobins and cytoglobins. *Respiratory Physiology & Neurobiology*. 2004;144:141-59.
98. Perutz MF. Species adaptation in a protein module. *Molecular Biology and Evolution*. 1983;1:1-28.
99. Palacios M, Voelker G, Arias-Rodriguez L, Mateos M, Tobler M. Phylogenetic analyses of the subgenus *Mollienesia* (*Poecilia*, Poeciliidae, Teleostei) reveal taxonomic inconsistencies, cryptic biodiversity, and spatio-temporal aspects of diversification in Middle America. *Molecular phylogenetics and evolution*. 2016;103:230-44.
100. Jourdan J, Kause ST, Lazar VM, Zimmer C, Sommer-Trembo C, Arias-Rodriguez L, et al. Shared and unique patterns of phenotypic diversification along a stream gradient in two congeneric species. *Scientific reports*. 2016;6:38971.
101. Weaver PF, Cruz A, Johnson SC, Dupin J, Weaver KF. Colonizing the Caribbean: biogeography and evolution of livebearing fishes of the genus *Limia* (Poeciliidae). *Journal of Biogeography*. 2016;43:1808-19.

102. Schartl M, Walter RB, Shen Y, Garcia T, Catchen J, Amores A, et al. The genome of the platyfish, *Xiphophorus maculatus*, provides insights into evolutionary adaptation and several complex traits. *Nature Genetics*. 2013;45:567-72.
103. Waits ER, Martinson J, Rinner B, Morris S, Proestou D, Champlin D, et al. Genetic linkage map and comparative genome analysis for the Atlantic killifish (*Fundulus heteroclitus*). *Open Journal of Genetics*. 2016;6:28-.
104. Evans TG, Hammill E, Kaukinen K, Schulze AD, Patterson DA, English KK, et al. Transcriptomics of environmental acclimatization and survival in wild adult Pacific sockeye salmon (*Oncorhynchus nerka*) during spawning migration. *Molecular ecology*. 2011;20:4472-89.
105. Evans DH, Claiborne JB, editors. *The physiology of fishes*. 3rd ed. Boca Raton, FL: Taylor & Francis; 2006.
106. Kelley JL, Arias-Rodriguez L, Patacsil Martin D, Yee MC, Bustamante C, Tobler M. Mechanisms underlying adaptation to life in hydrogen sulfide rich environments. *Molecular Biology and Evolution*. 2016;33(6):1419-34.
107. Tobler M, Henpita C, Bassett B, Kelley JL, Shaw J. H₂S exposure elicits differential expression of candidate genes in fish adapted to sulfidic and non-sulfidic environments. *Comparative Biochemistry and Physiology A: Molecular & Integrative Physiology*. 2014;175:7-14.
108. Krueger F. Trim Galore! version 0.3.7. http://www.bioinformaticsbabraham.ac.uk/projects/trim_galore/. 2014.
109. Li H, Durbin R. Fast and accurate short read alignment with Burrows-Wheeler transform. *Bioinformatics*. 2009;25(14):1754-60.
110. Shen Y-Y, Liang L, Zhu Z-H, Zhou W-P, Irwin DM, Zhang YP. Adaptive evolution of energy metabolism genes and the origin of flight in bats. *Proceedings of the National Academy of Sciences USA*. 2010;107:8666-71.
111. Zhang F, Broughton RE. Mitochondrial-nuclear interactions: compensatory evolution or variable functional constraint among vertebrate oxidative phosphorylation genes? *Genome Biology and Evolution*. 2013;5:1781-91.
112. McKenna A, Hanna M, Banks E, Sivachenko A, Cibulskis K, Kernytsky A, et al. The Genome Analysis Toolkit: a MapReduce framework for analyzing next-generation DNA sequencing data. *Genome Research*. 2010;20(9):1297-303.

113. Van der Auwera GA, Carneiro MO, Hartl C, Poplin R, del Angel G, Levy-Moonshine A, et al. From FastQ data to high-confidence variant calls: the genome analysis toolkit best practices pipeline. *Current Protocols in Bioinformatics*. 2013;43:11.0.1-.0.33.
114. DePristo M, Banks E, Poplin R, Garimella K, Maguire J, Hartl. C, et al. A framework for variation discovery and genotyping using next-generation DNA sequencing data. *Nature Genetics*. 2011;43(5):491-8.
115. Larkin MA, Blackshields G, Brown N, Chenna R, McGettigan PA, McWilliam H, et al. Clustal W and Clustal X version 2.0. *Bioinformatics*. 2007;23(21):2947-8.
116. Darriba D, Taboada GL, Doallo R, Posada D. jModelTest 2: more models, new heuristics and parallel computing. *Nature Methods*. 2012;9(8):772-.
117. Stamatakis A. RAxML version 8: a tool for phylogenetic analysis and post-analysis of large phylogenies. *Bioinformatics*. 2014;30(9):1312-3.
118. Hrbek T, Seckinger J, Meyer A. A phylogenetic and biogeographic perspective on the evolution of poeciliid fishes. *Molecular phylogenetics and evolution*. 2007;43:986-98.
119. Pollux BJA, Meredith RW, Springer MS, Garland T, Reznick DN. The evolution of the placenta drives a shift in sexual selection in livebearing fish. *Nature*. 2014;513:233-6.
120. Trapnell C, Williams BA, Pertea G, Mortazavi A, Kwan G, van Baren MJ, et al. Transcript assembly and quantification by RNA-Seq reveals unannotated transcripts and isoform switching during cell differentiation. *Nature Biotechnology*. 2010;28(5):511-5.
121. Rohlf RV, Harrigan P, Nielsen R. Modeling gene expression evolution with an extended Ornstein-Uhlenbeck process accounting for within-species variation. *Mol Biol Evol*. 2014;31(1):201-11.
122. Rohlf RV, Nielsen R. Phylogenetic ANOVA: the expression variance and evolution (EVE) model for quantitative trait evolution. *Systematic Biology*. 2015;64:695-708.
123. Yang Z. PAML 4: Phylogenetic analysis by maximum likelihood. *Molecular Biology and Evolution*. 2007;24(8):1586-91.
124. Löytynoja A, Goldman N. An algorithm for progressive multiple alignment of sequences with insertions. *Proceedings of the National Academy of Sciences*. 2005;102(30):10557-62.
125. Yang Z, Nielsen R, Goldman N, Pedersen AM. Codon-substitution models for heterogeneous selection pressure at amino acid sites. *Genetics*. 2000;155:431-49.

126. Zhang J, Nielsen R, Yang Z. Evaluation of an improved branch-site likelihood method for detecting positive selection at the molecular level. *Molecular Biology and Evolution*. 2005;22:2472-9.
127. Yang Z, Nielsen R. Codon-substitution models for detecting molecular adaptation at individual sites along specific lineages. *Molecular Biology and Evolution*. 2002;19:908-17.
128. Choi Y, Sims GE, Murphy S, Miller JR, Chan AP. Predicting the Functional Effect of Amino Acid Substitutions and Indels. *PloS one*. 2012;7(10):e46688.
129. Choi Y, Chan AP. PROVEAN web server: a tool to predict the functional effect of amino acid substitutions and indels. *Bioinformatics*. 2015;31(16):2745-7.
130. Hardison RC. Evolution of hemoglobin and its genes. *Cold Spring Harbor Perspectives in Medicine*. 2012;2:a011627.
131. Opazo JC, Butts GT, Nery MF, Storz JF, Hoffmann FG. Whole-genome duplication and the functional diversification of teleost fish hemoglobins. *Molecular Biology and Evolution*. 2013;30:140-53.
132. Culumber ZW, Hopper GW, Barts N, Passow CN, Morgan S, Brown A, et al. Habitat use of two extremophile, highly endemic, and critically endangered fish species (*Gambusia eurystoma* and *Poecilia sulphurophila*; Poeciliidae). *Aquatic Conservation-Marine and Freshwater Ecosystems*. 2016;26:1155-67.
133. Riesch R, Tobler M, Lerp H, Jourdan J, Doumas LT, Nosil P, et al. Extremophile Poeciliidae: multivariate insights into the complexity of speciation along replicated ecological gradients. *BMC Evolutionary Biology*. 2016;16:136.
134. Stuart YE, Veen T, Weber JN, Hanson D, Ravinet M, Lohman BK, et al. Contrasting effects of environment and genetics generate a continuum of parallel evolution. *Nature Ecology & Evolution*. 2017;1:0158.
135. Plath M, Pfenninger M, Lerp H, Riesch R, Eschenbrenner C, Slattery P, et al. Genetic differentiation and selection against migrants in evolutionarily replicated extreme environments. *Evolution; international journal of organic evolution*. 2013;67:2647-61.
136. Moore J, Gow J, Taylor EB, Hendry AP. Quantifying the constraining influence of gene flow on adaptive divergence in the lake-stream threespine stickleback system. *Evolution; international journal of organic evolution*. 2007;61:2015-26.

137. Tian R, Losilla M, Lu Y, Yang G, Zakon H. Molecular evolution of globin genes in Gymnotiform electric fishes; relation to hypoxia tolerance. *Bmc Evolutionary Biology*. 2017;17:51.
138. Poyart C, Bursaux E, Arnone A, Bonaventura J, Bonaventura C. Structural and functional studies of hemoglobin Suresnes (arg 141 alpha 2 replaced by His beta 2). Consequences of disrupting an oxygen-linked anion-binding site. *Journal of Biological Chemistry*. 1980;255(19):9465-73.
139. Poyart C, Krishnamoorthy R, Bursaux E, Gacon G, Labie D. Structural and functional studies of hemoglobin suresnes or a2 141(HC3) Arg → His β₂, a new high oxygen affinity mutant. *FEBS Letters*. 1976;69:103-7.
140. Dangre AJ, Manning S, Brouwer M. Effects of cadmium on hypoxia-induced expression of hemoglobin and erythropoietin in larval sheepshead minnow, *Cyprinodon variegatus*. *Aquatic Toxicology*. 2010;99:168-75.
141. Roesner A, Mitz SA, Hankeln T, Burmester T. Globins and hypoxia adaptation in the goldfish, *Carassius auratus*. *FEBS Journal*. 2008;275:3633-43.
142. Grispo MT, Natarajan C, Projecto-Garcia J, Moriyama H, Weber RE, Storz JF. Gene duplication and the evolution of hemoglobin isoform differentiation in birds. *Journal of Biological Chemistry*. 2012;287:37647-58.
143. Tobler M, Riesch R, Tobler CM, Plath M. Compensatory behaviour in response to sulfide-induced hypoxia affects time budgets, feeding efficiency, and predation risk. *Evolutionary Ecology Research*. 2009;11:935-48.
144. Gould SJ. *Wonderful Life: The Burgess Shale and the Nature of History*. New York: W. W. Norton and Company; 1990.
145. Orgogozo V. Replaying the tape of life in the twenty-first century. *Interface Focus*. 2015;5:20150057.
146. Blount ZD, Lenski RE, Losos JB. Contingency and determinism in evolution: replaying life's tape. *Science*. 2018;362:eaam5979.
147. Ballard JWO, Kreitman M. Is mitochondrial DNA a strictly neutral marker? *Trends in ecology & evolution*. 1995;10:485-8.
148. Hill GE. *Mitochondrial Ecology*. Oxford: Oxford University Press; 2019.
149. Friedman JR, Nunnari J. Mitochondrial form and function. *Nature*. 2014;505:335-43.

150. Woodson JD, Chory J. Coordination of gene expression between organellar and nuclear genomes. *Nature Reviews Genetics*. 2008;9:383-95.
151. Tobler M, Passow CN, Greenway R, Kelley JL, Shaw JH. The evolutionary ecology of animals inhabiting hydrogen sulfide-rich environments. *Annual Review of Ecology, Evolution and Systematics*. 2016;47:239-62.
152. Tobler M, Kelley JL, Plath M, Riesch R. Extreme environments and the origins of biodiversity: adaptation and speciation in sulfide springs. *Molecular ecology*. 2018;27:843-59.
153. Saraste M. Oxidative phosphorylation at the fin de siècle. *Science*. 1999;283:1488-93.
154. Shahak Y, Hauska G. Sulfide oxidation from cyanobacteria to humans: sulfide-quinone oxidoreductase (SQR). In: Hell R, Dahl C, Knaff DB, T L, editors. *Advances in Photosynthesis and Respiration*. 27. Heidelberg: Springer; 2008. p. 319-35.
155. Cooper CE, Brown GC. The inhibition of mitochondrial cytochrome oxidase by the gases carbon monoxide, nitric oxide, hydrogen cyanide and hydrogen sulfide: chemical mechanism and physiological significance. *Journal of Bioenergy and Biomembranes*. 2008;40:533-9.
156. Olson KR. H₂S and polysulfide metabolism: Conventional and unconventional pathways. *Biochemical Pharmacology*. 2018;149:77-90.
157. Pfenninger M, Lerp H, Tobler M, Passow C, Kelley JL, Funke E, et al. Parallel evolution of *cox* genes in H₂S-tolerant fish as key adaptation to a toxic environment. *Nature Communications*. 2014;5:3873.
158. Arndt S, Baeza-Garza CD, Logan A, Rosa T, Wedmann R, Prime TA, et al. Assessment of H₂S in vivo using the newly developed mitochondria-targeted mass spectrometry probe MitoA. *Journal of Biological Chemistry*. 2017;292:7761-73.
159. Brown AP, Arias-Rodriguez L, Yee MC, Tobler M, Kelley JL. Concordant changes in gene expression and nucleotides underlie independent adaptation to hydrogen-sulfide-rich environments. *Genome Biology and Evolution*. 2018;10:2867-81.
160. Jones FC, Grabherr MG, Chan YF, Russell P, Mauceli E, Johnson J, et al. The genomic basis of adaptive evolution in threespine stickleback. *Nature*. 2012;484:55-61.
161. Oziolor EM, Reid NM, Yair S, Lee KM, Guberman VerPloeg S, Bruns PC, et al. Adaptive introgression enables evolutionary rescue from extreme environmental pollution. *Science*. 2019;364:455-7.

162. Elmer KR, Meyer A. Adaptation in the age of genomics: insights from parallelism and convergence. *Trends in ecology & evolution*. 2011;26(6):298-306.
163. Palacios M, Arias-Rodriguez L, Plath M, Eifert C, Lerp H, Lamboj A, et al. The redesccovery of a long described species reveals additional complexity in speciation patterns of poeciliid fishes in sulfide springs. *PloS one*. 2013;8(8):e71069.
164. Brown AP, McGowan KL, Schwarzkopf EJ, Greenway R, Arias Rodriguez L, Tobler M, et al. Local ancestry analysis reveals genomic convergence in extremophile fishes. *Philosophical Transactions of the Royal Society B*. 2019;374:20180240.
165. Conte GL, Arnegard ME, Peichel CL, Schluter D. The probability of genetic parallelism and convergence in natural populations. *Proceedings of the Royal Society B*. 2012;279:5039-47.
166. Conway Morris S. *Life's solution: inevitable humans in a lonely universe*. Cambridge: Cambridge University Press; 2003.
167. Hildebrandt TM, Grieshaber M. Three enzymatic activities catalyze the oxidation of sulfide to thiosulfate in mammalian and invertebrate mitochondria. *FEBS Journal*. 2008;275:3352-61.
168. Losos JB. Convergence, adaptation, and constraint. *Evolution*. 2011;65:1827-40.
169. Alda F, Reina RG, Doadrio I, Bermingham E. Phylogeny and biogeography of the *Poecilia sphenops* species complex (Actinopterygii, Poeciliidae) in Central America. *Molecular phylogenetics and evolution*. 2013;66:1011-26.
170. Passow C, Arias-Rodriguez L, Tobler M. Convergent evolution of reduced energy demands in extremophile fish. *PloS one*. 2017;12:e0186935.
171. Greenway R, Drexler S, Arias-Rodriguez L, Tobler M. Adaptive, but not condition-dependent, body shape differences contribute to assortative mating preferences during ecological speciation. *Evolution; international journal of organic evolution*. 2016;70:2809-22.
172. Passow CN, Henpita C, Shaw JH, Quakenbush C, Warren WC, Scharl M, et al. The roles of plasticity and evolutionary change in shaping gene expression variation in natural populations of extremophile fish. *Molecular ecology*. 2017;26:6384-99.
173. Greenway R, Arias-Rodriguez L, Diaz P, Tobler M. Patterns of macroinvertebrate and fish diversity in freshwater sulphide springs. *Diversity*. 2014;6:597-632.
174. R Core Team. *R: A language and environment for statistical computing*. Vienna, Austria: R Foundation for Statistical Computing; 2018.

175. Dalziel AC, Martin N, Laporte M, Guderley H, Bernatchez L. Adaptation and acclimation of aerobic exercise physiology in Lake Whitefish ecotypes (*Coregonus clupeaformis*). *Evolution*. 2015;69:2167-86.
176. Kirby DM, Thorburn DR, Turnbull DM, Taylor RW. Biochemical assays of respiratory chain complex activity. *Methods in Cell Biology*. 2007;80:93-119.
177. Bates D, Maechler M, Bolker B, Walker S. Fitting linear mixed-effects models using lme4. *Journal of Statistical Software*. 2015;67:1-48.
178. Johnson JB, Omland KS. Model selection in ecology and evolution. *Trends in ecology & evolution*. 2004;19:101-8.
179. Burnham KP, Anderson DR. Model selection and multimodel inference: a practical information-theoretic approach. New York, NY: Springer; 2002.
180. Theissen U, Martin W. Sulfide:quinone oxidoreductase (SQR) from the lugworm *Arenicola marina* shows cyanide- and thioredoxin-dependent activity. *FEBS Journal*. 2008;275:1-9.
181. Ma Y-B, Zhang Z-F, Shao M-Y, Kang K-H, Tan Z, Li J-L. Sulfide:quinone oxidoreductase from echiuran worm *Urechis unicinctus*. *Marine Biotechnology*. 2011;13:93-107.
182. Lau GY, Barts N, Hartley RC, Tobler M, Richards JG, Murphy MP, et al. Detection of changes in mitochondrial hydrogen sulfide in vivo in the fish model *Poecilia mexicana* (Poeciliidae). *Biology Open*. 2019;8:bio041467.
183. Ferrick DA, Neilson A, Beeson C. Advances in measuring cellular bioenergetics using extracellular flux. *Drug Discovery Today*. 2008;13:268-74.
184. Rogers GW, Brand MD, Petrosyan S, Ashok D, Elorza AA, Ferrick DA, et al. High throughput microplate respiratory measurements using minimal quantities of isolated mitochondria. *PloS one*. 2011;6:e21746.
185. Commo F, Bot BM. nplr: N-Parameter Logistic Regression. R package version 01-7. 2016; <https://CRAN.R-project.org/package=nplr>.
186. Küstner A, Hoffmann M, Fraser BA, Kottler VA, Sharma E, Weigel D, et al. The genome of the Trinidadian guppy, *Poecilia reticulata*, and variation in the guanapo population. *PloS one*. 2016;11:e0169087.
187. Li H. Aligning sequence reads, clone sequences and assembly contigs with BWA-MEM. *arXiv Preprint*. 2013(arXiv:1303.3997v2).

188. Danecek P, Auton A, Abecasis G, Albers CA, Banks E, DePristo MA, et al. The variant call format and VCFtools. *Bioinformatics*. 2011;27:2156-8.
189. Zamani N, Russell P, Lantz H, Hoepfner MP, Meadows JRS, Vijay N, et al. Unsupervised genome-wide recognition of local relationship patterns. *BMC Genomics*. 2013;14:347.
190. Kelley JL, Passow C, Plath M, Arias-Rodriguez L, Yee MC, Tobler M. Genomic resources for a model in adaptation and speciation research: the characterization of the *Poecilia mexicana* transcriptome. *BMC Genomics*. 2012;13:652.
191. Warren WC, García-Pérez R, Xu S, Lampert KP, Chalopin D, Stöck M, et al. Clonal polymorphism and high heterozygosity in the celibate genome of the Amazon molly. *Nature ecology & evolution*. 2018:1.
192. Li H, Durbin R. Fast and accurate short read alignment with Burrows-Wheeler transform. *Bioinformatics*. 2009;25:1754-60.
193. Camacho C, Coulouris G, Avagyan V, Ma N, Papadopoulos J, Bealer K, et al. BLAST+: architecture and applications. *BMC Bioinformatics*. 2009;10(1):421.
194. Dunn CW, Zapata F, Munro C, Siebert S, Hejnal A. Pairwise comparisons across species are problematic when analyzing functional genomic data. *Proceedings of the National Academy of Sciences USA*. 2018;115:E409-E17.
195. Rohlf RV, Nielsen R. Phylogenetic ANOVA: the expression variance and evolution model for quantitative trait evolution. *Systematic biology*. 2015;64(5):695-708.
196. Rohlf RV, Harrigan P, Nielsen R. Modeling gene expression evolution with an extended Ornstein–Uhlenbeck process accounting for within-species variation. *Molecular biology and evolution*. 2014;31(1):201-11.
197. Benjamini Y, Hochberg Y. Controlling the False Discovery Rate: A Practical and Powerful Approach to Multiple Testing. *Journal of the Royal Statistical Society: Series B (Methodological)*. 1995;57(1):289-300.
198. Gene Ontology Consortium. The Gene Ontology (GO) database and informatics resource. *Nucleic Acids Research*. 2004;32:D258-D61.
199. Eden E, Navon R, Steinfeld I, Lipson D, Yakhini Z. GOrilla: a tool for discovery and visualization of enriched GO terms in ranked gene lists. *BMC Bioinformatics*. 2009;10:48.

200. Whitehead A. Comparative genomics in ecological physiology: toward a more nuanced understanding of acclimation and adaptation. *Journal of Experimental Biology*. 2012;215:884-91.
201. Auwera GA, Carneiro MO, Hartl C, Poplin R, del Angel G, Levy-Moonshine A, et al. From FastQ data to high-confidence variant calls: the genome analysis toolkit best practices pipeline. *Current protocols in bioinformatics*. 2013;11.0. 1-.0. 33.
202. DePristo MA, Banks E, Poplin R, Garimella KV, Maguire JR, Hartl C, et al. A framework for variation discovery and genotyping using next-generation DNA sequencing data. *Nature genetics*. 2011;43(5):491-8.
203. Li H, Handsaker B, Wysoker A, Fennell T, Ruan J, Homer N, et al. The sequence alignment/map format and SAMtools. *Bioinformatics*. 2009;25(16):2078-9.
204. Abascal F, Zardoya R, Telford MJ. TranslatorX: multiple alignment of nucleotide sequences guided by amino acid translations. *Nucleic acids research*. 2010;38(suppl_2):W7-W13.
205. Katoh K, Kuma K-i, Toh H, Miyata T. MAFFT version 5: improvement in accuracy of multiple sequence alignment. *Nucleic acids research*. 2005;33(2):511-8.
206. Felsenstein J. PHYLIP (Phylogeny Inference Package) version 3.6. Department of Genome Sciences, University of Washington, Seattle.: Distributed by the author. ; 2005.
207. Zhang J, Nielsen R, Yang Z. Evaluation of an improved branch-site likelihood method for detecting positive selection at the molecular level. *Molecular biology and evolution*. 2005;22(12):2472-9.
208. Yang Z, Wong WS, Nielsen R. Bayes empirical Bayes inference of amino acid sites under positive selection. *Molecular biology and evolution*. 2005;22(4):1107-18.
209. Mykles DL, Ghalambor CK, Stillman JH, Tomanek L. Grand Challenges in Comparative Physiology: Integration Across Disciplines and Across Levels of Biological Organization. *Integrative and comparative biology*. 2010;50(1):6-16.
210. Carey HV. Lessons Learned From Comparative and Evolutionary Physiology. *Physiology*. 2015;30(2):80-1.
211. Kohl KD. A Microbial Perspective on the Grand Challenges in Comparative Animal Physiology. *mSystems*. 2018;3(2):e00146-17.
212. Chang ES, Mykles DL. Regulation of crustacean molting: A review and our perspectives. *General and Comparative Endocrinology*. 2011;172(3):323-30.

213. Mykles DL, Chang ES. Hormonal control of the crustacean molting gland: Insights from transcriptomics and proteomics. *General and Comparative Endocrinology*. 2020;294:113493.
214. Papetti C, Lucassen M, Pörtner H-O. Integrated studies of organismal plasticity through physiological and transcriptomic approaches: examples from marine polar regions. *Briefings in Functional Genomics*. 2016;15(5):365-72.
215. Picard M, McEwen BS, Epel ES, Sandi C. An energetic view of stress: Focus on mitochondria. *Frontiers in Neuroendocrinology*. 2018;49:72-85.
216. Somero GN, Lockwood BL, Tomanek L. *Biochemical adaptation: response to environmental challenges, from life's origins to the Anthropocene*: Sinauer Associates, Incorporated Publishers; 2017.
217. Ghiselli F, Milani L. Linking the mitochondrial genotype to phenotype: a complex endeavour. *Philosophical Transactions of the Royal Society B: Biological Sciences*. 2020;375(1790):20190169.
218. Havird JC, Shah AA, Chicco AJ. Powerhouses in the cold: mitochondrial function during thermal acclimation in montane mayflies. *Philosophical Transactions of the Royal Society B: Biological Sciences*. 2020;375(1790):20190181.
219. Gillooly JF, Brown JH, West GB, Savage VM, Charnov EL. Effects of Size and Temperature on Metabolic Rate. *Science*. 2001;293(5538):2248.
220. Dillon ME, Wang G, Huey RB. Global metabolic impacts of recent climate warming. *Nature*. 2010;467(7316):704-6.
221. Sokolova IM, Frederich M, Bagwe R, Lannig G, Sukhotin AA. Energy homeostasis as an integrative tool for assessing limits of environmental stress tolerance in aquatic invertebrates. *Marine Environmental Research*. 2012;79:1-15.
222. Brown JH, Marquet PA, Taper ML. Evolution of Body Size: Consequences of an Energetic Definition of Fitness. *The American Naturalist*. 1993;142(4):573-84.
223. Sokolova IM, Sokolov EP, Haider F. Mitochondrial Mechanisms Underlying Tolerance to Fluctuating Oxygen Conditions: Lessons from Hypoxia-Tolerant Organisms. *Integrative and comparative biology*. 2019;59(4):938-52.
224. Elbassiouny AA, Lovejoy NR, Chang BSW. Convergent patterns of evolution of mitochondrial oxidative phosphorylation (OXPHOS) genes in electric fishes. *Philosophical Transactions of the Royal Society B: Biological Sciences*. 2020;375(1790):20190179.

225. Hayes JP. Altitudinal and seasonal effects on aerobic metabolism of deer mice. *Journal of Comparative Physiology B*. 1989;159(4):453-9.
226. Lau DS, Connaty AD, Mahalingam S, Wall N, Cheviron ZA, Storz JF, et al. Acclimation to hypoxia increases carbohydrate use during exercise in high-altitude deer mice. *American Journal of Physiology-Regulatory, Integrative and Comparative Physiology*. 2017;312(3):R400-R11.
227. Julian D, Crampton WGR, Wohlgemuth SE, Albert JS. Oxygen consumption in weakly electric Neotropical fishes. *Oecologia*. 2003;137(4):502-11.
228. da Fonseca RR, Johnson WE, O'Brien SJ, Ramos MJ, Antunes A. The adaptive evolution of the mammalian mitochondrial genome. *BMC Genomics*. 2008;9(1):119.
229. Hill GE. Cellular Respiration: The Nexus of Stress, Condition, and Ornamentation. *Integrative and comparative biology*. 2014;54(4):645-57.
230. Wolff JN, Ladoukakis ED, Enríquez JA, Dowling DK. Mitonuclear interactions: evolutionary consequences over multiple biological scales. *Philosophical Transactions of the Royal Society B: Biological Sciences*. 2014;369(1646):20130443.
231. Lane N. Mitonuclear match: Optimizing fitness and fertility over generations drives ageing within generations. *BioEssays*. 2011;33(11):860-9.
232. Hebert PD, Ratnasingham S, deWaard JR. Barcoding animal life: cytochrome c oxidase subunit 1 divergences among closely related species. *Proceedings Biological sciences*. 2003;270 Suppl 1(Suppl 1):S96-9.
233. Matoo OB, Julick CR, Montooth KL. Genetic Variation for Ontogenetic Shifts in Metabolism Underlies Physiological Homeostasis in *Drosophila*. *Genetics*. 2019;212(2):537.
234. Milani L, Ghiselli F. Faraway, so close. The comparative method and the potential of non-model animals in mitochondrial research. *Philosophical Transactions of the Royal Society B: Biological Sciences*. 2020;375(1790):20190186.
235. Havird JC, Weaver RJ, Milani L, Ghiselli F, Greenway R, Ramsey AJ, et al. Beyond the Powerhouse: Integrating Mitonuclear Evolution, Physiology, and Theory in Comparative Biology. *Integrative and comparative biology*. 2019;59(4):856-63.
236. Ballard JWO, Melvin RG. Linking the mitochondrial genotype to the organismal phenotype. *Molecular ecology*. 2010;19(8):1523-39.

237. Jeong H, Tombor B, Albert R, Oltvai ZN, Barabási AL. The large-scale organization of metabolic networks. *Nature*. 2000;407(6804):651-4.
238. Clark AG, Wang L, Hulleberg T. P-element-induced variation in metabolic regulation in *Drosophila*. *Genetics*. 1995;139(1):337-48.
239. Clark AG, Wang L, Hulleberg T. Spontaneous mutation rate of modifiers of metabolism in *Drosophila*. *Genetics*. 1995;139(2):767-79.
240. Montooth KL, Marden JH, Clark AG. Mapping determinants of variation in energy metabolism, respiration and flight in *Drosophila*. *Genetics*. 2003;165(2):623-35.
241. Barabási A-L, Oltvai ZN. Network biology: understanding the cell's functional organization. *Nature Reviews Genetics*. 2004;5(2):101-13.
242. Strogatz SH. Exploring complex networks. *Nature*. 2001;410(6825):268-76.
243. Weber APM, Horst RJ, Barbier GG, Oesterhelt C. Metabolism and Metabolomics of Eukaryotes Living Under Extreme Conditions. *International Review of Cytology*. 256: Academic Press; 2007. p. 1-34.
244. Nevo E. Evolution Under Environmental Stress at Macro- and Microscales. *Genome Biology and Evolution*. 2011;3:1039-52.
245. Muyzer G, microbiology AJMSNr, undefined. The ecology and biotechnology of sulphate-reducing bacteria. *naturecom*. 2008.
246. Olson KR, Straub KD. The Role of Hydrogen Sulfide in Evolution and the Evolution of Hydrogen Sulfide in Metabolism and Signaling. *Physiology (Bethesda)*. 2016;31(1):60-72.
247. Módis K, Bos EM, Calzia E, Van Goor H, Coletta C, Papapetropoulos A, et al. Regulation of mitochondrial bioenergetic function by hydrogen sulfide. Part II Pathophysiological and therapeutic aspects. *John Wiley and Sons Inc.*; 2014. p. 2123-46.
248. Greenway R, Barts N, Henpita C, Brown AP, Arias Rodriguez L, Rodríguez Peña CM, et al. Convergent evolution of conserved mitochondrial pathways underlies repeated adaptation to extreme environments. *Proceedings of the National Academy of Sciences*. 2020:202004223.
249. Kirby DM, Thorburn DR, Turnbull DM, Taylor RW. Biochemical Assays of Respiratory Chain Complex Activity. 2007. p. 93-119.
250. Rogers GW, Brand MD, Petrosyan S, Ashok D, Elorza AA, Ferrick DA, et al. High Throughput Microplate Respiratory Measurements Using Minimal Quantities Of Isolated Mitochondria. *PloS one*. 2011;6(7):e21746.

251. Ferrick DA, Neilson A, Beeson C. Advances in measuring cellular bioenergetics using extracellular flux. *Drug Discovery Today*. 2008;13(5):268-74.
252. Fangue NA, Richards JG, Schulte PM. Do mitochondrial properties explain intraspecific variation in thermal tolerance? *Journal of Experimental Biology*. 2009;212(4):514.
253. Brennan RS, Hwang R, Tse M, Fangue NA, Whitehead A. Local adaptation to osmotic environment in killifish, *Fundulus heteroclitus*, is supported by divergence in swimming performance but not by differences in excess post-exercise oxygen consumption or aerobic scope. *Comparative Biochemistry and Physiology Part A: Molecular & Integrative Physiology*. 2016;196:11-9.
254. Rosewarne PJ, Wilson JM, Svendsen JC. Measuring maximum and standard metabolic rates using intermittent-flow respirometry: a student laboratory investigation of aerobic metabolic scope and environmental hypoxia in aquatic breathers. *Journal of fish biology*. 2016;88(1):265-83.
255. Svendsen MBS, Bushnell PG, Steffensen JF. Design and setup of intermittent-flow respirometry system for aquatic organisms. *Journal of fish biology*. 2016;88(1):26-50.
256. Frenette BD, Bruckerhoff LA, Tobler M, Gido KB. Temperature effects on performance and physiology of two prairie stream minnows. *Conservation Physiology*. 2019;7(1).
257. Halsey LG, Killen SS, Clark TD, Norin T. Exploring key issues of aerobic scope interpretation in ectotherms: absolute versus factorial. *Reviews in Fish Biology and Fisheries*. 2018;28(2):405-15.
258. Borowiec BG, Hoffman RD, Hess CD, Galvez F, Scott GR. Interspecific variation in hypoxia tolerance and hypoxia acclimation responses in killifish from the family Fundulidae. *The Journal of experimental biology*. 2020;223(4):jeb209692.
259. Bates D, Mächler M, Bolker BM, Walker SC. Fitting linear mixed-effects models using lme4. *Journal of Statistical Software*. 2015;67(1):1-48.
260. Muggeo VM. Segmented: an R package to fit regression models with broken-line relationships. *R news*. 2008;8(1):20-5.
261. Callier V, Shingleton AW, Brent CS, Ghosh SM, Kim J, Harrison JF. The role of reduced oxygen in the developmental physiology of growth and metamorphosis initiation in *Drosophila melanogaster*. *The Journal of experimental biology*. 2013;216(23):4334.

262. Ultsch GR, Regan MD. The utility and determination of Pcrit in fishes. *The Journal of experimental biology*. 2019;222(22):jeb203646.
263. Burnham KP, Anderson DR. *Model selection and multimodel inference : a practical information-theoretic approach*. 2nd ed. ed. New York: Springer; 2002.
264. Alvarez M, Schrey AW, Richards CL. Ten years of transcriptomics in wild populations: what have we learned about their ecology and evolution? *Molecular ecology*. 2015;24(4):710-25.
265. Kita R, Fraser HB. Local Adaptation of Sun-Exposure-Dependent Gene Expression Regulation in Human Skin. *PLoS Genet*. 2016;12(10):e1006382-e.
266. Kadenbach B, Hüttemann M, Arnold S, Lee I, Bender E. Mitochondrial energy metabolism is regulated via nuclear-coded subunits of cytochrome c oxidase11 This article is dedicated to the memory of the late Professor Lars Ernster. *Free Radical Biology and Medicine*. 2000;29(3):211-21.
267. Sinkler CA, Kalpage H, Shay J, Lee I, Malek MH, Grossman LI, et al. Tissue- and Condition-Specific Isoforms of Mammalian Cytochrome *c* Oxidase Subunits: From Function to Human Disease. *Oxidative Medicine and Cellular Longevity*. 2017;2017:1534056.
268. Dudkina NV, Sunderhaus S, Boekema EJ, Braun H-P. The higher level of organization of the oxidative phosphorylation system: mitochondrial supercomplexes. *Journal of Bioenergetics and Biomembranes*. 2008;40(5):419.
269. Hatefi Y. The mitochondrial electron transport and oxidative phosphorylation system. *Annu Rev Biochem*. 1985;54:1015-69.
270. Lagoutte E, Mimoun S, Andriamihaja M, Chaumontet C, Blachier F, Bouillaud F. Oxidation of hydrogen sulfide remains a priority in mammalian cells and causes reverse electron transfer in colonocytes. *Biochim Biophys Acta*. 2010;1797(8):1500-11.
271. Goubern M, Andriamihaja M, Nübel T, Blachier F, Bouillaud F. Sulfide, the first inorganic substrate for human cells. *The FASEB Journal*. 2007;21(8):1699-706.
272. Szabo C, Ransy C, Módis K, Andriamihaja M, Murgheș B, Coletta C, et al. Regulation of mitochondrial bioenergetic function by hydrogen sulfide. Part I. Biochemical and physiological mechanisms. John Wiley and Sons Inc.; 2014. p. 2099-122.
273. Millidine KJ, Armstrong JD, Metcalfe NB. Juvenile salmon with high standard metabolic rates have higher energy costs but can process meals faster. *Proceedings Biological sciences*. 2009;276(1664):2103-8.

274. Norin T, Malte H. Intraspecific Variation in Aerobic Metabolic Rate of Fish: Relations with Organ Size and Enzyme Activity in Brown Trout. *Physiological and Biochemical Zoology*. 2012;85(6):645-56.
275. Yamamoto H, Morino K, Mengistu L, Ishibashi T, Kiriyama K, Ikami T, et al. Amla Enhances Mitochondrial Spare Respiratory Capacity by Increasing Mitochondrial Biogenesis and Antioxidant Systems in a Murine Skeletal Muscle Cell Line. *Oxidative Medicine and Cellular Longevity*. 2016;2016:1735841.
276. Scott GR, Guo KH, Dawson NJ. The Mitochondrial Basis for Adaptive Variation in Aerobic Performance in High-Altitude Deer Mice. *Integrative and comparative biology*. 2018;58(3):506-18.
277. Salazar JC, del Rosario Castañeda M, Londoño GA, Bodensteiner BL, Muñoz MM. Physiological evolution during adaptive radiation: A test of the island effect in *Anolis* lizards. *Evolution; international journal of organic evolution*. 2019;73(6):1241-52.
278. Scott GR, Schulte PM, Egginton S, Scott AL, Richards JG, Milsom WK. Molecular evolution of cytochrome c oxidase underlies high-altitude adaptation in the bar-headed goose. *Molecular biology and evolution*. 2011;28(1):351-63.
279. Decelle J, Andersen AC, Hourdez S. Morphological adaptations to chronic hypoxia in deep-sea decapod crustaceans from hydrothermal vents and cold seeps. *Marine biology*. 2010;157(6):1259-69.
280. Nilsson GE. Gill remodeling in fish—a new fashion or an ancient secret? *Journal of experimental Biology*. 2007;210(14):2403-9.
281. Kramer DL, McClure M. Aquatic surface respiration, a widespread adaptation to hypoxia in tropical freshwater fishes. *Environmental Biology of Fishes*. 1982;7(1):47-55.
282. Timmerman CM, Chapman LJ. Behavioral and physiological compensation for chronic hypoxia in the sailfin molly (*Poecilia latipinna*). *Physiological and biochemical zoology : PBZ*. 2004;77(4):601-10.
283. Seibel BA. Critical oxygen levels and metabolic suppression in oceanic oxygen minimum zones. *The Journal of experimental biology*. 2011;214(2):326.
284. Bickler PE, Buck LT. Hypoxia Tolerance in Reptiles, Amphibians, and Fishes: Life with Variable Oxygen Availability. *Annual Review of Physiology*. 2007;69(1):145-70.

285. Storz JF, Runck AM, Sabatino SJ, Kelly JK, Ferrand N, Moriyama H, et al. Evolutionary and functional insights into the mechanism underlying high-altitude adaptation of deer mouse hemoglobin. *Proceedings of the National Academy of Sciences*. 2009;106(34):14450-5.
286. Natarajan C, Hoffmann FG, Lanier HC, Wolf CJ, Cheviron ZA, Spangler ML, et al. Intraspecific polymorphism, interspecific divergence, and the origins of function-altering mutations in deer mouse hemoglobin. *Molecular Biology and Evolution*. 2015;32(4):978-97.
287. Cheviron ZA, Connaty AD, McClelland GB, Storz JF. Functional genomics of adaptation to hypoxic cold-stress in high-altitude deer mice: transcriptomic plasticity and thermogenic performance. *Evolution; international journal of organic evolution*. 2014;68(1):48-62.
288. Lau GY, Mandic M, Richards JG. Evolution of Cytochrome c Oxidase in Hypoxia Tolerant Sculpins (Cottidae, Actinopterygii). *Molecular Biology and Evolution*. 2017;34(9):2153-62.
289. Zhang Z-Y, Chen B, Zhao D-J, Kang L. Functional modulation of mitochondrial cytochrome c oxidase underlies adaptation to high-altitude hypoxia in a Tibetan migratory locust. *Proceedings of the Royal Society B: Biological Sciences*. 2013;280(1756):20122758.
290. Lagoutte E, Mimoun S, Andriamihaja M, Chaumontet C, Blachier F, Bouillaud F. Oxidation of hydrogen sulfide remains a priority in mammalian cells and causes reverse electron transfer in colonocytes. *Biochimica et Biophysica Acta (BBA) - Bioenergetics*. 2010;1797(8):1500-11.
291. Barve A, Wagner A. A latent capacity for evolutionary innovation through exaptation in metabolic systems. *Nature*. 2013;500(7461):203-6.
292. Keller SR, Taylor DR. History, chance and adaptation during biological invasion: separating stochastic phenotypic evolution from response to selection. *Ecol Lett*. 2008;11(8):852-66.
293. Stockwell CA, Hendry AP, Kinnison MT. Contemporary evolution meets conservation biology. *Trends in ecology & evolution*. 2003;18(2):94-101.
294. Reichard SH, White PS. Invasion Biology: An Emerging Field of Study. *Annals of the Missouri Botanical Garden*. 2003;90(1):64-6.
295. Rey O, Estoup A, Vonshak M, Loiseau A, Blanchet S, Calcaterra L, et al. Where do adaptive shifts occur during invasion? A multidisciplinary approach to unravelling cold adaptation in a tropical ant species invading the Mediterranean area. *Ecology Letters*. 2012;15(11):1266-75.

- 296.Sahu SK, Singh R, Kathiresan K. Multi-gene phylogenetic analysis reveals the multiple origin and evolution of mangrove physiological traits through exaptation. *Estuarine, Coastal and Shelf Science*. 2016;183:41-51.
- 297.Guo W-Y, Lambertini C, Nguyen LX, Li X-Z, Brix H. Preadaptation and post-introduction evolution facilitate the invasion of *Phragmites australis* in North America. *Ecology and evolution*. 2014;4(24):4567-77.
- 298.Carroll SP, Dingle H. The biology of post-invasion events. *Biological Conservation*. 1996;78(1):207-14.
- 299.Reznick DN, Ghalambor CK. The population ecology of contemporary adaptations: what empirical studies reveal about the conditions that promote adaptive evolution. *Genetica*. 2001;112(1):183-98.
- 300.Bøhn T, Terje Sandlund O, Amundsen P-A, Primicerio R. Rapidly changing life history during invasion. *Oikos*. 2004;106(1):138-50.
- 301.Phillips BL, Brown GP, Shine R. Evolutionarily accelerated invasions: the rate of dispersal evolves upwards during the range advance of cane toads. *Journal of evolutionary biology*. 2010;23(12):2595-601.
- 302.Tomarev SI, Piatigorsky J. Lens crystallins of invertebrates--diversity and recruitment from detoxification enzymes and novel proteins. *Eur J Biochem*. 1996;235(3):449-65.
- 303.Keys DN, Lewis DL, Selegue JE, Pearson BJ, Goodrich LV, Johnson RL, et al. Recruitment of a *hedgehog* Regulatory Circuit in Butterfly Eyespot Evolution. *Science*. 1999;283(5401):532.
- 304.True JR, Carroll SB. Gene Co-Option in Physiological and Morphological Evolution. *Annual Review of Cell and Developmental Biology*. 2002;18(1):53-80.
- 305.Gould SJ, Vrba ES. Exaptation—a Missing Term in the Science of Form. *Paleobiology*. 1982;8(1):4-15.
- 306.Bock WJ. PREADAPTATION AND MULTIPLE EVOLUTIONARY PATHWAYS. *Evolution; international journal of organic evolution*. 1959;13(2):194-211.
- 307.Salvidio S, Crovetto F, Adams DC. Potential rapid evolution of foot morphology in Italian plethodontid salamanders (*Hydromantes strinatii*) following the colonization of an artificial cave. *Journal of evolutionary biology*. 2015;28(7):1403-9.

308. Ridley CE, Ellstrand NC. Rapid evolution of morphology and adaptive life history in the invasive California wild radish (*Raphanus sativus*) and the implications for management. *Evolutionary Applications*. 2010;3(1):64-76.
309. Fisk DL, Latta LC, Knapp RA, Pfrender ME. Rapid evolution in response to introduced predators I: rates and patterns of morphological and life-history trait divergence. *BMC Evolutionary Biology*. 2007;7(1):22.
310. Blair AC, Wolfe LM. THE EVOLUTION OF AN INVASIVE PLANT: AN EXPERIMENTAL STUDY WITH *SILENE LATIFOLIA*. *Ecology*. 2004;85(11):3035-42.
311. Sherpa S, Blum MGB, Després L. Cold adaptation in the Asian tiger mosquito's native range precedes its invasion success in temperate regions. *Evolution; international journal of organic evolution*. 2019;73(9):1793-808.
312. MacDougall AS, McCune JL, Eriksson O, Cousins SAO, Pärtel M, Firn J, et al. The Neolithic Plant Invasion Hypothesis: the role of preadaptation and disturbance in grassland invasion. *New Phytologist*. 2018;220(1):94-103.
313. Alzate A, Onstein RE, Etienne RS, Bonte D. The role of preadaptation, propagule pressure and competition in the colonization of new habitats. *Oikos*. 2020;129(6):820-9.
314. Elst EM, Acharya KP, Dar PA, Reshi ZA, Tufto J, Nijs I, et al. Pre-adaptation or genetic shift after introduction in the invasive species *Impatiens glandulifera*? *Acta Oecologica*. 2016;70:60-6.
315. Bossdorf O, Lipowsky A, Prati D. Selection of preadapted populations allowed *Senecio inaequidens* to invade Central Europe. *Diversity and Distributions*. 2008;14(4):676-85.
316. Qin R-M, Zheng Y-L, Valiente-Banuet A, Callaway RM, Barclay GF, Pereyra CS, et al. The evolution of increased competitive ability, innate competitive advantages, and novel biochemical weapons act in concert for a tropical invader. *New Phytologist*. 2013;197(3):979-88.
317. Ricklefs RE, Guo Q, Qian H. Growth form and distribution of introduced plants in their native and non-native ranges in Eastern Asia and North America. *Diversity and Distributions*. 2008;14(2):381-6.
318. Randle AM, Snyder JB, Kalisz S. Can differences in autonomous selfing ability explain differences in range size among sister-taxa pairs of *Collinsia* (Plantaginaceae)? An extension of Baker's Law. *New Phytol*. 2009;183(3):618-29.

- 319.Schlaepfer DR, Glättli M, Fischer M, van Kleunen M. A multi-species experiment in their native range indicates pre-adaptation of invasive alien plant species. *New Phytologist*. 2010;185(4):1087-99.
- 320.Rejmanek M, Richardson DM. What Attributes Make Some Plant Species More Invasive? *Ecology*. 1996;77(6):1655-61.
- 321.Davidson AM, Jennions M, Nicotra AB. Do invasive species show higher phenotypic plasticity than native species and, if so, is it adaptive? A meta-analysis. *Ecology Letters*. 2011;14(4):419-31.
- 322.Schweitzer JA, Larson KC. Greater Morphological Plasticity of Exotic Honeysuckle Species may make them Better Invaders than Native Species. *The Journal of the Torrey Botanical Society*. 1999;126(1):15-23.
- 323.Zenni RD, Lamy J-B, Lamarque LJ, Porté AJ. Adaptive evolution and phenotypic plasticity during naturalization and spread of invasive species: implications for tree invasion biology. *Biological Invasions*. 2014;16(3):635-44.
- 324.Funk JL. Differences in plasticity between invasive and native plants from a low resource environment. *Journal of Ecology*. 2008;96(6):1162-73.
- 325.Hou Y-P, Peng S-L, Lin Z-G, Huang Q-Q, Ni G-Y, Zhao N. Fast-growing and poorly shade-tolerant invasive species may exhibit higher physiological but not morphological plasticity compared with non-invasive species. *Biological Invasions*. 2015;17(5):1555-67.
- 326.Sarà G, Romano C, Widdows J, Staff FJ. Effect of salinity and temperature on feeding physiology and scope for growth of an invasive species (*Brachidontes pharaonis* - MOLLUSCA: BIVALVIA) within the Mediterranean sea. *Journal of Experimental Marine Biology and Ecology*. 2008;363(1):130-6.
- 327.Hardy NB, Peterson DA, Ross L, Rosenheim JA. Does a plant-eating insect's diet govern the evolution of insecticide resistance? Comparative tests of the pre-adaptation hypothesis. *Evolutionary Applications*. 2018;11(5):739-47.
- 328.Dermauw W, Wybouw N, Rombauts S, Menten B, Vontas J, Grbic M, et al. A link between host plant adaptation and pesticide resistance in the polyphagous spider mite *Tetranychus urticae*. *Proceedings of the National Academy of Sciences of the United States of America*. 2013;110(2):E113-22.

329. Gleason LU, Burton RS. RNA-seq reveals regional differences in transcriptome response to heat stress in the marine snail *Chlorostoma funebris*. *Molecular ecology*. 2015;24(3):610-27.
330. Jenkins C, Keller SR. A phylogenetic comparative study of preadaptation for invasiveness in the genus *Silene* (Caryophyllaceae). *Biological Invasions*. 2011;13(6):1471-86.
331. Bell G, Collins S. Adaptation, extinction and global change. *Evolutionary Applications*. 2008;1(1):3-16.
332. Belyea LR, Lancaster J. Assembly Rules within a Contingent Ecology. *Oikos*. 1999;86(3):402-16.
333. Butler IB, Schoonen MA, Rickard DT. Removal of dissolved oxygen from water: A comparison of four common techniques. *Talanta*. 1994;41(2):211-5.
334. Pertea M, Pertea GM, Antonescu CM, Chang TC, Mendell JT, Salzberg SL. StringTie enables improved reconstruction of a transcriptome from RNA-seq reads. *Nat Biotechnol*. 2015;33(3):290-5.
335. Pertea M, Kim D, Pertea GM, Leek JT, Salzberg SL. Transcript-level expression analysis of RNA-seq experiments with HISAT, StringTie and Ballgown. *Nat Protoc*. 2016;11(9):1650-67.
336. Emms DM, Kelly S. OrthoFinder: solving fundamental biases in whole genome comparisons dramatically improves orthogroup inference accuracy. *Genome Biology*. 2015;16(1):157.
337. Emms DM, Kelly S. OrthoFinder: phylogenetic orthology inference for comparative genomics. *Genome Biology*. 2019;20(1):238.
338. Robinson MD, McCarthy DJ, Smyth GK. edgeR: a Bioconductor package for differential expression analysis of digital gene expression data. *Bioinformatics*. 2010;26(1):139-40.
339. Gutbrodt B, Dorn S, Unsicker SB, Mody K. Species-specific responses of herbivores to within-plant and environmentally mediated between-plant variability in plant chemistry. *Chemoecology*. 2012;22(2):101-11.
340. Vargas CA, Lagos NA, Lardies MA, Duarte C, Manríquez PH, Aguilera VM, et al. Species-specific responses to ocean acidification should account for local adaptation and adaptive plasticity. *Nature Ecology & Evolution*. 2017;1(4):0084.
341. Zhang J, Sun Q-l, Luan Z-d, Lian C, Sun L. Comparative transcriptome analysis of *Rimicaris* sp. reveals novel molecular features associated with survival in deep-sea hydrothermal vent. *Scientific reports*. 2017;7(1):2000.

342. Kleinsimon S, Longmuss E, Rolff J, Jäger S, Eggert A, Delebinski C, et al. GADD45A and CDKN1A are involved in apoptosis and cell cycle modulatory effects of viscumTT with further inactivation of the STAT3 pathway. *Scientific reports*. 2018;8(1):5750.
343. Brugarolas J, Lei K, Hurley RL, Manning BD, Reiling JH, Hafen E, et al. Regulation of mTOR function in response to hypoxia by REDD1 and the TSC1/TSC2 tumor suppressor complex. *Genes Dev*. 2004;18(23):2893-904.
344. Rossin A, Derouet M, Abdel-Sater F, Hueber A-O. Palmitoylation of the TRAIL receptor DR4 confers an efficient TRAIL-induced cell death signalling. *Biochemical Journal*. 2009;419(1):185-94.
345. Chaudhary PM, Eby M, Jasmin A, Bookwalter A, Murray J, Hood L. Death Receptor 5, a New Member of the TNFR Family, and DR4 Induce FADD-Dependent Apoptosis and Activate the NF- κ B Pathway. *Immunity*. 1997;7(6):821-30.
346. Lamkanfi M, Kanneganti T-D. Caspase-7: a protease involved in apoptosis and inflammation. *Int J Biochem Cell Biol*. 2010;42(1):21-4.
347. Olson KR. Mitochondrial adaptations to utilize hydrogen sulfide for energy and signaling. *Journal of comparative physiology B, Biochemical, systemic, and environmental physiology*. 2012;182(7):881-97.
348. An H-J, Shin H, Jo S-G, Kim YJ, Lee J-O, Paik S-G, et al. The survival effect of mitochondrial Higd-1a is associated with suppression of cytochrome C release and prevention of caspase activation. *Biochimica et Biophysica Acta (BBA) - Molecular Cell Research*. 2011;1813(12):2088-98.
349. Yasumoto K-i, Kowata Y, Yoshida A, Torii S, Sogawa K. Role of the intracellular localization of HIF-prolyl hydroxylases. *Biochimica et Biophysica Acta (BBA) - Molecular Cell Research*. 2009;1793(5):792-7.
350. Berardini TZ, Drygas-Williams M, Callard GV, Tolan DR. Identification of Neuronal Isozyme Specific Residues by Comparison of Goldfish Aldolase C to Other Aldolases. *Comparative Biochemistry and Physiology Part A: Physiology*. 1997;117(4):471-6.
351. Bröer S, Rahman B, Pellegrini G, Pellerin L, Martin J-L, Verleysdonk S, et al. Comparison of Lactate Transport in Astroglial Cells and Monocarboxylate Transporter 1 (MCT 1) Expressing *Xenopus laevis* Oocytes EXPRESSION OF TWO DIFFERENT MONOCARBOXYLATE

- TRANSPORTERS IN ASTROGLIAL CELLS AND NEURONS. *Journal of Biological Chemistry*. 1997;272(48):30096-102.
352. Pinheiro C, Albergaria A, Paredes J, Sousa B, Dufloth R, Vieira D, et al. Monocarboxylate transporter 1 is up-regulated in basal-like breast carcinoma. *Histopathology*. 2010;56(7):860-7.
353. Scrutton MC, Utter MF. The regulation of glycolysis and gluconeogenesis in animal tissues. *Annual review of biochemistry*. 1968;37(1):249-302.
354. Bermúdez-González MP, Ramírez-García A, Velázquez-García EdC, Queijeiro-Bolaños ME, Ramírez-Herrejón JP. Population structure of *Poecilia mexicana* (native) and *Poeciliopsis gracilis* (non-native) in a subtropical river. *Latin American Journal of Aquatic Research*; Vol 48, No 3 (2020). 2020.
355. Timmerman CM, Chapman LJ. Hypoxia and interdemec variation in *Poecilia latipinna*. *Journal of fish biology*. 2004;65(3):635-50.
356. Meffe GK, Snelson FF. An ecological overview of poeciliid fishes. In: Meffe GK, Snelson FF, editors. *Ecology and evolution of lifebearing fishes (Poeciliidae)*. New Jersey: Prentice Hall; 1989. p. 13-31.
357. Hopper GW, Gido KB, Pennock CA, Hedden SC, Frenette BD, Barts N, et al. Nowhere to swim: interspecific responses of prairie stream fishes in isolated pools during severe drought. *Aquatic Sciences*. 2020;82(2):42.
358. Lipsewers YA, Vasquez-Cardenas D, Seitaj D, Schauer R, Hidalgo-Martinez S, Sinninghe Damsté JS, et al. Impact of Seasonal Hypoxia on Activity and Community Structure of Chemolithoautotrophic Bacteria in a Coastal Sediment. *Applied and Environmental Microbiology*. 2017;83(10):e03517-16.
359. Roden EE, Tuttle JH. Sulfide release from estuarine sediments underlying anoxic bottom water. *Limnology and Oceanography*. 1992;37(4):725-38.
360. Ghalambor CK, Hoke KL, Ruell EW, Fischer EK, Reznick DN, Hughes KA. Non-adaptive plasticity potentiates rapid adaptive evolution of gene expression in nature. *Nature*. 2015;525(7569):372-5.
361. Ghalambor CK, McKay JK, Carroll SP, Reznick DN. Adaptive versus non-adaptive phenotypic plasticity and the potential for contemporary adaptation in new environments. *Functional Ecology*. 2007;21(3):394-407.

362. Leonard AM, Lancaster LT. Maladaptive plasticity facilitates evolution of thermal tolerance during an experimental range shift. *BMC Evolutionary Biology*. 2020;20(1):47.
363. Romero IG, Ruvinsky I, Gilad Y. Comparative studies of gene expression and the evolution of gene regulation. *Nature Reviews Genetics*. 2012;13:505-16.
364. Fischer EK, Ghalambor CK, Hoke KL. Can a Network Approach Resolve How Adaptive vs Nonadaptive Plasticity Impacts Evolutionary Trajectories? *Integrative and comparative biology*. 2016;56(5):877-88.
365. Riesch R, Plath M, Garcia de Leon FJ, Schlupp I. Convergent life-history shifts: toxic environments result in big babies in two clades of poeciliids. *Die Naturwissenschaften*. 2010;97(2):133-41.
366. Riesch R, Plath M, Schlupp I, Tobler M, Brian Langerhans R. Colonisation of toxic environments drives predictable life-history evolution in livebearing fishes (Poeciliidae). *Ecology Letters*. 2014;17(1):65-71.
367. Jeffery WR, Strickler AG, Yamamoto Y. To see or not to see: Evolution of eye degeneration in Mexican blind cavefish. *Integrative and comparative biology*. 2003;43(4):531-41.
368. Losos JB. *Lizards in an evolutionary tree: ecology and adaptive radiation of Anoles*. Berkeley, CA: University of California Press; 2009.
369. Losos JB, Jackman TR, Larson A, de Queiroz K, Rodriguez-Schettino L. Contingency and determinism in replicated adaptive radiations of island lizards. *Science*. 1998;279:2115-8.
370. Park C, Nagel R, Blumberg W, Peisach J, Maliozzo R. Sulfhemoglobin: properties of partially sulfurated tetramers. *Journal of Biological Chemistry*. 1986;261:8805-10.
371. Ghalambor CK, Hoke KL, Ruell EW, Fischer EK, Reznick D, Hughes KA. Non-adaptive plasticity potentiates rapid adaptive evolution of gene expression in nature. *Nature*. 2015;525:372-5.
372. Glover KA, Solberg MF, Besnier F, Skaala Ø. Cryptic introgression: evidence that selection and plasticity mask the full phenotypic potential of domesticated Atlantic salmon in the wild. *Scientific reports*. 2018;8(1):13966.
373. Grether Gregory F. Environmental Change, Phenotypic Plasticity, and Genetic Compensation. *The American Naturalist*. 2005;166(4):E115-E23.

374. Purchase CF, Moreau DTR. Stressful environments induce novel phenotypic variation: hierarchical reaction norms for sperm performance of a pervasive invader. *Ecology and evolution*. 2012;2(10):2567-76.
375. Burggren WW, Monticino MG. Assessing physiological complexity. *Journal of Experimental Biology*. 2005;208(17):3221.
376. van de Pol I, Flik G, Gorissen M. Comparative Physiology of Energy Metabolism: Fishing for Endocrine Signals in the Early Vertebrate Pool. *Frontiers in Endocrinology*. 2017;8(36).